

Advanced EEG Signal Processing with Applications in Brain-Computer Interfaces

*Evaluating user focused paradigms for the purpose of enhancing Brain-
Computer Interaction*

vorgelegt von
M. Sc.
Irina-Emilia Nicolae
ORCID: 0000-0002-9346-8467

von der Fakultät IV - Elektrotechnik und Informatik
der Technischen Universität Berlin (TUB)
und der Fakultät für Elektronik, Telekommunikation und Informationstechnologie
der Polytechnischen Universität Bukarest (PUB)
(im Rahmen des Doppel-Promotionsabkommens)

zur Erlangung des akademischen Grades

Doktor der Ingenieurwissenschaften
– Dr.-Ing. –

genehmigte Dissertation

Promotionsausschuss:

Vorsitzender (PUB): Prof. Dr. Ing. Gheorghe Brezeanu
Vorsitzender (TUB): Prof. Dr. Manfred Opper
Gutachter: Prof. Dr. Ing. Dan A. Stoichescu
Gutachter: Prof. Dr. Benjamin Blankertz
Gutachterin: Prof. Dr. Ing. Mihaela Neagu (Ungureanu)
Gutachter: Prof. Dr. Klaus-Robert Müller
Gutachter: Prof. Dr. Med. Gabriel Curio
Gutachter: Prof. Dr. Ing. Mihai Ivanovici

Tag der wissenschaftlichen Aussprache: 2. Oktober 2018
an der Polytechnischen Universität Bukarest

Berlin, 2019



Proiect cofinanțat din Fondul Social European prin Programul Operațional Sectorial Dezvoltarea Resurselor Umane 2007-2013

Investește în oameni!

Proiect KNOWLEDGE - POSDRU/159/1.5/S/134398

Dezvoltarea resurselor umane din cercetarea doctorală și postdoctorală: motor al societății bazate pe cunoaștere



UNIVERSITATEA POLITEHNICA DIN BUCUREȘTI

Facultatea: Electronică, Telecomunicații și Tehnologia Informației

Departmentul: Electronică Aplicată și Ingineria Informației



TECHNISCHE UNIVERSITÄT BERLIN

Faculty: Electrical Engineering and Computer Science

Institut: Software Engineering and Theoretical Computer Science

Nr. Decizie Senat: 271 din 31.08.2018

TEZĂ DE DOCTORAT

*METODE AVANSATE DE PRELUCRARE A SEMNALELOR EEG CU APLICAȚII
ÎN BRAIN COMPUTER INTERFACES*

*Evaluarea paradigmatelor orientate către utilizatori cu scopul îmbunătățirii
Interacțiunii Creier-Calculator*

***ADVANCED EEG SIGNAL PROCESSING WITH APPLICATIONS IN
BRAIN-COMPUTER INTERFACES***

*Evaluating user focused paradigms for the purpose of enhancing Brain-Computer
Interaction*

Autor: Ing. Irina-Emilia NICOLAE

COMISIA DE DOCTORAT

Președinte	Prof. Dr. Ing. Gheorghe BREZEANU	de la	Universitatea Politehnica București
Conducător de doctorat 1	Prof. Dr. Ing. Dan A. STOICHESCU	de la	Universitatea Politehnica București
Conducător de doctorat 2	Prof. Dr. Benjamin BLANKERTZ	de la	Technische Universität Berlin
Referent	Prof. Dr. Ing. Mihaela NEAGU (UNGUREANU)	de la	Universitatea Politehnica București
Referent	Prof. Dr. Klaus-Robert MÜLLER	de la	Technische Universität Berlin
Referent	Prof. Dr. med. Gabriel CURIO	de la	Charité – Universitätsmedizin Berlin
Referent	Prof. Dr. Ing Mihai IVANOVICI	de la	University Transilvania of Brașov

București 2018

To the memory of my beloved father, Nicolae Florin

ABSTRACT (EN)

(English)

Advances in signal processing push forward the Neurotechnology domain along with the Brain-Computer Interface (BCI) research which deals with the analysis of brain activity. Heading for a future that will most probably happen, where either healthy persons or people with disabilities communicate and control external devices without muscle control, a symbiotic relationship between humans and machines needs to be created. Moreover, the research direction should be guided to the users' side by evaluating users' interests and needs.

The main goal of this thesis is to provide suggestions and solutions to ease and facilitate the Brain-Computer Interaction, by the following: i) stimuli and tasks that refer to users' mental states and interests are optimized; ii) an interpretable system is created to reveal the neural information that can further determine a controlled BCI system to act; iii) and the most important aspect that make the first two key points possible: advanced and improved methodological approaches are developed to efficiently extract and interpret human neural activity from the Electroencephalogram (EEG).

The investigation is performed through two experimental studies, where the first one proposes improved stimuli and tasks regarding users' interests and preferences in a motor-imagery-based BCI. The second study considers users' cognitive mental states with the purpose to better control BCIs and investigates not only what the user has received from the external information, but also how and to which level of processing is the information encoded within the brain. The paradigms investigate the brain fluctuations induced by different stimuli and tasks, in order to provide the means to silently detect the meaningful neural information from the brain activity, which is critical for a BCI application. While the first paradigm considers Sensorimotor Rhythms (SMRs), the second paradigm is based on Event Related Potentials (ERPs). Most BCI paradigms consider either the temporal or the spectral information of the generated brain activity, but infrequently the investigation is performed in ensemble considering both domains. As it will be observed in this work, the analysis pipeline that considers only one domain might be suboptimal, while brain activity manifests additional information which is visible in both temporal and spectral domains. Therefore, this thesis deals with the methodological improvements that include complementary information, yielding to more accurate data analysis that outperforms most of the available methods.

ZUSAMMENFASSUNG (GE)

(German)

Fortschritte auf dem Gebiet der Signalverarbeitung beeinflussen auch die Entwicklungen (in der Neurotechnologie und somit auch die Erforschung) der Gehirn-Computer Schnittstellen (BCIs). Um Menschen mit körperlichen Einschränkungen, wie auch gesunden Menschen, die Möglichkeit zu geben ohne muskuläre Kontrolle über externe Geräte zu kommunizieren oder diese zu kontrollieren, muss eine symbiotische Beziehung zwischen Mensch und Maschine geschaffen werden. Hierfür sollte in der Forschung insbesondere ein größerer Fokus auf die Interessen und Bedürfnisse der Nutzer:innen gelegt werden.

Das Ziel dieser Arbeit ist es Lösungsvorschläge für eine verbesserte Gehirn-Computer-Interaktion zu untersuchen. Dabei werden: i) Stimuli und Aufgabenstellungen die sich auf den mentalen Zustand der Nutzer:innen beziehen optimiert, ii) ein interpretierbares BCI geschaffen, um die entscheidenden neuronalen Informationen zu bestimmen, iii) die beiden ersten Punkte werden vor allem durch verbesserte methodische Ansätze ermöglicht welche effizient neuronale Aktivitäten vom Elektroenzephalogramm (EEG) extrahieren und interpretieren.

Hierfür werden zwei EEG Studien analysiert. Erstere untersucht verbesserte Stimuli und Aufgabenstellungen bezüglich der Nutzerinteressen in einem motor-imagery basierten BCI. Die zweite Studie analysiert kognitive Zustände um herauszufinden wie externe Informationen im Gehirn ankommen und wie diese verarbeitet werden. Die beiden Studien untersuchen die Fluktuationen im Gehirn welche durch unterschiedliche Stimuli und Aufgabenstellungen induziert werden, um aussagekräftige neuronale Informationen, welche für die Anwendung des BCI wichtig sind, zu bestimmen. Während das erste Paradigma die sensormotorischen Rhythmen (SMRs) betrachtet, basiert das zweite Paradigma auf ereigniskorrelierten Potentialen (ERPs). Die meisten BCI Paradigmen betrachten entweder die zeitliche oder die spektrale Domäne der Gehirnaktivität, eher selten werden beide im ensemble analysiert. In dieser Dissertation kommen wir zu dem Schluss, dass die Analyse die sich nur auf eine der beiden Domänen stützt nicht optimal ist, da wichtige Informationen in beiden Domänen enthalten ist. Deshalb analysieren wir erweiterte Methoden die komplementäre Informationen aus beiden Domänen kombinieren, was zu einer genaueren Datenanalyse führt, die die Ergebnisse der bisherigen Methoden übertrifft.

REZUMAT (RO)

(Romanian)

Progresele în analiza semnalelor impulsionează domeniul neuro-tehnologiei împreună cu cercetarea Interfețelor Creier-Calculator (en., Brain-Computes Interfaces - BCI) care se ocupă cu analiza activității cerebrale. Îndreptându-ne către un viitor care cel mai probabil se va întâmpla cât de curând, în care fie persoane sănătoase, fie persoane cu handicap comunică și controlează dispozitive externe fără intermediul controlului muscular, o relație simbiotică între oameni și mașini trebuie să fie creată. Mai mult, direcția de cercetare ar trebui să fie ghidată către utilizatori, prin evaluarea intereselor și nevoilor utilizatorilor.

Scopul principal al acestei lucrări este de a oferi sugestii și soluții pentru a ușura și facilita interacțiunea creier-calculator, prin următoarele: i) stimulii și activitățile care se referă la stările mentale și interesele utilizatorilor, sunt optimizate; ii) un sistem interpretabil este creat pentru a dezvălui informația neuronală ce poate determina în continuare un sistem de tip BCI pe bază de control să acționeze; iii) și cel mai important aspect care face posibile primele doua puncte cheie: abordări metodologice avansate și îmbunătățite sunt dezvoltate pentru a extrage și interpreta, în mod eficient, activitatea neuronală umană relevată de Electroencefalogramă (EEG).

Investigarea se realizează prin două studii experimentale, în care primul propune stimuli și sarcini îmbunătățite privind interesele și preferințele utilizatorilor în cadrul unei Interfețe Creier-Calculator bazate pe imaginare motorie. Al doilea studiu consideră stările mentale cognitive ale utilizatorilor vizând îmbunătățirea ulterioară a controlului în cadrul Interfețelor Creier-Calculator și investighează nu numai ceea ce utilizatorul a prelucrat din informațiile externe, ci și modul și nivelul de prelucrare al informației codificate în creier. Paradigmele investighează fluctuațiile creierului induse de diferiți stimuli și activități, pentru a oferi mijloacele de a detecta informația neuronală semnificativă din activitatea creierului, care este critică pentru o aplicație de tip BCI. În timp ce prima paradigmă consideră ritmurile sensori-motrice (SMRs), a doua paradigmă se bazează pe potențiale legate de evenimente (en., Event-Related Potentials - ERPs). Majoritatea paradigmelor BCI consideră fie informațiile temporale, fie informațiile spectrale ale activității generate de către creier, însă rareori cercetarea se realizează în ansamblu, considerând ambele domenii, timp și frecvență. Așa cum se va observa în această lucrare, analiza care consideră un singur domeniu ar putea fi suboptimală, deoarece activitatea creierului prezintă informații suplimentare ce sunt vizibile atât în domeniul temporal, cât și în cel spectral. Prin urmare, această teză se ocupă cu îmbunătățirile metodologice ce includ informațiile complementare, obținând o analiză mai precisă a datelor ce depășește performanțele majorității metodelor disponibile.

ACKNOWLEDGEMENTS

Looking back from when I first took a step on the path to my PhD I am very grateful for all the support and advice I have received along the way. First, I want to express my deep appreciation and thanks to my supervisors Prof. Dr. Rodica Strungaru and Prof. Dr. Benjamin Blankertz who dedicated precious time and effort to guide and supervise the deployment and progress of my thesis, adding valuable suggestions and ideas from their expertise to improve or correct every detail of the scientific research that made possible the work presented here, today. Additionally, special thanks to the Prof. Dr. Dan Stoichescu, for guiding and supervising the necessities towards the public defence, due to Prof. Dr. Rodica Strungaru unavailability. Following, I want to thank to my advisor Prof. Dr. Mihaela Neagu (Ungureanu) for continuously supporting me with helpful reviews, improvements and comments along the research of this current piece of work. Humble thanks to the dissertation referees for their valuable review along with precious comments, suggestions, guidance and additional questions that helped clarifying unclear aspects of the thesis. Thus, special thanks are addressed to Prof. Klaus-Robert Müller and Prof. Dr. Gabriel Curio. Likewise, I offer my gratitude to Prof. Dr. Manfred Opper for his important guidance and supportive questions as a chair of the preliminary defence in Berlin, and for his availability on short notice in response to Prof. Dr. Henning Sprekeler unavailability. Further, I want to give thanks to Prof. Sever Paşca for his precious comments and observations as a second advisor of my thesis. Next, I want to thank to Laura Acqualagna who brought a lot of help and guidance along the development of my research.

Moreover, I want to sincerely thank to all the great people that helped me along this road with their helpful comments, suggestions and ideas. From the Neurotechnology and Machine Learning Departments of Technische Universität Berlin, namely Marija, Markus, Han-Jeong, Pieter-Jan, Sven, Stefan, Manon, Irene S, Irene W, Alex, Stephanie, Daniel, Matthias, Miriam and all the others that I did not mention here. Thanks also to Andrej and Naveen for their interest and collaboration. As well thanks to Dominik, Imke and Andrea for their administrative and technical support. Same thanks for the colleagues from the Department of Applied Electronics and Information Engineering, University Politehnica of Bucharest, among which I recall Bogdan, Dragoş, Miruna, Roxana, Andreea, Corina and may be many others. Also, thanks to Ing. Nicoleta Brănişteanu and Prof. Gheorghe Brezeanu for their guidance considering the administrative PhD issues. Further, I thank to all my co-authors and collaborators which I did not mention already, for the great team work performed within the projects that I participated during my PhD.

Further, I address many thanks for all the participants who dedicated precious time for being involved in the experiments and for having lot of patience and endurance in the tedious preparation of the experiments by mounting the EEG cap and tolerating the sticky gel on their hair. Among all, the scientific experiments would not be made possible without them.

We acknowledge financial support from the Sectoral Operational Programme Human Resources Development 2007-2013 of the Ministry of European Funds through the Financial Agreement POSDRU/159/1.5/S/134398. Further, the work leading to these results was sponsored by the European Union Seventh Framework Programme (FP7/2007-2013) under grant agreement no. 611570 and completed by the BMBF under contract 01GQ0850. Considering publication funds, we acknowledge support by the German Research Foundation and the Open Access Publication Funds of Technische Universität Berlin, and Prof. Dr. Mihaela Neagu (Ungureanu).

Contents

ABSTRACT (EN).....	iii
ZUSAMMENFASSUNG (GE)	v
REZUMAT (RO).....	vii
ACKNOWLEDGEMENTS.....	ix
Contents	xi
List of figures.....	xv
List of tables.....	xix
List of abbreviations	xxi
Introduction.....	1
1.1 The field of doctoral study	1
1.2 Purpose of the thesis.....	3
1.3 Outline of the thesis.....	4
1.4 Scientific contribution.....	6
1.5 List of contributions	8
1.5.1 Main contributions list.....	9
1.5.2 Additional contributions list	10
Fundamentals of neurophysiology.....	13
2.1 Neurophysiological background	13
2.2 Electroencephalography	14
2.3 Brain-Computer Interface	14
2.4 Neurophysiological signals that enable BCI control.....	15
2.4.1 Event Related Potentials	16
2.4.2 Oscillatory brain activity.....	17
2.5 Notation.....	21
Signal processing and machine learning methods in BCI research	23
3.1 Brain activity measurement.....	23
3.2 Preprocessing	24
3.2.1 Preliminary filtering and preprocessing.....	24
3.2.2 Enhanced artifact removal	25
3.3 Feature extraction.....	33
3.3.1 Feature selection and dimensionality reduction.....	34

Contents

3.3.2	Temporal methods	34
3.3.3	Spectral methods	35
3.3.4	Time-frequency measures	36
3.4	Classification and Regression	37
3.4.1	Linear Discriminant Analysis (LDA)	38
3.4.2	Binomial Logistic Regression (LR)	40
3.4.3	Multinomial Logistic Regression (MLR)	40
3.4.4	Regression	40
3.4.5	Classification validation	41
3.4.6	Classification evaluation	41
3.5	BCI applications	43
3.5.1	Applications for ERP-based paradigms	44
3.5.2	Motor-imagery based BCIs applications	44
3.5.3	Mental state BCIs applications	44
	Revealing the neural correlates of user efficient motor imagery tasks	47
4.1	Introduction and state of the art	47
4.2	Methods	49
4.2.1	Experimental design and scenarios for efficient user motor imagery tasks	49
4.2.2	Brain signal acquisition and equipment	51
4.2.3	Processing strategy to detect the specific motor imagery neural correlates	52
4.3	Findings	53
4.3.1	Behavioral data	53
4.3.2	Filtering measures comparison	54
4.3.3	Detecting the neural correlates of specific motor imagery tasks	54
4.3.4	Classification of specific motor imagery tasks	58
4.4	Discussion and conclusions	61
4.4.1	Comparison with previous studies	62
4.3.5	Open questions and conclusions	63
4.5	Limitations and future developments	64
4.6	Lessons learned	67
	Investigating the neural correlates of cognitive processing levels	69
5.1	Introduction and state of the art	69
5.2	Methods	71

5.2.1	Experimental design to elicit different cognitive processing levels	71
5.2.2	Neural signals acquisition	75
5.2.3	Analysis strategy to detect the neural correlates of different levels of cognitive processing	75
5.3	Findings	83
5.3.1	Investigating behavioral measures	83
5.3.2	Extracting the neural correlates for each cognitive processing level	84
5.3.3	Discrimination of different cognitive processing levels	95
5.4	Discussion and conclusions	103
5.4.1	Comparisons with other studies	103
5.4.2	Open questions and conclusions	104
5.5	Limitations and future directions	110
5.6	Lessons learned	112
Conclusions		113
6.1	General conclusions	113
6.2	Future perspectives towards BCI applications	115
Appendix		117
A.1	Additional theoretical foundations – Chapter 2	117
A.1.1	Statistical analysis	117
A.1.2	Measures of signal quality	120
A.1.3	Signal processing	120
A.1.4	Regularize a discriminant analysis classifier (Matlab implementation)	125
A.2	Supplementary material for the motor imagery study – Chapter 4	127
A.2.1	EEG activity detection	127
A.2.2	EMG activity detection	127
A.3	Supplementary material for the Depth of cognitive processing study – Chapter 5	131
A.3.1	Artifactual components	131
A.3.2	ERP analysis	133
A.3.3	ERD/ERS analysis	137
A.3.4	Discriminatory analysis	138
Bibliography		143

Contents

List of figures

Fig. 4.1 Timing for one experimental trial with right movement execution in this example.	50
Fig. 4.2 Power Spectral Density Estimate using the Welch method for the original signal and filtered signal	54
Fig. 4.3 Mean amplitude evolution over time for the arm lifting motor imagery task as response to Vis.-So. St	55
Fig. 4.4 Event related spectral perturbation for the right/left imagery trigger pull (Vo. St.) at electrodes C3 and C4	56
Fig. 4.5 Inter-Trial Coherence (ITC) for the left imagery trigger pull (Vo. St.) at electrode C3	56
Fig. 4.6 ERSP at the C3 and C4 electrodes for the right index finger motor imagery button press task (Vo. St.)	57
Fig. 4.7 Temporal evolution of the ERP components (average data) considering the right imagery button press with Vo. St.	57
Fig. 4.8 ICA components contributions to ERP and ERSP, considering the left imagery button press task (Vis. St.)	58
Fig. 4.9 The performance of the classifier given by the error rate, in relation to the number of features	59
Fig. 4.10 Average performance for multi-class and binary classification for the motor imagery tasks: button press (Vis. St.), button press (Vis.-So. St.), arm lifting (Vis.-So. St.), button press (Vo. St.), trigger pull (Vo. St.)	60
Fig. 4.11 Normalized confusion matrices over entire dataset for the multi-class motor imagery classification considering the no, left and right movements	61
Fig. 5.1 Representation of the stimuli categories (animals, fruits, mobility) and examples of their elements	72
Fig. 5.2 Experimental protocol examples for the cognitive processes investigated: memory, language and visual imagination	73
Fig. 5.3 Example of elements size indicators	74
Fig. 5.4 Timing of the trial: 500 ms for the fixation cross, 1250 ms for the stimulation period and 750 ms for the relaxation period	75
Fig. 5.5 Data analysis diagram	81
Fig. 5.6 Behavioral assesment – objective and subjective indicators for the Memory (M), Language (L) and Visual Imagination condition (VI): answers ratio and difficulty scores	83
Fig. 5.7 Grand average ERPs. (a) Memory condition; b) Language; c) Visual imagination	84
Fig. 5.8 Grand-average discriminations of the Event-Related Potentials given by signed r^2 considering Memory, Language and Visual imagination conditions	85
Fig. 5.9 Grand average power spectrum at location Pz, for the Deep (DT), shallow (ST) and no-processing (NT) levels in case of memory, language and visual imagination conditions.	86
Fig. 5.10 Grand-average spectrum discriminability given by signed r^2 at location Pz	87

List of figures

Fig. 5.11 Grand-average ERDs for the alpha band (8-14 Hz) considering all conditions (M, L, VI) and processing levels (NT, ST, DT) at electrode Pz	88
Fig. 5.12 Grand-average ERDs for the beta band (16-20Hz) at electrode Pz for all conditions (M, L, VI) and processing levels (NT, ST, DT)	89
Fig. 5.13 Binary CSP analysis (patterns) for the alpha frequency band (8-14Hz) after SSD considering NT-ST, NT-DT, ST-DT class pairs for each condition (Participant P4)	90
Fig. 5.14 Binary CSP with SSD patterns for the beta frequency band (16-20 Hz) considering all conditions and classification pairs (Participant P4)	91
Fig. 5.15 Multi-case CSP with SSD patterns of the 8-14Hz frequency band considering the NT, ST and DT classes for each condition (Participant P4)	92
Fig. 5.16 Multi-case CSP with SSD patterns of the 16-20Hz frequency band considering the NT, ST and DT classes for each condition (Participant P4)	93
Fig. 5.17 Spectrogram (ERSP and ITC) for the memory process at channels F7, P3, and Pz, considering the NT, ST and DT levels	94
Fig. 5.18 Spectrogram (ERSP and ITC) for the language process at channels F7 and Pz, considering the NT, ST and DT levels	94
Fig. 5.19 Spectrogram (ERSP and ITC) for the visual imagination process at channels Cz, P3, PO7, PO8 and Pz, considering the NT, ST and DT levels	95
Fig. 5.20 Pairwise classification mean performance over all trials for all cognitive processes (memory, language, visual imagination, light grey) given by the area under the ROC curve (AUC) based on ERP-mCSP	96
Fig. 5.21 Multi-class spatio-tempo-spectral classification performance (ERP & SSD-mCSP) for all conditions: Memory (M), Language (L) and Visual Imagination (Vi)	97
Fig. 5.22 Normalized confusion matrix for the Memory, Language and Visual Imagination condition across, showing the multi-class spatio-tempo-spectral classification performance (ERP & SSD-mCSP) between no (NT), shallow (ST) and deep processing (DT)	98
Fig. 5.23 Pair-wise spatio-temporal (ERP) classification performance between the levels of processing (NT – no-processing, ST – shallow processing, DT – deep processing)	99
Fig. 5.24 Pair-wise spatio-spectral (SSD-mCSP) classification performance between the levels of processing: NT – no-processing, ST – shallow processing, DT – deep processing	100
Fig. 5.25 The classifiers performance for the language condition considering the average AUC values	101
Fig. A.1.1 Scaling and wavelet functions for the Daubechies wavelet of order 5	123
Fig. A.2.1 Scatter plot of C3 vs C4 electrodes showing the distribution of the imagery trigger pull data (Vo. St.)	127
Fig. A.2.2 Average EMG signals over all trials for the left and right motor imagery movement (finger button press experiment with Vis. St.)	128
Fig. A.3.1 Example of artifactual components detected by ICA with MARA for participant P5 on the memory data, as compared to non-artifact neural component	132
Fig. A.3.2 Event-related potentials corresponding to the cognitive activity depicted in the temporal evolution of the EEG signal, at channel CPz	133
Fig. A.3.3 Temporal evolution of the trials and mean ERP corresponding to the memory condition, for NT, ST and DT, at channel CPz, for participant P5	134

Fig. A.3.4 Temporal and spatial distribution of the mean ERP of participant P5 for the NT, ST and DT processing levels considering the memory condition at electrode Pz	134
Fig. A.3.5 Grand average ERPs for the DT+ and DT- levels considering the memory, language and visual imagination conditions at electrode Cz	135
Fig. A.3.6 Grand average ERP considering all electrodes and all processing levels (NT, ST, DT- and DT+) for the language condition	135
Fig. A.3.7 Statistical temporal differences between classes considering signed r^2 at midline channels for the Memory, Language and Visual Imagination conditions	136
Fig. A.3.8 Grand-average ERD/ERS signed r^2 discriminability between DT and ST for the alpha (8-14 Hz) and the beta band (16-20Hz) at location Pz	137
Fig. A.3.9 Grand average ERD/ERS curves on 8-14 Hz considering all electrodes and all processing levels for the memory condition	137
Fig. A.3.10 Grand average ERD/ERS curves on 16-20Hz considering all electrodes and all processing levels for the memory condition	138
Fig. A.3.11 Scatter plot of Pz vs Cz electrodes showing the distribution of the language data considering the NT, ST and DT classes	138
Fig. A.3.12 The normal distribution graphs of the binary ERP-mCSP classifier performance	140
Fig. A.3.13 The variance distribution graph of the residuals between Language and Visual imagination for the NT-ST group, considering binary ERP-mCSP classifier performance.	140
Fig. A.3.14 The variance distribution graph of the residuals between Language and Visual imagination, considering the multi-class ERP-mCSP classifier performance	142

List of figures

List of tables

Tab. 2.1 Notation	21
Tab. 4.1 Motor imagery experiment types	51
Tab. 4.2 Signal quality estimation after filtering, based on the PSNR measure	54
Tab. 4.3 Features type, original features quantity and reduced features quantity	59
Tab. 5.1 Comparison over all conditions between the multi-class by JAD classification performance and the multi-class by OVR approach	102
Tab. A.3.1 ERP and multi band CSP with SSD binary classification performance with shrink rLDA over all conditions and participants	139
Tab. A.3.2 ERP-mCSP with SSD (JAD and OVR) multi-class classification performances with shrink rLDA over all conditions and participants	141

List of tables

List of abbreviations

Acc – Accuracy
AEP – Auditory Evoked Potentials
ANOVA – Analysis of Variance
AUC – Area under the ROC curve
BCI, BCIs – Brain-Computer Interface(s)
CDF – Cumulative Distribution Function
CMI – Continuous Motor Imagery
CSF, CSFs – Common Spatial Filter(s)
CSP, CSPs – Common Spatial Pattern(s)
CV – Cross-Validation
CWT – Continuous Wavelet Transform
DT – Deep Targets
DFT – Discrete Fourier Transform
DMI – Discrete Motor Imagery
EEG – Electroencephalography
EMG – Electromyography
EOG – Electrooculography
ERD, ERDs – Event Related Desynchronization(s)
RP, ERPs – Event Related Potential(s)
ERS, ERSs – Event Related Synchronization(s)
ERSP, ERPs – Event Related Spectral Perturbation(s)
FFDiag – Fast Frobenius Diagonalization
FFT – Fast Fourier Transform
FIR – Finite Impulse Response
fMRI – functional Magnetic Resonance Imaging
GA – Grand Average
GEVD – Generalized Eigenvalue Decomposition
HP – high-pass filter

List of abbreviations

IC, ICs – Independent Component(s)
ICA – Independent Component Analysis
IIR – Infinite Impulse Response
IN – multi-class problem divided to several binary decisions
ISI – Inter-Stimuli Interval
ITC – Inter-Trial Coherence
ITPC – Inter-Trial Phase Coherence
ITFE – Information Theoretic Feature Extraction
JAD – Joint Approximate Diagonalization
KS – Kolmogorov–Smirnov (test)
L – Language
LCD – Liquid-crystal-display
LDA – Linear Discriminant Analysis
LPN – Low Pass Notch filter
LR – Logistic Regression
M – Memory
MARA – Multiple Artifact Rejection Algorithm
mCSP – Multi-Band Common Spatial Pattern
MEG – MagnetoEncephaloGraphy
MI – Motor Imagery
MI – Mutual Information
MLR – Multinomial Logistic Regression
MSE – Mean Squared Error
NIRS – Near InfraRed Spectroscopy
NT – Non-Targets
OVR – One Versus Rest
PDF – Probability Density Function
PNG – Portable Network Graphics
PSD – Power Spectral Density
PSNR – Peak-Signal to Noise Ratio
QDA – Quadratic Discriminant Analysis
rLDA – Regularized Linear Discriminant Analysis

ROC – Receiver Operating Characteristic
RR – Ridge Regression
RMS – Root Mean Square
SDE – Spectral Density Estimation
SEM – Standard Error of the Mean
SI – International System of Units
SIM – Simultaneous Diagonalization
SMR – Sensorimotor Rhythms
SNR – Signal to Noise Ratio
SOA – Stimulus Onset Asynchrony
SPoC – Source Power Co-Modulation
SSD – Spatio-Spectral Decomposition
ST – Shallow Targets
STFT – Short-Time Fourier Transform
SVG – Scalable Vector Graphics
SVM – Support Vector Machine
TFR – Time-Frequency Representation
UTP – Unshielded Twisted Pair (cable)
USB – Universal Serial Bus
VEP – Visually Evoked Potentials
VI – Visual Imagination
WAV – Waveform Audio File Format
WT – Wavelet Transform

List of abbreviations

Chapter 1

Introduction

Non-invasive Brain-Computer Interfaces (BCIs) research benefits from a significant evolution in the last decades considering neural activity analysis. The vast majority of endeavors focus on identifying ascertained voluntary control commands, imposing strict activities to the user side, in order to control distinct devices or for communication purposes. On the other hand, the user state estimation from the ongoing brain signals was not granted much attention (Blankertz et al., [2010b,c](#); [2016](#)).

1.1 The field of doctoral study

The enhancement of technology gives us today more and more opportunities and utility to ease and improve our daily activities. In this regard, neurotechnology helps further by enhancing the connectivity between humans and technology. It involves the participation of different fields such as Computer Science, Neuroscience or Psychology, and many others. The applicability ranges from augmenting human capability by controlling external devices such as computer applications, wheelchair or any other electronic devices only with the brain signals; towards the restoration of a lost motor or cognitive function by neuro-rehabilitation or even to the replacement of a lost body part (mainly limbs), with the aid of neural prosthesis.

The first advancements in this field began to develop with the discovery of human brain signals, in 1924, by the German researcher and psychiatrist, Hans Berger (Berger, [1929](#)). After this time, multiple researches have been conducted and the field of Neurotechnology evolved for nearly half a century but only in the last twenty years has reached maturity. In general, it includes technologies that are designed to improve, repair and replace brain functions and allow researchers and clinicians to visualize the brain.

The neurotechnology research enhances step by step, mostly related to BCI systems (Dornhege et al., [2007](#); Wolpaw and Wolpaw, [2012](#)), providing enhancements of signal

acquisition (Nicolas-Alonso and Gomez-Gil, 2012), signal processing and machine learning techniques (Müller and Blankertz, 2006; Blankertz et al., 2008b;). Furthermore, new applications are developed each day and new discoveries are being reported (Wolpaw, 2007).

Although the main focus of the BCI research initially targeted clinical applications relating to lost brain functions replacement, involving for example, patients who lost their motor control, where the BCI provides a different option to communication (Birbaumer et al., 1999; Birbaumer and Cohen, 2007; Millán et al., 2010) or an alternative to movement execution by means of BCI prosthesis (Birbaumer, 2006; Mcfarland and Wolpaw, 2010), various experimental paradigms that targets alleviating daily activities have been also proposed. They are aiming to enhance the human capabilities of a normal and healthy individuals, for example as in the case of controlling a computer application with own brain signals (Bayliss and Ballard, 2000; Müller et al., 2008; Blankertz et al., 2010c; Zander and Kothe, 2011) and replacing the conventional peripheral input (e.g. mouse, keyboard) or in industrial settings by targeting workload reduction based on mental state detection (Venthur et al., 2010).

While primary research involves the use of motor imagery related brain activity for BCI control, activity which is hard to be controlled by the users, mostly because not everyone is capable of producing this specific type of brain signals (Guger et al., 2003; Blankertz et al., 2010a; Vidaurre et al., 2011b), a new interest arises in the BCI community which focuses on the user mental state detection, bringing many advantages and decision possibilities for the BCI system (Blankertz et al., 2016).

Another aspect that need to be taken into consideration when developing a BCI system, considers the analysis and decisions involved, that have to be properly checked in order to refer to the corresponding neural activity related to the BCI task and not to the non-cortical origins of activity such as eye, muscle movements and other types of noise activity. In this regard, a BCI system depends on advanced methods of signal processing and classification. By means of these machine learning techniques, the corresponding neural activity of interest is detected among a mixture of neural signals, problem always referred to as the ‘cocktail party’ problem (for example, detecting and understanding one person's speech from the amount of discussions, music and background noise which happen on a party environment).

Despite significant advances in BCI research, there is still no standard valid BCI system available on the market, but hopefully this is about to change in the decades to come, thanks to the involvement of the BCI research groups through the entire globe (Birbaumer and Cohen, 2007; Dornhege et al., 2007; Kohlmorgen et al., 2007; Wolpaw, 2007; Daly and Wolpaw, 2008; Galán et al., 2008; Mak and Wolpaw, 2009; Müller et al., 2008; Ariely and Berns, 2010; Haufe et al., 2011; Zander and Kothe, 2011; Wolpaw and Wolpaw, 2012; Collinger et al., 2013; Hwang et al., 2013; Borghini et al., 2014; Aricò et al., 2016a,b; Blankertz et al., 2016; Schultze-Kraft et al., 2016a,b; Naumann et al., 2017), and recently also the involvement of the industry sector (Neuralink Corp - <https://www.neuralink.com/>; Facebook, Inc. - Constine, (2017, Apr 19) and many more.

1.2 Purpose of the thesis

The most complex system in the universe - the brain, has fascinated researchers for a long time. The ability to control external devices only with the power of the mind is still a futuristic approach, yet many studies have proven this possibility and the most important aspect is that it is beneficial for the persons with disabilities, providing them the means for communication in case of loss of the ability to speech, the ability to control a wheelchair or any other external device, which offers them a significant aid in their daily activities.

This type of interaction, namely Human-Computer Interaction, could benefit if the attention of the scientific research and development will be more focused on the user itself.

The majority of present and past research is focusing on methods to achieve best performance in a HCI system by proposing tasks that can trigger a more powerful effect in the human brain, without driving the attention to the user needs and desires. In order to improve this interaction, the attention should be focused on the user, by searching for tasks related to user preferences, or by focusing on user decisions or on the current user state in order to control the respective application or an external device.

The key concept behind this enhanced BCI mental state detection technology, is the type of interaction, also called a symbiotic interaction, which derives from the well-known natural symbiotic relationship, where two different and conflicting organisms coexist together in a mutual relation. Each organism benefits from the other and the antagonistic condition that was present before is automatically cancelled out. As an example, the sea anemone and the clownfish coexist in a mutual intrinsic relationship by protecting from predators and nourishing each other. The anemone does not strike the clownfish with her stingers and the clownfish does not eat the nutrient tentacles of the anemone. Rather, the clownfish feeds itself with the leftovers from other fishes, cleans the anemone, and chases away anemone's fish predators, like the butterfly fish. In return, the anemone protects the clownfish with its toxic tentacles and receives nutrients in form of waste from the clownfish. In a similar way, a HCI should integrate this symbiotic relationship by carefully inspecting the desires and needs of the user and fulfilling them, in accordance.

Therefore, the long-term goal of this research is to infer implicit user variables in real-time and silently adapt the user interface within the Brain-Computer Interface or the Human-Computer Interaction systems. Firstly, user's interest and needs have to be taken into consideration; secondly, the current user's state and finally the interface has to be adapted accordingly.

The present thesis aims to establish experimental designs that focus on the user, in order to create an improved and more natural human-computer interaction. In this case, the potential applications of a system that allows real-time estimation of the current user state include enhanced human-computer interaction, such as information seeking application or operator assistance systems in industrial workplaces (as discussed in Venthur et al., 2010). Furthermore, we envision the use in any control BCI application involving healthy participants.

In view of the target scenario, the goal is to:

- Develop optimized stimulus and tasks to create user-friendly BCI paradigms;

- Relate to the user state – the BCI should focus on the user;
- Create interpretable BCI systems;
- Improve the signal processing methods to detect more accurately the processes originating from brain sources or to assist for a better reconstruction of the signals;
- Investigate deeper the information contained in the brain in order to increase our understanding of human brain processes;
- Take a step further towards a user-friendly BCI interaction system that can be further used for control or communication for healthy people or people with disabilities

Aiming reducing the complexity and interaction at the user side and also creating interpretable BCIs, the complexity has to be switched to the BCI system. Therefore, the objectives of this thesis relate to the development of improved BCI paradigms, tasks and scenarios that ease the interaction and to the development of advanced and improved methodological approaches for extracting and interpreting user neural activity from the electrophysiological signals recorded with EEG, while discarding the non-related cortical activity. As a reference, the neurophysiological interpretations will be compared to behavioral measurements.

The majority of current BCI systems recognize different mental states in rapport with preliminary training data. In this matter of classification, the general issue of BCIs is that they act as an unseen process, being hard for a researcher to verify and interpret what the system actually learns from the data. Recently, various researchers expressed the necessity to develop appropriate signal processing and classification techniques for BCI in order to gain knowledge and insights into the dynamics of the brain and the corresponding mental states (McFarland et al., 2006; Kübler and Müller, 2007; Müller et al., 2008; Blankertz et al., 2010; Blankertz et al., 2011; Vidaurre et al., 2015). This approach should become a necessity for a researcher or developer to correct a BCI to detect the corresponding neural processes.

Moreover, if the BCI will facilitate an asynchronous interaction (Mason and Birch, 2000), such as when the user can communicate with the interface at their own will or if the BCI will silently analyze user mental state, the human-computer interaction will become more natural, efficient and user-friendly.

Another issue that needs to be addressed relates to the number of classes generally used in BCI systems. Most BCI systems are constrained only to two classes, being hard for a user to control a BCI system especially when more degrees of freedom are requested. Therefore, a solution is clearly needed in this aspect by designing algorithms and BCIs that can efficiently identify a greather number of mental states and tasks (Dornhege et al., 2004a; Kronegg et al., 2007; Venthur et al., 2010).

1.3 Outline of the thesis

User mental state Brain-Computer Interfaces will break the ice of the interaction between a user or patient and an external machine, if the signals are silently recorded and the decisions are performed in real-time. Aiming this long-time purpose, we investigate via special designed BCI scenarios, the user-related tasks that could bring us closer towards this goal. In this topic, the thesis evaluates the signal processing and machine learning methods that could help investigating and discriminating the brain activity, while meantime leaning towards the

development of an interpretable BCI. The brain activity investigated in this research work, was non-invasive recordings via Electroencephalography.

Firstly, the neurophysiological concepts and basic principles that underlies a BCI system along with the key components of which it is composed, are primarily described in Chapter 2. Further, the signals types investigated in this thesis that can be used to drive a BCI system are detailed, namely the Event-Related Potentials (ERPs) and the oscillatory modulations given by cognitive activity and Sensorimotor Rhythms (SMRs). In addition, a standard notation for the mathematical concepts used in this thesis is detailed.

Further, a brief overview of the existing analysis methods within the scientific research is presented in Chapter 3, including the current BCI designs and applications (Chapter 3.5). The description of the existing signal processing and machine learning approaches, focusing more on those that are further used in this thesis, spans from the brain activity measurement (3.1), preprocessing of the EEG signals along with filtering and artifactual removal techniques (3.2), and continuing with the feature extraction and selection mechanisms (3.3) towards the classification (3.4).

To accomplish the purpose of this thesis described earlier, first user specific tasks were investigated in the well-used type of BCI, namely motor-imagery based BCI. The idea, described in more detail in Chapter 4, analyzes attractive and efficient tasks for the user in order to attract user's interest and therefore improve the interaction with the BCI. The brain responses elicited by the internal motor imagery event that generates changes in the oscillatory activity, namely sensori-motor rhythms (SMRs), are inspected considering the temporal, spatial and spectral information of the EEG activity. Specifically, the attenuations or increases in the alpha rhythm are closer investigated by the Event-Related (De)Synchronization (ERD/ERS) phenomena. The respective modulations changes can be easily observed by the event related brain dynamic responses in the power spectrum, therefore by studying the time-frequency representation given by the Event Related Spectral Perturbations measure (ERSP). Aiming a faster user reaction and a stronger brain response, two different types of stimuli, visual and auditory are evaluated in the experimental study. After appropriate preprocessing that clears the signal from unwanted artifacts and increases the signal to noise ratio of the signal, an enhanced classifier based on multi-modal features provides a very good discrimination of the motor imagery mental tasks. Further, the section 4.5 describes possible future developments and optimizations of this study. The work comprised in this chapter was performed at the Department of Applied Electronics and Information Engineering, Faculty of Electronics, Telecommunications and Information Technology, University Politehnica of Bucharest and was published in four scientific papers [5, 10, 11, 12] and a scientific report [13].

Furthermore, an innovative interface is investigated in Chapter 5, where the user mental state is taken into consideration, based on the depth of cognitive processing the external visual information. Implicit information about the current user's cognitive state, among different levels of cognitive state, could be later used in a Human Computer Interaction, for example in an information seeking application or an industrial operator monitoring setting, with the appropriate machine learning adaptations for online detection. The concept of differentiating between different levels of cognition, could be used to automatically adapt the application interface by reducing or increasing the amount of

information presented or the activities requested to be performed by the user. This will be a benefit for the interaction, making it more efficient, by firstly replacing or supplementing explicit input with the BCI's automatic brain state detection, and secondly by automatically adapting the interface according to user's needs and current state, without the need for additional setup. The feasibility of using BCI in such new contexts is investigated in this work by inducing different levels of cognitive processing, in order to: identify and study the corresponding neural correlates, investigate the related EEG features, and to adapt the necessary signal processing and machine learning techniques. The amount of cognitive processing is triggered by task instructions in a specific designed experimental paradigm, analogous to an odd-ball paradigm with visual stimulus presentation, in which the user takes decisions in accordance to the corresponding type of cognitive process (memory, language and visual imagination) and the level of processing (no-processing, shallow and deep processing). The brain responses investigated here are the Event Related Potentials (ERPs) and modulations of the oscillatory activity (Event Related De/Synchronizations), generated by the cognitive events. Considering data analysis, advanced signal processing methods were applied in order to reject non-neural components and keep only the brain activity related to the investigated user's state. Different spatial filtering methods are applied in order to reduce the effect of volume conduction and enhanced feature extraction methods are applied to detect the optimal neural components. Classification is applied in multi-modal form, by integrating the information extracted from the spatial, temporal and oscillatory domains. In addition, different classification techniques are evaluated for obtaining best performances. Firstly, binary classification is evaluated, and then multi-class discrimination is implemented to bring the classifier closer to a real application implementation, where the classifier has to automatically detect between different user states. Next, future developments are pointed out considering the signal processing and machine learning techniques that could be further improved and the directions that need to be taken further when switching towards real life applications. The research was performed at the Neurotechnology Group, Institute of Software Engineering and Theoretical Computer Science, Faculty of Electrical Engineering and Computer Science, Technical University of Berlin and a big part of the work presented in this chapter has been published in six scientific papers [2, 3, 6, 7, 8, 9], one in progress [1], and one database [4].

In the last chapter (Chapter 6), overall conclusions (section 6.1) are drawn for the work in this thesis, referring to the findings and the impact of this work on the scientific research. Further, the future developments and directions that could be taken starting from this research are discussed in section 6.2.

Supplementary figures and description considering single participant graphs, various electrodes and additional analysis are comprised in the [Appendix](#) section.

1.4 Scientific contribution

The thesis aims to contribute to the field of EEG analysis by considering advanced and adapted signal processing techniques for the corresponding paradigms and by proposing and evaluating specific BCI tasks and mechanisms towards mental state detection that could improve the brain-computer interaction. After careful evaluation of the existing methods and

practices and their short-comings, specific analysis scenarios were selected and proposed that better detect the corresponding neural activity and user related effective tasks are proposed that could drive more interest from the user's side and could ease the communication with a future BCI application. The proposed approaches are evaluated in two experimental studies with laboratory settings (Chapter 4 and 5) and published in [5, 10, 11, 12, 13] and [1, 2, 3, 4, 6, 7, 8, 9], respectively.

The core parts of this research are described hereunder:

- Concerning the user interest and his tendency of losing enthusiasm and becoming tired and disinterested in interacting with the BCI, specific user tasks are firstly investigated in a motor-imagery experiment that triggers interest, attention and forces continuous interaction with the corresponding BCI.
- The second main interest refers specifically to the user's side, by making use of the user's cognitive state, expressed in the corresponding neural correlates, triggered when cognitively processing the visual external information.
- The novel approaches are investigated in experimental studies on healthy participants, in order to test the applicability of these concepts to a more realistic scenario.
- For investigating and extracting the corresponding neural correlates that relate to the corresponding activities, powerful signal processing and machine learning approaches have been integrated for the neurophysiological and behavioral data analysis. Different data techniques were evaluated and combined to obtain highest performances, considering multi-variate analysis, by combining the spatial, temporal, and spectral domains.

The experimental studies focus on EEG, which is widely used due to its dramatically lower costs and better portability. The analysis discussed in this thesis refers primarily to EEG analysis, although the methods may be adapted and tested to other types of acquisition, but this aspect was not evaluated in this research.

The present thesis advances the BCI and Neurotechnology research field in various directions. While on one side, recent state-of-the-art machine learning techniques can expand the usability of BCI technology, on the other side, the research should focus towards BCI users. Therefore, two innovative BCI paradigms are proposed in order to inspect the neural correlates of specific user tasks or cognitive user's state. It was shown that such paradigms could improve the communication with BCI and could make it more practical and accessible compared to earlier approaches. The state-of-the-art analysis techniques were tested for the corresponding investigated neural correlates and combined when revealed shortcomings. Thus, novel approaches are constructed to improve the classification performance of brain data, particularly for EEG.

Shortly, the personal scientific contributions of me, the researcher in question, can be described by the following main developments:

- Two studies were carried out, both focusing on the user's side for the benefit of human-computer interaction. The studies show the applicability of the user related concepts to future Brain-Computer Interface applications (Section 4.1 and 5.1)
- The experimental designs and stimuli presentations necessary for the two studies were carefully planned and developed (based on the supervisors' proposals and under their guidance) in order to elicit the desired brain responses. Therefore, the graphical design of

the stimuli, the software setup for the presentations and the hardware setup for brain signal acquisition were entirely performed by the researcher in question (sections 4.2.1 and 5.2.1)

- For the first time, the context of levels of cognitive processing encountered in neuroscience and psychology are evaluated in a BCI scenario, in terms of a possible human-computer interaction application (Chapter 5)
- Specific schemes and investigations for effective analysis of the neural activity are proposed, tested and entirely developed for both studies (Section 4.2.3 and 5.2.3)
- Specific artifact removal techniques have been investigated and applied in order to reduce head, muscle and eye movements that are also present in more realistic scenarios (Section 4.2.3.1, 5.2.3.2, 5.2.3.3)
- Discriminative measures are applied in order to investigate into more detail the neural activity (Section 4.3.2, 5.2.3.4). Single-participant representations, as well as grand-average representations are carefully investigated (Section 4.3.3, 5.3.2, Appendix A.2.1, A.3.2, A.3.3). Special attention is given to the trial-by-trial and among participants' variability of the EEG data. Different feature extraction methods are implemented and optimized in order to extract the most relevant brain activity (Section 5.2.3.4).
- In addition, careful verification of the signals has been performed in order to assure that the extracted components which will be given to the classifier, highly reflect the cortical activity and not some artifacts (Section 4.3.3.3, 5.2.2.3)
- An improved ensemble classification approach is developed based on multi-modal analysis, taken advantage by the temporal, spatial and the spectral characteristics of EEG, in order to overcome the limitation of single domain analysis (Section 4.2.3.2 and 5.2.3.5)
- Appropriate multi-classification approach is implemented, necessary for further online classification (Section 4.3.4 and 5.3.3.2)
- New neurophysiological findings related to different levels of cognitive processing are detected and investigated (Section 5.3.2)
- Corresponding Matlab code was developed for each processing scenario and some adaptations to existing methods in order fit the corresponding processing pipelines are public available in the BBCI Toolbox (for example: [ssd-bank](#)) (Section A.1.4, A.2.2)
- Scientific research papers and articles that describe the corresponding approaches are published, further described in Section 1.5 [1 - 13].

1.5 List of contributions

The contributions performed on the research described in this thesis have been published in peer-reviewed journals and conference proceedings. The following section 1.5.1 list those articles, in chronological ordered starting with the most recent ones. The next Section 1.5.2, refers to all the additional peer-reviewed publications which were not included in the thesis, that I have authored or co-authored since the beginning of the PhD (October 2013) in the domain of signal processing. Specifically, they include additional research on Electroencephalography (EEG), Electrocardiography (ECG), Electrooculography (EOG), Electrohyserography (EHG), and image processing. A complete list of all the publications

including other domains such as synthetic biology or the manuscripts published before the beginning of the PhD (October 2013), can be found online on the following scientific research websites: [Researchgate](#) or [Academia](#). Considering the number of citations, the h-index was specified by [Google Scholar](#) on the 1th of March 2018 for all publications that have been published for at least 6 months and it represents the level h-3 which indicates that at least 3 manuscripts have been cited at least 3 times.

1.5.1 Main contributions list

Publications in preparation or under review

1. **I. E. Nicolae**, B. Blankertz, *Offline cognitive mental state detection: multi-classification approach for the use in BCI applications*, 2018, IEEE indexed, ISI. (in preparation)

Published publications

Journal papers

2. **I. E. Nicolae**, G. M. Neagu (Ungureanu), R. Strungaru, L. Acqualagna, B. Blankertz (2018) *Enhanced classification for the depth of cognitive processing depicted in neural signals*, **UPB Scientific Bulletin**, Series C, Vol. 80, Iss. 1, pp. 135-146, ISSN 2286-3540, WOS:000428622400012, ISI indexed.

3. **I-E Nicolae**, Acqualagna L and Blankertz B. (2017a). “Assessing the Depth of Cognitive Processing as the Basis for Potential User-State Adaptation”. *Front. Neurosci.* 11:548, 2017a, WOS:000412319200001, doi: <https://doi.org/10.3389/fnins.2017.00548>, ISI indexed.

Conference papers, book chapters, abstracts and data sets

4. **Nicolae I-E**, Acqualagna L and Blankertz B. (2017b). Assessing the Depth of Cognitive Processing as the Basis for Potential User-State Adaptation – Data set. Depositonce, Technische Universität Berlin. doi: <https://doi.org/10.14279/depositonce-6173>

5. **I. E. Nicolae**, M. M. C. Ştefan, B. Hurezeanu, D. D. Taralunga, R. Strungaru, T. M. Vasile, O. A. Bajenaru, G. M. Ungureanu (2016b) *Investigating Motor Imagery Tasks by Their Neural Effects – a Case Study*, **Proc. of the 38th Annual Intern. Conf. of the IEEE Engineering in Medicine and Biology Society**, 17-20 August, Orlando, Florida, pp. 5861-5864, WOS: 000399823506052, doi: <https://doi.org/10.1109/EMBC.2016.7592061>, IEEE Xplore indexed, ISI.

6. **I. E. Nicolae**, L. Acqualagna, B. Blankertz (2016a) *Investigating Depth of Cognitive Processing in the Brain Dynamics of Oscillations*, **Proc. of the Sixth Intern. Brain-Computer Interface Meeting**, May 30 - June 3, California, USA, p. 186, Published by Verlag der TU Graz, Graz University of Technology, ISBN 978-3-85125-467-9, doi: <https://doi.org/10.3217/978-3-85125-467-9-186>.

7. **I. E. Nicolae**, L. Acqualagna, and B. Blankertz (2015b) *Tapping Neural Correlates of the Depth of Cognitive processing for Improving Human Computer Interaction*, 4th Intern. Workshop on Symbiotic Interaction, Lecture Notes in Computer Science, **Springer**, Vol. 9359, pp. 126-131, Print ISBN 978-3-319-24916-2, doi: https://doi.org/10.1007/978-3-319-24917-9_13, BDI (Scopus) indexed.

8. **I. E. Nicolae**, M. Ungureanu, L. Acqualagna, R. Strungaru and B. Blankertz (2015c) *Spectral Perturbations reflect the Depth of Cognitive Processing for Brain-Computer Interface Systems*, **Proc. of the 5-th Intern. Conf. on e-Health and Bioengineering**, 19-21 November 2015, Iasi, Romania, pp. 1-4, WOS:000380397900126, doi: <https://doi.org/10.1109/EHB.2015.7391473>, IEEE Xplore indexed, ISI.
9. **I. E. Nicolae**, L. Acqualagna, and B. Blankertz (2015a) *Neural Indicators of the Depth of Cognitive Processing for User-Adaptive Neurotechnological Applications*, **Proc. Of the 37th Annual International Conference of the IEEE Engineering in Medicine and Biology Society**, August, Milano, Italy, pp. 1484-1487, WOS:000371717201190, doi: <https://doi.org/10.1109/EMBC.2015.7318651>, IEEE Xplore indexed, ISI.
10. **I.E. Nicolae**, G. M. Ungureanu and R. Strungaru (2014a) *ICA Analysis of Real and Motor Imagery Movements in a Brain-Computer Interface Stimuli System*, **Proc. of the xth Intern. Conf. of Electronics, Computers and Artificial Intelligence**, 23-25 oct, 2014, Vol. 6 – No. 6, 4 pages, WOS:000380489500047, doi: <https://doi.org/10.1109/ECAI.2014.7090216>, IEEE Xplore indexed, ISI.
11. **I.E. Nicolae**, G. M. Ungureanu, and R. Strungaru (2014b) *Motor Imagery Mental Tasks in Brain-Computer Interface Applications*, **Workshop on Smart Healthcare and Healing Environments**, AMI'14, 11-13 nov, Eindhoven, The Netherlands, 12 pages.
12. **I. E. Nicolae** (2013) *An improved stimuli system for brain-computer interface applications*, **Proc. of the 5th Intern. Conf. on Electronics, Computers and Artificial Intelligence**, 27 -29 June, Pitesti, Romania, Vol. 3, pp. 49 – 53, WOS:000343672500006, doi: <https://doi.org/10.1109/ECAI.2013.6636157> (Extended version published also in: *Intern. Journ. of Monitoring and Surveillance Technologies Research, Special Issue on Biomedical Monitoring Technologies*, 1(4), 1-8, Oct-Dec 2013, INSPEC:14907402, doi: <https://doi.org/10.4018/ijmstr.2013100101>), IEEE Xplore indexed, ISI.
13. **I. E. Nicolae**, “*Extracting signal from noise in Brain-Machine Interfaces*”, PhD Scientific Report, June 2014.

1.5.2 Additional contributions list

Publications in preparation or under review

14. **I. E. Nicolae**, M. Wenzel, B. Blankertz, et al., *Studying the neural correlates of high versus low focus user states for BCI applications*, 2018, IEEE indexed, ISI. (in preparation)

Published publications

Conference papers

15. R. Al. Cernat, A. M. Speriatu, D. D. Taralunga, B. E. Hurezeanu, **I. E. Nicolae**, R. Strungaru, G. M. Ungureanu (2017) *Stress Influence on Drivers Identified by Monitoring Galvanic Skin Resistance and Heart Rate Variability*, **Proc. of the 6th IEEE Intern. Conf. on E-Health and Bioengineering (EHB)**, June 22-24, Sinaia, Romania, pp. 261-264, INSPEC:17066086, doi: <https://doi.org/10.1109/EHB.2017.7995411>, IEEE Xplore, BDI (Scopus) indexed.

16. B. Hurezeanu, G. M. Ungureanu, D. Taralunga, **I. E. Nicolae**, W. Wolf, R. Strungaru (2016) *Real-time eye movement detection analysis: Comparison between image based algorithm and electrooculogram*, **Proc. of the 9th Intern. Conf. and Exposition on Electrical and Power Engineering (EPE)**, 20 oct 2016, Iasi, Romania, pp. 372-375, WOS:000390706300075, doi: <https://doi.org/10.1109/ICEPE.2016.7781365>, IEEE Xplore indexed, ISI.
17. D. D. Taralunga, G.M. Ungureanu, B. Hurezeanu, **I. E. Nicolae**, R. Strungaru (2016) *Non-contact heart rate estimation from a video sequence*, **Proc. of the 9th Intern. Conf. and Exposition on Electrical and Power Engineering (EPE)**, 20 oct, Iasi, Romania, pp. 348 – 351, WOS:000390706300070, doi: <https://doi.org/10.1109/ICEPE.2016.7781360>, IEEE Xplore indexed, ISI.
18. M. M. C. Ștefan, **I. E. Nicolae**, R. Strungaru, M. G. Ungureanu, M. Vasile; O. A. Băjenaru (2016) *A study on the efficient tracking of ERD based on the adaptive identification of the subject's reactive band*, **Proc. of the 9th Intern. Conf. and Exposition on Electrical and Power Engineering (EPE)**, 20 oct, Iasi, Romania, pp. 337 – 343, WOS:000390706300068, doi: <https://doi.org/10.1109/ICEPE.2016.7781358>, IEEE Xplore indexed, ISI.
19. M.M.C. Ștefan, **I. E. Nicolae**, R. Strungaru, T. M. Vasile, O. A. Băjenaru, G. M. Ungureanu (2016) *Adaptive Modelling of EEG Signals to Produce Accurate Time-Frequency Decompositions for Use in BCI*, **Proc. of the 8th Intern. Conf. of Electronics, Computers and Artificial Intelligence**, 30 June - 02 July, Ploiesti, Romania, 4 pages, vol 8, no. 2/2016, WOS:000402541200024, doi: <https://doi.org/10.1109/ECAI.2016.7861088>, IEEE Xplore indexed, ISI.
20. V. Straticiuc, **I. E. Nicolae**, R. Strungaru, T. M. Vasile, O. A. Băjenaru, G. M. Ungureanu (2016) *A preliminary study on the effects of music on human brainwaves*, **Proc. of the 8th Intern. Conf. of Electronics, Computers and Artificial Intelligence**, 30 June - 02 July, Ploiesti, Romania, 4 pages, vol 8, no. 2/2016, WOS:000402541200132, INSPEC: 16692514, doi: <https://doi.org/10.1109/ECAI.2016.7861196>, IEEE Xplore indexed, ISI indexed.
21. B. Hurezeanu, **I. E. Nicolae**, D. Taralunga, Rodica Strungaru, W. Wolf, I. Gussi, M. Ungureanu (2015) *Fetal monitoring: identifying the relevant biosignals interdependencies*, **Proc. of the 5-th Intern. Conf. on e-Health and Bioengineering**, 19-21 November, Iasi, Romania, 4 pages, WOS:000380397900098, doi: <https://doi.org/10.1109/EHB.2015.7391445>, ISI indexed.
22. R. Cojocaru, D. Popescu, **I. E. Nicolae** (2013) *Texture Classification based on Succolarity*, **Proc. of the 21st Telecommunications forum**, 26-28 November, Belgrade, Serbia, section 5, pp. 498-501, WOS:000349857500113, doi: <https://doi.org/10.1109/TELFOR.2013.6716275>, IEEE Xplore indexed, ISI.

Chapter 2

Fundamentals of neurophysiology

Foreword

When we think about the brain, we can think of the giant universe spread across billions of light-years, with constellations of information having billions of connections between them. Only size makes a difference with billions of light-years for the cosmos and only micrometers for the brain. Glancing through the microscope, the brain contains around 100 billion neurons with 100 trillion connections (synapses), which mean 700 billion times less than the estimated number of stars in the observable universe (The Australian National University, 2003). However, this tiny brain can „*contemplate even the vastness of interstellar space*” (Ramachandran, 2009). Now, as you probably visualized, we can barely scratch the surface of this huge amount of information. As telescopes investigate planets activity, so Electroencephalography (EEG) records the brain signals, getting closer to touch the unseen. By this means, you will feel like you almost hold petabytes of brain information with thousands of thoughts, memories and knowledge in the palm of your hand.

Now, how we can grab information from the brain, it will be described in this chapter. Starting from the theoretical aspects of the human brain and continuing with the measures and methods that help decipher and better understand the neural information.

2.1 Neurophysiological background

The neural activity generates changes of electrical fields (Buzsáki et al., 2012). The ionic current produced by the neurons within the brain that generates action potentials (postsynaptic potentials – PSPs, given by depolarizations of the neuronal membrane), propagates through the cortex until it reaches the surface of the scalp (Niedermeyer and Silva, 2005; Buzsáki et al., 2012). For this reason, the electrical activity arrived at the surface of the scalp will be weaker than the original activity, from millivolts (mV) down to microvolts (μV). The original electrical potentials from one source of the brain propagate differently within the

cortex due to different electrical conductivity of the brain and therefore, on the surface of the scalp the electrical potential could arrive at a distance from the original region of the brain. The effect is known as volume conduction (Rutkove, 2007).

2.2 Electroencephalography

The first attempt to record electrophysiological brain signals dating from 1875 belongs to Richard Caton who presented his findings about the electrical phenomena of cerebral hemispheres of animals (Caton, 1875). Later on, in 1924, after extensive experiments, Hans Berger (Berger, 1929), a German neurologist, discovered that besides animals, also the activity of the human brain can be gripped by placing an electrode on the surface of the scalp. Next, the signal is amplified and visualized as changes in voltage over time. This technique of brain signals recording (Niedermeyer and Silva, 2005) will be later called Electroencephalography (EEG). Over the decades, EEG proved to be very useful in scientific research and clinical applications, mainly due to its high temporal resolutions, not found by the other hemodynamic measures, such as: positron emission tomography - PET, functional near-infrared spectroscopy - fNIRS, functional magnetic resonance imaging - fMRI. Moreover, it is widely used due to its affordability, portability and non-invasive characteristics. Although, there is one drawback of EEG, namely low spatial resolution. To put it simply, EEG is similar to a symphony, composed by a complex mixture of sounds that change in time and space with varying phase, pitch, tone, volume (amplitude) and frequency. In EEG, there is mixture of brain signals coming from different sources of neural activity due to the volume conduction effect described earlier. However, this effect can be reduced to some extent based on advanced source separation techniques.

Apart from EEG, other brain measurement techniques may be used (briefly described later in Section 3.1), which do not constitute the purpose of this work.

2.3 Brain-Computer Interface

After almost 50 years from the discovering of human brain signals, a new type of interface dramatically developed, namely Brain-Computer Interface (BCI). The system unifies the interaction between a brain and a computer by measuring the neural activity and translating it into an action that could also be extended to an external device (Dornhege et al., 2007). The first records of the name BCI state from Jacques Vidal (Vidal, 1973) who first relied on visual evoked potentials to perform screen cursor control. As Wolpaw and Wolpaw (2012) describes, a BCI system aims to replace, restore, enhance, supplement or improve human sensory-motor or cognitive brain functions.

A real-time BCI system requires two main phases to be fulfilled: an offline training used to calibrate the system and an online phase where the BCI detects and interprets user's brain activity or user's current mental state and translates it in real-time into a command for a computer, which can be transferred to an external device. The online part of the BCI refers to a closed-loop process and is usually composed of six steps: neural activity recording, pre-processing, feature selection and extraction, classification, translation into a command and

providing feedback for the user (Mason and Birch, 2003). When the feedback is not provided, the BCI is considered an open-loop BCI. These steps are described in the following:

1) Neural activity recording: consists in recording the brain signals of a user reflecting the brain activity, by using different types of sensors or measurement techniques (Wolpaw et al., 2006). This signals acquisition step usually involves also a preliminary on-line cleaning of the signals to reduce the noise caused by electronic devices, cables, etc. In this research, we focus on the scalp electrical potential measurement technology, namely EEG.

2) Pre-processing: performs detailed cleaning and denoising of the brain data in order to improve the quality of the signals and increase the detection of relevant information incorporated in the signals (Bashashati et al., 2007).

3) Feature extraction and selection: detects the most relevant characteristics of the signals, named features that best describe the brain activity (Bashashati et al., 2007).

4) Classification: discriminates the group of features detected from the brain data by assigned them to a corresponding class, referring to the type of brain activity or mental state identified (Lotte et al., 2007a).

5) Translation into a command to a computer application or to an external device: After the specific mental state is identified, a command is associated to this brain activity or corresponding mental state that controls the given application. An example is an avatar in a virtual reality environment (Lécuyer et al., 2008), or a robot or prosthesis (Kübler et al., 2006).

6) Feedback/Neurofeedback/Biofeedback: the last and the most important step provides information (visual, auditory, tactile) to the user about the BCI decision (it can also be the actual output of the BCI application, e.g. the movement of a robotic arm). This closes the BCI loop and is useful for the user in order to control his brain activity and therefore the BCI (Wolpaw et al., 2002). The feedback is mostly given to the user in form of visual representations of the changes in the ongoing EEG (Neuper and Pfurtscheller, 2009), although it can comprise also auditory (Hinterberger et al., 2004; Hwang et al., 2009) or tactile (Chatterjee et al., 2007) feedback.

In this research, we refer to the offline part of the BCI, with the purpose of preliminary detecting the corresponding brain features for silently investigating the user's brain activity and mental state in a future feasible BCI application. This offline BCI consist in the following steps: measurement, pre-processing, feature extraction and classification, with no real-time feedback given to the user. Here, also a behavioral measure feedback is showed to the user, related to its performance, but is important not to confuse with the actual feedback of a BCI system as described above. Further in this thesis, when we refer to the BCI system, we mean the off-line BCI system.

2.4 Neurophysiological signals that enable BCI control

Different types of brain potentials have been studied by the BCI community and most of them are relatively easy to be identified by a computer, but a bit more cumbersome for a user to control his own potentials. Based on the type of the signal generator, two types of signals are investigated (Wolpaw et al., 2002; Curran and Stokes, 2003): Event-Related Potentials

(ERPs) as well as spontaneous brain signals. The Event-Related Potentials are unconsciously generated by the human brain when the user perceives an external stimulus, as a result of a sensory, cognitive or motor event. Here, we remind the commonly used potential, usually known as the P300 potential. The main advantage of ERPs, in comparison to spontaneous signals, is that they do not require user training, because they are naturally produced by the brain as response to a stimulus. This advantage makes it easier for the user to control a BCI system (Wolpaw et al., 2002; Curran and Stokes, 2003). Nevertheless, they require constant focus and repetitious stimuli, which can become exhausting and uncomfortable for the user.

On the opposite, spontaneous signals are voluntarily generated by the user, following an internal motor or cognitive process, without being triggered by an external stimulation. The widely used spontaneous signals are the sensorimotor rhythms (SMRs) and less used are the non-motor cognitive signals. Compared to the ERPs, the sensorimotor rhythms can be voluntarily controlled in amplitude by the user after intensive training (Wolpaw et al., 1991; Wolpaw and McFarland, 2004; Vaughan et al., 2006; Wolpaw et al., 2007). The spontaneous signals are observed as modulations of spontaneous brain rhythms, namely Event-Related Desynchronisation (ERD) in case of a decrease in spectral power of the corresponding frequency band (Pfurtscheller and Aranibar, 1977) or an Event-Related Synchronization (ERS) when an increase in power appears (Pfurtscheller and Silva, 1999; Lemm et al., 2009).

2.4.1 Event Related Potentials

As Donchin et al. (1973) describe, Event-Related Potentials, ERP (Vaughan, 1969) are spikes in the signal voltage caused by the occurrence of rare events. Triggered by an exogenous event, the ERPs signify the presence of cognitive processing the external information through our sensory systems, e.g. visual, auditory, tactile, etc. In the present time, they are usually investigated as a response to a sequence of stimuli divided in target and non-target, provided by a BCI, called an 'odd-ball' paradigm. This potential consists of a succession of positive deviations in amplitude (e.g. P100, P300) and negative deflections (e.g. N200, N400). In the case of a rare event (target), it will elicit a higher P300 potential (Handy, 2004; Luck, 2005) about 300 - 500 ms after the stimulus onset, compared to a lower peak in case of a frequent, un-attentive stimulus (non-target). The ERP shows huge variability between participants probably due to different folding of the cortex which influences the propagation of the signal through the scalp (Luck, 2005). Variability is observed also regarding one participant on different moments of the days, different participant state, or the level of tiredness (Polich and Kok, 1995). However, the analysis of ERP has different advantages: first compared to the behavioral measures it provides more information about the variations of a specific cognitive process, rather than the reaction time and accuracy, for example. Secondly, it provides a continuous measure of processing between a stimulus and a response, making it possible to determine which stage of processing is enlightened by a specific stimulus. Another advantage of ERP is that it can provide an on-line measure of the processing of stimuli (covert attention), even when there is no behavioral response. In addition, the user requires no training in order to use the system, because the effect is automatically generated in response to an external stimulus. A disadvantage is that it requires continuous attention and multiple repetitions of the stimuli.

Cognitive activity

The ERPs earlier described, also represent different components which are associated with several cognitive processes (Regan, 1989; Luck, 2014). In addition, the cognitive activities investigated in the oddball paradigms modify the amplitude and latency of the ERPs in relation to task difficulty (Ullsperger et al., 1987; Polich, 2007, Kim et al., 2008). The effect is observed by an increased P300 and longer latencies, influenced by complex processes and stronger attentional demand. This cognitive potential is characterized by a peak around 300 - 500 ms after the stimuli in the centro-parietal cortex (Polich, 2007).

2.4.2 Oscillatory brain activity

Complementary to the observed effects of the neural activity over time, oscillations in the spectrum given by the Event Related De/Synchronization (ERD/ERS) of the Sensorimotor Rhythm (SMR) provides also necessary information of the neural processes. These electrophysiological rhythmic activities (Buzsáki, 2006), are generated by the firing of groups of neurons in different frequency bands. A change in the mental state of a healthy hominid generates a change in a frequency band over the entire brain. The corresponding frequency ranges vary between participants, due to different anatomical structure. Additionally, the location of the brain activity sources provides information about the corresponding brain function involved. In continuation, a description of the frequency bands (Groppe, 2013) along with the functional behavior that is associated to, are detailed hereunder.

Brain waves

- **Delta rhythm (δ , 0.5-4 Hz of 20 to 100 μ V):** The functional description of the delta frequency band relates to a sleep stage, mostly for adults. (Armitage, 1995)
- **Theta rhythm (θ , 4-8 Hz with >10 μ V):** Theta signifies drowsiness or arousal in teenagers and adults. In addition, changes in amplitude related to cognition and workload have also been observed (Gundel and Wilson, 1992; Gevins et al., 1997; Klimesch, 1999).
- **Alpha rhythm (α , 8-13 Hz of 20-100 μ V):** The alpha frequency band is mostly generated by visual activity originating from the occipital cortex (e.g. Vanni et al., 1997). Alpha waves could refer also to attention in the frontal area (Niedermeyer, 1997) or a relaxed state (Hughes and Crunelli, 2005). Opening and closing the eyelids also activates or suppress in the generation of the alpha frequency band. In general, experimenters take advantage of this effect in order to verify the quality of the EEG signals.
- **Mu rhythm (μ , 8-10 Hz):** A special case of oscillations which involves the same frequency range as the alpha band (Feshchenko, 2001) is represented by the mu rhythm, except that is generated by a motor or sensorimotor event which modulates the rhythm amplitude (Wolpaw and Wolpaw, 2012). More exactly suppression in the μ -rhythm (8-10Hz) is encountered in the motor cortex regions and is generated by motor or motor-imagery activities (Pfurtscheller and Silva, 1999).
- **Beta rhythm (β , 13-30 Hz with 5-30 μ V):** A higher frequency, named as beta band, relates to more active processes like motor activity (Pfurtscheller and Silva, 1999; Pfurtscheller and Neuper, 2001), concentration, actively thinking (mental effort) (Lachaux et al., 2005).

- **Gamma rhythm (γ , 30-100 Hz, $<10\mu\text{V}$):** The gamma frequency band appears in higher cognitive functions, e.g. in learning processes, or motor functions (Niedermeyer and Silva, 2005).

While most of the EEG research focuses on the spectrum analysis from 1Hz to 50Hz (Cohen, 2014), the EEG comprises prominent relevant information also in higher frequency ranges (Curio, 1999; Gotz et al., 2009; Scheer et al., 2009; Nikulin et al., 2011; Telenczuk et al., 2011; Buzsáki and Silva, 2012; Fedele, 2014).

❖ *Note:* The frequency bands intervals are not fixed and might slightly exceed the specified ranges, especially between individuals (see below).

Variability between and within participants

When aiming the development of a general functional online BCI system, it is important to consider the variability between and within participants. Variability in the temporal, spatial or spectral distribution of the neural information, termed non-stationarity is often encountered in the EEG. Changes can be generated by a series of factors such as: anatomical and biological (e.g. age, neurological diseases, brain structure), non-related neural signals (e.g. muscle artifacts or other physiological artifacts, mental state, mood, tiredness), technical (e.g. electrode conductivity or electrode position changes), task-related changes (e.g. different task involvement, memory performance), and so on. Explicitly, changes in amplitude, spectral power and spatial patterns between participants arise, that can drastically influence the performance of a SMR BCI system (Blankertz et al., 2010a). Moreover, the variability is encountered as well within participants (Dähne et al., 2011). Several studies show these variabilities while trying to solve this issue (Lemm et al., 2005; Blankertz et al., 2008a; Sannelli et al., 2011; Vidaurre et al., 2011a,c; Christensen et al., 2012; Samek et al., 2012, 2014; Dähne et al., 2014a,b). Two approaches are identified that aim a robust BCI: (1) detecting signal representations invariant to nonstationarities (Bünau et al., 2009) or (2) detecting and alleviating them (Kohlmorgen and Lemm, 2001; Schlögl et al., 2010; Vidaurre and Blankertz, 2010; Blythe et al., 2011; Vidaurre et al., 2011b;). The second suitable solution invariant to fluctuations that can increase the performance of a BCI system (Blankertz et al., 2002, 2008a; Müller et al., 2004, 2008) considers a participant-dependent classifier based on a preliminary BCI training, in which the individual frequency ranges are detected and the corresponding features are set to the classifier.

2.4.2.1 Modulations of spontaneous brain rhythms

The decrease in amplitude of spontaneous brain rhythms is well-known as Event Related-Desynchronization (ERD) (Pfurtscheller and Aranibar, 1977). In general, the ERD is followed by an increase in amplitude called Event-Related Synchronization (ERS) (Pfurtscheller and Silva, 1999; Lemm et al., 2009). These modulations of the amplitude (hull curves) can span in the alpha and beta bands (Pfurtscheller and Klimesch, 1992; Nikulin et al., 2007) and can be time-locked to the external stimuli or triggered by internal functions (such as voluntary movements, or cognitive processes). Uncommon activities tend to produce higher modulations than frequent activities, effect known and demonstrated in many studies within the scientific community. For example, left hand movement execution for right-handed individuals, produces increased activity as compared to the usual right-hand

execution (Klöppel et al., 2007), or the observation of uncommon activities for infancy produces stronger motor activation, represented by a pronounced desynchronization in the mu frequency band, as compared to ordinary actions. (Stapel, 2010).

As applications, these EEG band power modulations are used to control electronic devices, either via motor imagery or cognitive processes (Section 3.5).

Non-motor cognitive activity

Besides the use of motor imagery tasks, cognitive processes are also used to drive a BCI system, for instance: memory, language, visual imagination, mental numerical calculations, mental imagery rotation of geometric shapes, etc. (Keirn and Aunon, 1990; Anderson et al., 1998; Millán et al., 2000; Curran and Stokes, 2003). Each of them generate specific variations in the respective band power and cortical regions, such as: enhanced ERD in the alpha band for memory processes (Mecklinger et al., 1992; Klimesch et al., 1994; Klimesch, 1999; Stipacek, 2003; Jensen and Colgin., 2007; Pesonen et al., 2007), or in the processing and production of words (Klimesch et al., 1997).

On the other side, the cognitive perception of external stimuli produces in particularly a short ERS followed by a sustained ERD arising in the α band (Klimesch et al., 1992; Klimesch et al., 1993), after the P300 potential (Yordanova et al., 2001). The alpha band is known to desynchronize concurrently with mental activity, namely to decrease in amplitude with cognitive difficulty, visible in the centro-parietal area (Gevins et al., 1997; Venthur et al., 2010). For more complex cognitive activities, oscillations in the beta band are also encountered (Pesonen et al., 2007; Okazaki et al., 2008; Sheth et al., 2009), as desynchronizations for complex reasoning (Basile et al., 2013), decision making (Nakata et al., 2013) or in the transition between different cognitive states (Sheth et al., 2009). On the opposite, synchronizations are observed in the theta band according to task difficulty (Klimesch, 1999), for example in higher memory load (Gundel and Wilson, 1992; Gevins et al., 1997) or the encoding of new information.

In addition, cognitive phenomena, have been also shown to correlate with band-power modulations (Varela et al., 2001; Buzsáki and Draguhn, 2004), for example: perceptual encoding and attentional process (Sergeant et al., 1987; Başar et al., 1997; Debener et al., 2003; Klimesch, 2003; Schack et al., 2005; Bauer et al., 2006; Polich, 2007), vigilance in operational environments (Gevins et al., 1995; Holm et al., 2009), perception (Plourde et al., 1991; Makeig and Jung, 1996; Thut et al., 2006) and decision making (Haegens et al., 2011a,b).

2.4.2.2 *Sensorimotor rhythms*

When motor or motor-imagery actions are intended and executed, for example the real or imagined movement of a body part (Pfurtscheller and Neuper, 2001; Pfurtscheller et al., 2006), the motor cortex is characterized by an oscillatory idle rhythm, called sensorimotor rhythm (SMR), in the μ (\approx 8-13 Hz) and β (\approx 13-30 Hz) frequency bands. Specifically, the movements of the upper body parts, such as hands, generate a decrease in power called Event Related Desynchronisation (ERD), in the μ rhythm, over the contra-lateral motor cortex area (the opposite hemisphere) and an increase in band power called Event Related Synchronisation (ERS) in the ipsi-lateral hemisphere (Pfurtscheller and Silva, 1999). For the

inferior body parts, for example feet, the oscillations are observed in the central motor cortex. As for the beta frequency (Pfurtscheller et al., 2005), the SMR's amplitude shows a de/synchronization during motor execution which precedes a short synchronization that appears after the movement, termed as the 'beta rebound'.

Comparing the type of movement: real or imagery execution, many similarities are encountered starting with resembling ERDs (McFarland et al., 2000; Neuper et al., 2005) in the contralateral site according to the respective movement (left or right) and ERSs present in the ipsilateral cortex modulated in the mu and beta bands.

The drawback of using SMRs for driving a BCI is that the control commands options are constrained by the number of body parts. Moreover, a subject which has lost a body part in an accident, might find it hard to imagine its movement, firstly due to the emotional connection and secondly, due to the lack of movement execution for a long period of time. Also, when aiming prosthesis control, the system's decision is constrained by the amount of body parts, which will involve a higher complexity to the user side when performing multiple body parts movements. Generally, in a BCI based on sensorimotor rhythms, the user has to modify the amplitude of his SMRs for the purpose of controlling the BCI system (Wolpaw and McFarland, 2004; Wolpaw et al., 2007). Based on this fact, not all users are capable of controlling the system (Guger et al., 2003; Blankertz et al., 2010a; Vidaurre and Blankertz, 2010). Another disadvantageous factor is that it requires prolonged training time for the user to learn to control the BCI system. However, using advanced signal processing and machine learning algorithms, the amount of training is increasingly reduced to zero (Blankertz et al., 2006a).

These ERD/ERS modulations can be investigated by analyzing the Event-Related Spectral Perturbations, ERSP (Section 3.3.4.1) or the envelope of the signal filtered in the mu band (Appendix A.1.3.2).

2.5 Notation

In this section, the concepts and notations used in this thesis are further detailed. Firstly, as stated before in Section 2.3, a ‘BCI system’ term will refer to the off-line part of a BCI system, if not specified otherwise. Another notion used here refers to a mental state, meaning at the same time a brain activity pattern.

The detailed notation used in this manuscript for equations is presented in the table below (Tab. 2.1). Matrices are denoted with boldface uppercase letters, vectors as boldface lowercase letters, scalar values as Roman uppercase letters or small Greek letters and indices of vector or matrices as lowercase italic letters.

Tab. 2.1 Notation

Symbol	Description
\mathbf{X}	a matrix (bold capital letters), where \mathbf{I} denote the identity matrix, \mathbf{W} the filtering matrix, \mathbf{A} the patterns matrix
\mathbf{y}	a vector (bold small letters), where $\mathbf{y}(t)$ denotes a temporal signal, where specifically, \mathbf{b} is the bias and \mathbf{z} is the z-score
A or α	scalar values (capital Roman or small Greek letters), where $\alpha, \beta, \gamma, \theta, \delta$ denote the EEG frequency bands
i, j, k	indices of vectors or matrices (small italic Roman letters), except p which is the probability value (p -value)
E or N_e	number of epochs (trials) of a recorded signal
N or N_c	number of EEG recorded channels
T or T_e	number of samples of a measurement signal
$\ \cdot\ , \cdot $	absolute value of a scalar, vector or a complex norm
$\ \cdot\ _2$	Euclidean distance/ L^2 -norm of a vector or a complex number
$\ \cdot\ _2^2$	Squared Euclidian distance
$\ \cdot\ _F$	Frobenius-norm
$\langle \cdot \rangle$	inner product of two vectors
$(\cdot)^T$	matrix or vector transpose
$(\cdot)^{-1}$	Inverse of a matrix
$(\cdot)^+$	(Moore Penrose) Pseudoinverse of a matrix
$(\cdot)^*$	complex conjugate of a matrix or vector
Σ	Covariance matrix, where e.g. $\sum_{k=1}^N$ is used to represent the sum of elements from $k=1, \dots, N$
$\hat{\Sigma}$	estimated covariance matrix
$\hat{P}(f)$	estimated power of the signal
\mathcal{F}	Fourier transform
\mathcal{H}	Entropy
\mathbb{E}	Expected value
$\psi(t)$	Mother wavelet
$\varphi(t)$	Father wavelet
MI	Mutual Information

Chapter II. Fundamentals of neurophysiology

f	frequency
μ	mean
σ	standard deviation
σ^2	variance
$x \sim \mathcal{N}(\mu, \sigma^2)$	multivariate random variable x , Gaussian (normal) distributed with mean μ and variance σ^2
λ	eigenvalue, where λ_1 express the largest eigenvalue
sgn	sign function
$sgn r^2$	signed and squared point biserial correlation coefficient (<i>signed r^2</i>)
log, ln	Natural logarithm
log_{10}	decimal logarithm
$tanh$	hyperbolic tangent
Hz	Hertz – frequency unit in the International System of Units (SI)
dB	Decibels – power measurement unit in the International System of Units (SI)
cm	Centimeter – distance unit in the International System of Units (SI)
ms	Milliseconds – time unit in the International System of Units (SI)

Chapter 3

Signal processing and machine learning methods in BCI research

For more than a century, scientists investigated brain activity to gain insights into perceptual, cognitive and motor functions.

This chapter provides a short description of the existing methods and techniques used to accomplish each step of a BCI system, followed by an overview of the main BCI designs and applications. The methods described here refer to off-line BCIs, but might be applicable also for on-line systems, with corresponding adaptations. In more detail, the chapter will cover the steps composing a BCI, starting with the measurement types of brain activity in Section 3.1, followed by the pre-processing approaches in Section 3.2 and the feature extraction methods in Section 3.3, and continuing with the classification techniques described in Section 3.4, comprising linear methods overall. The last Section 3.5 presents the most used BCI applications developed, by emphasizing the possible applications related to the experimental designs proposed in this thesis.

3.1 Brain activity measurement

Various techniques have been developed that measure the brain activity (de Moor, 2003; Wolpaw et al., 2006). Some of them require invasive methods, such as: ElectroCorticoGraphy (ECoG) (Leuthardt et al., 2006) where a grid of electrodes is placed over the dura-mater, or implanted electrodes placed under the skull (Lebedev and Nicolelis, 2006). As non-invasive techniques, we remind the hemodynamic measurements, such as MagnetoEncephaloGraphy (MEG) (Mellinger et al., 2007; Besserve et al., 2008), functional Magnetic Resonance Imaging (fMRI) (Weiskopf et al., 2004) or Near InfraRed Spectroscopy (NIRS) (Coyle et al., 2007). Also non-invasive is ElectroEncephaloGraphy (EEG) (Wolpaw et al., 2006), one of the most widely used acquisition technique due to its relatively accessible

price, non-invasiveness, portability and a very good temporal resolution. In this thesis research, we have restricted to EEG as an acquisition measure for the BCI designs, due to its numerous advantages.

3.2 Preprocessing

3.2.1 Preliminary filtering and preprocessing

After the brain signals have been recorded using the measurement types (in this case, EEG), the raw signals must be cleaned and denoised of unwanted perturbations. A preliminary filtering of the raw signals is performed online by the hardware while the signals are recorded. Usually, it consists of a combination of a high-pass filter (HP) of 0.1 Hz or less, a low pass filter (LP) and a notch filter (LPN), in order to remove the interfering frequencies, the DC ripple and cables movement artifacts.

Next, offline filtering of the input signals is needed to have a clearer signal and to increase the Signal to Noise Ratio (SNR). This is done by temporal (Section 3.2.1.1) or spatial filters (Section 3.2.2.2) or even the combination of both if the signal is noisy or contains movement artifacts, for example. Regarding temporal filters, the idea is to perform band pass filtering or a succession of high-pass and low-pass filtering in the frequency band of interest, which are further described below.

3.2.1.1 Temporal filters

The temporal filters can remove various undesired effects such as slow variations in the EEG signal, caused by electrodes polarization or by power-line interference (50 Hz in Europe). In addition, they can reduce the influence of noisy frequencies that are outside the frequency range of the brain activity investigated. Generally, the filtering can be achieved using Discrete Fourier Transform (DFT) (Appendix A.1.3.1.1), Finite Impulse Response (FIR) (Appendix A.1.3.1.3), Infinite Impulse Response (IIR) filters (Appendix A.1.3.1.4) and many others. Because the filters may introduce artifacts and phase shifts, strongly altering the neural signals, it is advisable to apply the filters in reverse in the offline scenario in order to produce a zero-phase shift. This tactic is not applicable in the online case, therefore causal filters must be considered (which do not depend on the future inputs) (Lemm et al., 2004).

3.2.1.2 Downsampling

In general, the EEG signals are recorded with a sampling rate of 1000 Hz for a higher signal quality (given 500Hz maximum bandwidth according to the Nyquist frequency) and are amplified with an order of 20000 from tiny nanovolts to microvolts, so they can be easily investigated in the signal analysis on a bigger level. Further, because the human brain generates frequencies between 0 and 100Hz (Niedermeyer and Silva, 2005), the signals are usually downsampled to 100 Hz or more after filtering, in order to reduce the amount of data and to keep only the necessary information.

3.2.1.3 Re-referencing

In order to reduce the perturbations in amplitude produced by the hardware (different voltages and electrode conductivities between single channels recordings), the signals can be

offline re-referenced to a baseline (Delorme et al., 2011). While for the EEG data acquisition, the voltage is already measured with respect to a reference electrode, electrode measurement which can be compromised due to artifacts or electrical activity, affecting therefore all the other electrodes, re-referencing aims at mitigating this effect (Lepage et al., 2014). For example, referencing to electrodes placed on the mastoids (linked mastoids), to forehead reference electrodes, or even to an average channels signal (common average referencing) can be performed. This can be achieved by linearly transforming the recorded data, namely by subtracting the reference signal from each EEG channel (Tallon-Baudry et al., 2001; Luck, 2014; Staudigl et al., 2015).

3.2.1.4 *Baseline correction*

After the segmentation of the data (where each trial includes a pre-stimulus and a post-stimulus interval), baseline correction (Kronegg et al., 2007) regarding the selected pre-stimulus interval is performed for each trial. The reference interval, also referred to as baseline interval, is usually selected from -200ms or -100ms to zero (where zero is the stimulus onset). An averaged amplitude or spectrum value computed on this reference interval is subtracted from each trial, aiming at diminishing the non-stationarity effects of EEG signals and reducing the background noise activity.

3.2.2 **Enhanced artifact removal**

As mentioned in the aim of the thesis, one important aspect that need be considered when developing a BCI system is related to its decision basis, such that it is not based on signals that do not constitute cortical origins. In addition, the aim is to create a system that does not act as a ‘black box’ system, but rather an interpretable BCI where researchers can visualize and interpret what the BCI has detected. Pursuing this goal, the EEG artifact correction (Section 3.2.2.1) and source localization functions (Section 3.2.2.2) are mandatory in a BCI system.

Different types of artifacts (Fisch and Spehlmann, 1999) affect the task-related or mental state brain activity, produced by electronic devices, e.g. loose electrodes, outer electric fields, drifts; or by biopotentials generated by participant’s body such as: eye movements, muscular activity, etc. Corresponding filters are applied depending on the type of noise: FIR/IIR filters for removing electronic noise, and adaptive filters for rejecting the body biopotential artifacts. These artifacts are characterized by high amplitudes and frequency ($\gg 100\mu\text{V}$ and > 60 Hz) exceeding the neural activity ($\leq 50\mu\text{V}$ in adults; < 80 Hz) (Muthukumaraswamy, 2013).

The data is primarily filtered in the necessary frequency range (below 50Hz) corresponding to the investigated neural activity (Section 3.2.1.1). Therefore, a part of the frequencies related to body biopotential artifacts (e.g. muscular activity) are automatically excluded.

Further, a rough pre-cleaning of the data is necessary to be performed in order to improve the quality of the data by rejecting the noisy epochs (trials) and channels while keeping only the good quality ones. Secondly, projection methods are implemented to extract the relevant brain activity and discard the noisy activity (artifactual sources). A further description of these last two approaches follows below.

3.2.2.1 Rejection Methods

The rejection methods (Muthukumaraswamy, 2013; Samek, et al., 2017) detect the artifactual epochs or channels and remove them based on thresholds given by specific characteristics of the artifacts, such as high amplitude or high frequency, depending on the type of artifacts; or by analyzing the deviation of the signals. Two approaches used in this thesis are further described below, namely max-min and variance criterions.

1. Max-min criterion

The max-min method rejects artifactual epochs by analyzing the features of an epoch and detecting if it's out of a normal threshold range. For example, for strong eye movement artifacts which are considered greater than 100 μV in amplitude, it is implied a threshold of maximal difference of about 150 μV between the maximum and the minimum amplitude values for one epoch, searched within the electrodes providing information over vertical (AF3, AF4, Fp1, Fp2 and EOG channels) and horizontal eye movements (F9 and F10). If the maximal difference of the epoch in at least one channel exceeds the threshold, then the epoch is discarded from analysis.

2. Variance criterion

In addition to the frequency filtering described in Section 3.2.1.1, which removes a portion of the artifacts with higher frequencies ($> 50\text{Hz}$), a further check over the signals has to be performed for the artifacts (e.g. jaw clenching in the 20-40 Hz range (Khoshnam et al., 2017) which are interleaved with the neural related frequency. The solution involves a variance check over the broad band-power 5-40 Hz. The epochs are rejected when are characterized by excessive variance in more than 20% of the channels. In addition, channels dropping to zero (loose electrodes) represented by variance lower than $0.5\mu\text{V}^2$ in more than 10% of the trials were also removed.

3.2.2.2 Projection Methods – spatial filters

In contrast to the rejection approach, projection methods do not remove artifactual epochs, but the artifactual sources based on decomposition. This provides a spatial filtering of the data, resulting in a cleaner EEG most likely composed by neural sources.

The recording of the electrical brain activity is strongly influenced by the eyes and muscles movements (Fatourechhi et al., 2007), especially that these artifacts have higher amplitude and cover up the neural activity. Moreover, it is mandatory to neglect the background brain activity that is not related to the neural activity of interest, procedure that is not covered by the rejection methods. Removing the undesired noise, increases the signal to noise ratio of the signals and reduces the effect of volume conduction. This is performed by temporal, spatial (Parra et al., 2005) or spectral filters (McFarland et al., 1997; Ramoser et al., 2000; Lemm et al., 2005; Dornhege et al., 2006; Tomioka et al., 2006), such as Independent Component Analysis (Makeig et al., 1996; Makeig et al., 2000a; Naeem et al., 2006; Kachenoura et al., 2008), blind source separation (Ziehe and Müller, 1998), Common Spatial Patterns (Ramoser et al., 2000; Dornhege et al., 2004a; Blankertz et al., 2008a,c; Grosse-Wentrup and Bus, 2008), Spatio-Spectral Decomposition (Nikulin, et al., 2011), etc. Moreover, the spatial filtering (CSP) contributes to the enhancement of the BCI performance

(Dornhege et al., 2004b; Blankertz et al., 2006c). Altogether, the application of spatial filters is highly recommended for EEG analysis.

1. Independent component analysis (ICA) – Infomax

A well-used method that separates the signal into artifactual components and neuronal activity assuming independently generated sources is Independent component analysis (ICA) (Makeig et al., 1996; Hyvärinen et al., 2004). By separating the mixed signal into additive subcomponents, it attempts therefore to solve the ‘cocktail party’ problem. The basic assumption that the analysis is based on, considers non-Gaussian subcomponents and statistically independent sources¹. ICA considers two choices for independence (Haykin, 2009): minimizing Mutual Information (*MI*) (e.g. Infomax algorithm - Bell and Sejnowski, 1995; Amari et al., 1996) or maximizing non-Gaussianity (e.g. Maximum Likelihood estimation – Stone, 2004; FastICA algorithm - Hyvärinen and Oja, 2000).

In general, the ICA algorithm can be described as follows. For a random variable represented by the vector $\mathbf{x} = [\mathbf{x}_1, \dots, \mathbf{x}_m]^T$ and the source components that we want to extract as $\mathbf{s} = [\mathbf{s}_1, \dots, \mathbf{s}_n]^T$, the generative forward model is expressed by $\mathbf{x} = \mathbf{A} \cdot \mathbf{s}$, with \mathbf{A} being the mixing matrix, where the independent components are detected by maximizing the cost function. Considering zero-mean and uncorrelated Gaussian noise $\mathbf{n} \sim \mathcal{N}(0, \sigma^2)$, the related equation is: $\mathbf{x} = \mathbf{A} \mathbf{s} + \mathbf{n}$, where the component \mathbf{x} is composed of the sum of independent components $\mathbf{x} = \sum_{k=1}^n \mathbf{a}_k \mathbf{s}_k$. The original sources \mathbf{s} can be recovered by multiplying the observed signals \mathbf{x} with the inverse of the mixing matrix $\mathbf{W} = \mathbf{A}^{-1}$, also known as the unmixing matrix. Therefore, this is performed by means of a linear transformation, $\mathbf{s} = \mathbf{W}^T \mathbf{x} + \mathbf{n}$, termed the backward model.

Considering the Infomax approach (Bell and Sejnowski, 1995; Amari et al., 1996), ICA acts like a multivariate projection algorithm, extracting M multiple signals in parallel, whereas the projection (\mathbf{W}) extracts a succession of signals (\mathbf{y}) from a set of M signal mixtures. Starting from the set of signal mixtures \mathbf{x} and a mutual independent set \mathbf{g} given by Cumulative Distribution Functions (CDFs), the aim is to detect the unmixing matrix \mathbf{W} that maximizes the joint entropy of the signals $\mathbf{Y} = \mathbf{g}(\mathbf{y})$, where $\mathbf{y} = \mathbf{W}^T \cdot \mathbf{x}$. Based on the optimal unmixing matrix \mathbf{W} , the signals \mathbf{Y} are independent characterized by maximum entropy, implying independency also in the extracted signals $\mathbf{y} = \mathbf{g}^{-1}(\mathbf{Y})$. When the source Probability Density Function (PDF) of the source $p(\mathbf{s})$ fits the PDF of the extracted signal $p(\mathbf{y})$, then the maximization of the joint entropy of \mathbf{Y} also maximizes the mutual information $MI(\mathbf{x}, \mathbf{Y})$.

Now, the entropy of the signals $\mathbf{Y} = \mathbf{g}(\mathbf{y})$, can be assessed by:

¹ With respect to EEG, the signals generated from distinct sources propagate through the cortex and mix up towards the surface of the scalp where they are recorded. Therefore, the EEG signals are considered as a linear mixture of unknown sources that can be solved by blind source separation. Even though the signals correlate in their flow of information (Makeig et al., 2004), the main assumption of ICA regarding spatially independent sources holds for cortical areas while they are spatially and neuroanatomically differentiable. For this reason, components such as eye movements can be separated from neural components. Furthermore, the ICA unmixing process can be performed not only in the spatial domain (spatial ICA), but also in the temporal domain (temporal ICA, Jung et al., 2000), where the assumptions consider temporally independent underlying components with possible overlapping spatial topographies and is generally applied for discriminating ERP components.

$$\mathcal{H}(\mathbf{Y}) = \frac{1}{N} \sum_{k=1}^N \ln(p(\mathbf{Y})), \quad (3.1)$$

where \mathbf{p}_Y is given by: $p(\mathbf{Y}) = p(\mathbf{y})/|\mathbf{J}|$, with $|\mathbf{J}| = |\partial\mathbf{Y}/\partial\mathbf{y}| = \mathbf{g}'(\mathbf{y}) = p(\mathbf{s}, \mathbf{y})$ the Jacobian matrix. This gives:

$$\mathcal{H}(\mathbf{Y}) = -\frac{1}{N} \sum_{k=1}^N \ln\left(\frac{p(\mathbf{y})}{p(\mathbf{s}, \mathbf{y})}\right) \quad (3.2)$$

When PDF($p(\mathbf{s})$) fits PDF($p(\mathbf{y})$), $p(\mathbf{Y})$ has an uniform distribution and $\mathcal{H}(\mathbf{Y})$ is maximized. Then, based on:

$$p(\mathbf{y}) = p(\mathbf{x})/|\partial\mathbf{y}/\partial\mathbf{x}| = p(\mathbf{x})/|\mathbf{W}| \quad (3.3)$$

the entropy of \mathbf{Y} is:

$$\mathcal{H}(\mathbf{Y}) = -\frac{1}{N} \sum_{k=1}^N \ln\left(\frac{p(\mathbf{y})}{\mathbf{w} \cdot p(\mathbf{s}, \mathbf{y})}\right) = \frac{1}{N} \sum_{k=1}^N \ln(p(\mathbf{s}, \mathbf{y})) + \ln(|\mathbf{W}|) + \mathcal{H}(\mathbf{x}). \quad (3.4)$$

In the end, $\mathcal{H}(\mathbf{Y})$ is maximized to accomplish the independency of \mathbf{y} . $\mathcal{H}(\mathbf{x})$ can be ignored in this case, because it is not affected.

Now for M signal mixtures, $p(\mathbf{s})$ can be expressed by a logistic function, usually chosen as the hyperbolic tangent function, \tanh : $p(\mathbf{s}) = (1 - \tanh(\mathbf{s})^2)$. The entropy of \mathbf{Y} is:

$$\mathcal{H}(\mathbf{Y}) = -\frac{1}{N} \sum_{i=1}^M \sum_{k=1}^N \ln(1 - \tanh(\mathbf{w}_i^T \mathbf{x}(k))^2) + \ln(|\mathbf{W}|). \quad (3.5)$$

And the optimal unmixing \mathbf{W} can be found using the gradient descent method:

$$\mathbf{W}_{m+1} = \mathbf{W}_m + \lambda_m (\mathbf{I} - \tanh(\mathbf{Y})\mathbf{Y}^T) \mathbf{W}_m. \quad (3.6)$$

After the ICA decomposition, a decision has to be made regarding the type of component: neural or artifactual. This decision and selection of the neural components to be kept is performed in two manners: manually or automatically. The manual selection inspects the components by checking the spatial pattern and the power spectrum. While this approach requires longer time as well as scientist expertise, an automatic approach suits better in this context. One good approach in this sense is implemented by Winkler et al., (2011), algorithm named as Multiple Artifact Rejection Algorithm (MARA).

2. ICA with automatic artifactual component selection (MARA)

The Multiple Artifact Rejection Algorithm (MARA) (Winkler et al., 2011) detects the artifactual ICs (Independent Components) using a classifier based on six features. One feature represents the ICs temporal evolution and targets outliers' detection based on mean local skewness. Three features relate to the power spectrum, in which two characterize the distribution of the normal logarithmic decreased spectrum shape; and one detects the standard alpha peak specific to neural components, based on the average logarithmic power of the alpha band (8-13 Hz). Two features identify the spatial distribution of the ICs, in which one indicates the source distribution and its type based on l_2 -norm (neural source given by minimal l_2 -norm and artifactual signal by maximal l_2 -norm); and one determines localized spatial distributions which refer to loose electrodes or muscle artifacts, providing additional information of source locations as compared to the ICA method which is computed by means of the logarithmic difference between the maximum and minimum activation in a scalp map.

Overall, its application successfully cleans the EEG data of small eye movement artifacts, muscular artifacts and loose electrodes.

3. Spatio-Spectral Decomposition (SSD)

In most cases, the neural activity of interest overlaps with the background noise activity, therefore enhanced separation techniques are requested. Based on the premise that noise sources outspread over few Hz or even tens of Hz and knowing that are usually modeled as white or 1/f noise, the noise interferences can be reduced or even canceled by inhibiting the noise in the spectral neighborhood of the frequency range of interest that characterize the investigated neural process. Mathematically, the Spatio-Spectral Decomposition (SSD) method (Nikulin et al., 2011) represents a linear decomposition algorithm that maximizes the signal variance of a desired frequency band, while simultaneously diminishes it at the neighboring noise frequencies, enhancing therefore the signal-to-noise ratio. SSD enhances the extraction of oscillatory activity, especially in the alpha band characterized by the alpha peak and it has been shown that SSD performs better than the ICA method (Nikulin et al., 2011; Winkler et al., 2015). Moreover, SSD could be further used as a dimensionality reduction method. For more details on this aspect, please see the heuristic dimensionality reduction approach proposed by Haufe et al., (2014a).

Given a set of recorded signals \mathbf{X} of size $t \times c$, with t – the number of samples and c – the number of channels, the measured signal \mathbf{X} is filtered in the frequency of interest f , giving \mathbf{X}_s , and in the neighboring frequencies $f \pm \Delta f$ (with Δf in the range 1-2 Hz) which will be considered further as noise, resulting in \mathbf{X}_N . Filtering in the frequency of interest is performed by band-pass filtering of f (e.g. 8-13 Hz) and the neighboring frequencies (the left and right side bands) can be obtained by applying a band-pass filter on the entire range $[f - \Delta f; f + \Delta f]$ and subsequently applying a band-stop filter for removing the band of interest and keeping only the signals in the neighboring frequencies (e.g. 7-8 Hz and 13-14 Hz for $\Delta f = 1$ Hz). Now, denoting the covariance matrices of the filtered signal of interest and the filtered signal noise, by Σ_s and Σ_N , the aim is to find the spatial filter \mathbf{w} that maximize the signal to noise ratio (SNR) between the variance of the frequency of interest and the variance of the noise (the surrounding frequency bins). The maximization of the SNR of the projected signal can be defined by maximizing the objective function:

$$SNR(\mathbf{w}) = \max_{\mathbf{w}} \frac{\sigma^2(\mathbf{w}^T \mathbf{x}_s)}{\sigma^2(\mathbf{w}^T \mathbf{x}_N)} = \max_{\mathbf{w}} \frac{\mathbf{w}^T \Sigma_s \mathbf{w}}{\mathbf{w}^T \Sigma_N \mathbf{w}} \quad (3.7)$$

Taking the derivative \mathbf{w} and imposing the equality to zero, gives:

$$\lambda \Sigma_N \mathbf{w} = \Sigma_s \mathbf{w}, \quad (3.8)$$

which can be solved by the generalized eigenvalue decomposition (GEVD) (Francis, 1961; Kublanovskaya, 1962), where λ is the generalized eigenvalue related to the eigenvector \mathbf{w} .

For neurophysiological investigation, the spatial patterns \mathbf{A} , where each column of \mathbf{A} indicates component's contributions (strength and polarity) in the measured channels, are determined by transforming the backward models (the filters which can not be interpreted) into forward models (the patterns which are neurophysiologically interpretable) (Haufe et al., 2014b), considering the following transformation: $\mathbf{A} = \Sigma \mathbf{W} \Sigma_c^{-1} = \Sigma \mathbf{W} (\mathbf{W}^T \Sigma \mathbf{W})^{-1}$ (Haufe et al., 2014b), with Σ being the data covariance matrix, \mathbf{W} the spatial filter matrix and Σ_c the covariance matrix of the component.

4. Common Spatial Patterns (CSP)

Another powerful technique for spatial filtering is the Common Spatial Patterns (CSP) algorithm (Fukunaga, 1990; Koles, 1991; Ramoser et al., 2000; Lemm et al., 2005; Lotte et al., 2007a; Blankertz et al., 2008a,c; Tomioka and Müller, 2010; Sannelli et al., 2011; Samek et al., 2012; Vidaurre et al., 2015). The method is further used as a feature extraction method in which the common spatial filters (CSF) are applied to extract the neural sources specific for class discrimination. Shortly, CSP facilitates the discrimination of different brain states by spatial filtering, enhancing the signal of interest while suppressing the background activity.

a. Binary case

For spatial filtering and as a feature extraction process, CSP filters are frequently applied in BCI in order to reduce the effect of volume conduction and extract the corresponding oscillatory features. Moreover, CSP extracts class discrimination spatial patterns that relate to neural sources. Standardly, the CSP approach functions for binary cases, detecting the discriminative modulations between the two classes. Previously described by Fukunaga (1990), Koles (1991), Müller-Gerking et al. (1999), Ramoser et al. (2000), CSP detects the spatial projection of the band-pass filtered data that maximizes the variance for one class while minimizing the variance for the other class.

Considering Σ_1 and Σ_2 as the covariance matrices of the two classes for the band-passed filtered data, one procedure consists in simultaneously diagonalizing Σ_1 and Σ_2 such that the eigenvalues sum to 1:

$$\begin{aligned} \mathbf{W}^T \Sigma_1 \mathbf{W} &= \mathbf{D}_1, \\ \mathbf{W}^T \Sigma_2 \mathbf{W} &= \mathbf{D}_2, \text{ s.t. } \mathbf{D}_1 + \mathbf{D}_2 = \mathbf{I} \end{aligned} \quad (3.9)$$

The generalized eigenvectors \mathbf{W} are computed by:

$$\Sigma_2 \mathbf{W} = (\Sigma_1 + \Sigma_2) \mathbf{W} \mathbf{D}$$

where \mathbf{D} is the diagonal matrix containing the generalized eigenvalues of Σ_2 (with values between 0 and 1) and \mathbf{w}_j , the column vectors of \mathbf{W} represent the spatial filters.

The enhanced discriminative activity between the two classes can be obtained as a ratio between the variance of one class and the variance of the joint activity $\Sigma_1 + \Sigma_2$. Then, the objective function for detecting the \mathbf{w} filters that maximize the variance for the two conditions is described by:

$$\max_{\mathbf{w} \in \mathbb{R}^c} \frac{\mathbf{w}^T \Sigma_2 \mathbf{w}}{\mathbf{w}^T (\Sigma_1 + \Sigma_2) \mathbf{w}} \quad (3.10)$$

This can be resolved by computing the generalized eigenvalue problem:

$$\Sigma_2 \mathbf{w} = \lambda (\Sigma_1 + \Sigma_2) \mathbf{w} \quad (3.11)$$

which yields a set of eigenvectors \mathbf{w}_i and λ_i eigenvalues for $i = 1, \dots, N$ with N – the number of channels. The eigenvectors corresponding to the first largest eigenvalues maximizes the variance for one condition and minimizes the variance for the other condition and vice-versa for the last lowest eigenvalues. Hence, the spatial filters that best maximize the variance between classes correspond to opposite eigenvalues. A good practice is to choose several eigenvectors from both sides (e.g. up to 6, with three from each side - Blankertz et al., 2008c) selected based on a score related to the ratio of the medians which is more robust to outliers, as compared to the classical eigenvalue score.

After the decomposition and the corresponding common spatial filters have been extracted and the signals were projected to the CSPs, the features are composed by considering the band power of the detected sources, which is generally approximated in BCI research based on the logarithm of the spatial filtered data (log-power of the band-pass filtered signal, $\log(P(x))$) (Blankertz et al., 2008c). An important step before CSP filtering (before estimating the band-power of the projected signals) is represented by computing a linear projection of the data, as detailed in (Dähne et al., 2014b; Haufe et al., 2014b).

Another important remark must be mentioned regarding the evaluation of the CSP algorithms. Due to the fact that the CSP technique considers label information, the computation of the filters is mandatory to be performed on the training data, with appropriate application on the test data by linear derivation. Otherwise, it may lead to considerable underestimation of the generalization error (Blankertz et al., 2008c).

Further, it is imperative to notice that the neurophysiological interpretation must focus only on the spatial patterns, without considering the spatial filters which cannot be interpretable due to their mosaic spatial structure, simultaneously relating to signal and noise components (Bießmann et al., 2012; Haufe et al., 2014b). The spatial patterns can be easily computed by inverse transformation in relation to the spatial filters: $\mathbf{A} = (\mathbf{W}^T)^{-1}$. When the spatial filter matrix \mathbf{W} is not invertible, the pseudoinverse is computed: $\mathbf{A} = (\mathbf{W}^T)^+$. However, when \mathbf{W} does not have full rank, the patterns do not coincide any more with the entries of the pseudoinverse (Haufe et al., 2014b), therefore, respective transformation has to be performed, as in Section 3.2.2.2.3.

Despite the major advantages of the classic CSP algorithm, such as: producing high signal-to-noise ratio, its computational efficiency and easy implementation, an important challenge arise referring to artifacts and non-stationarity. Various modifications and extensions to the CSP algorithm have been proposed to tackle this problem (Lemm et al., 2005, 2011, Dornhege et al., 2006, Lotte et al., 2007a; Sannelli et al., 2011; Samek et al., 2014). Some of them focus on invariance and robustness to noise and artifacts (Blankertz et al., 2008a; Kawanabe et al., 2014) and others to non-stationarities in the data (Samek et al., 2012, 2014).

b. Multi-class approach

First, we need to understand why a multi-class approach is necessary to be performed. While targeting multiple decisions choices to be inferred in the BCI adaptation, the answer comes from the primary goal of a BCI application which requires online implementation and real-time classification of the brain signals. Towards this goal, a multi-class approach suits better compared to multiple binary discriminations.

While generally suited for binary cases, some CSP extensions have been developed for the multi-class approach (Müller-Gerking et al., 1999; Dornhege et al., 2004a; Dornhege et al., 2004b), namely the IN approach (Müller-Gerking et al., 1999, Allwein et al., 2000), One Versus the Rest approach (OVR) (Wu et al., 2005) and Simultaneous Diagonalization (SIM) (Grosse-Wentrup and Bus, 2008). While the IN approach considers reducing the multi-class problem to several binary decisions (Müller-Gerking et al., 1999, Allwein et al., 2000) and requires longer time to be performed. an appropriate multi-class approach is necessary to distinguish faster the corresponding class membership. An appropriate extension of the CSP

to the multi-class problem has been previously considered by (Dornhege et al., 2004a) and involves computing the CSPs for each class in relation to the other classes. This method is referred to as one over rest (OVR) strategy. Furthermore, a Simultaneous Diagonalization (SIM) method or Joint Approximate Diagonalization (JAD) method (Cardoso and Souloumiac, 1996; Ziehe and Müller, 1998; Ziehe et al., 2000, Pham, 2001; Ziehe et al., 2004; Grosse-Wentrup and Bus, 2008), considers estimating the CSPs for each of the multi-classes. In the presented thesis, the last enhanced approach is further investigated.

One Versus the Rest CSP approach (OVR)

An improvement to the IN approach is represented by the OVR approach (Dornhege et al., 2004a). While IN does binary classification on all binary pairs and assigns the trials to the class membership based on the highest voting out of the three classifiers, OVR performs multi-classification on all one versus rest binary CSP patterns. The EEG data is of course projected onto the CSPs and all the variances, log-band power of the CSP features, are fed to the classifier.

Joint Approximate Diagonalization (JAD)

While in a binary case (IN or OVR), the CSP filters are computed based on a simultaneous diagonalization of the two covariance matrices with their eigenvalues sum to one (Eq. 3.9), the multi-class JAD approach (Grosse-Wentrup and Bus, 2008) finds a matrix that follows the same rule for decomposition but related to multi covariance matrices. When in the binary case the solution can be easily found, in the multi-class approach an approximation of the solution is computed based e.g. on approximate simultaneous diagonalization. Meaning that for the covariance matrix Σ of each k class ($k = 1, \dots, N$, where N is the number of classes), the decomposition finds an approximation solution for the \mathbf{W} matrix that satisfies $\mathbf{W}^T \Sigma_k \mathbf{W} = \mathbf{D}_k$, where \mathbf{D}_k is a diagonal matrix fulfilling $\sum_{k=1}^N \mathbf{D}_k = \mathbf{I}$, with \mathbf{I} being the identity matrix. In our implementation, this joint diagonalization problem is computed with the FFdiag (Fast Frobenius Diagonalization) algorithm (Ziehe et al., 2004). The algorithm is based on the Frobenius-norm formulation and computes the diagonalization using non-orthogonal transformation and a recursivity computation based on a multiplicative iteration, assuring the invertibility of \mathbf{W} .

In more detail, it finds an approximate solution of the following optimization problem, by minimizing the Frobenius norm of the off-diagonal elements of \mathbf{D}_k :

$$\min_{\mathbf{W} \in \mathbb{R}^{M \times M}} \sum_{k=1}^N \sum_{i \neq j} ((\mathbf{W}^T \Sigma_k \mathbf{W})_{ij})^2 \quad (3.12)$$

While the above cost function can converge to zero, the invertibility of the matrix \mathbf{W} prevents this effect from happening: $\mathbf{W}_{(it+1)} = (\mathbf{I} + \mathbf{V}_{(it)})\mathbf{W}_{(it)}$, where it is the current iteration and $\mathbf{V}_{(it)}$ is the iteration matrix.

Further, after the approximate diagonalization has found a solution, the relevant activity sources have to be considered. Because there is no canonical way to choose the relevant CSP patterns, the selection is performed by considering the first m eigenvalues with highest mutual information (out of maximum M sources). This selection is similar to ICA, where these m sources denote the brain activity related to the corresponding information on the decisions and intentions of the BCI user, and the other brain sources that do not relate to the BCI task, are considered as noise sources. This spatial filtering composed by ICA and

derived approximation of mutual information to identify the signal subspace is termed as Information Theoretic Feature Extraction (ITFE):

$$MI(c, \mathbf{w}_j^T \mathbf{x}) \approx - \sum_{k=1}^N p(c_k) \log \sqrt{\mathbf{w}_j^T \sum_k \mathbf{w}_j} - \frac{3}{16} \left(\sum_{i=1}^N p(c_k) ((\mathbf{w}_j^T \mathbf{D}_k \mathbf{w}_j)^2 - 1) \right)^2,$$

where $MI(c, \mathbf{w}_j^T \mathbf{x})$ is the mutual information of the class label c and the linear transformation $\mathbf{w}_j^T \mathbf{x}$, calculated based on negentropy for each eigenvector \mathbf{w}_j (column $j=1, \dots, M$) of \mathbf{W} , with $\mathbf{w}_j^T \sum_k \mathbf{w}_j = 1$; and $p(c_k)$ is the class probability. For more details, see Grosse-Wentrup and Bus, (2008).

In the end, a set of optimal linear spatial filters can be interpreted as the m columns of \mathbf{W} with the highest mutual information.: $MI(c, \mathbf{W}^T \mathbf{x}) = \sum_{k=1}^m MI(c, \mathbf{w}_j^T \mathbf{x})$. Therefore, according to the ICA model, all the important information on the classes is contained in the first m sources (the first m ICs).

3.3 Feature extraction

The purpose of the feature extraction step for data analysis is to detect the specific values and characteristics of the neural signals in the temporal, spatial and spectral domain that best characterize the investigated neural activity, whilst discarding the artifacts and background noise of the EEG. These values, termed ‘features’ are then stored in a ‘feature vector’ which is further used for classification.

While some researchers focus more on the classification step of a BCI, granting more attention to the preprocessing and feature extraction steps is more important in a BCI system in order to identify and select the optimal neural features, which will automatically lead to a correct and enhanced classification performance (Pfurtscheller et al., 2003; Hammon and de Sa, 2007). These features should relate to the neurophysiological signals that describe the corresponding mental state or brain activity, and not to other activities or body potential artifacts.

In the following, a description of the extraction methods used through this thesis is further presented, considering the temporal (Section 3.3.2), spatial and spectral (Section 3.3.3) signals characteristics.

A good improvement for the brain analysis and for the classification performance of a BCI is represented by combined feature approaches such as spatio-temporal, spatio-spectral, tempo-spectral methods and so on (Dornhege et al., 2004a; Gysels and Celka, 2004; Boostani et al., 2007).

In this case of multi-modal features, especially in case of features with different type of units, normalization should be performed on the combined feature vector. The feature types have to be centered around zero with a standard deviation of one, in order to have the features on the same scale which will ease the classifier decision. A common approach is to use z-score normalization which is computed by subtracting the mean and dividing by the standard deviation for each feature type: $\mathbf{z} = (\mathbf{x} - \mu)/\sigma$.

3.3.1 Feature selection and dimensionality reduction

An often-encountered problem in the BCI refers to high feature vectors dimensions, especially for multi-modal analysis which combine different types of features such as spatial, temporal, or spectral, leading in the end to an increase in the computation time of the system or an overestimation of the data considering classification. In order to treat this problem, the feature vector should be reduced to an adequate number that in general will improve performances. Therefore, feature selection and dimensionality reduction become a preferable approach (Millán et al., 2002; Garret et al., 2003; Schroder et al., 2003; Subasi 2010; Nikulin et al., 2011; Haufe et al., 2014a). When reducing the number of features, it is also important to relate the number of features to the amount of data, such that the dimensionality of the training data in one class exceeds the number of features with a couple of factors. Otherwise, the classification will overfit, issue caused by the ‘course of dimensionality’ phenomena (Friedman, 1997; Jain et al., 2000).

Throughout this thesis, feature selection methods, manually or heuristically implemented, have been used to reduce the feature vector dimensionality, and are described in the corresponding feature extraction or spatial filtering method, e.g. ICA, SSD, CSP.

3.3.2 Temporal methods

Considering ERP based BCI paradigms, the relevant ERP amplitudes may be considered for the feature extraction step. The amplitude evolutions of the signals within each epoch are carefully investigated. Preliminarily, the baseline correction is applied (Section 3.2.1.4). For a closer inspection and overview of the ERPs, a visual representation is usually carried out referring to average trials for all trial repetitions. In this sense, averaged single-participant ERP representations can be analyzed or Grand Averages (GA) considering all participants. Next, relevant time intervals are manually or automatically detected, and the corresponding temporal amplitudes are considered as features. While the manual procedure requires additional involvement from the researcher side, automatic methods (e.g. based on discriminability measures) are more efficient regarding feature extraction.

3.3.2.1 Spatio-temporal feature detection based on signed r^2 discriminability measurement

Spatio-temporal features are extracted considering a heuristic selection of the intervals with maximum discriminability and a constant spatial pattern between the two classes, based on the method presented in Blankertz et al. (2011). Relevant time intervals are selected with high signed and squared point biserial correlation coefficient (*signed r^2*) values.

1. The signed r^2 discriminability measure

For binary discrimination between classes, the *signed r^2* measure can be applied. Considering two signals \mathbf{x}_1 and \mathbf{x}_2 , and their class membership label \mathbf{y}_1 and \mathbf{y}_2 that relate to two different classes (class 1 and class 2), the *signed r^2* measure detects the high differences between the signals based on the point biserial correlation coefficient, $r(\mathbf{x}_1, \mathbf{x}_2)$. The signed and squared r value is given by:

$$\text{signed } r^2(\mathbf{x}_1, \mathbf{x}_2) = \text{sgn}(r(\mathbf{x}_1, \mathbf{x}_2)) \cdot r(\mathbf{x}_1, \mathbf{x}_2)^2, \quad (3.13)$$

where the point biserial correlation coefficient is computed by considering the signal and the class label information:

$$r(\mathbf{x}, \mathbf{y}) = \frac{\sqrt{N_1 \cdot N_2}}{N_1 + N_2} \cdot \frac{\mu_1 - \mu_2}{\sigma(\mathbf{x})} \quad (3.14)$$

with N_1 and N_2 – the numbers of samples in class 1 and 2, and μ_1 , μ_2 – the mean of class 1 or 2, respectively.

This discriminability measure can be also applied in the frequency domain, in order to detect relevant frequency bands with high class differentiation of the oscillatory signals (Blankertz et al., 2006b, 2007, 2009).

2. Discriminability matrix visualization of signed r^2

For visualization purposes, the temporal and spatial discriminability can be graphically visualized as time evolution and scalp plots. For a more complete overview of the temporal distribution within each channel, which is not observed in the scalp plots that presents information only for a short time interval (e.g. Fig. 5.7 upper plots) and neither in the temporal evolution plots that shows the information only for one or few channels (e.g. Fig. 5.7 bottom plots), a more detailed representation is given by the discriminability matrix (e.g. Fig. A.3.7), where the *signed r^2* information of each time point is graphically represented with a colormap for all channels, a time versus channels representation.

3.3.3 Spectral methods

Besides the temporal domain, the spectral information also provides valuable information, which may be complementary to the temporal features depending on the type of brain information investigated. An overview of the extracted spectral feature is presented in the following.

3.3.3.1 Band power features

A good characterization of the neural oscillations can be expressed by the power of representative frequency bands. The signal is therefore band-pass filtered in the relevant frequency band and the band power features are computed by squaring the resulted signal or extracting the logarithm of the band-power of the signals or components as specified in (Blankertz et al., 2008c), in order to obtain an approximate normal distribution of the features (Pfurtscheller and Neuper, 2001). Different frequency bands may be considered for feature extraction, depending on the analyzed BCI task or mental state, for example the μ frequency band for motor imagery tasks (Pfurtscheller and Neuper, 2001; Scherer et al., 2008; Zhong et al., 2008; Nicolae et al., 2016b) and a various range of frequency bands such as theta, alpha, beta for cognitive processing tasks (Palaniappan, 2005; Lotte et al., 2007a,b; Nicolae et al., 2016a, 2017a).

3.3.3.2 Power spectral density features

In order to obtain more information over brain oscillations, the power spectrum also referred to as the Power Spectral Density (PSD) is often analyzed in the BCI research (Keirn and Aunon, 1990; Millán et al., 2002; Millán and Mouriño, 2003). It shows the distribution of the signal power over different frequencies and can be computed with the Fourier transform (Appendix A.1.3.1.2), periodogram (Appendix A.1.3.3.1), or any other time to frequency

transformation. The PSD features are then obtained, for example, by taking the filtered signals or the square of the filtered signals (Lalor et al., 2005).

3.3.4 Time-frequency measures

The neurophysiological signals present different characteristics in the time and also frequency domains, therefore another feature extraction method relates to a combined temporal and spectral approach, named time-frequency decomposition. The approach allows the simultaneous analysis in both time and frequency domains via time–frequency representations (TFR) (Cohen, 1995; Sejdić et al., 2009), like Short-time Fourier Transform (STFT) (Appendix A.1.3.4.2), Wavelet Transform (WT) (Appendix A.1.3.4.3), or representations based on Power Spectral Density (PSD) (Appendix A.1.3.4.1).

One measure that helps describing and visualizing the changes in the power spectrum related to an event is the Event-Related Spectral Perturbation (ERSP) method (Makeig, 1993) computed based on a spectrogram (more details in Section 3.3.4.1).

Another frequency measure that is commonly used in BCI for measuring the interactions between signals, for example the phase synchronization or coherence between channels or epochs at different time points is given by the Inter-Trial Coherence (Gysels and Celka, 2004) measure, further described in Section 3.3.4.2).

3.3.4.1 Event-Related Spectral Perturbations (ERSP)

The Event Related Spectral Perturbation (ERSP) method, introduced by Makeig (1993), quantifies amplitude dynamic changes of the EEG frequency spectrum in time, triggered by an external or internal event. As well known in the scientific literature, the oscillations vary with multiple frequency bands and the ERSP method allows the simultaneous investigation of the full spectrum, as compared to the narrow-band ERD/ERS curves, for example. It shows valuable applications in practice (Makeig, 1993; Makeig et al., 2004; Fuentemilla et al., 2006; Huang et al., 2007a,b; Li et al., 2011; Nicolae, 2013; Nicolae et al., 2015c).

The computation of ERSP starts from generating the power spectrum of an epoch (the time which follows an event) or a continuous signal using Short-Time Fourier Transform (STFT) or Wavelet Transform. In more detail, a signal (or epoch) is split into overlapping segments of a given window length and the average amplitude spectra of these windows is computed. From each time point of the spectrum, the average baseline spectrum computed on the baseline interval (the time that precedes the event) is then subtracted in order to reduce the signal background perturbation. In this sense, a similar and preferred approach is to normalize the signal (or epoch) spectrum by division with the average baseline spectra. Finally, the logarithmic spectral amplitude $10 \cdot \log_{10}(\text{power})$ dB is represented in a time by frequency plane, called spectrogram. For a general overview of the perturbations for one class, the ERSP of the corresponding epochs are then averaged. The time-frequency representation provides then a larger overview of the Event-Related (De)Synchronization (ERD/ERS) phenomena (Pfurtscheller and Aranibar, 1979) in multiple frequency bands and their durations and latencies, simultaneously.

The mathematical formulation of the ERSP (Delorme and Makeig, 2004) is given by:

$$ERSP(f, t) = \frac{1}{T} \sum_{k=1}^T |P_k(f, t)|^2, \quad (3.15)$$

where P_k is the spectrum of epoch $k = 1, \dots, T$ for the frequency f and time t .

3.3.4.2 Inter-Trial Coherence (ITC)

The ERD and ERS phenomena are time locked to a stimulus, not phase locked to an event, therefore a good measure investigates the local phase coherence across consecutive trials, namely Inter-Trial Coherence (ITC) or ‘phase-locking factor’ (Tallon-Baudry et al., 1996; Delorme and Makeig, 2004; Makeig et al., 2004). In contrast to the ERSP method (Section 3.3.4.1), the ITC calculates the EEG phase coherence between trials for a specific Independent Component, channel, time point or frequency interval and may indicate the timing of firing of neurons groups. ITC is a frequency measure of the neural activity synchronization for a given time point and frequency for different time locked EEG epochs. Mathematically, ITC is defined by the power spectrum, normalized by the Root Mean Square (RMS) power of single trial estimation:

$$ITC(f, t) = \frac{1}{T} \sum_{k=1}^T \frac{P_k(f, t)}{|P_k(f, t)|} \quad (3.16)$$

where $|\cdot|$, in this case, is the complex norm. For a specific time-point, ITC measure ranges from zero to one, explicitly from no synchronization between the EEG epochs to strong synchronization. For a given frequency range, it provides the magnitude and phase of the spectral estimation. Moreover, phase coherence between trials can be also estimated by Inter-Trial Phase Coherence (ITPC) showing the event-related phase representation.

3.4 Classification and Regression

Based on the optimal feature set detected on the feature extraction and selection processes, the class discrimination is performed by means of a classifier in order to decode the corresponding user mental state or task. For example, in the ERP-based BCIs (Chapter 2.4.1), the classifier discriminates between target and non-target neural responses, while for motor-imagery based BCIs (Chapter 2.4.2.2) it discriminates between different motor imagery tasks (e.g. left/right hand movement). On a closer look into the classifier process, the data is split into a labeled training set and a non-labeled test set of feature vectors; and the classifier will assign the class memberships for the test set considering what it learned on the training set.

Although, various methods have been developed for classification (Müller et al., 2003; Lotte et al., 2007a; Bishop, 2007; Lemm et al., 2011) or regression (Duda et al., 2001; McFarland, and Wolpaw, 2005), for example supervised learning methods such as Linear Discriminant Analysis (LDA) (Friedman, 1989; Blankertz et al., 2011), Quadratic Discriminant Analysis (QDA) (McLachlan, 2004), Logistic Regression (LR) (Tomioka et al., 2007), Ridge Regression (RR) (Hoerl and Kennard, 1970) few of them provide high performing results for EEG data (Bashashati et al., 2007, Lotte et al., 2007a). As the complexity of a classifier is increased, so is the generalization error and the classifier performance will degrade. Therefore, simple linear algorithms, such as Linear Discriminant Analysis (LDA), are better suited in this context (see also results in Section 5.3.3.3). Further, referring to the high number of features that could characterize a BCI system, for example a large set of temporal features in the case of an ERP-based BCI, the classifier must be regularized by shrinking the estimated covariance matrix (Tomioka and Müller, 2010; Blankertz et al., 2011; Bartz and Müller, 2013). The regularization will help preventing overtraining and is more robust with respect to outliers, due to the reduction of the

generalization error (Jain et al., 2000; Duda et al., 2001). In addition, classifiers can be applied for binary decisions or even more for multi-class discrimination. While some of them needs some tuning in order to be applied, e.g. Logistic Regression (LR) adapted to Multinomial Logistic Regression (MLR) (Böhning, 1992; Greene, 2012), others can easily work in both cases, e.g. LDA. Multi-class classification is necessary when aiming to decode multiple user states, and obtaining faster performance as compared to the use of multiple binary discrimination (Dornhege et al., 2004a).

3.4.1 Linear Discriminant Analysis (LDA)

Linear discriminant analysis (LDA) is a simple classification method due to its linearity, facile use and easy implementation, and a powerful method providing high performances. It is well suited for EEG data, because it starts from the assumptions that: *i*) the data is Gaussian distributed; *ii*) all classes have equal covariances; and *iii*) the true distributions of the classes, means μ_i , and covariance matrix Σ , are known. While the characteristics of the EEG data type approximately fulfills already the first two points, the true distributions: the means μ_i , and covariance matrix Σ still have to be estimated. The decision boundary for separating between classes consists of a hyperplane, described by: $\mathbf{w}^T \mathbf{x} + \mathbf{b} = \mathbf{y}(\mathbf{x})$ with $\mathbf{y}(\mathbf{x}) = 0$, where \mathbf{w}^T is the weight vector that describes the orientation of the hyperplane and \mathbf{b} is the bias representing the location of the hyperplane. The class belonging is defined by the position in relation to the hyperplane: negative for one class ($\mathbf{y}(\mathbf{x}) < 0$) and positive for the second class ($\mathbf{y}(\mathbf{x}) > 0$). Referring to two classes discrimination, the weight matrix is given by $\mathbf{w} = \hat{\Sigma}^{-1}(\hat{\mu}_2 - \hat{\mu}_1)$ and the bias is given by: $\mathbf{b} = \mathbf{w}^T(\hat{\mu}_2 + \hat{\mu}_1)/2$. Moreover, LDA seeks the linear projection \mathbf{w} that best separates the classes: such as minimizes the within-class variance σ_w while maximizes the variance between classes σ_b , mathematically defined by maximizing the ratio of the distributions:

$$\max_{\mathbf{w}} \frac{\sigma_b^2}{\sigma_w^2} = \max_{\mathbf{w}} \frac{(\mathbf{w}^T(\hat{\mu}_2 - \hat{\mu}_1))^2}{\mathbf{w}^T(\hat{\Sigma}_2 - \hat{\Sigma}_1)\mathbf{w}} = \max_{\mathbf{w}} \frac{\mathbf{w}^T \Sigma_b \mathbf{w}}{\mathbf{w}^T \Sigma_w \mathbf{w}} \quad (3.17)$$

with Σ_b and Σ_w denoting the corresponding between-class and within-class covariance. For multi class discrimination, the between class variability can be defined by the covariance of the class means μ : $\Sigma_b = 1/N_C \sum_{i=1}^{N_C} (\hat{\mu}_i - \hat{\mu})(\hat{\mu}_i - \hat{\mu})^T$.

3.4.1.1 Regularization with Shrinkage of the Covariance Estimation (rLDA shrink)

As described earlier, regularization is mandatory in order to avoid overfitting. One common approach to reduce the distortions for the estimated covariance that appear due to the curse of dimensionality effect, is to perform shrinkage of the covariance matrix (Friedman, 1989). Therefore, the estimated covariance $\hat{\Sigma}$ is shrunk by a regularization parameter $\gamma \in [0, 1]$ and a scaling parameter ν :

$$\tilde{\Sigma}(\gamma) = (1 - \gamma)\hat{\Sigma} + \gamma\nu\mathbf{I} \quad (3.18)$$

While ν is computed as the average eigenvalue of the estimated covariance, the computation of the optimal regularization parameter γ requires more effort and is comprised between zero (no shrinkage) and one (spherical covariance). Since earlier approaches of estimating γ in the cross-validation step is computationally intensive (Friedman, 1989), analytical approaches that minimize the Mean Squared Error are more efficient (Ledoit and Wolf, 2004; Schäfer and Strimmer 2005).

For N feature vectors: $\mathbf{x}_1, \dots, \mathbf{x}_N \in \mathbb{R}^d$, $Z_n = (\mathbf{x}_n - \hat{\boldsymbol{\mu}})(\mathbf{x}_n - \hat{\boldsymbol{\mu}})^\top$ is defined for each trial n , with $\hat{\boldsymbol{\mu}} = \frac{1}{N} \sum_{n=1}^N \mathbf{x}_n$, the empirical mean. The optimal shrinkage parameter γ^* , can be analytically computed by:

$$\gamma^* = \frac{N}{(N-1)^2} \frac{\sum_{i,j=1}^d \sigma_{n=1,\dots,N}^2(Z_n)_{i,j}}{\sum_{i,j=1}^d (\hat{\boldsymbol{\Sigma}} - v\mathbf{I})_{i,j}^2} \quad (3.19)$$

where $\sum_{i,j}^d$ is the sum of the entities; $\sigma_{n=1,\dots,N}^2(Z_n)$ is the variance of Z_n ; $(\hat{\boldsymbol{\Sigma}} - v\mathbf{I})_{i,j}$ represent the element of $(\hat{\boldsymbol{\Sigma}} - v\mathbf{I})$ at position row i and column j ; and $\hat{\boldsymbol{\Sigma}}$ is the standard estimator of the true covariance matrix $\boldsymbol{\Sigma}$, namely the empirical covariance matrix: $\hat{\boldsymbol{\Sigma}} = \frac{1}{N-1} \sum_{n=1}^N (\mathbf{x}_n - \hat{\boldsymbol{\mu}})(\mathbf{x}_n - \hat{\boldsymbol{\mu}})^\top$.

3.4.1.2 Sliding LDA

An LDA based approach useful to discriminant ERP potentials without aligning them, relates to a sliding window approach. Mainly, the LDA classifier is trained for a particular temporal interval in sliding manner. The features are considered as different time delays from the onset of the event. In addition, the method can help for the feature selection process by detecting the most relevant time intervals for classification by estimating the highest classification performance among all slides.

3.4.1.3 Quadratic Discriminant Analysis (QDA)

The Quadratic Discriminant Analysis (QDA) uses quadratic boundaries to separate between classes (e.g. circle, ellipse, parabola, hyperbola or can also be linear), as compared to only linear separation performed by LDA. QDA requires also Gaussian distributed data as LDA, except the constraint regarding the equality of the class covariance matrices which is not required (Hastie et al., 2008). Therefore, because the class covariance matrices are not identical, the covariance matrix $\boldsymbol{\Sigma}_k$ has to be estimated separately for each class $k = 1, \dots, N$, which gives quadratic terms in the discriminant function:

$$\delta(\mathbf{x}) = -\frac{1}{2}(\log \boldsymbol{\Sigma}_k) - \frac{1}{2}(\mathbf{x} - \boldsymbol{\mu}_k)^\top \boldsymbol{\Sigma}_k^{-1}(\mathbf{x} - \boldsymbol{\mu}_k) + \log \pi_k \quad (3.20)$$

Then, the classification rule is similar, finding the class k that maximizes the discriminant function: $\hat{G}(\mathbf{x}) = \underset{k}{\arg \max} \delta_k(\mathbf{x})$.

Due to its flexibility regarding the covariance matrix, QDA inclines towards a better estimate of the data as compared to LDA, although it's also more complex, with more parameters to be estimated. Moreover, if the data is almost linearly distributed, QDA might have higher model variance and so leaning to overfitting. Moreover, for limited data, the computed covariance matrix of the training data might be inaccurate. Therefore, it might be better to reduce the complexity of the model in this case and refer to a common covariance matrix assumption as in LDA.

When choosing a classifier model, it is important to select the best compromise between fitting the data in a better way while having a complex model that can induce more errors or using a simpler classifier, but which does not fit the data accurately. In any case, a perfect classifier model is almost impossible to be achieved, especially for complex and mixed data distributions. In addition, the performance of the classifier on the unseen data

might be higher in case of a simpler model, because it is more robust to outliers and variability in the data.

3.4.2 Binomial Logistic Regression (LR)

In case of a Logistic regression (LR) model (Cox, 1958; Long 1997; Tomioka et al., 2007; Greene, 2012), the outcome (the dependent variable) is categorical, expressed in binary format (0 and 1). The binary logistic model estimates the percentage that a risk factor affects the probability of a specific response.

Considering a set of n observations represented by the vectors \mathbf{x}_k , aggregated in the data matrix \mathbf{X} of size $n \times k$, with \mathbf{y} the outcome and ε the vector of disturbances, the model can be described by:

$$\mathbf{y} = \mathbf{x}_1\beta_1 + \dots + \mathbf{x}_k\beta_k + \varepsilon, \quad (3.21)$$

equivalent with the form: $\mathbf{y} = \mathbf{X}\beta + \varepsilon$.

The goal is therefore to estimate β . After appropriate transformation, the linear model can be expressed in the form: $\mathbf{y} = \mathbf{A}\mathbf{x}^\beta + e^\varepsilon$, which can be unfolded to:

$$\ln \mathbf{y} = \beta_1 + \beta_2 \ln \mathbf{x}_2 + \dots + \beta_k \ln \mathbf{x}_k + \varepsilon. \quad (3.22)$$

For multiple outcome categories, the discrimination is analyzed by multinomial logistic regression, described in the following subsection.

3.4.3 Multinomial Logistic Regression (MLR)

Multinomial Logistic Regression (MLR) extends the binomial Logistic Regression (LR) by predicting a nominal dependent variable with more than two categories. The multinomial logistic function (Böhning, 1992; Greene, 2012) that describes the response probabilities of a nominal model (Bock, 1997) in relation to the linear combination of predictors \mathbf{X}_β , is described by:

$$\ln \left(\frac{\pi_i}{\pi_r} \right) = \beta_{i0} + \sum_{j=1}^{pr} \beta_{ij} \mathbf{X}_{ij} \quad (3.23)$$

with $i=1, \dots, k-1$, where k is the number of categories, pr is the number of predictors, π is the categorical probability and r is the reference category.

3.4.4 Regression

Generally, regression describe the relation between the variations of the output and the predictors (or features). The relation is generally estimated by the conditional expectation, expressed by the average of the output when the input is fixed. Various regression approaches can be used, such as linear regression, ridge regression, logistic regression for binary classification or multinomial logistic regression for multi-class discrimination.

As a reference method for more complex regression models, we first describe the linear model in the following.

Having a set of predictors $\mathbf{x}_1, \dots, \mathbf{x}_N$, the goal is to predict the outcome \mathbf{y} given a new input \mathbf{x} . Then, the linear model is defined by: $\hat{\mathbf{y}} = \mathbf{w}^T \mathbf{X}$ and the optimal weight vector \mathbf{w} is computed by minimizing the loss between the true output \mathbf{y} and the prediction $\hat{\mathbf{y}}$. The commonly used loss function to be minimized is the Least-Square Error (LSE) method:

$$\min \varepsilon(\mathbf{w}) = \sum_{k=1}^N (\mathbf{y}_k - \mathbf{w}^T \mathbf{x}_k)^2. \quad (3.24)$$

After derivation and equation calculation, \mathbf{w} is expressed by:

$$\mathbf{w} = (\mathbf{X}\mathbf{X}^T)^{-1}\mathbf{X}\mathbf{y} \propto \Sigma^{-1}\mathbf{X}\mathbf{y}.$$

3.4.4.1 Ridge Regression shrink (RR shrink)

In addition to a linear regression approach which is mainly similar to LDA (Duda et al., 2001), the regularized version namely ridge regression, is better tailored for high dimensional data, making the model more robust to outliers. The regularization can be achieved by shrinkage of the covariance matrix, similarly to the rLDA shrink method described in Section 3.4.1.1.

Therefore, a regularization term (Hoerl and Kennar, 1970) is added to the loss function:

$$\varepsilon(\mathbf{w}) = (\mathbf{y} - \mathbf{w}^T\mathbf{X})^2 + \lambda\|\mathbf{w}\|_2^2, \quad (3.25)$$

where the parameter λ enforce the shrinkage from high values of \mathbf{w} , towards zero (no shrinkage, linear model). The optimal \mathbf{w} is computed by:

$$\mathbf{w} = (\Sigma + \lambda\mathbf{I})^{-1}\mathbf{X}\mathbf{y}. \quad (3.26)$$

3.4.5 Classification validation

3.4.5.1 Cross-validation

Considering classification, an important procedure is to estimate the true error rate of the given classifier, especially when an independent set of testing samples is not available, or the dataset is limited. Therefore, in offline analysis, a good approach such as Cross-Validation (CV) is customary employed. The technique evaluates the predictive values of a classifier in order to analyze the unseen data (Lemm et al., 2011). Specifically, the data is split into K data segments also called as folds, of which a bigger part (usually 90%) is used as training data and one part (10%) is kept as testing data. The CV procedure is applied K times while choosing different segments for the validation (e.g. every segment is used exactly one time as a test set). The final estimation is computed by averaging the performance values for all K repetitions. In addition, in order to diminish the variance of the cross-validation estimator, a repeated CV procedure can be performed, in which every CV is repeated T times by shuffling the entire dataset and dividing again into K folds as described above. The resulted performances are then averaged over K folds and T repetitions.

The features in the training set are used for learning the classifier model and the corresponding generalized features within the test set are used to validate the classifier.

Note: It is very important that the training features and test features are independent, such as no information from the test set, especially label information, has been used to compute the training features or other model paramters! This is the main characteristic of an unseen test set. Therefore, greater precaution has to be employed in the feature extraction and selection processes (For more details, please see Blankertz et al., 2008c; Lemm et al., 2011; Haufe et al., 2014a).

3.4.6 Classification evaluation

Assessing the performance (accuracy) of a BCI system is also an important process and requires careful implementation and investigation, not to incorrectly estimate system's performance. Generally, it indicates the final decision of the system that relates in one way or

another to the percentage of correctly classified epochs. A commonly used measure for binary class evaluation performance is represented by the Area Under the ROC Curve (AUC), while for multi-class estimation normalized loss can be used, for example. These measures along with some other important procedures are described in the following.

3.4.6.1 Area Under the ROC Curve (AUC)

The Area Under the ROC Curve (AUC) (Hanley and McNeil, 1982) is a good common measure for estimating binary classification performance, computed based on the Receiver-Operator Characteristics (ROC) curve (Green and Swets, 1966). The ROC curve is a graphical representation expressing the “True Positive Rate (TPR)” also named “sensitivity”, in relation to the “false positive rate” also known as “1-specificity”. The area under the ROC curve (AUC) can be viewed as a generalization of the ROC curve to a single rational value. The AUC measure ranges between 0 and 1, where a value over 0.5 is targeted for binary discrimination, representing a good performance better than chance level, undoubtedly considering the appropriate statistical significance measures (Appendix A.1.1).

3.4.6.2 Normalized loss

In order to assess the accuracy of a multi-class classification, when the AUC measure cannot be applied anymore, the method to be referred to has to include normalization. Additionally, the class-wise normalized loss helps with weighting in case of unbalanced classes:

$$loss = \frac{1}{n_{cls}} \sum_{i=1}^{n_{cls}} \frac{N_{err-C_i}}{N_{C_i}}, \quad (3.27)$$

where n_{cls} – the number of classes; N_{err-C_i} – the number of wrongly estimated samples in class C_i ; N_{C_i} – the number of samples in class C_i . While this result represents the loss ratio out of 1, the accuracy is complementary to the loss, given by: $Acc = 1 - loss$. When cross-validation is applied, the normalized loss is computed inside folds, and then averaged over all folds.

3.4.6.3 Confusion matrices

The classification accuracy value can be misleading in case of different number of observations between classes, or for multi-class discrimination. In this sense, computing confusion matrices is a useful approach, which provides a detailed overview of the classification errors and performance. To put it simply, a confusion matrix (Kohavi and Provost, 1998) is a table layout that describes the amount of correct and mislabeled (confounded) samples for each class. The columns refer to the predicted class instances and the rows show the true class instances, showing the correct classified samples in each class on the diagonal.

For unbalanced classes, normalized confusion matrices have to be performed. For a larger overview of the classification performance, confusion matrices can be represented for single participants, or as grand average over all participants.

The amount of errors and the type of misclassifications that are described by the confusion matrix, arise from the resubstitution.

1. Resubstitution error and accuracy

The resubstitution error shows the misclassification costs, namely the difference between the response given by the classifier on the training data and the predictions responses performed on the test data with the information from the training data. A high value of the resubstitution error, will imply a weak performance of the classifier and a poor prediction of a new data. In any case, the opposite is not valid: a small resubstitution error does not necessarily imply a good fit on new data. However, it still gives a good overview of the estimation and the performance of the classifier.

An accuracy measure, Acc , can be computed using the general confusion matrix, \mathbf{R} , of the classifier that relates to the resubstitution errors:

$$Acc = \frac{\sum_{i=1}^k \mathbf{R}_{ii}}{\sum_{i=1}^k \sum_{j=1}^k \mathbf{R}_{ij}}, \quad (3.28)$$

where k represents the number of classes and \mathbf{R}_{ij} is the number of observations of class i , estimated as class j .

3.4.6.4 Statistical testing

In order to reinforce the performance of a classifier, it is crucial to test the statistical significance of the model outcome. In addition, for example when interpreting and correlating differences and similarities in the ERPs among trials and participants, or for extracting inferences over the data, statistical analysis is mandatory to be performed. The statistical evidence assures if the inferences conducted on the diverse sample data are valid (not due to chance) and can be deduced in general from a larger data. Among the wide range of statistical tests (Fukunaga, 1990, 2013), the common tests can be classified in the following categories: descriptive statistics (e.g. normality test, correlation coefficient measure, means comparison tests), hypothesis testing (e.g. t-test, chi-squared test), analysis of variance (e.g. ANOVA, F-test, chi-squared test for variance, Barlett test), multiple comparisons (e.g. Bonferroni correction), and non-parametric testing (e.g. Wilcoxon rank test, Kolmogorov-Smirnov test). The choice of the statistical test depends on the experiment design, the type of variables in the data set, and the distribution of the data. Considering data distribution for example, parametric tests are suitable in case of normally distributed data, while on the other hand, non-parametric tests can be applied to non-normal data.

For data visualization purposes regarding the statistical distribution of the data, statistical charts such as histograms and box charts are usually represented. Shortly, the main statistical tests used in this thesis are described in Appendix A.1.1.

3.5 BCI applications

A brief overview over existing BCI paradigms and applications is described in this section, mainly focusing on those relevant for the context of this thesis. As follows, the common ERP-based BCI paradigms using visual and auditory stimuli are described. Further, motor-imagery based BCIs are briefly discussed, followed by the general research and applications on mental state detection. The possible BCI applications range from entertainment (Krepki et al., 2007; Lécuyer et al., 2008) to control or communication (Vidal, 1973; Dornhege et al.,

2007; Wolpaw and Wolpaw, 2012). While initially, the BCI technologies have been developed by the research community as assistive devices for patients with disabilities (Pfurtscheller and Neuper, 2001; Neuper et al., 2003; Kübler et al., 2005; Birbaumer et al., 2008; Mak and Wolpaw 2009), the purpose of BCI research has expanded also towards non-medical applications for healthy individuals (Müller et al., 2008; Blankertz et al., 2010c, 2016; Zander and Kothe, 2011; van Erp et al., 2012; Allison et al., 2012; Gamberini et al., 2015). Primarily initiated in controlled laboratory settings, BCIs developed to the extent of home use, industrial environmental settings (Venthur et al., 2010), or even outdoor activities such as driving (Haufe et al., 2011; 2014c), air traffic control (Aricò et al., 2016a,b), piloting (Borghini et al., 2014).

Moreover, the range of possible BCI applications is even wider (Moore, 2003), and the type and context of applications will certainly expand in the following years.

3.5.1 Applications for ERP-based paradigms

Starting from the vital ERP-based BCI paradigm with visual stimuli developed for the purpose of communication, namely the matrix speller by Farwell and Donchin (1988), more and more complex and diverse paradigms have been developed for different purposes. Controlling BCIs through ERPs (Vidal, 1973; Blankertz et al., 2011) is a vast well-known approach, relying on different ERP components like P300 (Farwell and Donchin, 1988; Treder and Blankertz, 2010), or on some other subtypes of ERPs, such as visually evoked potentials (VEP) (Müller-Putz et al., 2005), or auditory evoked potentials (AEP) (Schreuder et al., 2010; Höhne et al., 2011a). The applications range from controlling a computer application or a virtual environment and games (Bayliss and Ballard, 2000; Lécuyer et al., 2008) towards more artistic use, such as brain painting (Kubler et al., 2008).

3.5.2 Motor-imagery based BCIs applications

The applications based on motor-imagery BCIs include motor control (Pfurtscheller et al., 2003), communication (Kübler et al., 2005; Blankertz et al., 2007, 2008b), controlling computer applications (Wolpaw et al., 1991), robots, prosthesis, wheelchairs (Vanacker et al., 2007; Galán et al., 2008) and other electronic devices. The respective application or device can be controlled by the BCI users through self-induced amplitude variations of the sensorimotor rhythms (SMRs) (Wolpaw et al., 2002; Wolpaw and McFarland, 2004; Blankertz et al., 2007).

3.5.3 Mental state BCIs applications

An emerging paradigm nowadays relates to the investigation of the ongoing EEG activity, by detecting user's mental state and intentions for the benefit of humans. Using a non-control BCI interaction based on "implicit information" obtained from the neurophysiological activity, which does not requires a direct user interaction (Kohlmorgen et al., 2007; Müller et al., 2008; Blankertz et al., 2010c, 2016; Allison et al., 2012, Zander et al., 2014; Brunner et al., 2015; Schultze-Kraft et al., 2016b; Naumann et al., 2017), exceeds the possibilities offered by "explicit control" available within control-BCI systems (Birbaumer et al., 1999, Blankertz et al., 2007; Wolpaw and Wolpaw, 2012). Specifically, different BCI designs have been used to monitor and investigate the user cognitive mental state, represented by attention,

workload, stress, task engagement, decision-making (Klimesch, 1999; Kohlmorgen et al., 2007; Müller et al., 2008; Venthur et al., 2010; Borghini et al., 2014; Haufe et al., 2014c; Gamberini et al., 2015; Schultze-Kraft et al., 2015), and many other factors, for example investigating the brain activity related to music (Makeig et al., 2011; Treder et al., 2014; Sturm et al., 2015; Vaid and Singh, 2015). This type of BCIs that monitors and interprets user's state and learn to adapt the interface according to user's cognitive and affective state, without the restriction of conscious user control and continuous interaction with the system, are termed passive BCIs. This approach brings noticeable advantages to the BCI interaction, compared to the BCI control based on voluntary brain activity modulations which require considerable amount of time for user training in order to learn how to modify their brain activity and additional time to obtain good performances.

Considering this fact, it can be extended to adapt information seeking applications (Nicolae et al., 2017a), industrial operator monitoring systems (Venthur et al., 2010) and many others (Müller et al., 2008; Blankertz et al., 2010c, 2016; Zander and Kothe, 2011; Erp et al., 2012).

Although online mental state BCI applications are still in the research and development step, the advancement of powerful machine learning techniques will materialize them into practice (Blankertz et al., 2002; Krauledat et al., 2004; Müller et al., 2004, 2008).

Chapter 4

Revealing the neural correlates of user efficient motor imagery tasks

As described in the introduction of this thesis, it is important that for the development of improved Brain-Computer Interfaces, the interest should be focused on the user. This study investigates different stimuli applied in a synchronous BCI system, to determine the most effective ones by analyzing the user reaction time during real motor movements and the brain activity during motor imagery movements, under the assumption that some BCI stimuli may generate faster reactions and stronger cortical potentials than others. Visual and auditory stimuli were chosen for investigation, and the corresponding brain potentials were further compared. In addition, different efficient motor imagery tasks that attracts users' attention and interest, while targeting stronger brain activity and fast and accurate mental movement execution for allowing a facile and agile BCI interaction. These user efficient tasks could provide a new mental control strategy for future BCI applications. As an acquisition method for brain signal recording the Electroencephalography (EEG) method is used in this study.

4.1 Introduction and state of the art

Motor imagery-based Brain-Computer Interfaces (BCIs) are the most largely investigated systems in BCI research (Grimm et al., 2010). The BCI decisions are founded on two or more motor imagery tasks, which can be expressed by the mental practice of different motor actions without the use of muscles or any body part activity, but only the brain. Aiming at improving and supplementing daily life activities, the BCI applications involve communication or control purposes (Wolpaw et al., 2002), or even rehabilitation (Mokienko et al., 2014). The implementation is possible by the replacement, enhancement or the repairment of motor or cognitive functions, for example controlling a prosthesis or a wheelchair device via brain signals for the individuals who lost a body part in an accident

(Kübler et al., 2006; Vanacker et al., 2007; Galán et al., 2008), or rehabilitating the capability to execute a real motor movement using motor imagery training for patients after stroke with small impairment or severe paresis (Mokienko et al., 2014; Morone et al., 2015; Carrasco and Cantalapiedra, 2016).

As described in the Fundamentals Chapter (2.4.2.2), the neural signals that are used to drive a motor imagery BCI system, generally involving hand and/or foot movements, are characterized by a decrease in the mu band power (8-13 Hz), namely desynchronization, appearing in the contralateral sensorimotor cortex, followed by a synchronization in the ipsilateral cortex (Pfurtscheller and Aranibar, 1977; Pfurtscheller and Neuper, 1997, 2001; Pfurtscheller and Silva, 1999; Pfurtscheller et al., 2006).

Despite the tremendous research in the last decades over the motor imagery BCI systems, some shortcomings still exist for this approach and this feasibility study aims to diminish the effect of one of them, namely the bothersome and tiredness effects on the users when performing the same tedious motor imagery motion for several repetitions (Pomer-Escher et al., 2014; Trejo et al., 2015; Talukdar and Hazarika, 2016). By choosing proper stimuli, efficient tasks and captivating paradigms, the users can gain interest in using the BCI and his performance and similarly the BCI's performance could increase over time.

Targeting this goal, different efficient motor imagery tasks are investigated in this study and one type particularly relates to user's interest and hobby. After the completion of the study, the user expressed strong interest in benefiting from such a BCI system. The study investigates the oscillatory activity considering the Sensori-motor rhythms (SMRs) observed as spectral perturbations (Makeig, 1993) which generates (de)synchronizations in the mu band, consistent with the scientific literature. The efficiency of the proposed tasks was further demonstrated by an increased classification performance of the neural activity. Overall, we recommend using pre-defined efficient motor imagery tasks for rehabilitation, cognitive functions enhancement, or any other possible motor imagery based BCI application. Specifically, finger button press, arm lifting and a user defined trigger pulling activity in form of imagery movements are investigated, considering visual or auditory stimuli in a BCI paradigm. While the motor imagery tasks that we use as a basis for comparison, namely finger movements (Blankertz et al., 2006a; Stavrinou, 2007; Furman et al., 2016; Kaplan et al., 2016) and arm movements (Badia et al., 2013; Tavakolan et al., 2016) receive a lot of attention in the scientific community, no user-defined imagery tasks are investigated to the best of our knowledge, making this investigation a novel concept in the BCI community.

The visual and auditory stimuli of the BCI system, were carefully chosen to improve the reaction time of the BCI user and enhance its brain activity, envisaging the limitations and capabilities of the visual and auditory human system. Different visual and auditory stimuli types were tested via the interface with a real movement execution experiment given by the easier task of finger button press. The most efficient stimuli were selected for the motor imagery experiment by investigating the PSNR of the signals and the user reaction time. While this evaluation of the stimuli in real motor execution experiments is not presented in this thesis, detailed information and results are presented in Nicolae, (2013).

In terms of investigation and methods approach (Section 4.2.3), the selection emerged from the following. Generally, the motor imagery brain response is mostly analyzed considering the spectral domain (Lee et al., 2009; Lee et al., 2010), which only considers one

aspect of information encoded in the neural data. The temporal information, ERPs, could also provide intrinsic knowledge of the activity within the patterns. While ERP alone can not entirely disclose the brain response characteristics as response to external stimuli (Makeig, 1993), the ERSP measure may offer information that is not contained in the ERP, through its investigation over the power modulations changes (Makeig et al., 2004). Therefore, combining the time and frequency domains seem a reasonable approach to be considered in order to provide additional complementary information which could highly provide not only in-depth understanding of the neural activity, but also advantageous classification outcome (Makeig et al., 2004).

4.2 Methods

4.2.1 Experimental design and scenarios for efficient user motor imagery tasks

4.2.1.1 Participants

The experiment is a preliminary case study performed on a male participant of 27 years old, with no experience in BCI. The participant is right-handed and has normal eyesight and normal hearing. The participant gave his written informed consent regarding the involvement in the study and the permission to record his brain signals and behavioral measures during the experiment for research purposes. The experiments were performed during evening, in a laboratory environment, with 35 dB background noise. For the moment, only one participant was chosen in order to investigate the impact of the efficient tasks and to adapt the signal processing and machine learning methods for an enhanced discrimination of the motor tasks. After the feasibility of efficient motor imagery tasks is analyzed and demonstrated, the next future study will include an adequate statistical number of participants.

4.2.1.2 Experimental paradigm

4.2.1.2.1 Stimuli

The timing and structure of the experimental design is detailed in Fig. 4.1, and is composed of three periods: *i)* relaxation, *ii)* attention and *iii)* trial. The first relaxation segment lasts for 2s and is represented by a black screen. The next attention segment which lasts for 0.5s, prepares the participant for the actual trial by presenting a cue with the “+” symbol of a 218×218 pixels size for the visual stimuli experiment and by playing a beep sound for the auditory stimuli experiment. The motor imagery task is performed in the trial segment of 3s long and is triggered by a left/right arrow symbol of size 392×214 in case of visual stimulation, or the pronunciation of the left/right word by a female voice of 250 Hz frequency with 70dB in the auditory (voice) stimuli experiment. The visual stimuli are scaled 1 to 3 as compared to the total screen size and the format used is PNG. For auditory stimuli, the format used is WAV.

Shortly, three stimuli scenarios were investigated (as in Tab. 4.1), considering different stimuli types: 1) Visual Stimuli (*Vis. St.*) referring to the use of visual arrows for the task and visual cue for the attentional period; 2) Visual Stimuli with an auditory attention cue

represented by a digital Sound (*Vis.-So. St.*); 3) Auditory Stimuli and auditory cue given by Voice Stimuli for the task and a digital sound for the attentional cue (*Vo. St.*).

The effective visual stimulus related to color was selected from the real left/right finger button press experiments by analyzing the results regarding user accuracy rate and reaction time. Although the efficient and simple visual stimuli that triggered the faster response considering real button press movement was the green stimuli on white background (Nicolae, 2013), we decided to select white stimuli on black screen for motor imagery, in order to have neutral stimuli for the general use (e.g. regarding color blindness). For the auditory attentional cue, the sound was selected with 3300Hz, 75 kbps and 80 dB amplitude.

The participant stayed seated with 50cm in front of the LCD screen and was requested to focus in the center of the screen and to complete a randomized series of 40 trials for each experiment: 20 trials for each left or right movement. The reduced number of trials was imposed in order to test the feasibility of using, as possible, a reduced number of task repetitions for a BCI system that will increase the interaction speed, reduce the tiresome effect at the user side, while still obtaining a good system performance in terms of classification.

The stimuli presentation was shown on a 22" LCD display (HP LE2201w) with 60 Hz frequency rate and built-in speakers. The software used for presenting the stimuli is SuperLab 4.0 (Cedrus Corporation). For the button press response, the RB-730 Response pad was used connected with the computer via USB cable.



Fig. 4.1 Timing for one experimental trial (with $t=0$ the stimulus onset) composed by the relaxation time (2s), the attention cue (0.5s), and the actual task period (3s) with right movement execution in this example. Same timing is considered for the auditory stimuli, where the digital sound is presented for 500ms in place of the attentional cue. (Figure taken from Nicolae, 2013, with permission)

4.2.1.2.2 Mental tasks

Aiming a stronger activation in the motor cortex (Guillot et al., 2009), kinesthetic motions from first person perspective are performed in the experiments, which consist in mental execution of all the muscle contractions and actions required by the respective movement, implying therefore a much more complex process than a visual imagination of the movement. The participant was trained three days in advance and couple of times in the day of the experiment in order to practice and get familiarized with the motor imagery concept. The neurofeedback shown for this motor imagery training phase was represented by the ongoing EEG signals as an amplitude evolution in time. During the experiment, different motor imagery mental tasks are inspected which involve left/right arm and finger movements, namely: index finger button press (index flexion), arm lifting, and a specific task related to user background and hobbies. For the arm lifting task, the user was asked to imagine the movement as if he would try to reach the presented visual stimulus. Considering the specific

task, the user freely selected the mental strategy that he is most comfortable with, and he chose ‘gun trigger pulling’, based on his main hobby and experience in shooting games. This involves an imagery left or right arm lifting as if the user holds and raises a virtual gun as in a gaming scenario, followed by an imagery index finger flexion representing pulling the trigger of the gun.

Considering the auditory experiments with voice stimuli, the participant concentrated on the voice speaking the current tasks, with eyes closed, and performed the corresponding imagery movements. In total, ten experiments are performed considering a mixture of stimuli and mental tasks, as in the table below (Tab. 4.1). Further, for the purpose of a viable comparison between different experiment types, we choose to perform the analysis (section 4.3) on only one run (first experiment) for each task, in order to have an equal number of trials.

At the end of the experimental study, the participant completed a questionnaire regarding his interest in the experiments and provided a personal estimation of his performance considering the stimuli types and the imagery motor tasks.

Tab. 4.1 Motor imagery experiment types (Table taken from Nicolae et al., 2014b, with permission)

<i>Stimulus type</i>	<i>Presented Stimuli</i>	<i>Attention type</i>	<i>Mental task</i>	<i>No. of experiments</i>
Visual (<i>Vis. St.</i>)	white and black stimuli	white cue	button press	4
Visual and sound (<i>Vis.-So. St.</i>)	white and black stimuli	1200 Hz sound	button press	2
Visual and sound (<i>Vis.-So. St.</i>)	white and black stimuli	1200 Hz sound	arm lifting	1
Auditory (<i>Vo. St.</i>)	female voice stimuli	1200 Hz sound	button press	2
Auditory (<i>Vo. St.</i>)	female voice stimuli	1200 Hz sound	trigger pull	1

4.2.2 Brain signal acquisition and equipment

The EEG activity was recorded using the BIOPAC system (BIOPAC Systems, Inc.), with a 1000 Hz sampling frequency and amplified with 20000 Gain. The BIOPAC hardware acquisition system consists in the MP150 acquisition unit, the UIM100C amplifier module, two EEG100C amplifiers necessary to record signals from the two hemispheres and the electrode cap CAP100C. The C3 and C4 gel-based electrodes were used, relating to the specific brain areas corresponding to the left and right arm movement. In addition, Electromyography (EMG) was also recorded for real movements detection, but this setting and analysis is not presented here (For more details, please see Nicolae et al., 2014a and shortly in Appendix A.2.2). As software acquisition system, Acqknowledge 4.0 was used. The recorded data are transmitted from the acquisition system to the computer via an UTP Intel (R) 82567M-3 Gigabit Ethernet network of 100 Mbps speed. The connection between the BIOPAC equipment and the software stimuli system is done via an I/O address bus.

For brain signal processing and data analysis, the MATLAB (The MathWorks, Natick, MA, USA) analysis software was used, including the MATLAB Signal Processing

Toolbox, the Statistics and Machine Learning Toolbox and the Wavelet Toolbox. Additionally, the EEGLAB (Makeig et al., 2000; Delorme and Makeig, 2004) toolbox was used regarding the time-frequency analysis domain.

4.2.3 Processing strategy to detect the specific motor imagery neural correlates

4.2.3.1 Preprocessing

First, for removing the interfering frequencies, a sequence of online hardware filtering was applied composed by a 0.1 Hz high pass filter and a 35 Hz 4 pole low pass Besselworth filter with a 50 Hz notch filter (40 dB attenuation). Next, the recorded data were off-line analyzed in MATLAB and EEGLAB. For removing the remaining noise, two filtering approaches were chosen and tested after careful investigation of the magnitude and spectrum response of different filters: 1) a combination of temporal filters and 2) wavelet filtering. The quality of the signals was analyzed by the Peak Signal-to-Noise Ratio (PSNR) measure (Appendix A.1.2) and the best method was selected thereafter for the processing pipeline.

1) The temporal filters approach consists in a sequence of an IIR comb filter of order 20 with 0.5 Hz bandwidth and 1 dB magnitude limits, applied twice on the signals. Next, it is followed by a FIR band stop equiripple filter of order 50 with the following constraints: 49.5 Hz – 50 Hz pass band, 50 – 50.5 stop band and 50.5 – 51 pass band intervals with and 0.5 to 40 dB magnitude pass for the frequencies lower than the pass band interval and 1 to 40 dB magnitude pass for higher frequencies. This schema is designed to filter the jitters and the noise line frequency of 50 Hz.

2) The second filtering approach employs the Interval-dependent wavelet denoising method (Appendix A.1.3.1.5), using Daubechies mother wavelet of level 5 with 3 intervals (Fig. A.1.1).

After filtering, the epochs were segmented in the interval (-2.5; 3 s) with baseline correction (-2.5; 0 s) and the noisy trials were manually removed from the data by visual inspection. Additionally, the artifact rejection technique, namely the Independent Component Analysis (ICA) using the Infomax approach (Section 3.2.2.2.1) was applied on the data, in order to detect the relevant neural patterns and check the activity sources (and remove the noisy components in case of an improper acquisition). The components selection was manually performed by visual inspection considering the spatial distribution (power topographic maps), power spectrum and components temporal activity among trials. The components related to channel pop artifacts (when channel goes off or the electrode drops or gets loose) are intended to be discarded from the data. Finally, no components were removed by ICA, relating to no noisy electrodes within the available spatial resolution (two channels).

4.2.3.2 Neural correlates detection

In order to analyze the corresponding oscillatory activity revealing the sensorimotor synchronization or desynchronization, the ERSP time-frequency transformation was applied on the data after the ICA decomposition. The ERSP method (Section 3.3.4.1) was computed using different transformation: Short-Time Fourier Transform (Appendix A.1.3.4.2) and wavelet transform (Appendix A.1.3.4.3). The transformation based on Fourier analysis

considers a Hamming window of 128 samples and 100 overlays, over the spectrum range from 3 to 35 Hz. The ERSP based on wavelet transform considers sinusoidal Morlet wavelets of 3-cycles which are increased slowly with frequency, reaching half the number of cycles as in the equivalent FFT window of the highest frequency (applied with a Hanning overlapping window).

Spectral perturbations are expected to appear in the mu frequency band (8-12 Hz) and possibly in beta (13-30 Hz), relating to the Event Related (De)Synchronization (ERD/ERS) variations (Chapter 2.4.2.2). In addition, the inter-trial variability of the trials is inspected by analyzing the local phase coherence with the Inter-Trial Coherence method (Section 3.3.4.2).

For the classification, regularized Linear Discriminant Analysis (rLDA) with shrinkage of the covariance matrix was applied (Appendix A.1.4) in form of a multi-class discrimination, deciding between left, right and no movement. Aiming a robust and efficient classifier, the classifier is fitted by setting the optimal parameters according to the distribution of each class and the redundant features are removed. The best regularizations parameters (γ and δ) were explored within 25 levels and detected by considering the lowest error rate of crossvalidation. The redundant features as detected by the two parameters are further removed (as in Appendix A.1.4). The classifier considers multi-modal features considering the temporal, spatial and spectral domains. The amplitude values for each trial in the 300 - 2300 ms interval within the 1 - 49 Hz frequency range are considered for the temporal features (filtered using 1 Hz FIR high pass filter of order 30 and a Chebyshev type II of order 10 with 3 dB of ripple in the passband up to 42 Hz and 50 dB of attenuation in the stopband starting at 49 Hz). The temporal features are concatenated with the power spectral features of the corresponding mu and beta frequency bands (8-12 Hz; 18-25 Hz) where the strongest perturbations appear, and both features types relate to the two channels (C3 and C4) as spatial distribution information. The spectral features are estimated by the Fast Fourier Transform (FFT) method and computed on the same time interval, 300-2300ms. For the no movement condition, the temporal and spectral features as amplitude and power values are considered from the relaxation interval before each trial: from -2500ms to -500ms. The feature types are normalized using z-score normalization and concatenated in the feature vector which is given to the classifier.

The classifier was validated using 5 folds cross-validation and the performance was assessed in terms of accuracy given by the normalized confusion matrix and the resubstitution errors (Section 3.4.6.3).

4.3 Findings

4.3.1 Behavioral data

Information over the behavioral data is offered by the subjective questionnaire, in which the participant stated an increased interest, performance and attention for the voice stimuli and for the trigger pull task. As regarding subjective performance, the participant expressed no errors regarding a mistaken trial between left or right and no trial misses.

4.3.2 Filtering measures comparison

When comparing the temporal and wavelet filtering responses regarding the PSNR, a significant better quality of the signal is observed for the wavelet filtering approach. The C3 and C4 electrode signals regarding real movement button presses are considered for the comparative analysis and the wavelet filtering results in a PSNR of almost 5 times higher than in the FIR filtering (Tab. 4.2), effect which is significant with the one-way ANOVA statistical test ($p = 0.0052$).

Tab. 4.2 Signal quality estimation after filtering, based on the PSNR measure (Table taken from Nicolae et al., 2014b, with permission)

Signal	Movement	PSNR	
		FIR filtering	Wavelet filtering
Channel C4	Left button press	10.7859	51.1709
Channel C3	Right button press	6.0897	55.6603

The result of the noise removal over the quality of the signal is investigated also considering the power spectrum. The power spectral density (PSD) of the signal was estimated using the Welch method (Appendix A.1.3.3.2) with 1024 Kaiser windows of 256 size length and no overlap. Fig. 4.2 shows the PSD of the C3 signal before and after temporal filtering, while the spectrum for the C4 signal coincides². We can observe a cleaner signal, with no strong peaks at 50 Hz and above as interferences from the 50 Hz power line source, compared to the original signal. The power spectrum from 0 to 100 Hz corresponding to the brain activity, follows the 1/f shape and contains the 10 Hz alpha peak.

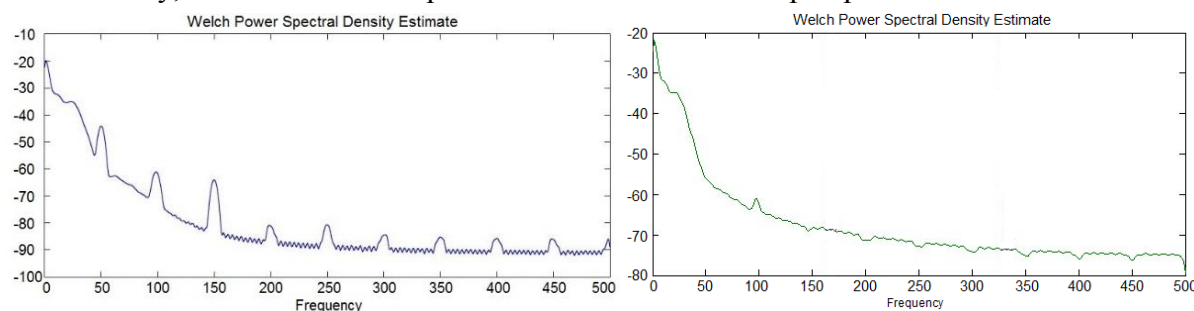


Fig. 4.2 Power Spectral Density Estimate using the Welch method for the original signal (left plot) and filtered signal (right plot). (Figure taken from [14], with permission).

For further analysis, the wavelet filtering was applied as preprocessing step due to its improvement in terms of PSNR.

4.3.3 Detecting the neural correlates of specific motor imagery tasks

4.3.3.1 Temporal analysis

Firstly, we have a look over the evolution of the amplitude modulations over time in the mu band, corresponding to the imagery movement. After corresponding band-pass filtering in the 8-12 Hz range, the signals can be further investigated. For example, in case of the arm lifting

² In order to investigate the filters effects for line noise diminuation (including the 50Hz line noise echos: 100Hz, 150Hz, etc.), the entire frequency range was analyzed as the purpose of comparison (0-500Hz), while later on in the analysis the pass-band filtered signal of 0-50Hz was considered.

task (Fig. 4.3) as response to visual stimuli and auditory attentional cue (*Vis.-So. St.*), after the 300 ms point which relates to the timing perception of the stimulus, the modulations change on average, with stronger fluctuations (higher amplitude) for the left imagery movement as compared to a decreased amplitude for the right imagery movement. The lag in phase synchronicity between hemispheres and conditions is more clearly observed on single trial (right image in Fig. 4.3 and further in Fig. 4.5)

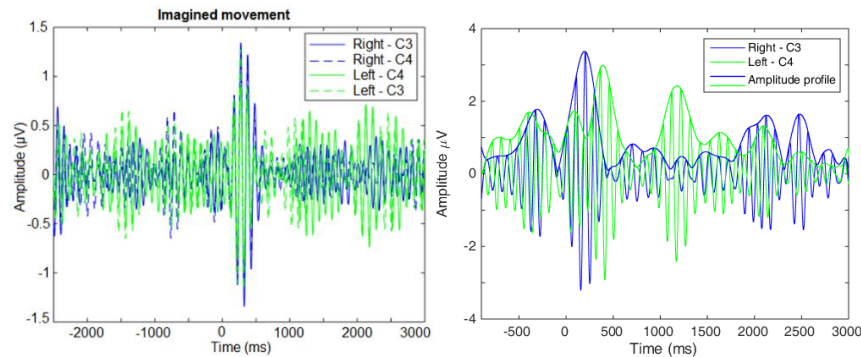


Fig. 4.3 Mean amplitude evolution over time for the arm lifting motor imagery task as response to *Vis.-So. St* (left image) and single trial amplitude representation (right image). The thicker line on top of the single trial representation highlights the amplitude profile (envelope) and it was estimated with Hilbert transform. (Left figure from Nicolae et al., 2016b, with permission)

4.3.3.2 Time-frequency analysis

Secondly, the spectral perturbations generated by the sensori-motor rhythm (SMR) are investigated via time-frequency representations. The Event Related Spectral Perturbations (ERSP) phase locked to the event are presented for example in case of the motor imagery trigger pull task as reaction to voice stimuli in Fig. 4.4. Related to the motor imagery movement, the most significant pronounced perturbations according to a 0.01 bootstrap significance level appear in the mu 8-13 Hz frequency band in form of a desynchronization (-4 dB) for the 500 - 1500ms temporal interval considering the contralateral hemisphere (electrode C3 for right movement and electrode C4 for left movement). This is followed by a synchronization (4 dB) in the same frequency band for the 1600 - 2100ms interval. Similar follow up with a delay appears in the beta band, 18-25Hz, starting with a desynchronization and is followed by a synchronization. The ERSP also shows a brief but significant increase in power at about 30Hz. Considering the ipsilateral hemisphere, interestingly ERD appears in the mu and beta band. Another increase in power is observed at 500-1000ms in the theta range.

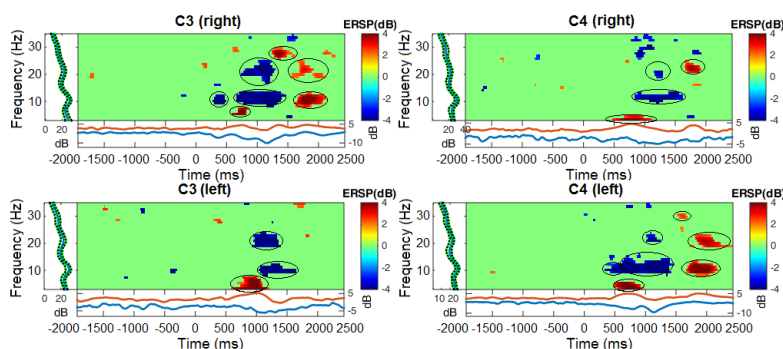


Fig. 4.4 Event related spectral perturbation for the right/left imagery trigger pull (Vo. St.) at electrodes C3 and C4. The color bar at the right side of the graphs show the scale of the plots in terms of dB for the power spectral density (-4 to 4 dB). The lateral left panel shows the baseline mean power spectrum, and the lower panels show the ERSP envelope (low and high mean dB values, relative to baseline, at each time in the epoch). The circled areas represent significant ERD/ERS with bootstrap level 0.01, which are found also at the 0.001 significance level. The ERSP was computed using the Morlet wavelet transform for the 2.9 – 35 Hz range, on the interval -2000 – 2500ms, relative to the baseline period of -2500 – 0ms. (Figure modified from Nicolae et al., 2016b, with permission).

Considering the temporal and spectral synchronization within EEG, the ITC in Fig. 4.5 illustrates the timings where phase-locking occurs or not. Some significant ITC at about 15-20Hz for the -500 – 0 ms interval is observed (which may correspond to the decrease in power at 0ms in Fig. 4.4, bottom left plot), which might indicate therefore that the EEG activity becomes phase-locked in single trials (with respect to the stimulus). However, the time and frequency points relating to significant ITC and ERSP are not necessarily identical. Furthermore, this effect is insignificant at the 0.001 bootstrap significance threshold. Considering the other conditions, similar ITC is encountered, where it hardly reaches significance and cannot be interpreted. While searching for other influences, the oscillatory activity, for example, does not significantly influence the ERP trace, according to ITC (bottom plot in Fig. 4.5).

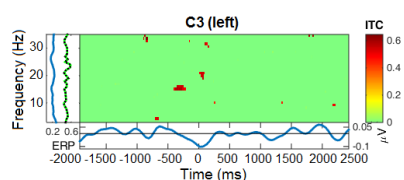


Fig. 4.5 Inter-Trial Coherence (ITC) for the left imagery trigger pull (Vo. St.) at electrode C3. The color bar at the right side of the graphs show the strength considering coherence (red - statistically significant phase coherence; green – no significant phase coherence). The bottom panel shows the mean ERP trace. Bootstrapping was used to identify significant levels of ITC (with 0.01 significance threshold). (Figure modified from Nicolae et al., 2016b, with permission).

Considering imagery right finger button press with voice stimuli in Fig 4.6, more information is encountered in the beta band, according to the bootstrap significance level of 0.01. Beta desynchronization is encountered at 1000 -1500 ms, followed by and beta synchronization in the 1500-2000 ms interval in the contralateral area for the right movement. For the left movement, an ERS is observed in the alpha band, simultaneous with ERD in the

beta band. Regarding the ipsilateral information, strong perturbations appear in form of ERD at the same timing related to the imagery movement.

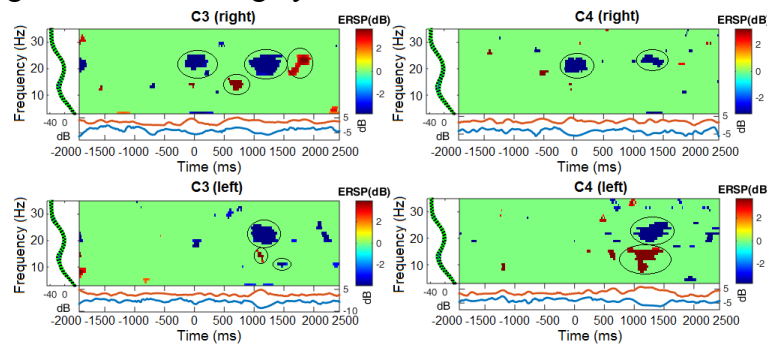


Fig. 4.6 ERSP at the C3 and C4 electrodes for the right index finger motor imagery button press task (*Vo. St.*). The ERSP (-4 to 4 dB) was computed using the STFT method on the 2.9 – 35Hz frequency range and -2000 to 2500ms timing interval, with -2500 ms baseline, highlighted by 0.01 bootstrap significance level (with the circled areas significant also for a 0.001 level).

In the other motor imagery activities, similar spectral perturbations are revealed (detailed investigations without bootstrapping in Nicolae et al. (2014b)).

4.3.3.3 Neural components

The temporal evolution of the ERP components, as available with the limited spatial resolution, can be observed in Fig. 4.7, for the right imagery button press with voice stimuli. The component's evolution starts with a slight amplitude decrease in the contralateral side, which becomes more pronounced around 800 ms, during the presumed imagery movement and is complemented by an increase in the ipsilateral side, around 1400ms.

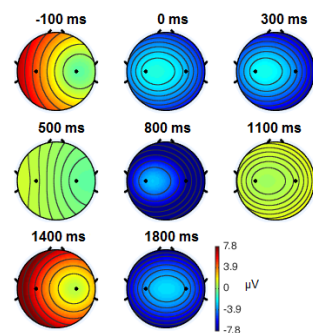


Fig. 4.7 Temporal evolution of the ERP components (average data) considering the right imagery button press with *Vo. St.*; (Figure is taken and extended from Nicolae et al., 2016b, with permission).

In addition, to investigate the contribution of the ICA components to the time series (ERP) and oscillatory domain (ERSP), Fig. 4.8. shows, for example, ICA components activations for all trials, considering left imagery finger button press with visual stimuli. The ERP image plot in Fig. 4.8 (left side) shows an increase in amplitude (coded in red) observed at 400 ms after the stimulus related to the P300 potential, and is followed by a decrease in amplitude starting from 600 ms until 1000ms (coded in blue), and continues with a slight increase in amplitude for the 1000-2000ms interval. In terms of variability between trials, differences exist in the range 800-2000ms, due to different motor imagery latencies, which

slightly influences also the ERP. The other analyzed measures suggest that Component 1 accounts for a few of the EEG power at 10 Hz (around 400ms in the ERSP mean power trace) and for little of the average ERP (around 400ms and 1400ms in the averaged ERP trace). The phase at the analyzed frequency (9 - 11 Hz) is evenly distributed, except in the 400ms vicinity where ITC shows a value of 0.7 suggesting phase synchronization according to the bootstrap significance level (0.01). Overall, the analysis relates to an ERP component, with more contributions to the time series.

On the other hand, the second component contributes multiple times throughout the oscillations (ERSP at 9-11 Hz) and slightly to the time series (to an amount of $0.5\mu\text{V}$). Furthermore, the component may likewise contribute to other oscillatory phenomena present at different frequencies, which are not visible here due to one frequency phase-sorting. No significant phase synchronization is shown given by no ITC values higher than 0.5. These contributions along with the pattern spatial distribution and the power spectrum of the component strongly suggest a mu component, offering additional information from the neural oscillations rather than the time domain.

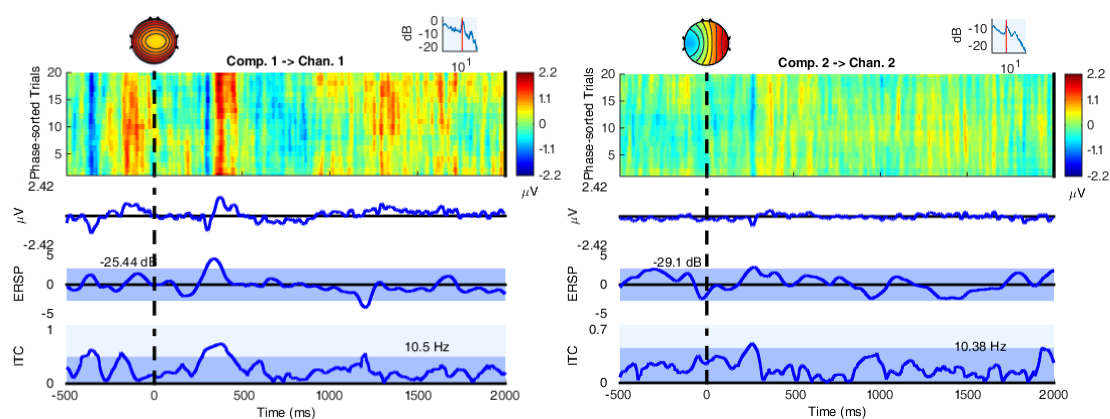


Fig. 4.8 ICA components contributions to ERP and ERSP, on the time interval -500ms to 2000ms (stimulus onset at 0ms), considering the left imagery button press task (Vis. St.). The small top figure shows component's power spectrum for the 2-35Hz band. The ERP image plot under shows the amplitude evolution of all trials ($-2.2\mu\text{V}$ to $2.2\mu\text{V}$), phase-sorted at the alpha frequency band (9-11 Hz). The three blue trace plots underneath show: • component's contribution to the average ERP time evolution ($-2.42\mu\text{V}$ to $2.42\mu\text{V}$); • component's contribution to the ERSP mean power at 9-11Hz (-4 to 4dB); • and phase synchronicity over all trials (ITC values in the 0–1 range with bootstrap significance level of 0.01). For an absolute representation of component's activity at an electrode (absolute value and polarity), the components were back-projected to the corresponding channel: Component 1 \rightarrow Channel 1 (C3) and Component 2 \rightarrow Channel 2 (C4). (Figure extended from Nicolae et al., 2016b, with permission.)

4.3.4 Classification of specific motor imagery tasks

For an overview over the distribution of the data, see for example the scatter plot of the imagery trigger pull data, shown in Appendix A.2.1, Fig. A.2.1.

Aiming enhanced classification performance, the optimal regularization parameters gamma (γ), and delta (δ) are searched and detected from the training data. In addition, dimensionality reduction is performed by removing the redundant features. The minimum

number of features that still produce a good quality of the classifier is selected thereafter. Depending on each case, an optimal tradeoff has to be considered between the model size and accuracy. For example, in case of the data from the arm lifting motor imagery task with visual and sound stimuli in Fig. 4.9, the smallest optimal number of features that generates a small mean classifier error rate of about 0.2, was selected as 2600. This reduces to a fifth portion of the features, which automatically decreases the computational complexity of the classifier. As it can be seen in the figure, using more features in this case does not produce a considerable classification enhancement (with less than 0.2 error rate), while choosing less features could weaken the classifier reliability (more errors). The error rate in this case is the misclassification error rate, computed by the average fraction of misclassified data in crossvalidation on the whole dataset. The regularization parameters selected here for 2600 features are: $\gamma = 0.9167$ and $\delta = 0.1076$. For other tasks, even less features are enough, e.g. 2000 features for the imagery trigger pull task with *Vo. St.* (Tab. 4.3).

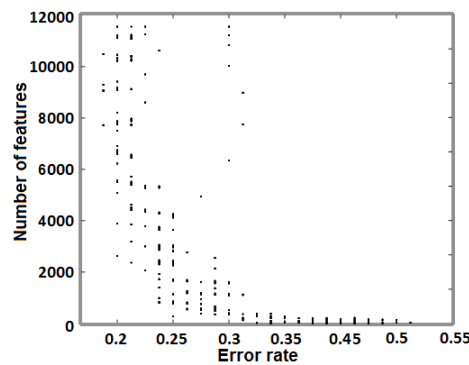


Fig. 4.9 The performance of the classifier given by the error rate, in relation to the number of features. The data refers to the arm lifting motor imagery task (*Vis.-So. St.*). Figure modified from Nicolae et al., 2016b, with permission (more features).

Tab. 4.3 Features type, original features quantity and reduced features quantity

<i>Motor imagery tasks</i>	<i>Features type</i>			<i>Total quantity (number of features)</i>	<i>Final quantity (reduced number of features)</i>
	<i>Temporal (amplitude in time: 300ms - 2500ms, for 0-50Hz)</i>	<i>Spectral (power in time: 8-12Hz and 18-25Hz)</i>	<i>Spatial (C3 and C4 electrodes)</i>		
finger button press (<i>Vis. St.</i>)	2000	4000 (2000×2)	× 2	12000 (6000 × 2)	2000
finger button press (<i>Vis.-So. St.</i>)					2600
arm lifting (<i>Vis.-So. St.</i>)					2600
finger button press (<i>Vo. St.</i>)					3000
trigger pull (<i>Vo. St.</i>)					2000

After setting the optimal parameters and the number of features, the multi-class classification is performed for the motor imagery tasks (Fig. 4.10, left image). Referring to the type of stimuli, highest mean performances are observed considering the visual and visual-sound stimuli with 0.7 to 0.84 normalized accuracy. Good performances of 0.61-0.65 are also observed considering the voice stimuli regarding the imagery trigger pull and button press tasks, but lower than the visual and visual-sound experiments.

Comparing between imagery tasks, the arm lifting, and finger button press with *Vis.-So. St.* experiments seem to result in the best performances (0.81 – 0.84), followed by the other finger button press tasks (0.61-0.7) and the proposed efficient task of trigger pull (0.65). Although the proposed trigger pull task classification did not exceed the classical finger button press tasks, the trigger pull task accuracies are still highly significant above chance level (t-test with $\alpha = 0.01$). Notice that all performances are high above chance level (33%), confirmed by the two-sample statistical t-test at the 0.01% significance level or higher.

Furthermore, the binary classification results between left and right imagery movements, performed with the same features and settings, are significantly high of 78-90% (Fig. 4.10, right image).

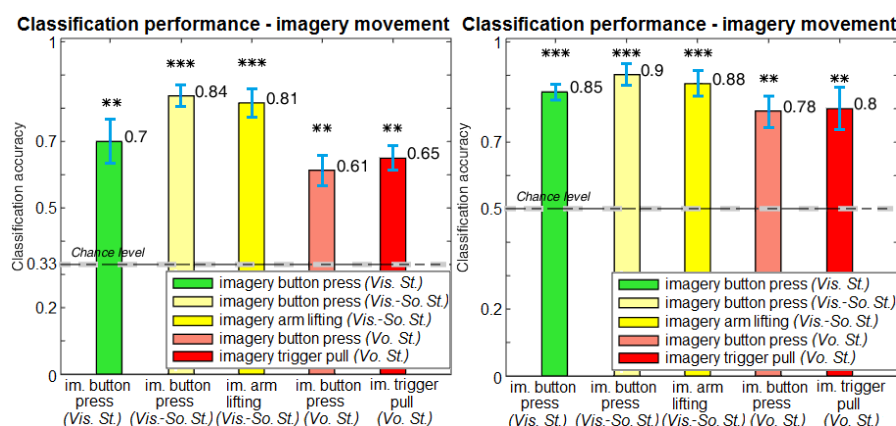


Fig. 4.10 Average performance (5 folds) for multi-class (left image) and binary classification (right image) for the motor imagery tasks: button press (*Vis. St.*), button press (*Vis.-So. St.*), arm lifting (*Vis.-So. St.*), button press (*Vo. St.*), trigger pull (*Vo. St.*). The blue error bars represent the standard error of the mean, SEM. The dotted black with grey horizontal line represents the chance level of 33% or 50%, respectively. Performances are statistically significant over chance level with t-test (** for $\alpha = 0.01$; *** for $\alpha = 0.001$; multi-class: $p=0.0052/ 0.0001/ 0.0004/ 0.0035/ 0.001$; binary: $0.0002/ 0.0001/ 0.0007/ 0.0042/ 0.0093$). Figure modified from Nicolae et al., 2016b, with permission (related to more classification features).

Moreover, the results of the classification discrimination are detailed in the confusion matrices showing the resubstitution errors for each class (Fig. 4.11). The confusion matrices show few misclassifications between left and right movement, and almost no assignments of a movement (left or right) to the no-movement class. For example, in the trigger pull with *Vo. St.* experiment (Fig. 4.11), 16 no-movement trials are classified as left/right movements (13 left and 3 right), 6 left movements are wrongly classified (2 no-movement and 4 right), and 7 right movement trials are wrongly classified as 2 no-movement and 5 left movements. In this case, the classification accuracies within each class are: 0.6 for no movement, 0.7 for left movement and 0.65 for the right movement task.

signals in terms of temporal (ERPs), spectral (power spectrum, spectrogram, ERSP) and spatial information (spatial distribution over channels in form of scalp maps).

4.4.1 Comparison with previous studies

An accurate comparison between different studies is difficult to be performed due to different experimental settings and different signal processing scenarios and machine learning techniques involved, but for the purpose of highlighting the presented research in the scientific community, some important differentiations with the state-of-the-art studies will be pointed out in the following.

Considering classification performances, similar or even smaller classification performances were found in other studies, as compared to the case study in question. For example, in Furman et al. (2016), researchers investigated imagery finger flexion as reaction to auditory stimuli. They investigated the thumb and pinky finger flexions of each hand, and the simultaneous flexion of both thumbs and both pinkies, giving 6 classes in total and 30 trials for each task. As features, normalized covariance matrices in time and space from 64 channels are considered, along with normalized wavelet filter bank features. The multi-class discrimination uses a one versus one multi-class SVM (Support Vector Machine) with a linear kernel classifier evaluated with 10 folds cross-validation, resulting in a single-participant classification accuracy of a maximum 36.2% and a minimum of 22.83%, compared to the chance level for 6 classes of 16.71%. If we extrapolate to a 3-class discrimination with 33.33% chance level, the results could imply a range of 45.54% - 72.21% in accuracy, smaller than the classification accuracy of 61-84% obtained in our case study for the imagery finger flexion.

In an online BCI experiment for controlling a virtual avatar by imagery arm extension, Badia et al. (2013) obtained good performances for a similar three class discrimination between no imagery movements, left and right imagery, using a linear classifier regarding alpha, beta and gamma frequency bands. The classification accuracies are similar as in our study, ranging from 65% to 97% with an average of 85% as compared to 81% in our arm lifting task. While considering participant interest, the participants in the Badia et al. (2013) experiment, expressed that control of the avatar's arms was difficult, rating on average with a 2.52 score out of 5. Considering combined features for the classification could increase the system performance as in our study, and therefore ease the control process, while contributing to an increased interest for the user considering more effective and attractive tasks.

A recent study by Rimbert et al. (2017), investigated and proposed the use of discrete motor imagery (DMI) as compared to continuous motor imagery (CMI), in order to overcome participants's fatigue and boredom effects in a motor imagery based BCI and to improve efficiency such as detecting faster a motor imagery task. Where CMI refers to a continuous and repetitive execution of a motor imagery task, the DMI considers short lasting imagery movements. As comparison, they investigated 4s of four repetitive imagery right finger flexions for the CMI and short imagery flexions of 2s. In this way, the DMI movement distinguished from the CMI movement by the repetition of the imagined movement and the timing requested for performing the movement. Although, their findings considering classification show no difference between CMI vs. rest (0.714%) and DMI vs. rest (0.719%),

DMI could have a future impact in the BCI domain regarding a faster detection of the movement (faster information transform rate), while also avoiding user's fatigue by reducing the repetitive movement and shortening the execution. Considering neurophysiology, the grand average power spectrum of the DMI showed a decreased amplitude of the ERS compared to the CMI task, which might be due to the summation of the overlapping patterns in the CMI, more precisely by the concatenation of several ERDs and ERSs produced by several motor imagery executions. In addition, authors detected a bigger variability between participants for the ERD and ERS modulations in the CMI task, which might be due to the same reason. This variability may also give a negative impact on the classification rate. In our study, we also performed a short DMI of 3s, and in addition we use effective tasks to improve participant's interest, the classification performance of 78-90% for the two-class discrimination is higher compared to the range of 57-90% in the binary classification of the Rimbart et al. (2017) study. However, their experiment considers 16 participants and their classification involves CSP features based on the spatial information from 9 electrodes, which brings additional improvement and spatial representation and is of interest to be investigated in the future.

Other works that successfully considers feature combinations in multi-class paradigms of imagined movements (left hand, right hand and foot) are presented in Dornhege et al., (2004a) and Fazli et al., (2015) and shows once more that these combined approaches significantly boost BCI performances.

4.3.5 Open questions and conclusions

Prior to EEG analysis the signals were preprocessed in order to remove the interferences and noise sources and to obtain a cleaner signal. The wavelet filtering performed better than the temporal filtering, resulting in a more increased PSNR of the signal. Next, the relevant components and features that relate to the corresponding motor imagery neural activity were detected and extracted from the data.

Considering the signal processing steps (Section 4.3.2), the filtering and artifact removal techniques using wavelet filtering provided good signal quality and the non-neural artifacts were removed as possible. Next, the Independent Component Analysis helped to detect the corresponding motor imagery components.

The motor imagery tasks elicited the well-known sensori-motor rhythms observed in the ERD/ERS effects of the corresponding brain hemisphere. In addition, the effect of higher amplitude modulations for left imagery compared to right imagery, shown in the amplitude evolution over time of the pass band data (Fig 4.3), is consistent with the scientific demonstrated neural effect, which states that uncommon activities give a higher potential than regular activities and stronger desynchronization in the mu-frequency band, i.e. for left arm movement for right-handed user (Klöppel et al., 2007), or for extraordinary compared to ordinary actions observation (Stapel et al., 2010).

Based on the preliminary investigation in this case study, the efficient imagery tasks relating to user's hobby, namely the trigger pull task, resulted in good performances of the classifier. However, the 'trigger pull' classification task resulted in a decrease as compared to the basic tasks of imagery finger button press and arm lifting. When referring to the areas and

brain processes involved in the motor imagery tasks, it was expected to obtain higher classification accuracy for the arm lifting and trigger pulling tasks as compared to finger button press, because the motor imagery of a bigger body part (e.g. arm) covers a larger area of brain activation as compared to a small size body part (e.g. finger) (Kandel et al., 2000). However, no discrepancies are obtained between arm lifting and finger button press for visual and sound stimuli ($p=0.587$ two-sample t-test, $\alpha=0.0001$) and similarly for the trigger pull task as compared to the button press task with voice stimuli ($p= 0.3739$ two-sample t-test, $\alpha=0.0001$). For the trigger pull task, because it comprises a more complex imagery process, involving arm lifting and finger flexion, maybe it becomes harder to be discriminated due to many processes involved and limited spatial information available (two channels). Another reason of this opposite performance obtained might be due to specific brain reaction on the type of stimuli: voice stimuli, because smaller accuracies were obtained also for the finger button press in scenario with the voice stimuli. Even so, the use of this type of stimuli for further applications is supported by increased user interest described in the experiment's questionnaire, where the participant stated an increased interest, performance and attention for the voice stimuli. The reduced classification performances can be also due to an increased tiredness for the participant at the end of the experiment (*Vo. St.*) as compared to more energy in the beginning of the experiment (*Vis. St., Vis.-So.St.*). All-inclusive, the hypothesis presented here have to be further investigated in a more detailed study, with aspects highlighted in the next section (Section 4.5).

In another train of thoughts, when one might expect not so high classification performances of 61-84% in case of imagery movements (three classes), note that these results might be due to the reduced data and one participant classification. The small number of trials was enforced to test the feasibility of using a small number of repetitions that can be later used in a BCI system, while obtaining high classification accuracies. The feasibility of few repetitions was successful here in the offline case, although a comparison with multiple trials repetitions is necessary in the online case. In addition, the combined feature approach which considers the complementary temporal and spectral information contributed to enhanced performances.

On the basis of the available neurophysiological effects observed in the ERPs, ERD/ERS and power spectrum, the investigated efficient motor imagery scenarios are feasible and can be further investigated in a larger experimental study. The use of the effective tasks in the context of BCI applications is reinforced by the classification results, offering comparable performances with respect to a basic task, while also taking into consideration user's interest and reducing therefore the bothersome effect within a BCI.

4.5 Limitations and future developments

As the effective tasks seem worthwhile to be considered for the purpose of BCI applications, some limitations and potentials flows which are described below can be improved and investigated further. The investigation can be deepened in a more detailed study considering more participants, e.g. 15 or more aiming a statistically significant group and more channels, e.g. 32 channels or more (Sannelli et al., 2010). Compared to the current case study in which we could not draw concrete conclusions considering the sources and the spatial distribution

of the activity based only on two channel data, the future in-depth study should consider more channels. This will provide a better spatial representation of the activity over the sensorimotor area and an efficient artifact removal. For the artifact removal case, additional channels in the occipital and in the frontal area will help removing the noise activity generated by the visual cortex and the eye movements.

In terms of hardware equipment and recording, it was inconvenient to connect multiple channels due to many amplifier modules and lots of cables (one amplifier module per channel). Furthermore, the use of active electrodes (with built-in amplifier) will greatly improve the EEG signal quality (MettingVanRijn et al., 1996) and controlling the impedance will help for a better conductivity, producing an enhanced signal quality (Kappenman and Luck, 2010). For future studies, it is recommended that the notch hardware filter, or other hardware filters in general, are to be avoided while they tend to introduce distortions in the data (Luck, 2005; Dickter and Kieffaber, 2013), in form of phase shifts (and delays), "ringing" in the data stream.

Considering experimental design, more trials can be integrated aiming statistically significance in case of higher trial to trial variability, and also as a comparison medium with the reduced trials case. While the current study did not evaluate the contribution of the amount of trials for BCI systems, a follow up study might be useful in this direction. Related to stimuli, the enhanced visual and audio stimuli as selected in Nicolae, (2013) can be further investigated within the motor imagery experiments (e.g. green stimuli on white background). For the stimulus paradigm, the position of the arrows in the visual stimuli experiment should be placed in the center of the screen. This will reduce the horizontal eye movements and the possible involved issue in the current study can be avoided, which relates to the fact that the classifier may learn the corresponding left or right eye movements instead of the actual motor imagery activity. If equivalent experimental setup is desired, then the eye movements contribution may also be overcome to an extent within signal processing (Section 3.2.2). Furthermore, the dissimilarities in the stimulation between the rest period (no visual/audio stimulus) and the trial period (visual/audio stimulus) generates strong inconsistencies in the EEG which might affect the classification. Without a good spatial representation and removal of the non-task related components, the current classifier might strongly relate to the visual brain responses generated by the external stimuli, and not to the motor imagery itself. A simple solution requests similar stimulation in the experimental paradigm for all conditions (left, right and rest) to avoid any discrepancy.

In terms of experimental scenario, more experiment combinations for each type of stimuli and imagery task should be performed for more accurate comparisons: e.g. the trigger pull task in scenario with visual stimuli and visual with sound stimuli, in addition to the voice stimuli experiments. Moreover, all task scenarios should be considered with eyes opened, as for a viable comparison between them. On this line, 'eyes closed' have a different amplitude modulation, topography and power level as compared to 'eyes open' when the alpha band is suppressed (Berger, 1933; Adrian and Matthews, 1934; Barry et al., 2007; Gomez-Ramirez et al., 2017). These important differences produced in the EEG signals and in the neural components might be involved in the classification differences between the tasks with visual or sound and voice stimuli.

While in the current study, the classification performances are reduced for the proposed effective tasks as compared to the classical motor imagery tasks, a bigger range of effective motor imagery tasks that stimulate user's interest and takes into consideration his preferences is intuitively to be considered. Moreover, the tasks should be selected to consider uncommon activities in the users' area of interest, which may elicit a more powerful brain response, as compared to known, common activities (Klöppel et al., 2007; Stapel, 2010).

Another aspect that has to be included is a more specific user neuro-feedback in the motor imagery training process, for a better overview and control of user's own signals. As compared to the current simple feedback, where only the evolution of the EEG signals was shown, a better way for example, is to consider the envelope of the signals in the mu band for a better representation of the ERD and ERS effects (Clochon, 1996), or the power band values in the mu, alpha and beta frequency bands representative for the motor imagery activity, or moreover, topographical maps of the cortical activity in the mu band (Hwang, 2009). Motor imagery is a complex process and requires intense concentration and attention and as it has been variously shown in different studies that not all participants are capable of controlling their sensori-motor rhythms (Guger et al., 2003; Kübler and Müller, 2007; Vidaurre and Blankertz, 2010; Blankertz et al., 2010a; Vidaurre et al., 2011b). Therefore, closer investigation has to be performed on the participants' brain signals in the training phase, in order to check the existence of the corresponding mu power band modulations.

Considering the signal processing and machine learning steps, there is always place for improvements. First, automatic trial removal can be implemented (as in Section 3.2.2.1) in contrast to the manual selection based on visual inspection that is used here. Further, appropriate treatment of eye movements and muscle artifacts should be considered, so the artifacts have low to no implications in the classifier decision. This can be performed by applying for example, the ICA method with MARA feature selection as presented in Section 3.2.2.2.

For a more accurate extraction of the neural information, decomposition methods can be used, SSD or CSP for example, as in Section 5.2.3.4, for the case with a higher number of channels. For a closer relation to the task-related neural activity, the amplitude evolution of the signal over time (envelope) which decreases or increases with respect to motor imagery, can be considered instead of the FFT spectral features, while FFT has a large noise sensitivity and can not capture transient features in a signal, nor time-frequency information.

While motor imagery produces changes in both temporal and spectral domains, an interesting approach from Lu and Yin (2015) which combines the ERP information with the ERSP information and produces enhanced classification discrimination, is of interest to be considered. On this line, it will be interesting to further evaluate the contribution of the motor imagery activity to each measure (ERP, ERSP, spectra), detecting where, when and how much is involved, extending the investigation from Section 4.3.3.3. In addition, one can consider, for example, intelligent feature selection algorithms based on weighting (Sugiyama et al., 2007) in order to detect which features are the most representative for the corresponding neural process, temporal or spectral, and to which extent.

4.6 Lessons learned

- ✓ The motor imagery tasks elicited the well-known sensori-motor rhythms observed in the ERD/ERS effects of the corresponding brain hemisphere.
- ✓ The specific motor imagery tasks corresponding to user background proved to be efficient by user's prolonged attention during the experiment and its subjective evaluation stating increased interest and performance.
- ✓ The classification discriminations between left, right (and no imagery movements) considering all types of motor imagery tasks resulted in very good performances for both multi- and binary cases, as compared also to other motor imagery studies.
- ✓ Using complementary information from the temporal and spectral domains, brings additional information to the classifier, producing therefore enhanced performance.
- ✓ Albeit a low number of data points are available due to the reduced number of stimuli, the simple LDA classification method still performs very good.
- ✓ The wavelet filtering method resulted in better signal quality compared to temporal filtering, considering the current available data.
- ✓ After the feasibility was analyzed in this case study, the next in-depth experimental study should consider a statistically significant group of participants.
- ✓ More scenarios combinations in terms of stimuli and tasks should be further implemented and investigated for appropriate comparisons.
- ✓ More channels need to be integrated in the next in-depth study for a more detailed spatial distribution of the brain activity.
- ✓ To assure a correct execution of the motor imagery paradigm, a more specific neurofeedback needs to be implemented in the future study.
- ✓ Carefull treatment and rejection of artifacts (eye and muscle activity) has to be performed in the future study.
- ✓ Carefull consideration is further requested for the experimental design, to avoid additional eye movements and dissimilarities in the stimuli between conditions (left/right/rest), which might induce different visual responses.

Chapter 5

Investigating the neural correlates of cognitive processing levels

The functionality of general BCI systems are based on choosing one type of task and request the user to perform the corresponding mental task and voluntary control the variations of his brain activity, such as motor-imagery based systems. This comes with a high drawback that affects the user ability to control the BCI, based on the variability of its brain signals for the same task in different moments of the day, or different user emotional state, and so on. The idea investigated in this research study, is to create a method to silently detect the user mental state and effectuate the control in every moment, without requesting a strict mental task involving extensive learning to the user side in order to control his brain signals. This will provide a relaxed, more natural and faster interaction with the BCI. As an example, we can think about an information seeking application, such as a research engine where the content can be automatically highlighted, reduced, or changed based on the current mental state detected. In this case, the BCI will still require a training phase to infer the characteristics and thresholds for each mental state, but without the exhausting requirements for the participant as having to continuously control and modify his brain signals. This ultimate goal is discussed also in the future perspectives and it is validated based on the feasibility of the inferred mental state detection based on the experimental study described further in this chapter. Moreover, this chapter encloses the investigation of the cognitive user mental state by detecting the corresponding neural correlates of the depth of cognitive processing.

5.1 Introduction and state of the art

While Brain-Computer Interface (BCI) research mostly focuses on the detection of voluntary motor controls which require intensive user training and strict tasks, as also shown in the previous chapter (Chapter 4), the detection of the momentary user state (Blankertz, et

al., 2016) did not receive too much attention. In real world applications, where the interaction is co-adapted with the computer, the goal is to replace or supplement the explicit information given by the user (keyboard, mouse or gestural input) with implicit input directly from the human brain considering the current intentions or brain state. In such a way, the interface should be aware of which information is more significant for the user (Acqualagna and Blankertz, 2015) and access implicit information from the user state (Nicolae et al., 2015a,b,c, 2016a, 2017a; Ušćumlić and Blankertz, 2016; Wenzel et al., 2016) in order to allow a smooth adaptation of the interface according to the current situation. More specifically, in information seeking applications for example, when one wants to search for more information about a specific topic from a scientific online database, the interface could display meaningful keywords in appropriate positions in association with the desired topic and additionally refine the results based on continuous user state detection. As another example, considering operator monitoring applications (e.g. in industrial workplaces Venthur et al., 2010), the interface can reduce the number of actions that are required to be performed by the operator and even take over control with an automated process in extreme cases. This approach may offer a dramatical improvement in the application by diminishing the number of errors and accidents in the workplace, while avoiding critical mental states of the operators and user frustration, leading to a stressless and safer working environment.

Different mental states have been scrutinized to monitor cognitive user's state and refer to different levels of attention (Vecchiato et al., 2016), task engagement (Venthur et al., 2010), fatigue, workload (Berka et al., 2007; Kohlmorgen et al., 2007; Schmidt et al., 2007, 2009; Borghini et al., 2014; Schultze-Kraft et al., 2016b), movement intention (Haufe et al., 2011, 2014b) and many others (Müller et al., 2008; Zander and Kothe, 2011; van Erp et al., 2012; Sturm et al., 2015; Blankertz et al., 2010c, 2016).

Targeting information seeking applications, user's state might be also estimated by evaluating the current level of cognitive processing the presented information. In this sense, we are interested in the brain natural fluctuations of cognitive processing (Polich and Kok, 1995), which are caused, for example, by: mind wandering (Melinscak et al., 2014; Hohmann et al., 2016), distraction (Schubert et al., 2008) and fluctuations in vigilance (Beatty et al., 1974; Matousek and Petersén, 1983; Birbaumer, 2006; Schmidt et al., 2007, 2009; Ji et al., 2012; Vecchiato et al., 2016). However, based on our previous experience in earlier studies (Venthur et al., 2010), these variations are difficult to be analyzed and validated in an experimental setting. Therefore, the present study takes the approach of inducing different levels of cognitive processing by task instructions. This research work aims to investigate the feasibility of employing the depth of cognitive processing for future user state adaptation, and to detect the feature markers characteristic to different levels of cognitive processing, exploitable in the future BCI interaction. Specifically, the depth of cognitive processing refers to the degree to which information can be processed. In our scenario, the amount of cognition spreads on three cognitive levels: from no processing, towards shallow and deep processing (McLeod, 2007). Where no processing suggests no retention of information, a shallow process refers to a mild processing of information detected by attention considering the structural form, such as color appearance or categorization, while a deep process requires more elaborated processes, e.g. semantic correlations (Craik and Tulving, 1975; Anderson and Reder, 1979) or quantitative measures. While the concept of depth of cognition has been

widely investigated in psychology (Craik and Lockhart, 1972; Cohen and Waters, 1985), to the best of our knowledge, no research has been performed that investigates its effects considering the electrophysiological signals towards BCI applications. Separately, the EEG activity during different cognitive processes (Section 2.4.2.1) has been widely investigated (Klimesch, 1996, 1999; Başar et al., 1999, 2001; Debener et al., 2006). In our current research work, three cognitive processes have been investigated, namely memory encoding and decoding, language and visual imagination that can be present during a human-computer interaction. The memory process requires visual or auditory memory recall for the necessary information (short-term memory retention of information) in an n -back task form (Pesonen et al., 2007, Chen, et al., 2008), considered mostly in the frontal, temporal and parietal lobes (Berger et al., 2014; Onton et al., 2005; Scholz et al., 2017). The language process considers word-retrieval functions and phonemic representations, namely syllables, that are processed in the language phonology area (Brodmann Areas – Kandel et al., 2000; Lloyd, 2007; Dubin, 2017), in the pre-frontal, frontal and temporal areas (Baars and Gage, 2010), mostly lateralized (Bear et al., 2007; Griggs, 2012). The visual imagination process demands more extensive processes like long-term memory retrieval and imagination, generated in the pre-frontal, central, parietal, and parietal-occipital areas (Osaka, 1984; Roland and Gulyás, 1995; Ganis et al., 2004, 2013) and uses quantitative measurements for discrimination.

The depth of cognition has been quantified by tapping the corresponding components of brain activity, in a specific scenario inspired by the odd-ball paradigm (Section 5.2.1). The neural components arising from cognitive processes are distinguished by the Event-Related Potentials and the oscillatory activity. Moreover, discriminative neurophysiological markers considering each level of processing are extracted using separability measures applied to the ERPs waveforms and tackled by the spectral modulations which are further quantified by enhanced classification methods based on this multivariate data analysis (Section 5.2).

5.2 Methods

5.2.1 Experimental design to elicit different cognitive processing levels

5.2.1.1 Participants

The experiment was conducted in a laboratory environment with seventeen participants aged between 22 and 35 years old. The experimental study involving human participants described in this research work was approved by the ethics committee of the Department of Psychology and Ergonomics of the Technische Universität Berlin. Normal or correct-to-normal visual acuity was considered for the study and no participant expressed a history of neurological disease, injury or heart problems. The data from two participants was discarded from further analysis due to improper recording. Considering the experience in BCI from the remaining fifteen participants, the group was mixed, ranging from no experience in BCI (5 participants) to familiar (4 participants) and experts in BCI (6 participants). Participants had different mother tongues, namely German (11 participants), English (one participant) and other languages (3 participants), therefore a good command of English or German was required in order to fulfill the task in the language condition. Twelve participants were right handed and

with regard to gender, 4 females and 11 males took part in the experiment. To countenance their motivation, participants were financially remunerated for their participation.

5.2.1.2 Experimental scenario

The experiment started with an introductory discussion for the participant into the experiment, followed by practice tests in order to familiarize with the tasks. The total duration of the experiment lasted between three and three and half hours, depending on the introductory discussion time and the time requested by each participant to get familiarized with the experiment.

The experiment elicits the levels of cognitive processing by considering a visual experimental paradigm similar to an odd-ball paradigm. The user is requested to stay still, relaxed and seated with 30 cm in front of the LCD screen and focus in the center of the screen while visualizing the sequence of stimuli and performing the mental tasks as instructed.

1. Stimuli

The visual stimuli are represented by a pair of cartoon-drawing images having same color (red/green/blue/magenta) and showing a different object chosen from one out of three categories (animals, fruits and mobility) (example in Fig. 5.1). The pair of images is formed by a random selection from a corresponding category, where each category consists of a total of ten elements.

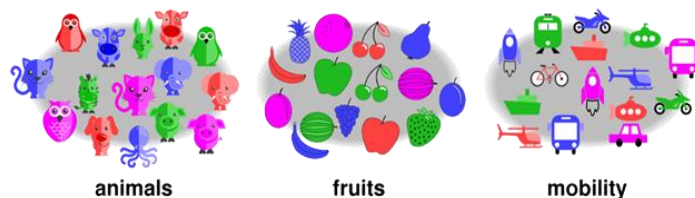


Fig 5.1 Representation of the stimuli categories (animals, fruits, mobility) and examples of their elements (cat, penguin, apple, banana, bus, rocket, etc.). Each category contains 10 elements and they can be represented in 4 colors (red/green/blue/magenta). For the stimuli presentation, a pair of elements are randomly selected from a category, with same color. (Figure taken from Nicolae et al., 2017a, with permission.)

The cognitive processes, namely Memory (M), Language (L) and Visual Imagination (VI), termed further as *conditions* are evaluated in this order, one after another, each in five runs with 120 stimuli per run (accumulating a total of 15 runs and 600 stimuli). In order to avoid confusions between the tasks, which were already quite demanding, the conditions were not alternated after each run. Each run of the experiment started with a short question considering participant's current mood, expressed by a good, ok or bad state. Next, the first image of the experiment shows the target cue: a pair of images showing the target color and the target category (Fig. 5.2). When the participant is ready and has memorized the target information, the participant presses the space bar and the sequence of images starts. During the presentation, the participant had to be attentive and focused and for each stimulus it had to distinguish the color first and then the category in comparison with the target cue. To keep the participant engaged during the experiment and to obtain a measure of task performance,

the participants were instructed to perform mentally counting and additions, in accordance with the presented stimuli.

The *levels* of processing are modulated by the requested tasks and are triggered by non-targets (NT) which requires no processing, shallow targets (ST) associated with a 'shallow level' of processing and deep targets (DT) triggering a deep level of processing.

Referring to the target cue, the instructions are as follows: *i)* In case of NT (non-targets) stimuli, the color does not match the target cue color → the participant neglects the NT stimuli; *ii)* For ST (shallow targets) stimuli, only the color matches with the target cue color, but the category does not match → the participant performs mental counting (+1); *iii)* For DT (deep targets) stimuli, the color and the category match the target cue → the participant is requested to mentally count +1 and additionally to evaluate a question task corresponding to the cognitive process (M/L/VI) (see below *Mental tasks*) and in case of positive answer (positive Deep Targets, DT+) → to additionally count +10, otherwise (negative answer) do nothing additional (Negative Deep targets, DT-).

Participants entered the final result at the end of each run and obtained feedback about the correct number. After the experiment is completed, the participants filled in a questionnaire detailing the difficulty of the experiment referring to the type of cognitive processes and the category types. The difficulty is acquired by scoring from zero to two, representing easy, medium or hard difficulty.

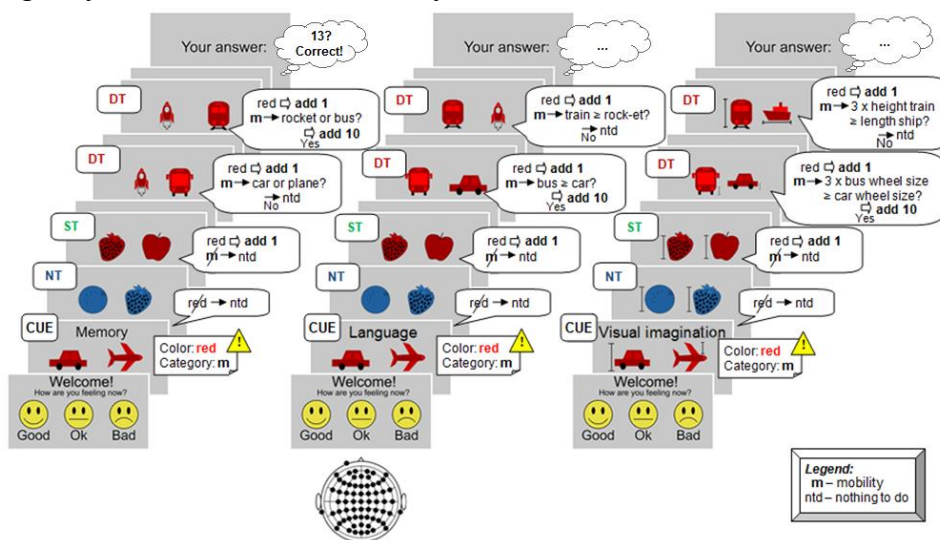


Fig. 5.2 Experimental protocol examples for the cognitive processes investigated: memory, language and visual imagination (from left to right). For each stimulus, the participants had to perform or not mental computations and decisions. Each experiment run starts with the current mood evaluation and ends with the final number insertion and receiving feedback about the correct number. Note that the presentation included in addition the fixation and relaxation screens before and after each stimulus accordingly, but these screens are omitted here. (Figure taken from Nicolae et al., 2017a, with permission.)

2. Mental tasks

Memory

For the memory task, resembling a complex n -back task, the users have to memorize the target cue pair, and while the sequence of images is presented, they have to keep in mind the last target pair which refers to a DT stimulus (color and category matching the target cue).

For each DT stimuli, the users have to evaluate if at least one of the current stimulus elements was also present in the last stimulus target pair. In case of a positive answer (positive deep target), they have to mentally add 10 to the current number counted and memorize the new target pair for the next trials in any of the cases.

Language

The language task refers to the words that represent the image elements. The user has to decide whether the number of syllables of the element in the left side is greater or equal than the number of syllables of the right element. Again, if the answer is true, add 10 to the number counted. English or German language was considered, depending on the participant's mother tongue.

Visual imagination

For the visual imagination task, users have to perform mental representations of the stimulus elements referring to the real objects (not to the cartoon drawings) and make comparisons based on dimensions. Such as, to answer the following question: Is three times the dimension of the left element greater than or equal to the right element dimension? The dimensions have to be considered as average dimensions and not to refer to a specific object type and may refer to the entire elements size or to parts of the elements. The corresponding dimensions are indicated with a black marker, as in Fig. 5.3. For a constant complexity regarding the size comparisons between different trials, the selection of the stimuli elements pairs while generating the stimuli, was constraint to a threshold interval, to avoid big discrepancies such as too large or too small size differences.

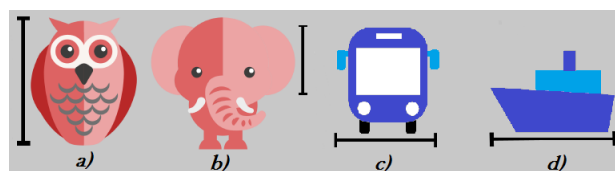


Fig. 5.3 Example of elements size indicators: (a) a vertical marker placed on left side represents the entire object ; b) a vertical marker placed on the right side represents a part of the object (i.e. elephant's ear); c) a horizontal marker for a front view representation indicates element's width; d) a horizontal marker for a lateral view representation indicates element's length. (Figure taken from Nicolae et al., 2015a, with permission, where the images a) and b) were designed by Freepik <http://www.freepik.com/>)

5.2.1.3 Experimental design

The timing, the speed and the complexity of the stimuli presentation was set based on a pilot study without the EEG cap on four participants. The timing of each trial is represented in Fig. 5.4, starting with 500ms for fixation, continuing with the stimulation period of 1250ms and followed by the relaxation period of 750ms, with a total of 2500ms Inter-Stimuli Interval.

The average ratio of the stimuli was chosen to be $75:12.5:12.5 \pm 2\%$ for NT:ST:DT. The number of deep targets (DT) and shallow targets (ST) was chosen to be approximately the same, such as the difference in the ERPs will not be correlated to the frequency of their occurrence. Within the deep targets, approximately 36% are negative deep targets (DT-) and 64% are positive deep targets (DT+). In order to maintain this occurrence and not to increase too much the variability and the complexity of the experiment, only 2/3 categories were

selected for each run. The order of the sequence was set to start with an easier target category (fewer object details, transportation or fruits), to continue with a harder category (more object details: animals) and to end with an easier category (transportation or fruits).

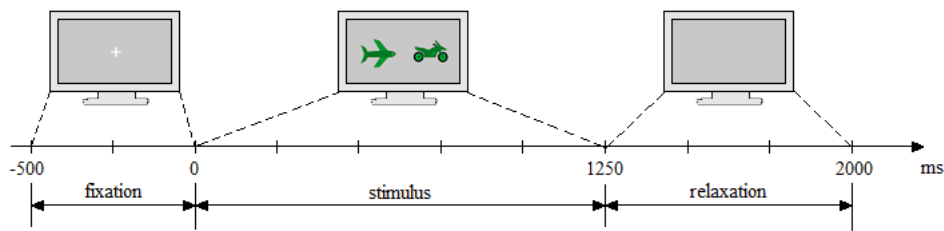


Fig. 5.4 Timing of the trial: 500ms for the fixation cross (white), 1250ms for the stimulation period and 750ms for the relaxation period. The stimulus background screen is light grey. (Figure taken from Nicolae et al., 2017a, with permission.)

The stimuli presentation was developed with the Processing software version 3.0a4 (<https://processing.org/>). The images (cartoon-like drawings) were drawn with the Inkscape software (<https://inkscape.org/>), except from the elements in the animals category, which were downloaded from an on-line free database (<http://www.freepik.com/>). The images format used is Scalable Vector Graphics (SVG) with a resolution of 480x480. The images were placed close to the center of the screen with a 2" distance between them, presented on a 23" screen with 60Hz refresh rate and 1920x1080 resolution (Dell U2410).

5.2.2 Neural signals acquisition

The neural signals were recorded using 64 EEG channels using the ActiCAP system with active electrodes (Brain Products GmbH, Munich, Germany) and distributed according to 10-20 international system. One electrode was placed under the left eye to record the EOG signal movements. Unipolar recording was used with the ground placed at the AFz scalp position and referenced at left and right mastoids. For good quality recording, the skin–electrode impedance was kept below 20 k Ω using the ActiCAP control software. Signals were recorded with BrainVision Recorder at 1 kHz sampling frequency (fs) and amplified using BrainAmp MR plus. The main script to connect between the software products was developed in MATLAB (release R2014a, The MathWorks, Inc., Natick, MA, USA). The recorded EEG and behavioral data is available from the DepositOnce repository of Technische Universität Berlin (Nicolae et al., 2017b).

5.2.3 Analysis strategy to detect the neural correlates of different levels of cognitive processing

The signal processing methods and machine learning techniques for data analysis were developed with the MATLAB software (The MathWorks, Natick, MA, USA), and the BCI toolbox (Blankertz et al., 2016; https://github.com/bbci/bbci_public), the MATLAB Signal Processing Toolbox, the Statistics and Machine Learning Toolbox, the Wavelet Toolbox and the EEGLAB toolbox (Makeig et al., 2000a; Delorme and Makeig, 2004). Furthermore, for more complex and vivid graphical representations the Python programming language was used along with the package Matplotlib (Hunter, 2007).

5.2.3.1 Behavioral assessment

As described in the experimental scenario section, subjective indicators were considered for the participant's behavioral assessment, referring to the current personal mood (good, ok and bad state) and personal overview for the difficulty of the conditions (0 - easy, 1 - medium, 2 - hard). In addition, an objective indicator was also integrated in relation to participant's responses that refers to the number counted. This was assessed by a ratio of the absolute difference between the participant's response and the correct number, divided by the correct number (Eq. 5.1). The resulted ratio varies between 0 and 1, showing high or weak performance. The final assessment value was computed for each condition and averaged between all runs.

$$a_{p,C} = \frac{\sum_{r=1}^5 \frac{pr_r - c_r}{c_r}}{5}, \quad (5.1)$$

where

$a_{p,C}$ – the assessment value for the behavioral data of the participant $p \in \overline{1-15}$ for the condition C (M, L or VI);

pr_r – the participant's response for the run r , $r \in \overline{1-5}$;

c_r – the correct number for the run r .

5.2.3.2 Pre-processing (filtering and epochs rejection)

Downsampling to 100 Hz was performed (Section 3.2.1.2) in order to reduce the dimensionality of the data, while preserving only the related human brain frequency range. The data was then low-pass filtered for anti-aliasing using the Chebyshev type II filter of order 10, with a 42 Hz pass-band edge frequency and less than 3 dB ripple and a 49 Hz stop-band edge frequency with 50 dB attenuation. In addition, for removing the signal drifts, a 1 Hz FIR high-pass filtering of order 300 with zero-phase shift, designed using least-squares error minimization, was applied (For future online classification, appropriate causal filters must be considered). The signals were re-referenced to the left and right mastoids channels. Next, the data was divided into epochs corresponding to the timing described in Fig. 5.4. Prior to ERP analysis, artifact rejection was applied based on variance and max-min criterion (Section 3.2.2.1) to remove the epochs with ocular and muscle artifacts and the channels dropping to zero. Baseline correction (Section 3.2.1.4) was performed using 100 ms of pre-stimulus period (fixation timing).

5.2.3.3 Artifact removal

For a better artifact cleaning of the data such as strong eye movement artifacts, muscular artifacts and loose electrodes Independent Component Analysis (ICA) was applied with artifactual components selection given by the MARA algorithm (Section 3.2.2.2.2). The artifactual components were rejected based on a threshold of artifact probability of 0.20. In addition, the artifacts selection is further verified by visual inspection of the independent components considering the time series, components spectrum and scalp maps, and looking for characteristics of muscle activity, eye blinks, horizontal and vertical eye movements or loose electrodes (e.g. in Fig. A.3.1). After the artifactual ICs have been identified, the EEG signal was reconstructed without them.

5.2.3.4 Multi-modal discriminative analysis

The multi-modal analysis investigates the neural correlates from the temporal (Event-Related Potentials, ERPs) and spectral domain (Event-Related (De)Synchronizations, ERDs/ERSs), or both (Event-Related Spectral Perturbations, ERSP). As a measure of discriminability between two classes of each condition, the signed and squared point biserial correlation coefficient (*signed r^2* , Section 3.3.2.1.1) is used, showing the differences in the ERPs modulations, in the power spectrum and in the ERD/ERS effects in accordance with the selected relevant frequency bands. The ERD/ERS is computed based on Hilbert Transform (Appendix A.1.3.2) and the result is then smoothed (Bracewell, 1999). The Event-Related Spectral Perturbation (ERSP) method is computed based on Short-Time Fourier analysis (Appendix A.1.3.4.2) and phase coherence across trials is investigated with the Inter-Trial Coherence (ITC) measure (Section 3.3.4.2). For visualizing the neurophysiological effects, grand averages representations of the ERPs, spectrum and ERD/ERS curves are obtained for each condition by averaging across all trials and participants. The baseline interval used for normalizing the graphical representations is selected as 200 ms before the stimulus onset, referring to the fixation period. Changes in the oscillatory power generated at different frequencies are assessed by extracting the spectrum from 3 to 40Hz, using Fourier transform with Kaiser window.

The brain sources corresponding to the neural oscillations of cognitive activity are detected by advanced decomposition methods (Section 3.2.2.2), namely: Spatio-Spectral Decomposition (SSD) and Common Spatial Pattern (CSP). For neurophysiological investigation, the CSP patterns applied on SSD filtered signals are linearly constructed in the opposite sense as they were applied, by multiplying the CSP patterns with the SSD patterns: $\mathbf{A}_{\text{SSD}\&\text{CSP}} = \mathbf{A}_{\text{CSP}} \times \mathbf{A}_{\text{SSD}}$, where $\mathbf{A}_{\text{CSP}} = (\mathbf{W}_{\text{CSP}}^T)^+$ and $\mathbf{A}_{\text{SSD}} = \sum \mathbf{W}_{\text{SSD}} (\mathbf{W}_{\text{SSD}}^T \sum \mathbf{W}_{\text{SSD}})^{-1}$, as described in Section 3.2.2.2.4 and 3.2.2.2.3.

5.2.3.5 Multi-modal classification and validation

In order to join complementary information about the neural activity, information contained in different domains is combined in a fruitful manner. Spatio-temporal features based on ERPs are combined with the oscillatory features, further described below. The corresponding level of cognitive processing is primarily estimated by regularized Linear Discriminant Analysis (Section 3.4.1) and further tested by other classification and regression methods, in order to obtain best performances. While a binary discrimination is firstly investigated, a multi-class approach is further analyzed to approach the detection towards a real application scenario. In the multi case, LDA and multinomial Logistic Regression (Section 3.4.3) are investigated as classifiers.

❖ **Classification features**

1. Combined spatio-temporal and spatio-spectral features (for binary classification)

a) Spatio-temporal features

The spatio-temporal features (channels and time) were extracted as described in Blankertz et al., (2011) and Section 3.3.2.1. Five temporal windows are detected for each participant based on a heuristic selection of the intervals with maximum *signed* r^2 discriminability and a constant pattern between the two classes. The windows were searched over the stimulus interval, from 0 to 1250ms.

b) Spatio-spectral features

As described in Section 2.4.2.1, the cognitive processes also generate modifications in the oscillatory activity. Therefore, we considered extracting the valuable information from the involving frequency bands according to each cognitive process. The most significant frequency bands were selected based on the discriminative analysis (Section 5.2.3.4). To enhance the discrimination of activity in the frequency band of interest, Spatio-Spectral Decomposition (SSD) was performed (Nikulin et al., 2011) and the respective Common Spatial Patterns (CSPs) (Blankertz et al., 2008c) were extracted for the corresponding frequency bands.

- *Spatio-Spectral Decomposition, SSD*

Aiming an enhanced discrimination of mental states expressed by the spectral modulations depicted by the ERD/ERS phenomena, linear spatial filtering was applied prior to CSP detection. The neural activity of interest can be covert in the fluctuations of the background noise activity due to overlapping frequency content or to reduced variance for the activity of interest as compared to a background process. Therefore, it seems useful to apply SSD (Section 3.2.2.2.3) in order to enhance the variance in the frequency range specific to the type and the level of cognitive processing, and reduce the variance of the noise. Specifically, the optimal spatial filters are detected by maximizing the frequencies of interest, considering the alpha and beta frequency bands selected by the signed r^2 discriminability measure over the ERD/ERS modulations (as will be shown in section 5.2.2.2), and minimizing the signal power in the neighboring frequencies. The neighboring frequencies are considered as 1Hz band width aside the frequency band of interest, followed or respectively preceded by a gap (stop band) of 1 Hz. Because this requires frequency filtering before the decomposition, continuous data was used to avoid filter edges artifacts. Following closely the decomposition, SSD extracts the components primarily expressing the signal of interest that better relates to the oscillation's variance. Thus, for the SSD decomposition we consider only the highest components that contribute to 10^{-6} of the highest eigenvalue (see low-rank factorization in Haufe, et al., 2014b), which generally resulted in about 15 to 35 components per discrimination pair.

- *Multi-band Common Spatial Patterns, mCSP*

In order to reduce the effects of volume conduction and to decode the cognitive intentions by distinguishing the spatial localization of the oscillatory activity, we make use of the widely used Common Spatial Patterns (CSP) method as described in Section 3.2.2.2.4, successful as shown in different studies (Winkler et al., 2011; Acqualagna et al., 2015; Acqualagna et al., 2016; Schultze-Kraft et al., 2016b). In our case, the binary technique increases the variance of a higher level of cognitive processing while diminishes the variance of a lower level of processing and vice versa. The components reaching this goal were automatically selected (as in Blankertz et al., 2008) to a maximum of three spatial filters per class and individually checked for each participant with careful visual inspection. As highlighted by the ERD/ERS phenomena (Section 5.3.2.2.2), the relevant time interval characterizing the cognitive activity was selected starting from 350 ms after the stimuli and until 2000ms, approximately corresponding to the moment when the cognitive processing starts, after the appearance of the P300. In addition, more specific intervals were considered as given by the ERD/ERS discriminability, in accordance with the discrimination pair (e.g. 800-1500ms for the ST-DT discrimination) and the results are presented in Section 5.3.2.2.2. A deeper cognitive processing requires longer time to be fulfilled, time which exceeds the stimulus presentation, as described also in Duncan-Johnson and Kopell (1981). The most significant CSPs representative for the relevant frequency bands, alpha (8-14 Hz) and beta (16-20 Hz), are detected as given by discriminative analysis (Section 5.3.2.2.3). The CSPs were separately computed on each band, the logarithm of the variance is computed for each CSP (Section 3.3.3.1) and all values are finally cumulated as band power features in the feature vector. The entire process was performed on the precursory band-pass filtered data with SSD.

- c) *Combined spatio-temporal and spatio-spectral features (ERP-mCSP)*

Furthermore, the spatio-temporal and spatio-spectral features were combined, such that complementary information from both domains will be simultaneously exploited. The corresponding processing pipeline is described in Fig. 5.5. Firstly, the signals are preliminary preprocessed (by filtering, epochs and channels rejection and artifact removal) and segmented, followed by appropriate feature extraction considering the feature type: time or power. The obtained optimal spatio-temporal features related to the highest *signed r^2* difference between classes are concatenated with the spatio-spectral features given by the mCSP process, while considering the cross-validation scheme (10 folds with 10 repetitions). Specifically, in the spectral domain, due to label information integration, the relevant CSPs are computed on the training data (CSP W) and used to spatially filter the testing data by linear derivation (W), for each cross-validation fold. The resulted band-power features (log-variance) are introduced in the feature vector along with the relevant temporal features. While in our case, the features are roughly on the same scale, no normalization was initially performed on the feature vectors. However, for comparison purposes, z-score normalization of the feature vectors was later applied by subtracting the mean and dividing by the standard deviation on each feature type.

❖ **Classification and regression**

a) *LDA Classification*

The discrimination was first evaluated by regularized Linear Discriminant Analysis with shrinkage of the covariance matrix (Section 3.4.1.1), where the optimal shrinkage parameters are automatically determined (as in Blankertz et al., 2011; Schäfer and Strimmer, 2005).

b) *sliding LDA classification*

Separately, a shrinkage LDA classifier (similar as in Ušćumlić, 2016) is applied only for the temporal features, in sliding manner for each trial with 50ms time shifts on different significant intervals depending on the condition. The intervals are selected according to the discriminability evaluations. Then, the classifier is set to slide from 0 to 1500ms for the memory condition, until 1000ms for the language and until 1400ms for the visual imagination condition. Preliminary, the classifier is trained on the 550-650ms interval for memory, 850-950ms for language and 800-900ms for visual imagination. The final result considers average performance for a trial.

c) *QDA*

In addition to LDA, Quadratic Discriminant Analysis (Section 3.4.1.3), was also applied to investigate the performance. The results are further provided in Section 5.3.3.3.1.

d) *Regression*

Furthermore, regression approaches are also investigated (Section 5.3.3.3.1), namely Ridge Regression shrink (Section 3.4.4.1) and Logistic Regression (Section 3.4.2).

❖ **Validation**

The pairwise classification was validated with 10 folds cross-validation (Section 3.4.5.1) and the performance is assessed by the area under the ROC curve scores (Section 3.4.6.1). For the regression case, class-wise normalized loss measure (Section 3.4.6.2) was applied.

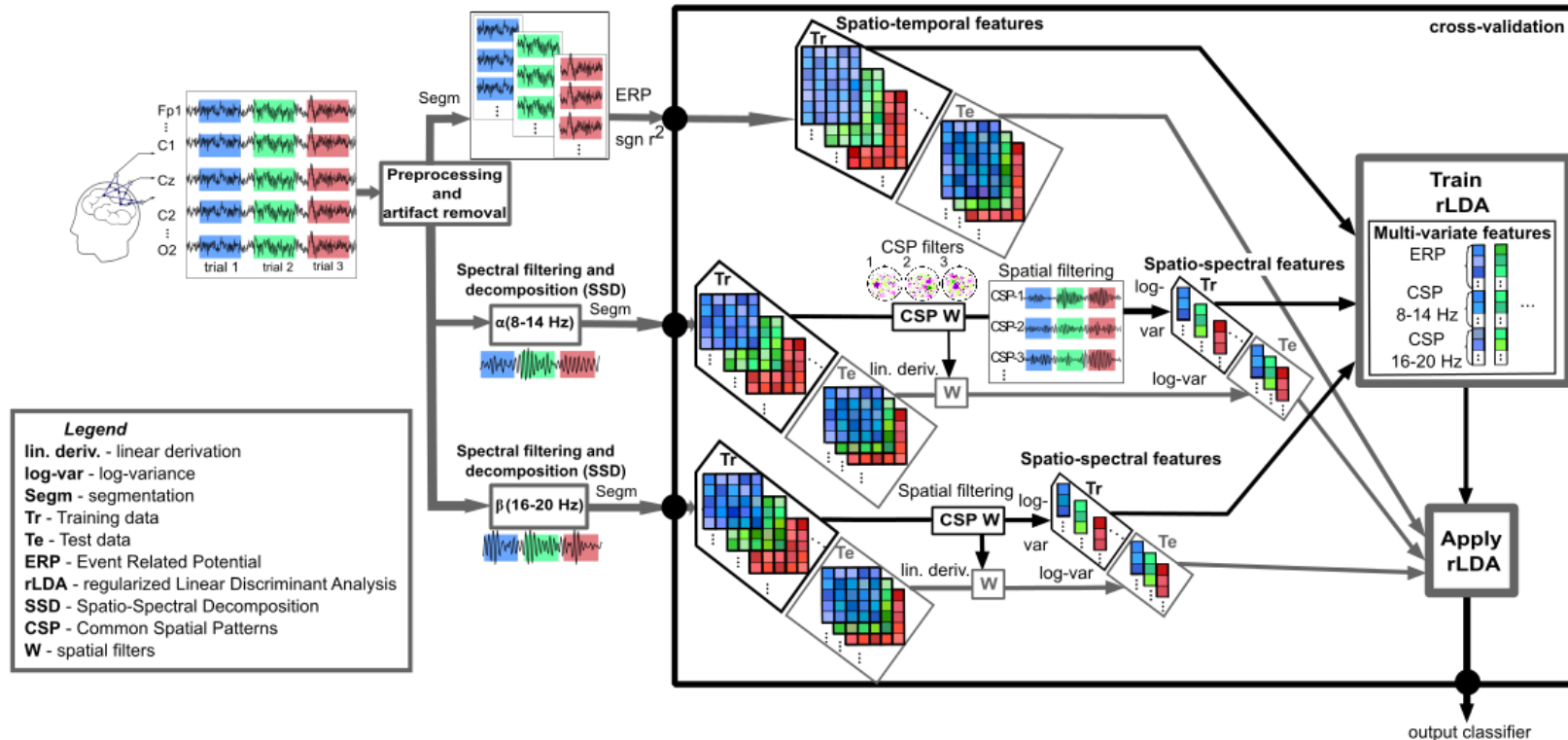


Fig. 5.5 Data analysis diagram. The neural data is analyzed in the temporal (ERPs), spatial and spectral domains (α , 8–14 Hz and β , 16–20 Hz). The three types of feature vectors: the spatio-temporal features (the most relevant temporal points based on the maximum signed r^2 intervals between classes), the spatio-spectral features (log-band power of the CSPs) in the α and β bands, are concatenated and given to the classifier within crossvalidation. Due to label information employment, spatio-spectral filtering considers the optimal channel and frequency band using CSP analysis with automatic filter selection computed on the training set (CSP W) and applied to the test set by linear derivation (W). SSD and the interval selection method based on signed r^2 were applied to the entire dataset and not within crossvalidation. While this aspect of the validation is not perfectly sound, the expected overestimation of the performance is limited. Finally, the classifier (regularized Linear Discriminant Analysis with shrinkage of the covariance matrix) decides the corresponding class membership for each trial (output classifier), representing the cognitive processing level. (Figure taken from Nicolae et al., 2017a, with permission.)

2. *Combined spatio-temporal and spatio-spectral features (for multi-class classification)*

In relation to the combined approach described in the previous sub-section for binary classification (5.2.3.5.1), few modifications have to be implemented. While the *signed r^2* discrimination as well as the CSP method are specific to binary discrimination, appropriate discrimination approaches have to be considered, applicable for multi-class classification. The temporal features are selected considering the relevant and unique signed r^2 intervals for the ST-DT and ST-NT discrimination pairs. Regarding spectral features, multiple CSPs are computed with the JAD method (Section 3.2.2.2.4.2) selecting two CSPs per class and the classifier performances are compared when using the CSP features with the OVR strategy (Section 3.2.2.2.4.2). Since this algorithm makes use of the label information, the CSPs were computed in crossvalidation form, in the same way as the binary CSP approach in section 5.2.3.5.1. Similarly, the log-variance features (section 3.3.3.1) are considered for classification, for both frequency bands and preliminary SSD filtered data.

Linear Discriminant Analysis with shrinkage of the covariance matrix (Section 3.4.1.1) is employed for classification. In addition, multinomial logistic regression (Section 3.4.3) is also investigated (Section 5.3.3.3.2). The classifiers are evaluated with the class-wise normalized loss measure (Section 3.4.6.2). For more details regarding the accuracy for each class, normalized confusion matrices (Section 3.4.6.3) were computed.

5.3 Findings

Firstly, the behavioral performances were studied, followed by the neurophysiological analysis and interpretation, which gives detailed insights for the corresponding cognitive processes.

5.3.1 Investigating behavioral measures

The behavioral data was analyzed considering the ratio of participants responses (described in Section 5.2.3.1), the participants state evaluated at the beginning of each run, and participants feedback regarding the application in terms of interest and complexity. Considering user's mood, eleven participants expressed a 'good' condition for 53% of the experiment and six participants maintained their 'ok' mood for 47% of the experiment. No single participant reported a bad mood during or after the experiment.

Regarding participants responses (Fig. 5.6, left side), more accurate responses are observed for the language condition, with the 25% and 75% percentiles of the ratio closer to zero (however, this effect is not statistically significant: $p = 0.2465$ with 1-way independent rm-ANOVA). Referring to a trend over time considering performance, no improvement or decrease was observed considering the answers ratio, showing insignificant correlations by the Spearman rank-order correlation (memory: $p = 0.3367$; language $p = 0.3982$; visual imagination $p = 0.1211$; and in total over all 15 runs: $p = 0.6192$).

Considering tasks difficulty for each condition (Fig. 5.6, right side), lower score is depicted in the language condition, characterizing an easier process rated by the participants (statistically significant: $p = 0.0451$, one-way ANOVA statistical test considering one factor (participants) and three levels (conditions)). The memory and visual imagination conditions received equal scoring representing similar difficulty, higher than the language condition.

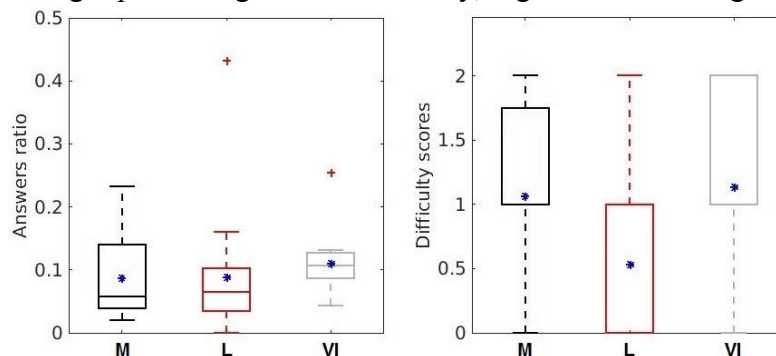


Fig. 5.6 Behavioral assesment – objective and subjective indicators for the Memory (M), Language (L) and Visual Imagination condition (VI): answers ratio (left image); difficulty scores (right image). Ratios closer to zero correspond to better performance. The blue asterisk indicates the corresponding mean values and the outliers are represented by the red crosses. (Figure taken from Nicolae et al., 2017a, and adapted from Nicolae et al., 2015b, with permission).

5.3.2 Extracting the neural correlates for each cognitive processing level

5.3.2.1 Temporal analysis

The first view over the neurophysiological characteristics in relation to the processing of the cognitive tasks considers the event-related potentials (ERPs). The following figure (Fig. 5.7) shows the grand averages for each condition across all participants and trials. Strong differences between the levels of processing are depicted considering amplitude and duration of the potentials. No strong differences are encountered in the temporal evolution of the first potential peaking at approximate 250ms, across all conditions, characterized by a fronto-central positive component, representing visual processing of the external stimuli. However, a negative component at the lateral occipital location is present in this early interval, more pronounced in the visual imagination condition. Its amplitude is gradually modulated by the type of target (DT < ST < NT). Furthermore, different amplitudes and duration are encountered for the later positive component, corresponding to the P300 potential, present at 400ms. It is characterized by a strong positive activation in the centro-parietal area and is modulated in amplitude by an increasing level of cognitive processing (NT < ST < DT). For an overview over the ERPs on all electrodes, see Appendix A.3.2, Fig. A.3.6 and for an example on single participant ERPs, see Appendix A.3.2, Fig. A.3.4.

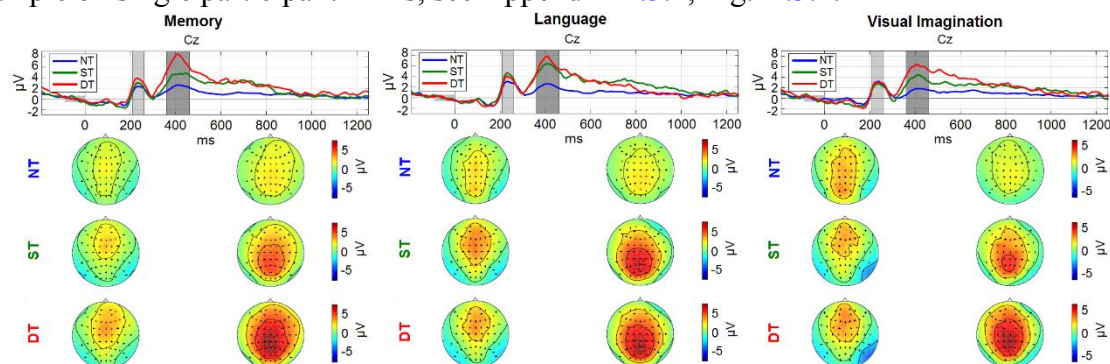


Fig. 5.7 Grand average ERPs. (a) Memory condition; b) Language; c) Visual imagination. The upper plots represent the time evolution from -200 ms to 1250 ms, with 0ms, the stimulus onset, at representative electrode Cz. The scalp plots underneath show the topographies referring to the shaded areas highlighted in the time evolution plots: 210–260 ms; 360–460 ms. (Figure taken from Nicolae et al., 2017a and adapted from Nicolae et al., 2015a, with permission.)

Two decisions are involved in each task. Firstly, participants decide on the type of the stimulus (NT, ST or DT), which further triggers no (NT), mild (ST), or intense (DT) processing. The related processes according to the decisions influence the ERPs exposed in Fig. 5.7. While the components amplitudes are graded in accordance with the level of processing, their latencies are similar, representing the same decision task. For deep targets (DT), a second decision has to be performed (more detail in Appendix A.3.2, Fig. A.3.5). In this case, representative ERP components are not clearly distinguishable, due to different time execution variations between trials (Appendix A.3.2, Fig. A.3.3).

Grand average signed r^2 differences between the levels of processing are analyzed referring to the spatial distribution shown as scalp topographies in the top plots and to the temporal discriminability presented in the underneath time plots (Fig. 5.8). However, because

the r^2 values depend on the number of samples, the comparison across different pairs with respect to the absolute value of r^2 is biased, because NTs are in greater number than ST and DT. The highest discrimination between the levels of processing is encountered in the centroparietal area, corresponding to the P300 component. The amplitude and duration of these P300 differences differ between conditions and indicate different cognitive processing of the stimuli. While differentiating between a deeper level of processing and an easier level (ST-NT, DT-NT, DT-ST), the most prominent signed r^2 difference can be described as a positive deviation starting around 300 ms and gradually increasing until 1000 ms or less, strictly depending on the condition.

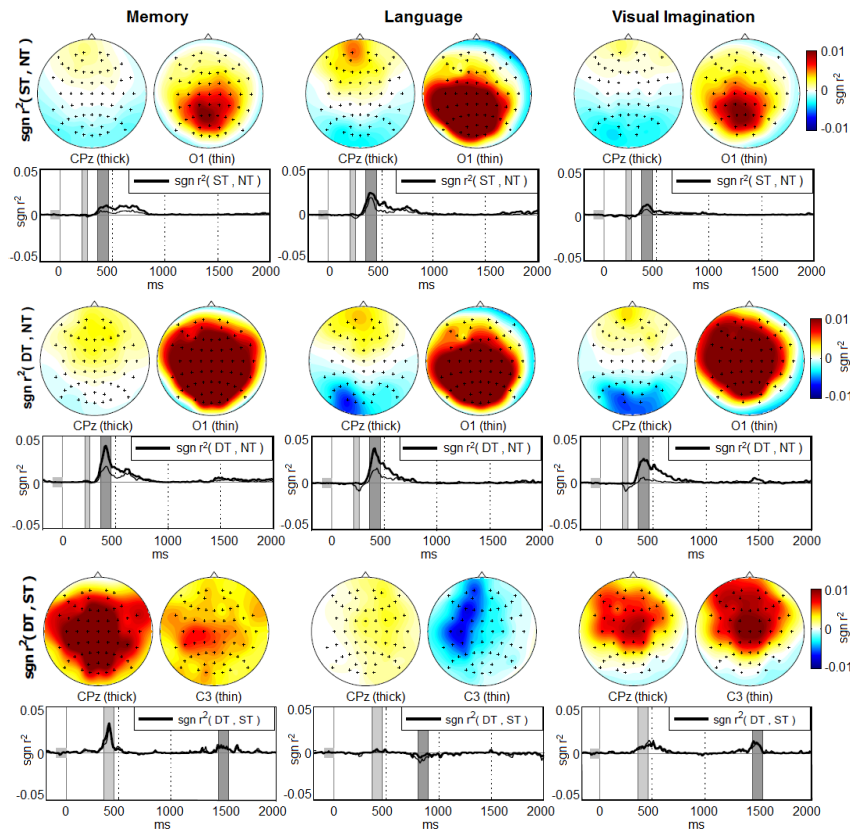


Fig. 5.8 Grand-average discriminations of the Event-Related Potentials given by signed r^2 considering Memory, Language and Visual imagination conditions for the -200 ms to 2000 ms interval. From top to bottom: ST – NT and DT – NT at channels CPz (thick line) and O1 (thin line), and DT – ST at channels CPz (thick) and C3 (thin). The scalp topographies correspond to the time intervals highlighted by the shaded areas in the temporal evolution plots: 210-260 ms; 360-460 ms; 800-900 ms; 1450-1550 ms. (Figure taken from Nicolae et al., 2015b, with permission from Springer Publication.)

In addition to the other discrimination pairs, the deep and shallow amplitude evolution discrimination (DT-ST) shows a late activation in form of a negative difference around 850 ms for the language condition and a positive difference, around 1500 ms for the memory and visual imagination processes. Left lateralized spatial distribution is observed in form of a decreased activation, specifically in the language condition. The potential at 1500 ms (more detail in Appendix A.3.2, Fig. A.3.2) resemble a P2 potential corresponding to the appearance of the blank screen (relaxation period) and peaking 250 ms after. These potentials are similar for no- and shallow processing, but for deep processing the potential is higher.

Except the biased signed r^2 measure, another plausible reason might relate to the trend of the ongoing signal which is higher in amplitude for a longer period of time for DT (see Fig. 5.7), due to the additional decision which requires longer time to be fulfilled.

For a detailed view of the discriminability over all channels, the *signed r^2* computed pair-wise between classes using additional Bonferroni correction is shown in Appendix A.3.2, Fig. A.3.7.

5.3.2.2 Spectral analysis

1. Power spectrum

The neurophysiological markers that represent the cognitive processes are complementary investigated in the power spectrum by evaluating the neural activity generated in theta (5-7Hz), alpha (8-14Hz) and beta (16-20Hz) frequency bands, as depicted in Fig. 5.9, computed on the trial timing 350-2000ms. Discriminative information can be observed over the alpha (8-12Hz and 12-14Hz), showing desynchronization with 2-3 dB less during deep processing as compared with shallow processing. The theta (5-7Hz) and beta (16-20Hz) bands do not show substantial differences.

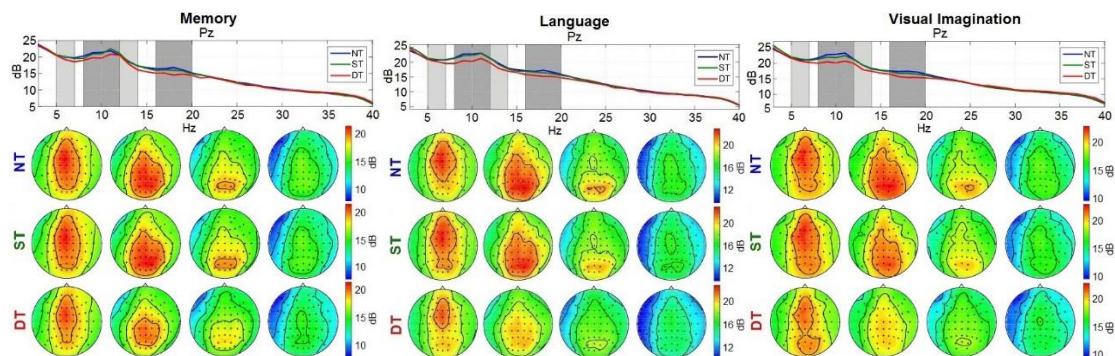


Fig. 5.9 Grand average power spectrum at location Pz, computed on the 350-2000ms timing, for the Deep (DT), shallow (ST) and no-processing (NT) levels in case of memory, language and visual imagination conditions. The top plots show the power spectrum at different frequency bands and the bottom plots show the scalp maps corresponding to the grey shaded areas from above. (Figure adapted – different timing, from Nicolae et al., 2016a, with permission from Verlag der TU Graz.)

A closer investigation of the neural fluctuations of the cognitive processes in the spectral domain is revealed by the signed r^2 discriminability, more pronounced at the parietal location, presented in Fig. 5.10. This helps depicting the most informative frequency bands involving the cognitive processes. Higher discrimination is observed for the alpha band (8-14 Hz) followed by a smaller discrepancy in the beta band (16-20 Hz). Considering their prominent difference encountered in the frontal and parietal sites, both frequency bands were selected for further analysis in a multi-band approach. A small modulation is visible also in the theta band (5-7 Hz), observed for the shallow and no-processing discrimination and between deep and shallow processing (the upper and bottom graphs in Fig. 5.10). This effect in the theta band is insignificant compared to the discrimination in the alpha and beta frequency bands and it is not found for all processing levels, therefore the theta band is not considered further for the analysis.

Continuing the investigation, more pronounced difference in the spectrum is observed for the deep-shallow discrimination, as compared to the shallow and no-processing discrimination. This effect coincides with the fact that complex processing has a stronger influence in power compared to a superficial level of processing (Jaušovec and Jaušovec, 2000; She et al., 2012; Naumann et al., 2017). However, it should be noted that the same issue occurs here related to the biased r^2 values which depend on the number of samples, therefore more biased towards the NT case.

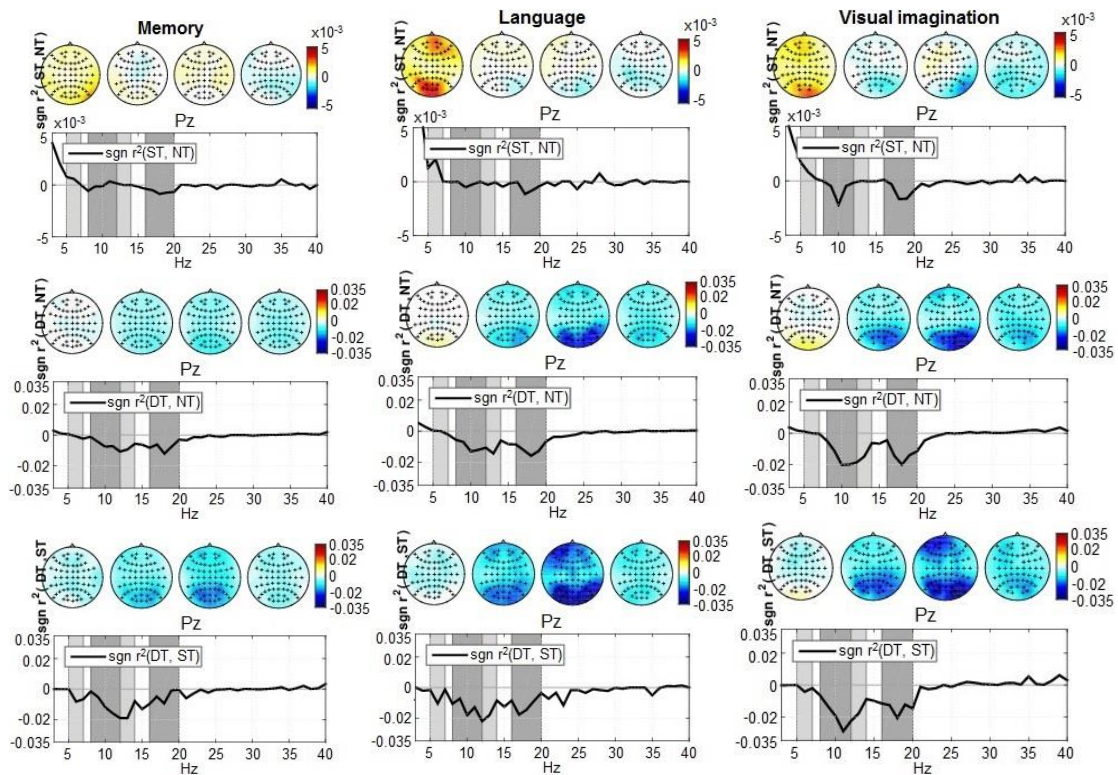


Fig. 5.10 Grand-average spectrum discriminability given by signed r^2 at location Pz. From top to bottom: ST-NT, DT-NT, DT-ST discriminations, computed on the 350-2000ms timing for ST-NT and DT-NT and 800-2000ms for DT-ST. The four scalp plots refer to discriminative signed r^2 values, corresponding to theta (5-7Hz), alpha (8-12Hz; 12-14Hz), and beta (16-20Hz) frequency bands (shaded in grey). Note the scale difference: the upper ST-NT graphs scale from -0.005 to 0.005 $sgn r^2$, compared to the other graphs which scale from -0.035 to 0.035 $sgn r^2$. (Figure adapted – different timing, from Nicolae et al., 2017a, with permission from Springer.)

2. ERDs/ERSs

Further, a deeper overview of the modulations in different frequency bands, such as the (de)synchronization (ERD/ERS) effects, outlined by the modulation of the amplitudes in the temporal domain, resp. the hull curves of the specific chosen bands is investigated in Fig. 5.11 and Fig. 5.12. For appropriate visualization, considering parietal area as the main area for cognitive processes, the midline parietal electrode Pz is selected (For other electrode patterns, see Fig. A.3.9, A.3.10 in Appendix A.3.3.). The envelope ranges from -1 to $0.5\mu\text{V}$ (Fig. 5.11) for the alpha band and between -0.4 to $0.4\mu\text{V}$ for the beta band (Fig. 5.12). The evolution of the envelopes begins with a similar synchronization for all processing levels and conditions until 300ms, corresponding to the same type of processing the external

information. Further, desynchronization follows in both alpha (8-14Hz) and beta (16-20Hz) frequency bands, stronger around 500ms, showing user's preparation for a more complex cognitive task. Next it is completed by a synchronization starting around 800 ms and peaking at 1800ms. The amplitude evolution of the hull curves is modulated by the amount of processing: the shallow (ST) and deep processes (DT) elicits more pronounced desynchronizations in comparison to the reference of no-processing (NT). In addition, the deep process has a more pronounced ERD compared with the shallow process (signed r^2 discriminability in Fig. A.3.8 of Appendix A.3.3).

Considering the spatial distributions, more pronounced synchronization ($0.1 - 0.35\mu\text{V}$) is observed for shallow processing in the centro-parietal area compared to no-processing ($0 - 0.25\mu\text{V}$) and stronger desynchronization ($-0.3 - 0\mu\text{V}$) in the temporal, central and parietal area for complex processing. When comparing between complex cognitive processes (DT), higher ERS in amplitude and spatial distribution is found for the memory processes, in opposition with a stronger ERD for language and visual imagination. This effect might be explained by the fact that visual imagination is a more complex process, requiring additional processes and functions, namely memory and imagination, contrasting with the other two processes. On the other way around, the memory process produces the highest impact in amplitude and reduced spatial distribution, contrasting with the behavioral point of view, where the participants stated, on average the language as the easiest method.

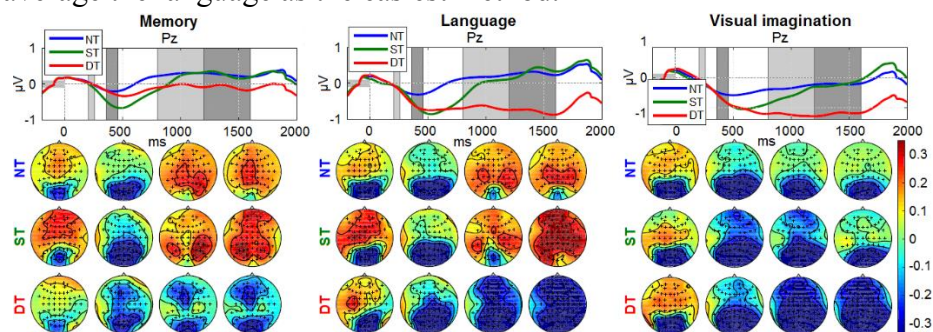


Fig. 5.11 Grand-average ERDs for the alpha band (8-14 Hz) considering all conditions (M, L, VI) and processing levels (NT, ST, DT) at electrode Pz. The baseline interval is equivalent to 200 ms of pre-stimulus interval (the grey horizontal strip). The amplitude limits for all graphs is -1 to $1\mu\text{V}$ for the time evolution and -0.35 to $0.35\mu\text{V}$ for the scalp distributions. The four scalp plots are computed on: 210 – 260 ms, 360 – 460 ms, 800 – 1200 ms, 1200 – 1600 ms intervals (shaded in grey). (Figure from Nicolae et al., 2017a, with permission from Springer.)

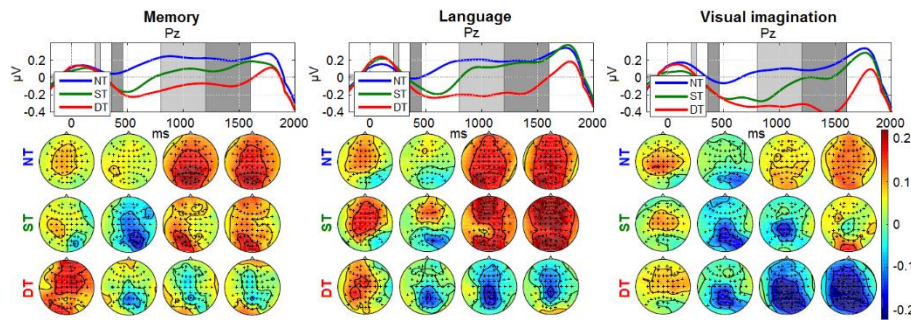


Fig. 5.12 Grand-average ERDs for the beta band (16-20Hz) at electrode Pz for all conditions (M, L, VI) and processing levels (NT, ST, DT) and baseline corrected (-200 - 0ms). Amplitude limits for all graphs: -0.4 to $0.4 \mu V$ for the temporal evolution and -0.22 to $0.22 \mu V$ for the spatial distributions. (Figure from Nicolae et al., 2017a, with permission from Springer.)

3. CSPs

Furthermore, the Common Spatial Patterns analysis provide information about the presumed sources of the neural activity which are optimally projected on the surface of the scalp (as explained in Section 5.2.3.4). In the following, the binary and multi-class CSPs are further investigated.

a) Binary case

In Fig. 5.13 and Fig. 5.14, the relevant common spatial patterns referring to the selected alpha and beta frequency bands, are shown as scalp topographies considering participant P4. Fig. 5.13 shows the patterns for the alpha frequency band (8-14 Hz) and the patterns of the beta band (16-20 Hz) are presented in Fig. 5.14. Clear patterns are observed, no eye or muscle artifacts. The first components, with eigenvalues larger than 0.5, refer to a maximization of the variance for the first class and a minimization of the variance for the second class. On the opposite, the last components with an eigenvalue lower than 0.5 represents the second class maximization of the variance and in the same time first class minimization of the variance. Participant P4 chosen for visualization showed highest classification accuracy (77% accuracy for ST-DT, 92% for NT-DT and 80% for NT-ST discrimination) and the best behavioral response (46.66% perfect runs out of 15, with an average behavioral ratio considering all conditions of 0.04708). The components which maximize the variance of no-processing level are characterized by diffused activation patterns at different scalp locations relating to random activity, in comparison with the components which maximize the variance of shallow and deep processes, which illustrate activity in the central, temporal or parietal area, with increased or decreased variance (green or purple). The color coding and sign of the activation patterns are not relevant in this context. In general, more relevant components are detected in the case of discriminating a higher level of processing which involves more activity, in comparison with lower level or no-processing discrimination cases, where less sources of activity are detected.

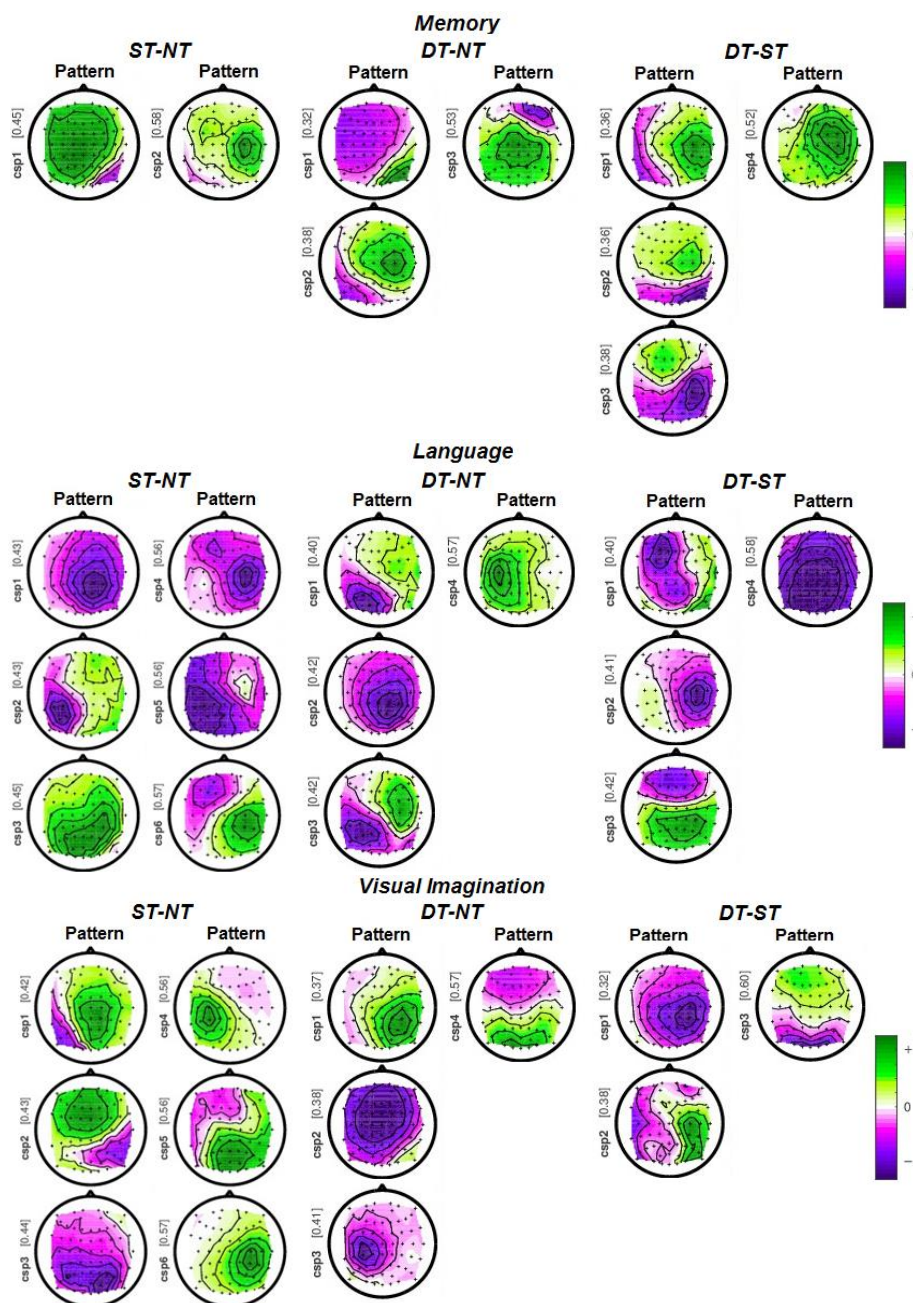


Fig. 5.13 Binary CSP analysis (patterns) for the alpha frequency band (8-14Hz) after SSD considering NT-ST, NT-DT, ST-DT class pairs for each condition (Participant P4). The components with an eigenvalue less than 0.5 maximize the first class variance and the others greater than 0.5 maximize the second class variance, and were computed for the first fold of cross-validation, on the 350-2000ms interval. (Figure taken from Nicolae et al., 2017a, with permission from Springer.)

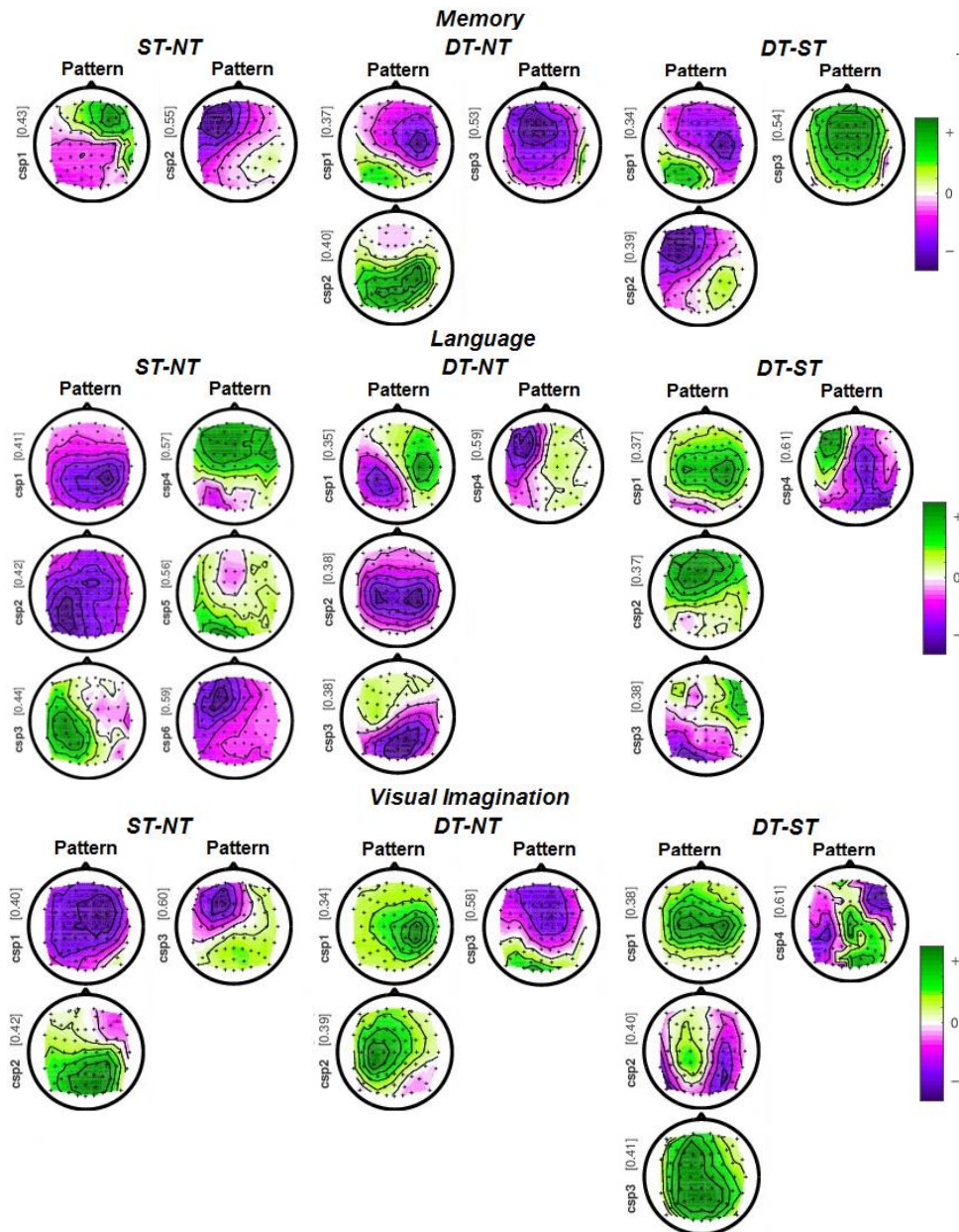


Fig. 5.14 Binary CSP with SSD patterns for the beta frequency band (16-20 Hz) considering all conditions and classification pairs (Participant P4). The components represent the first fold of cross-validation, computed on the 350-2000ms interval. (Figure taken from Nicolae et al., 2017a, with permission from Springer.)

b) Multi-class case

Apart from the two class CSP discrimination, we can further investigate the spatial patterns of neural activity specific to each class, considering the multi-case approach, as explained in the JAD method (Section 3.2.2.2.4.2). Two components ($m = 2$) have been chosen for each of the three classes, represented in the first six CSP components given by the highest eigenvalues. These patterns are presented in Fig. 5.15 for the alpha band (8-14 Hz) and in Figure 5.16 for the beta band (16-20 Hz).

Considering the no processing class, no particularly localized activity is observed, resembling for example mind wandering and attention as a background process. On the other

hand, the shallow processing components consider frontal and parietal activations referring to attention and processing of the stimuli. The deep processing components involve participations from different regions (frontal, temporal, central, parietal), corresponding to the type of cognitive process. For example, the deep processing components of the memory condition show more variance in the ante-frontal, fronto-central, right temporal, centro-parietal, and parietal areas corresponding to attention, short-term memory, memory (non-verbal), object recognition, visual association and organization processes, in accordance. The CSPs for the language condition relate to higher variance in the fronto-central, centro-parietal, parietal and parietal-occipital areas, most likely relating to language, working memory and sequential thinking, non-verbal memory and reasoning processes. For visual imagination, pronounced activations are disclosed in the central, centro-parietal, left temporo-parietal and parietal regions corresponding to spatial representations and constructions, recognition, short-term memory, picture images, cognitive reasoning, and imagination mechanisms. (Dohrmann, 1983; Kolb and Wishaw, 1980; Lezak, 1983; Netter, 1983; Kandel et al., 2000; Thompsn and Thompson, 2003; Kolak et al., 2006; Lloyd, 2007; Carter, 2014; Dubin, 2017).

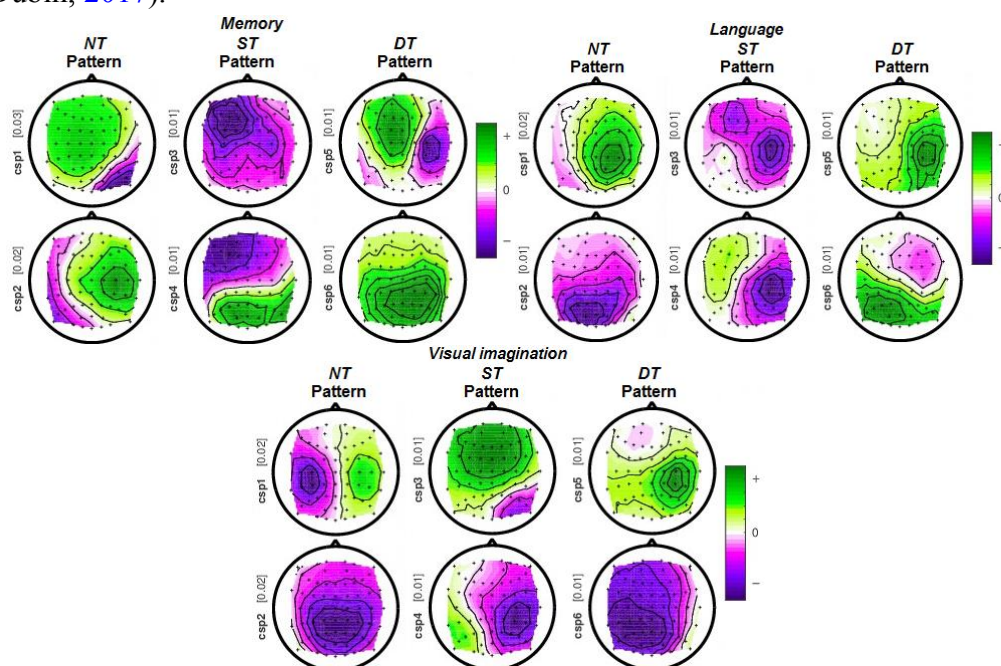


Fig. 5.15 Multi-case CSP with SSD patterns of the 8-14Hz frequency band considering the NT, ST and DT classes for each condition (Participant P4). The two components for each class are presented on rows, with the corresponding eigenvalue. The components were computed for the first fold of cross-validation.

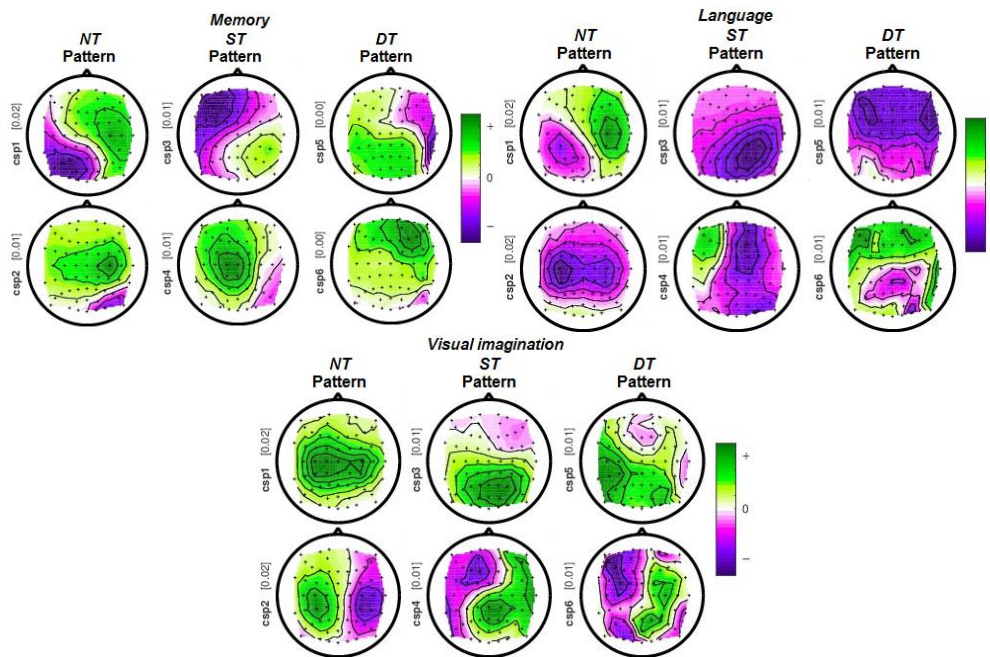


Fig. 5.16 Multi-case CSP with SSD patterns of the 16-20Hz frequency band considering the NT, ST and DT classes for each condition (Participant P4).

5.3.2.3 Tempo-Spectral analysis

More information of the neural oscillations in the temporal domain is depicted by the Event-Related Spectral Perturbations, visible in the time-frequency representation. The corresponding spectral perturbations of the cognitive processes, are captured by electrodes F7 and P3 for the memory process in Fig. 5.17, by F7 for the language task in Fig. 5.18, and by Cz, P3, PO7 and PO8 for the visual imagination in Fig. 5.19, in accordance with the characteristic brain locations. In addition, the parietal area generally covers all the cognitive processes represented with the corresponding electrode Pz.

The time-frequency representations show that after the first phase-locking perturbations at 10-20 Hz, an increase in power follows in different bands according to the processing level. The average coherence across trials and participants in the alpha and gamma bands in the parietal and frontal area shows high local phase consistency of the neurophysiological waveform across successive trials, represented by a sharp transient increase centered at 500ms and a small increase locked on 1700ms.

Looking over the spectral perturbations of the memory process (Fig. 5.17), a continuum positive activity (>1dB) is observed in the gamma frequency (>30Hz) at the parietal area (P3, Pz) for the deep level of processing (DT), corresponding with a complex and continuous mental activity state, such as: concentration, focus, memory access and contrasting with a negative deflection (<-1dB) in lower bands (<30Hz). For the shallow level of processing (ST), variable positive perturbations are observed in high beta and gamma frequencies corresponding to the counting task and also later in the alpha band corresponding to reduced processing (color appearance detection), more evidenced in the frontal area (F7). On the contrary, the non-processing of the stimuli (NT) shows more variations in the alpha band corresponding to mind wandering and no cognitive activity. The Inter-Trial Coherence (ITC) shows, for deep processing, higher values of 0.6–0.8 at around 400–600ms and below

20Hz, and smaller values of 0.4 at 1700-1800ms and below 18 Hz, showing the time when the trials become phase-locked with respect to the event.

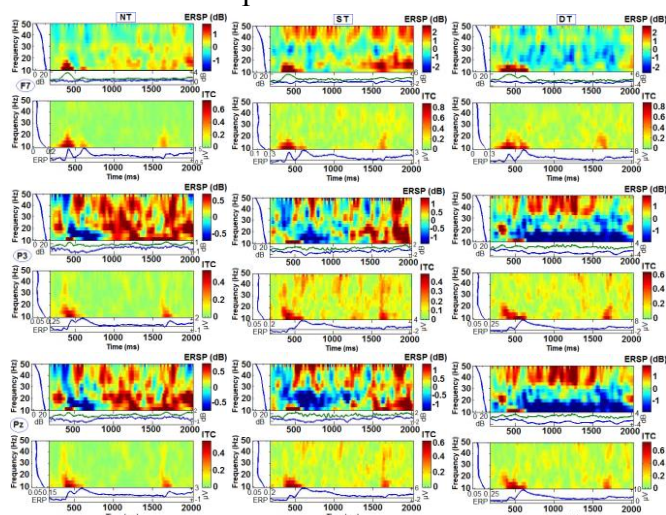


Fig. 5.17 Spectrogram (ERSP and ITC) for the memory process at channels F7, P3, and Pz (on rows from top to bottom) considering the NT, ST and DT levels (on columns from left to right). For ERSP: right colorbar shows the scale of the power spectral density (dB); the lateral left panel shows the baseline mean power spectrum; the lower panels show the ERSP envelope - low and high mean dB values over time, relative to baseline (-200ms, 0ms). For ITC: the right colorbar shows coherence strength scale (ITC values); the bottom panel shows the mean ERP trace. (Figure taken from Nicolae et al., 2015c, with permission from IEEE.)

Considering the language condition, the processing levels are more differentiated, as shown in Fig. 5.18, with reduced perturbations for no processing and some variations in higher bands (> 30Hz) due to mind wandering, small perturbations between 20 and 30 Hz for the shallow process, and stronger perturbations in the gamma range for deep processing.

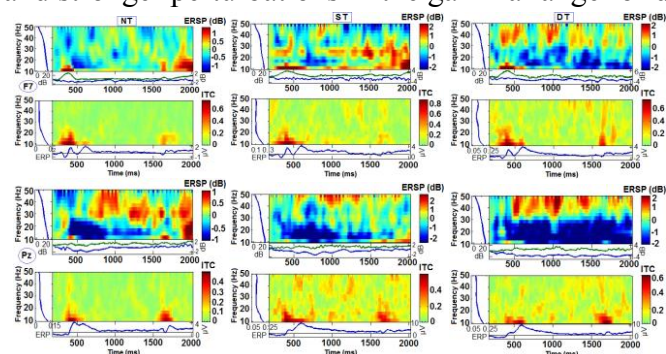


Fig. 5.18 Spectrogram (ERSP and ITC) for the language process at channels F7 and Pz (on rows from top to bottom) considering the NT, ST and DT levels (on columns from left to right). (Figure taken from Nicolae et al., 2015c, with permission from IEEE.)

Distinctive perturbations are observed for the visual imagination process (Fig. 5.19) in accordance with the level of processing, namely: small perturbations between 30Hz and 40 Hz for shallow processes and stronger perturbations between 30 Hz and 50 Hz for the deep process. The ITC is similar for all the processing levels. For the second potential observed in the ERP of Fig. 5.19, the P2 around 1700 ms, an interesting effect is the absence of perturbations in the gamma band for the deep process.

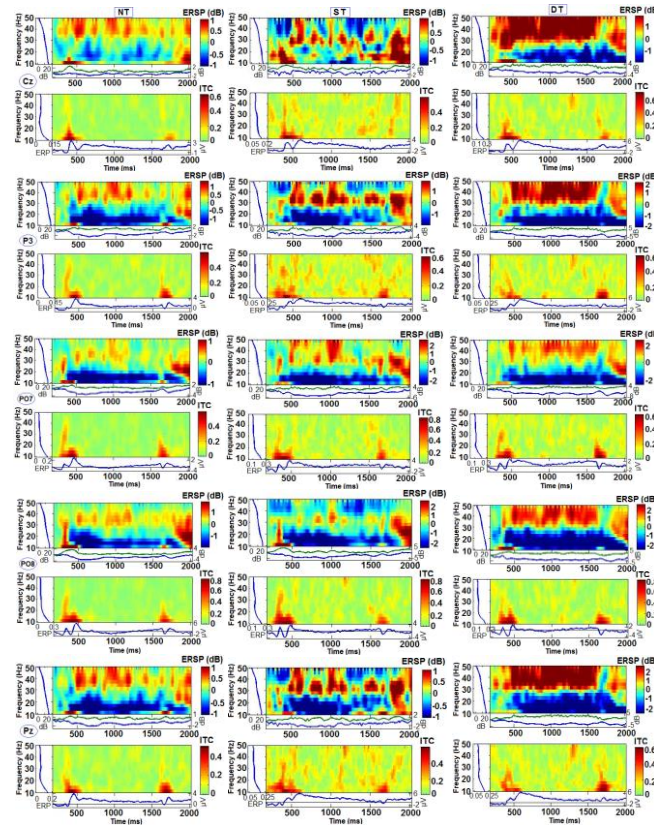


Fig. 5.19 Spectrogram (ERSP and ITC) for the visual imagination process at channels Cz, P3, PO7, PO8 and Pz (on rows from top to bottom), considering the NT, ST and DT levels (on columns from left to right). (Figure from Nicolae et al., 2015c, with permission from IEEE.)

5.3.3 Discrimination of different cognitive processing levels

5.3.3.1 Binary classification

The evaluation of the binary multi-modal classification based on the combined spatio-temporal and multi-band CSP (ERP-mCSP) features, are presented hereunder. More details over the separate ERP classification are presented in sub-section 5.3.3.3.1, [Additional classification results](#), corresponding to Nicolae et al., (2015b) and Nicolae et al., (2018).

The classification performances across participants and for all conditions are presented in Fig. 5.20 in form of box-plots, considering the area under the roc curve values (detailed single participant values in Appendix A.3.4, Tab. A.3.1). Very good performances are observed with means beyond 70% for ST-DT discrimination, around 75-80% for NT-ST pair and the highest performance for NT-DT discrimination, around 85-90%. A 2-way repeated measure of ANOVA was performed over the AUC values with the factors: condition and classification pairs, which provide a statistically significant difference between the classification pairs ($p < 0.001$, $F = 64.99$). Based on the condition factor, the results in Fig. 5.20 expose higher average accuracy for the language condition comparing the others two, but this observation was not proved statistically significant ($p = 0.2112$). All performances for all participants and condition pairs are significantly above chance level (indicated by Wilcoxon signed-rank test with $\alpha = 0.001$). The ANOVA assumptions were checked with

Shapiro Wilk for the normality distribution of the residuals, Bartlett test for homogeneity of variance, and Mauchly's test for data sphericity (more detail in Appendix A.3.4).

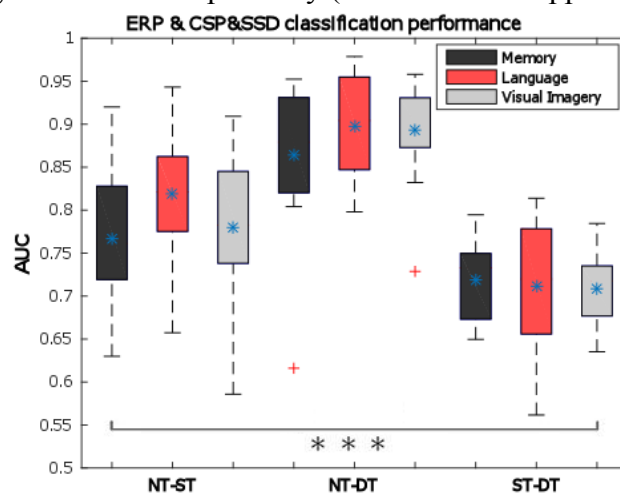


Fig. 5.20 Pairwise classification mean performance over all trials for all cognitive processes (memory – dark grey, language – light red, visual imagination – light grey) given by the area under the ROC curve (AUC) based on ERP-mCSP. The bottom and upper whiskers of each box-plot corresponds to the minimum and maximum values regarding all participants, the rectangular horizontal sides of the box considers the 25% and 75% percentiles of the data, the blue star represents the mean values, and the red cross points the outliers. The high achievements exceeds 55% and range until 97% in total. All pairs show statistically significant accuracy over chance level, marked with three black asterisks in the bar plot (Wilcoxon signed-rank test; $p < 0.001$). (Figure taken from Nicolae et al., 2017a, with permission.)

Considering standardization of the feature vectors, the performances are similar with a difference of $\pm 1-3\%$ compared to the results with no normalization presented in Fig. 5.20. For example, the 0.74, 0.72, 0.72 AUC values for the M, L, VI conditions considering the ST-DT classification with standardization, seem higher compared to 0.71, 0.72, 0.70 AUC for no standardization. However, considering all classification pairs the results are not significantly different (n -way ANOVA: $p = 0.0601$).

5.3.3.2 Multi-class classification

The following figure (Fig. 5.21) shows the multi-class classification results considering the combined tempo-spectral JAD approach, as described in Section 5.2.3.5.2. The normalized accuracy shows 0.59% performance for the memory condition, 0.62% for the language and 0.60% for the visual imagination. The results show an increased performance over the chance level (33% considering the 3 classes: NT, ST, DT), significant by Wilcoxon signed-rank test ($p < 0.001$). No significant difference is encountered between conditions by the one-way ANOVA statistical test with $\alpha = 0.05$ ($p = 0.3384$). The ANOVA assumptions were checked with Shapiro Wilk for the normality distribution of the residuals, Bartlett test for homogeneity of variance, and Mauchly's test for data sphericity (see Appendix A.3.4, with more details also on single participant classification performances, Tab. A.3.2).

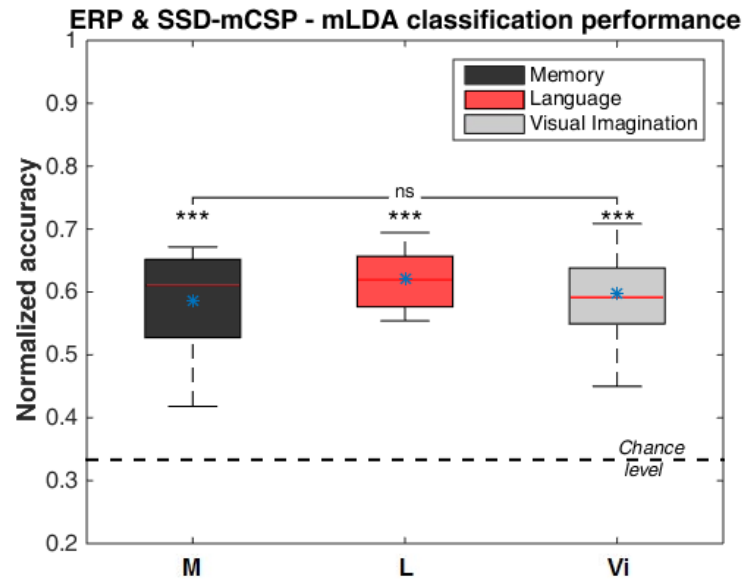


Fig. 5.21 Multi-class spatio-tempo-spectral classification performance (ERP & SSD-mCSP) for all conditions: Memory (M; dark grey/dark), Language (L; red/medium dark) and Visual Imagination (Vi; light grey/light).

In addition, in order to have a detailed understanding of the classification performance, we can check the trials assignment to classes in terms of normalized confusion matrices. The following figures show the normalized summed confusion matrices over all participants, calculated by summing all the predicted trials across all participants and all folds and normalized by dividing the number of predicted trials for each class by the actual number of trials in that class, as shown by the ratio within each confusion matrix block.

Fig. 5.22 sketch the confusion matrix for the memory condition. The classification of the neural signals corresponding to the no processing level assigned the highest correct number the trials, with a rate of 72.7%, followed by shallow and deep processing classes. The highest number of misclassified trials occurred for shallow class, where 29% of the trials were classified in the no processing class. In each case, the misclassification ratio is smaller than the correct trials classification. For the language condition, the highest classification ratio among classes is also observed for the no processing level.

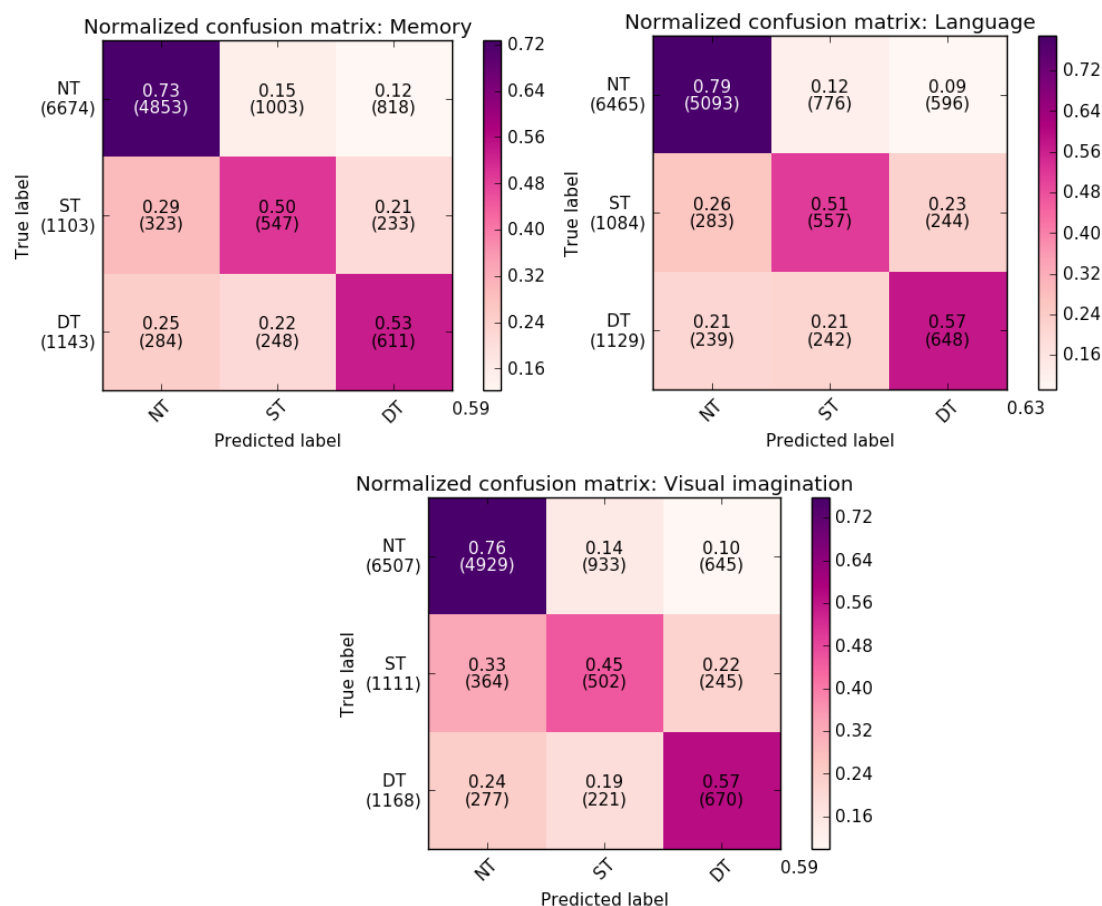


Fig. 5.22 Normalized confusion matrix for the Memory, Language and Visual Imagination condition across all participants, showing multi-class spatio-tempo-spectral classification performance (ERP & SSD-mCSP) between no (NT), shallow (ST) and deep processing (DT). The rows show the true class labels and the total number of trials for each class in brackets, whereas the columns provide the output of the classification. The correct assigned trials for each class are depicted on the diagonal with the overall mean classification accuracy in the bottom right corner. The ratio of the corresponding assigned trial class is shown in each cell and the total number of trials is provided underneath each ratio, in brackets.

❖ Note:

Notice that there is a small difference, lower than 1% between the average classification results presented in the box-plot in Fig. 5.21 and in the confusion matrices in Fig. 5.22, but this effect is mainly due to different average calculations. For the normalized loss, the accuracy is computed by averaging the normalized ratio within folds, which is given by the number of predicted trials in that fold and divided by the size of the corresponding fold. While for the confusion matrices, the accuracy is computed by summing up all predicted trials of all folds and participants and computing the normalized ratio. We have computed this normalized sum for the confusion matrices, in order to have a larger overview of the classified and misclassified trials in general.

5.3.3.3 Additional classification results

1. Binary case

a) Spatio-temporal classification with shrink *rLDA*

As comparison, in this section we show the separate uni-modal classification results. In Fig. 5.23, the averaged classification performances over trials and participants considering the spatio-temporal features are presented by the area under the roc curve values. The classification performances show significant values comparing between classification pairs ($F = 55.18$; $p < 0.001$ with rm-ANOVA), exceeding 0.75 AUC for the NT-ST discrimination. Higher performances are also observed for the NT-DT classification, reaching mean performance up to 0.85. While the ST-DT discrimination shows smaller performances around 0.67, corresponding to reduced discriminability between ERPs given by the signed r^2 in Fig. 5.8. Considering conditions, AUC values seem higher for the language condition for the first two classification pairs, although this effect is not statistically significant ($p = 0.1479$ with 2-way independent rm-ANOVA with factors conditions and classification pairs and $\alpha = 0.05$).

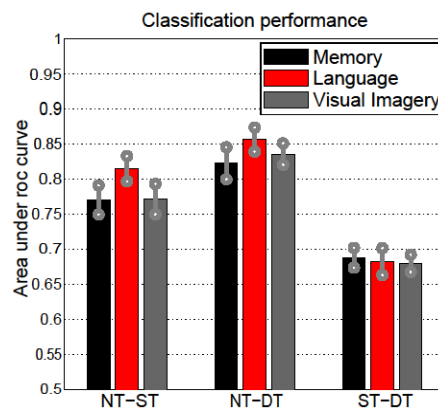


Fig. 5.23 Pair-wise spatio-temporal (ERP) classification performance between the levels of processing (NT – no-processing, ST – shallow processing, DT – deep processing). The standard errors of the means, SEM, are highlighted by the grey antennas on top of the bar plots. (Figure taken from Nicolae et al., 2015b, with permission from Springer Publication.)

For an overview over the distribution of the data, see the scatter plot in Fig. A.3.11 of Appendix A.3.4.

b) Spatio-spectral classification with shrink *rLDA*

As it can be observed on the mean average classification performance (Figure 5.24), the SSD-mCSP classification outperforms the ERP classification for the ST-DT pair, e.g. 74% on average for the language condition, compared to 68% ($F = 11.21$; $p = 0.0013$ with rm-ANOVA), but at the same time the ERP classification performs better for the NT-ST pair, 79% compared to 60% for the SSD-mCSP classification ($F = 104.85$; $p < 0.001$ with rm-ANOVA). Therefore, a combined approach was necessary in order to take advantage of both temporal and spectral features.

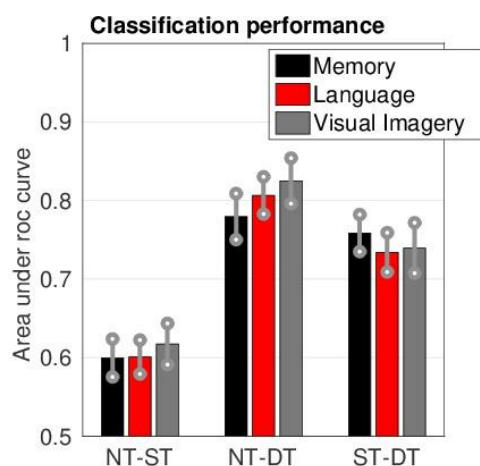


Fig. 5.24 Pair-wise spatio- spectral (SSD-mCSP) classification performance between the levels of processing (NT – no-processing, ST – shallow processing, DT – deep processing)

c) Spatio-temporal classification with sliding shrink rLDA

Considering the sliding ERP classification approach, we have a look over the classifier performance. The average classification output for the language condition presented in Fig. 5.25, shows 0.69 AUC values ± 0.016 SEM for the NT-ST discrimination, 0.68 AUC ± 0.012 SEM for NT-DT and 0.71 AUC ± 0.0010 SEM for ST-DT.

d) Spatio-temporal, spatio-spectral and spatio-tempo-spectral shrink rLDA classification comparisons

In addition, we can have a look, in comparison, over all the classification approaches and feature-based types, in the following.

As it can be seen in Fig. 5.25, the CSP classification on the 5-7 Hz frequency band gives the lowest performance. An improvement is observed for the 8-14 Hz and 16-20 Hz frequency bands, which were selected also for the combined classification. The Spatio-Spectral Decomposition method enhances the classification, more emphasized for the ST-DT discrimination of the 8-14 Hz frequency band. Next, the multi-band classification based on SSD which considers both 8-14 Hz and 16-20 Hz frequency bands, shows a small improvement when discriminating the deep processing class. The majority of the methods provide classification performances greater than the chance level 0.5 (significant t-test: $p < 0.05$; exceptions: CSP 5-7 Hz for the NT-ST and ST-DT pairs and CSP 16-20 Hz and CSP 16-20 Hz & SSD for the NT-ST pair; $p > 0.2$). The temporal classification based on ERP offers increased classification when discriminating the non-processing class (NT-ST), but decreased classification for the ST-DT pair. The ERP classification with sliding window show small performance around 70%, compared to the interval selection method based on signed r^2 that goes beyond 80% for NT-ST and NT-DT discrimination. Then, by applying the combined method which joints the ERP based on signed r^2 with the multi-band CSP with SSD classification, therefore taking into account both temporal and spectral features, an enhanced classification is obtained, even for the ST-DT pair (extended information on each participant in Appendix A.3.4, Tab. A.3.1). Note for example that the CSP 8-14 Hz with SSD classification performance look similar as the multiband-CSP & SSD classification. However, this effect was not found for the other conditions, where the combined approach

produces higher performances (even though not significant, $p > 0.27$ with Wilcoxon signed rank test).

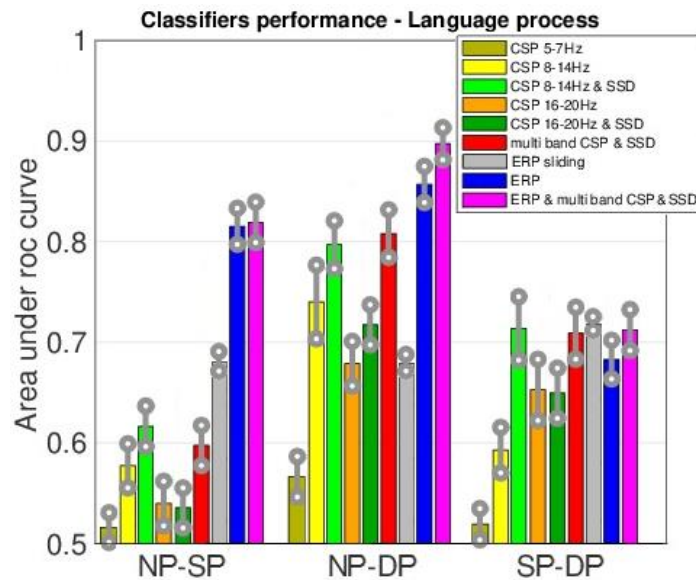


Fig. 5.25. The classifiers performance for the language condition considering the average AUC values. The grey antennas represent the standard error of the mean (SEM). Figure taken from Nicolae et al., 2018, with permission.

e) *Spatio-tempo-spectral shrink rLDA classification with selected CSP timing*

Further improvements for the combined classification approach were tested considering the selection of the CSP components. While in the method specified in section 5.2.3.5.1, the entire trial timing from 0 to 2000ms is considered for the selection of the CSP features, here, specific timing is considered detected by the highest ERDs discrimination in section 5.3.2.2.2. The selection interval was trimmed to 800 – 1500ms and therefore, the classification performance is improved by 1-3%. For example, in the ST-DT case, mean AUC values of 0.7294, 0.7328 and 0.7296 ($\pm 0.0156, 0.0221, 0.0135$ SEM) are obtained for the memory, language and visual imagination condition, but this increase is not significantly higher in statistical terms ($p = 0.1995$; 2-way independent rm-ANOVA).

f) *Spatio-tempo-spectral classification with Ridge regression shrink*

While searching for improvements considering classification, the ridge regression shrink method is also evaluated compared to the LDA approach. Specifically, for the ST-DT discrimination which is of higher importance, lower AUC values are obtained for all conditions: 0.6558, 0.6713 and 0.6628 ($\pm 0.0116, 0.0148, 0.0106$ SEM), significantly smaller than the LDA performances with 4-6% ($F = 18.77$; $p < 0.001$; 2-way independent rm-ANOVA).

g) Spatio-tempo-spectral classification with Logistic Regression

Considering Logistic Regression, the ST-DT discrimination provides mean AUC values of 0.4021 (± 0.0122 SEM), 0.3921 (± 0.0128 SEM), 0.3939 (± 0.0152 SEM) for the three conditions, below chance level ($p < 0.001$, p , Wilcoxon signed rank test rejected the chance level significance for $\alpha = 0.01$).

h) Spatio-tempo-spectral classification with QDA

For the QDA classification of the ST-DT pair, AUC values smaller than the LDA and the Ridge regression results are obtained: 0.5817, 0.5735, 0.5675 mean AUC (± 0.0197 , 0.0135, 0.0150 SEM), but beyond the chance level ($p < 0.001$ with one sample t-test).

i) Spatio-tempo-spectral classification with shrink rLDA considering DT- and DT+ classes

When trying to discriminate between DT- and DT+, which relates to user's decision when evaluating the cognitive question task, good AUC values are obtained of 0.5548, 0.5937, 0.6125 mean AUC (± 0.0329 , 0.0238, 0.0264 SEM), that exceeds chance level. However, the performance is not statistically significant for the memory condition ($p = 0.1180$ not significant, $p = 0.0015$, $p = 0.0008$; one sample t-test with $\alpha = 0.05$).

2. Multi-class case

a) Multi-class CSP, the OVR approach with shrink rLDA (3 classes)

When performing the multi-class CSP based on the One Versus Rest approach for the NT, ST and DT classes, the classification accuracy appears higher for all conditions compared to the JAD method (Tab. 5.1), showing 60.08% average performance for the memory condition, 63.13% for the language and 61.07% for the visual imagination. However, this difference is not statistically significant (rm-ANOVA: $p = 0.3751$). More details on single participant classification performances in Appendix A.3.4, Tab. A.3.2.

Tab. 5.1 Comparison over all conditions between the multi-class by JAD classification performance and the multi-class by OVR approach, both considering the spatio-tempo-spectral features

Participant	Memory		Language		Visual imagination	
	JAD	OVR	JAD	OVR	JAD	OVR
Mean	0.5931	0.6008	0.6276	0.6313	0.6034	0.6107
SEM	0.0200	0.0204	0.0117	0.0122	0.0176	0.0174

In addition, in terms of performance time, the classification execution time for one participant for the JAD method is three time faster than the OVR method, since fewer CSP patterns are provided to the classifier. For example, for one participant in 10 folds cross-validation form, the computation for JAD is 87.60 sec, as compared to 276.034 sec for OVR.

b) Multinomial logistic regression (3 classes)

When performing the multi-class (3 classes) classification for the combined spatio-temporal and spatio-spectral features (JAD approach) considering the Multinomial logistic regression method instead of LDA, the results are not improved. The performances show normalized accuracies of 0.4216 (± 0.0198 SEM), 0.4570 (± 0.0120 SEM), 0.4323 (± 0.0176 SEM) for the

memory, language and visual imagination conditions, significantly above chance level ($p < 0.001$; one sample t-test), but significantly smaller than the multi-classification with LDA results in section 5.3.2 ($F = 152.92$; $p < 0.001$; 2-way independent rm-ANOVA).

c) Multi-class JAD approach with shrink rLDA (4 classes)

When performing the multi-class LDA with spatio-tempo-spectral features (JAD approach) considering the four classes NT, ST, DT- and DT+, highest performances are obtained, namely 0.4352, 0.4617, 0.4424 (± 0.0163 , 0.0101, 0.0159 *SEM*) exceeding the 0.25 chance level ($p < 0.001$ with one sample t-test). However, the DT- and DT+ classes were not accurately discriminated with several misclassifications. Therefore, the four classes discrimination needs further investigation.

5.4 Discussion and conclusions

5.4.1 Comparisons with other studies

Firstly, the Event Related Potentials components have been widely investigated in the scientific community and previous works investigating the cognitive activity in oddball paradigms show likewise amplitude modulations and latency changes of the ERPs depending on the task difficulty (Donchin et al., 1973; Ullsperger et al., 1987; Polich, 2007; Kim et al., 2008). Specifically, the P300 amplitude increases and latencies are extended proportional with an increase in processes complexity and a stronger attentional demand.

In addition to the P300 amplitude modulations in the temporal domain, frequency modulations also appear, according to the difficulty of the cognitive processes. While some studies focus on the α band desynchronizations that appear at the centro-parietal sites during mental activity and cognitive judgement (Gevins et al., 1997; Klimesch, 1999; Venthur et al., 2010), which proportionally decreases in amplitude with the difficulty of cognitive processing, other studies consider the β oscillations that appear at the central and parietal sites (Pesonen et al., 2007; Okazaki et al., 2008; Sheth et al., 2009), decreasing with more complex cognitive activity. Furthermore, other studies relate to the changes in the θ activity, showed as synchronizations with respect to task difficulty (Gundel and Wilson, 1992; Klimesch, 1999), in the frontal midline scalp location (Gevins et al., 1997). Additionally, other studies have found power changes even in the delta and gamma frequency bands (Brouwer et al., 2012; Christensen et al., 2012). In a recent study of Naumann et al. (2017), gradual differences in task difficulty are investigated in the ongoing EEG considering the difficulty level of a video game. Their investigation shows strong modulations in the θ (4–7 Hz) and α (8–13 Hz) frequency bands, essential to changes in task difficulty, similar to older studies (Pope et al., 1995; Gevins and Smith, 2003).

However, in our study we found significant modulations in the α and the β bands and reduced in the θ band. These variations between studies are produced by the type of the experimental paradigm and the specific cognitive tasks performed.

As for the neural investigation and feature selection, few studies consider the multi-modal approach by integrating the temporal and also the spectral neural information (Dornhege et al., 2003; Brouwer et al., 2012; Martel et al., 2014; Mühl et al., 2014), as successfully proven in the present research. Moreover, the heuristic approach of selecting the

temporal intervals with highest discrimination that refer to the most significant spatio-temporal features, is not so frequently found in other studies, as in e.g. Blankertz et al. (2011), Scholler et al. (2012), Acqualagna and Blankertz (2013).

Considering the classification model, shrink rLDA provides the highest performance as compared to other classification methods (Parra et al., 2002; Müller et al., 2003; Bartz and Müller, 2013; Farquhar and Hill, 2013), e.g. the shrink rLDA classification is higher with 4-6% compared to ridge regression shrink as shown in our evaluation, effect proved also in other studies (Schultze-Kraft et al., 2016b) where shrink rLDA performs better with about 3%. In addition, the use of the Spatio-Spectral Decomposition is effective as shown in other studies (Cohen, 2016; Halme and Parkkonen, 2016; Schultze-Kraft et al., 2016b). Moreover, spatial filtering via CSP or other approaches should be customary integrated in BCI studies, in order to investigate the neural components and verify what the system learns. Unfortunately, many studies report very good classification accuracies with no reference to the type of components, leaving the decision to the machine side, which cannot consider only the neural information without proper setting. In this case, we are left to think with the ambiguity that the signals and components may or may not consider movement artifacts associated with the corresponding task executed in the experiment. Transferring the interpretability to the expert view is a good start for developing a reliable BCI. Additionally, a good choice of an artifact removal technique plays an important role here, as shown in our study considering the ICA with MARA technique which disregards many eye and muscular artifacts, loose electrodes, or artifacts from technical sources, providing a clear signal, with components originating from neural sources.

Numerous studies have investigated the feasibility of considering a variety of approaches for mental states decoding, for example workload (Gevins and Smith, 2003; Kohlmorgen et al., 2007; Holm et al., 2009; Borghini et al., 2014), alertness (Jung et al., 1997), fatigue (Stikic et al., 2011), and so on. However, to the best of our knowledge, no study has undertaken the challenge of assessing the cognitive processing levels for the purpose of monitoring user mental state, as reference to the involvement of the cognitive processes in many real-life applications.

5.4.2 Open questions and conclusions

5.4.2.1 Behavioral data

As behavioral data is a good measure of user performance and may show to some extent (depending on the paradigm) the relation to user decisions, how deeply the presented information is processed in the brain cannot be obtained by behavioral data. In this line of research, the user states are accessible through the user's brain signals.

5.4.2.2 Discriminant EEG analysis

1. Temporal analysis, ERP

In the average ERPs (Fig 5.7), two peaks appear: first at 250ms after the stimuli and the second at 400 ms with a distinguished prolongation. The first smaller peak relates to the decision considering the type of stimulus (NT, ST, or DT). No significant modulation is encountered for this P250 peak, correlating with a similar degree of cognition for all levels of

processing, namely color and category perception. The second peak, however, refers to different levels of processing (no processing (NT), shallow (ST), or deep (DT) processing), being modulated in amplitude in correspondence with an increase level of processing. No differences in latencies appear, owing to the fact that the processing levels relate to the same decision task of mental computation. On the other hand, the deep processing task involves the execution of an additional task, according to the type of cognitive process. Conducting the requested cognitive task in order to answer the respective question will imply differences in latencies between trials (as depicted in Fig. A.3.3, Appendix A.3.2), not clearly visible on grand averages.

The graduated differences between shallow and deep processing observed in the ERPs (Fig 5.7) and ERDs/ERSs (Fig. 5.11 and Fig. 5.12) correlate with different levels of processing, and are not generated by targets occurrence, namely the odd-ball effect. This influence was avoided by integrating the same stimuli percentage of 12.5% between shallow (ST) and deep targets (DT). Referring to the differences between shallow or deep processing and no processing, it cannot be disentangled which differences are generated by the rarity of the occurrence (oddball effect) and which by the additional processing demands of the task. The differences in the time course of the ERDs (Fig. 5.11 and Fig. 5.12) encountered even after 500 ms, implies that the different modulations might probably be generated by the additional cognitive processing task in ST and DT.

While interpreting the patterns of the neural correlates by signed r^2 discrimination, left lateralized scalp topography (parietal and temporal areas) was observed for the language condition (Fig. 5.8), endorsing the scientific research which showed that language activation mostly involves left hemisphere participation (Spironelli and Angrilli, 2010; Griggs, 2012). The lateral occipital location for the visual imagination condition (Fig. 5.7) shows likewise negative potential underlying visual mechanisms, memory access and interpretation (Ganis et al., 2004).

The ERP spatial components showed no evidence of saccades, such as lateralized activity in the frontal area corresponding to horizontal eye movements, albeit the participants were permitted to freely explore the visual stimuli by eye gaze. The successful artifact removal belongs to the ICA artifact correction with semiautomatic selection of the artifactual components based on MARA (e.g. in Fig. A.3.1, Appendix A.3.1). However, on grand average the eye movements could average out, because they do not follow the same timing across trials.

2. *Tempo-spectral analysis, ERSP*

The cognitive state of a user is also reflected in the brain dynamics of locally generated oscillations at various frequencies. The spectral perturbations (Fig. 5.17, Fig. 5.18) show therefore additional information considering the memory (Berka et al., 2007), language or visual imagination conditions, more prominent for the gamma band (>30 Hz). A shallow level of processing is depicted in higher beta frequencies (20 – 30 Hz, 28 – 38Hz) relating to an alert and focused state (Lafrance and Dumont, 2000; Levin et al., 2000). Perturbations in the alpha band are detected for no cognitive processing (10 – 13 Hz), corresponding to a visual processing of information, an alert state but no mental processing (Thut et al., 2006).

Whereas the current channel-wise activity analysis integrates a cumulation of potentials collected from different parts of the brain, more source related information could be detected by considering time-frequency decompositions of the independent components.

3. *Spectral analysis, PSD, ERD, CSP*

The power spectrum discriminability in the range of 3-40 Hz (Fig. 5.10), showed pronounced spectral components considering the α (8–14 Hz) and β band (16–20 Hz) and less noticeable for the θ band (5–7 Hz). Comparing between conditions, the θ band is emphasized for the memory and language conditions, reflecting memory retrieval (Meyer et al., 2015), cognitive activity (Klimesch, 1999), and sustained attention (Huang et al., 2007b). These signed r^2 differences encountered in the θ band are considerably smaller than the differences occurred in the α and the β band. Therefore, the θ band was discarded from further analysis, decision reinforced by a separate classification evaluation considering only the θ band (e.g. 0.51, 0.56, 0.51 mean AUCs for the language condition with respect to the binary discriminations: NT-ST, NT-DT, ST-DT; showing insignificance for the NT-ST and ST-DT classification pairs with t-test at $\alpha = 0.0056$ and Bonferroni correction for multiple comparisons, given $p > 0.0195$ and barely significance for the NT-DT discrimination with $p = 0.0052$).

The ERD/ERS curves considering the α and β bands are modulated by the degree of cognitive processing, better evidenced after 500 ms. The degree of modulation in the α band relate to the presence of mental coordination (Palva and Palva, 2007), alert states (Klimesch, 1999), cognitive processing, access to stored information (Klimesch, 2012). On the other side, strong β ERS show complex processing and analyzation of the presented information (Lachaux et al., 2005). Between conditions, higher synchronization is observed for the deep processing level considering memory condition, suggesting an easier process. However, this effect contrasts with the subjective participants scoring relating, on average, to an easier language condition (difficulty scores in Fig. 5.6).

As further measures for discrimination, the spatial filtering distinguishes the activity sources with maximum variance between conditions, such as e.g. higher variance in the frontal area for the shallow processing and higher variance in the parietal area for the deep processing (Fig. 5.13 and Fig. 5.14). Moreover, the CSP components show an estimation of the originating activity which do not suggest influences from eye movements and visual processing, such as strong frontal or occipital activity, respectively. This assures a reliable classification discrimination based on the neural correlates alone. Furthermore, the spatial activation patterns allow an additional physiological interpretation, by providing information regarding the spatial region of the cerebral sources that engender the activity of the component.

4. *Classification*

The three levels of cognitive processing (no-processing, shallow and deep processing) were successfully binary distinguished from 0.70 up to 0.90 mean performance considering multivariate data analysis applied on a single-trial basis on the temporal and spectral domains (ERPs and CSPs), considering regularized LDA with shrinkage.

When interpreting the classification results in relation with the signed r^2 discrimination for the ERD/ERS curves, an important observation is conspicuous, that the

combined classification performs remarkably, even in the NT-ST case when no considerable difference is encountered by the signed r^2 . This is due to the involvement of both temporal and spectral features in the classes' discrimination.

Further, it is important to note that the user error, shown in the behavioral data, may influence the performance of the classifier, due to the lack of true labels. And generally, a higher level of cognition might involve higher participant error rate. However, we can not draw any conclusion with the available data, since we do not have behavioral measure to relate strictly to the levels of processing. On the other side, participants error rate may not have a significant influence, because the behavioral performances are quite good (answers ratio close to zero as shown in Section 5.1). In addition, no correlation has been found between answers ratio and classification performances (binary or multi-class) considering conditions ($p > 0.16$ Spearman rank-order correlation), even though a slight trend is observed for language over the other conditions in terms of fewer behavioral error rates and higher classification performances. Furthermore, it is essential to point out the classification success considering participants free viewing between the two stimulus objects. Following this permissiveness, different levels of processing unwittingly might induce different eye dynamics between stimuli (e.g., DT might induce more alternations of the gaze between the two objects of a stimulus as compared to NT which may not require eye movements at all). For this reason, appropriate artifact removal strategies (ICA with MARA) and careful verification was performed, and the resulted signals seem to have no artifacts intrusions (ERP, ERD, CSP). Furthermore, an evaluation of potential contamination by artifacts was performed by detecting the level of decoding based on the EOG activity alone. In this regard, the difference between the EOG (measured below the left eye) and Fp1, F10 and F9 channels was considered as features, corresponding to the vertical and horizontal eye movements. The binary classification (rLDA shrink) show chance level AUCs considering all conditions and classification pairs. For example, the discrimination of the NT-ST, NT-DT, and ST-DT pairs for the language condition provides: 0.51, 0.55 and 0.46 mean AUCs). All results were statistically tested by Wilcoxon signed rank test showing insignificance ($p > 0.17$).

Considering the multi-class classification approach, good performances around 60% are obtained for the three classes (NT, ST, DT) considering appropriate multi-modal classification based on rLDA shrink. Targeting user mental state decoding based on the depth of cognition which involves the prediction from multiple cognitive processing levels (at least three: no-, shallow and deep processing), a multi-class classification approach is more appropriate. However, improvements are expected in this regard, targeting increased discriminations for the shallow and deep processing levels which show more misclassifications. A supposition on this fact is considering participants error rate, which might be modulated by the level of difficulty (e.g. higher the level of cognition, higher the error rate, higher the misclassification rate). This involves a different strategy (Porbadnigk et al., 2015) which is hardly investigated with the current data. Another reason could possibly be due to other more stochastic aspects of brain activity, or less likely to the structure of the experiment.

5. *Additional classification results*

Firstly, the use of SSD improves the classification performance, as shown also in other works, Schultze-Kraft et al., (2016b).

Moreover, when comparing the multi-modal performances (ERP-mCSP) with the separate uni-modal classification results (ERPs or CSPs) in sub-section 5.3.3, it is noticed that higher performances are obtained and that the temporal and spectral features plays a role specific to the discrimination pair. In the NT-ST discrimination, most probable the temporal features bring enhancements (due to higher temporal classification performances), while for the ST-DT discrimination, the CSP features contribute to higher performances (due to higher spectral classification performances).

Regularized LDA with shrinkage of the covariance matrix provides the best classification performances. When considering logistic regression, the classification drastically decreases and moreover, it goes below chance level, meaning that more samples are classified in the opposite class. At first view, this might be considered due to the temporal dependence among the trials. On this line, the classifier might learn something related to the precedence of the events and therefore, the below chance level effect is obtained, instead of the pure chance distribution. More in deeply, it might be thought that there is some physiological or instrumental signal in the data which has some harmonic at frequency close to autocorrelation present within the labeling of the trials. Then, the classifier might simply learn that 'frequency'. Due to non-100% coherence between autocorrelation of labels and that rhythm in the data, the hold-out set in the crossvalidation might always be in the 'anti-phase', which should give "null-distribution". In this case, the permutation testing would not provide reliable assessment, since it obliterates autocovariance within the labeling. A solution might be the 'anti-learning' phenomenon, the reversal of classifier decisions when the classifier is trained to learn the wrong labels (Kowalczyk and Chapelle, 2005). In case of marginally sparse design, a possible solution to get away from anti-learning, may be to perform N-3 cross-validation, i.e. holding out three samples, not folds (one sample from each category) and repeated on sufficiently number of times (arbitrarily select one sample from class NT, one from class ST and another one from class DT).

However, the same effect was not obtained in the linear separation case, with LDA. Therefore, this might have something to do with the linear vs. non-linear separation of the data, and in the logistic non-linear case, the data is overfitted. Further testing needs to be implied considering the separation mode between training and test data (one sample crossvalidation). This was not further tested here, because it did not constitute the scope of this research.

Firstly, random label shuffling needs to be performed and the results investigated: around chance level performances should be obtained. When below chance accuracy occurs in permutation testing experiments with nearly similar probability to that of above chance accuracy, this imply that below chance and above chance could both be stochastic. It is possible that, in the case of only one participant is giving below chance accuracy, then, this could be due to different sources of noise (e.g., electrodes noise, head motion during acquisition, participant's attention, etc.). In this case, the particular participant can be neglected, or further processing has to be performed on that participant. However, in our

case, the number of below chance participants is close to the number of above chance participants, then, there is no correlation between the EEG and the stimuli. Furthermore, the cross-validation approach with 10 folds shows below chance performance on most of the test iterations (and always below chance level overall), so this doesn't seem to be a fluke of noise recording, cumulative participant motion, etc.

A different investigation is to consider 10-folds crossvalidation separately within each run and check if the results are over chance level. Furthermore, to check whether the results of training on one session alone and testing on another session give below chance level. If the verifications are true, it might indicate that the classifier is able to learn from the data within each session separately and cannot transfer the knowledge to other sessions.

The number of class NT, class ST and class DT examples in the training and test set are unbalanced, therefore the classifier might develop some bias to guess one class more than the other. For example, the classifier guesses class NT more often than class ST and DT. However, class ST and class DT are balanced, so the classifier should roughly guess an equal amount, although the guesses just tend to be more often wrong than correct.

Additional work that treats this issue can be found in Kowalczyk and Chapelle, (2005).

5.4.2.3 *On the line of research*

In addition to the standard BCI research, the present study inferred different levels of cognitive processing by activities that exceeds conventional target/non-target approaches and provide further insights on how the information was perceived by the user and to which processing degree. Furthermore, a higher variability and complexity of the visual stimuli is present and in conjunction with the free viewing permission for the inspection of the stimuli, gives more freedom to the user side. This work expands previous research on the effect of task complexity over ERPs and brain oscillations.

The fruitful extraction and discrimination of the cognitive processing levels based on novel machine learning methods and advanced signal processing techniques, demonstrates the usability of the depth of cognitive processing for the use in neurotechnological applications considering the EEG signals. Overall, the present study is a step forward toward applications that estimate the level of cognitive processing in realistic settings of Brain-Computer Interfacing, or moreover considering Symbiotic Interactions (Blankertz et al., 2015; Gamberini et al., 2015) where the system can automatically adapt to the user state, intentions and needs, for example considering safety critical workplaces (Venthur et al., 2010).

5.5 Limitations and future directions

Starting from the fact that feeble discrimination was obtained between shallow and deep processing in the multi-case approach and the bizarre effect in the logistic regression case, further investigations are necessary. As we have a good reason to believe that the stimuli randomness did not introduce additional temporal dependency to the ERP responses (Tangermann et al., 2012a), a hidden background process may still be involved, relating to a continuous increased attentional demand during the entire experiment. If this supposition is true or not, this aspect needs to be taken into consideration for future investigations. In the unfortunate case, adapted classification approaches have to be considered (e.g. Höhne and Tangermann, 2014).

On the other side, optimized adaptation of the current multi-modal classification can be considered related to features weighting, based on correlation (Sugiyama et al., 2007). In such way, the corresponding weights for the two types of features (temporal and spectral) will relate to their amount of involvement for the corresponding neural component. Another classification approach in order to detect the correct neural responses and to neglect the error potentials can be considered by an unsupervised classification (Vidaurre et al., 2011a; Schultze-Kraft et al., 2016b).

The discrimination between fulfilled and unfulfilled tasks within the deep process requires additional engaging activity and processing and needs further investigation. The trial-to-trial variability of the neural responses caused by different latencies in judgement of each decision, should be investigated in more detail. For instance, investigating differences in remembered and not remembered trials for the memory process, differences in the language semantics, or differences in the quantitative measures of the visual imagination process will provide further information on the underlying internal mechanisms of user intentions that correspond to natural fluctuations of the respective cognitive process. The discriminations can be evaluated for example by sub-class shrinkage classification (Höhne et al., 2016). Following this line of natural fluctuations in user decisions, another scenario with more flexible options regarding decisions and tasks can be evaluated, for example the case where the user can willingly choose a task or not.

The current experimental paradigm involved induced levels for investigating the depth of cognitive processing, while an intended real-time BCI application would involve spontaneous fluctuation in the level of processing. The neural correlates could be different, and it is of interest to investigate how could the proposed approach transfer to the realist situation and how to calibrate the classifier for that scenario. As a starting point, the investigated experimental paradigm in form of a serial stimulus presentation with body movements constrains and less eye movements, and the reduced number of artifacts, made it easier to retrieve the neural components, but it constrained the user freedomness. When considering transferring the present findings to a real BCI application, such as an information retrieval system, more flexibility considering viewing and movements should also be investigated (as in Schultze-Kraft et al., 2012; Kauppi et al., 2015; Ušćumlić and Blankertz, 2016) and a more natural task scenario (Schultze-Kraft et al., 2012). However, allowing free

movements and viewing comes with a drawback in form of increased artifacts, which require additional care by spatial filtering in order to refer only to the activity from neural sources.

While controlled paradigm and stimuli were appropriate for primarily investigating the levels of cognitive processing in form of an ERP study, more complex and variate stimuli, with richer structure are available in real applications which might generate different ERP responses and introduce additional jitter, needing therefore throughout investigation. In depth investigation should be performed also considering words instead of pictures, while in an information retrieval system for example, linguistic stimuli such as words and text are more appropriate (Acqualagna and Blankertz, 2015).

One step further towards the implementation in real-life scenarios is to develop online quantification of the level of cognitive processing considering the successful multi-modal decoding. Corresponding adaptations have to be properly considered for online settings, e.g. causal filters considering pre-processing, appropriate classification (Blankertz et al., 2010a; Schultze-Kraft et al., 2012). For an optimal extraction of the neural components, methods such as CSP, Source Power Co-modulation, SPoC (Dähne et al., 2014a) and Canonical Source Power Co-modulation, cSPoC (Dähne et al., 2014b) can be used, as in Schultze-Kraft et al., (2016b). Source Power Co-Modulation (SPoC) analysis can be used to extract cognitive power modulations in accordance with the ongoing level of processing. SPoC finds the spatial filters of which their corresponding bandpower dynamics maximally covary with a given target variable (Dähne et al., 2014a), namely the level of cognition. While canonical SPoC (Dähne et al., 2014b) can be used in unsupervised settings where no label information is available, perfect suitable for online BCI applications.

Targeting novel neuro-technological applications that are able to adapt to the momentary state of the user, a real-time estimator to detect the natural occurring fluctuations in the levels of cognitive processing needs to be developed, as similarly investigated in Venthur et al. (2010) or for example considering workload detection in Naumann et al. (2017) and Schultze-Kraft et al. (2012; 2016b).

5.6 Lessons learned

- ✓ The stimuli paradigm turned out to be captivating for the participants which were engaged the entire duration of the experimental sessions.
- ✓ The well-designed complex stimuli paradigm successfully elicited different levels of cognition, namely no processing, shallow and deep processing.
- ✓ Discriminative patterns of cognitive processing are reflected in the temporal fluctuations represented by the ERPs and in the spectral modulations visible by the ERD/ERS phenomena.
- ✓ Enhanced artifact projection methods (such as ICA with MARA) are a valuable signal processing tool by successfully removing several artifacts caused by e.g. ocular and muscular activity, electronic noise or loose electrodes.
- ✓ The resulted components and modulations (ERP, ERD/ERS, CSP) show clear activity with no perturbations originating from artifactual sources.
- ✓ Multi-modal decoding (spatio-tempo-spectral features) is successful and feasible for BCI systems. It resulted in a higher performance (higher AUC) compared to uni-modal decoding, with performances increased by at least 10%.
- ✓ Best classification performance was obtained by regularized linear discriminant analysis with shrinkage of the covariance matrix considering the binary and the multi-class case.
- ✓ Several misclassifications are encountered for the DT- and DT+ discrimination and a more suitable approach should be further investigated. E.g. a specific exploitation and classification adapted to the subclass features, aiming the discrimination of not only the processing levels, but also user decisions within the deep processing task.
- ✓ First step towards an online mental state detection BCI system has been taken in this study. However, when targeting the detection of natural fluctuations in user decisions within a BCI application, a complementary scenario should be investigated, with more flexible options considering user decisions and tasks, e.g. a situation where the user can willingly choose a task or not.
- ✓ Furthermore, in a future scenario based on natural fluctuations, the neural correlates will most likely be different and is questionable how well the proposed approaches here would transfer to the realist situation and how the classifier should be calibrated for that case. Further investigations are needed in this regard.
- ✓ While the classification considered the paradigm labels and therefore prevented the knowledge of the 'ground truth', future unsupervised classification should be considered to suit also the online application case when no label information is available;
- ✓ The feasibility of considering the depth of cognitive processing for a neuro-technological application based on mental state detection has been proved in this research ERP study.
- ✓ To approach a more realistic application, a research study that considers more flexibility considering movements and viewing, with natural brain fluctuations and not induced processing should be further investigated;

Chapter 6

Conclusions

The advancement of technology along with novel signal processing and machine learning algorithms provides a great tool for a better understanding of the human brain and its processes. Further, it is up to expert researchers and well-trained experimenters to design intelligent scenarios that reveal the concealed neural processes. This thesis contributes to the investigation of neural signals and proposes scenarios that focuses more towards user's interest. Firstly, by developing specific paradigms and proposing tasks to investigate user's corresponding brain activity. Secondly, by using improved signal processing and machine learning techniques as shown in this thesis, the BCI system will become more reliable and relying on the neural signals and not on noise, and easily interpretable where a researcher can verify what the system actually classifies. We investigated advanced techniques in the processing step to remove artifacts that come from noisy sources and propose intelligent approaches regarding the classification selection. In such ways, the BCI performance is improved, user's interest is increased, and the Brain-Computer Interaction will be further facilitated.

6.1 General conclusions

This PhD thesis contributes to the field of Brain-Computer Interfaces and Neurotechnology by two offline studies that investigate optimized stimulus and tasks considering user interest, targeting the improvement of the BCI interaction. Both studies highlight the importance to rigorously choose the stimuli setup for visual or auditory paradigms in the context of user-friendly BCIs. Advanced signal processing and machine learning techniques were evaluated, which may lead to an efficient and fully interpretable BCI system. The aforementioned system would be able to distinguish different mental states and inform the BCI expert about the corresponding brain rhythms and regions involved.

Specifically, the system could also inform the BCI experts which neural activity corresponds to which mental state, considering specific brain regions and specific rhythms.

Firstly, on Chapter 4, improved stimuli in a motor imagery based BCI system were evaluated. After selecting effective stimuli, specific attractive and efficient user motor imagery tasks were investigated, based on user's interests, preferences, background and skills. In such a way, the study aimed to design specific user task that engage the user in the BCI system and would trigger a more powerful brain process that can be easier detected by the BCI. By the careful selection of the stimuli and user defined tasks, the user was continuously involved and showed increased interest in the BCI. A remark for future studies is to carefully select an activity related to user's interest, but an uncommon activity that could trigger a more powerful neural effect. By considering corresponding advanced signal processing and an ensemble approach that uses complementary information from the temporal and the spectral characteristics of the brain activity, our evaluations obtained high performances.

After providing improvements to the most frequently used type of BCI system, the motor imagery based BCI, the research focused towards more beneficial applications that go beyond the conventional communication and control goals of the BCI systems, towards more convenient approaches of mental state monitoring (Müller et al., 2008; Zander and Kothe, 2011). The study investigated different levels of cognitive processing (Chapter 5) for the purpose of user mental state detection, scenario which has not been previously used in the BCI research, to the best of our knowledge. This can later be used to drive the corresponding BCI applications based on the current user state evaluated from the ongoing EEG activity. Enhanced discrimination between different levels of cognitive processing has been detected while investigating the neurophysiological processes. The behavioral assessment additionally showed very good user performance for the complex stimuli paradigm. Participants expressed interest along the experiment, also observed in the questionnaire fulfilled at the end of the experiment. The careful selection of the advanced pre-processing (temporal and spectral filtering), data analysis (spatial filtering, multi-modal discriminability) and machine learning techniques, resulted in clear signals and an interpretable BCI system, where the researcher can easily verify what the system selected as relevant for the corresponding brain activity. The multi-modal analysis of the brain activity and the multi-feature approach efficiently detected the corresponding brain processes and enhanced the discrimination of the neural correlates given by the ensemble classification approach. The regularized Linear Discriminant Analysis with shrinkage of the covariance matrix was successful in case of multi-dimensional features, showing an enhanced classes discrimination supported by high classification accuracies, exceeding the performances of other classification techniques.

Both experimental studies results showed that the proposed processing and classification strategies revealed the neural activity related to the involved brain processes and neglected the noisy background activity together with artifacts caused by movements and hardware noise.

The behavioral measures with respect to user error rate and personal feedback considering the experiment, suggested that developing an interface centered on the user, reduces the bothersome effect and keeps him engaged for a prolonged time.

In terms of pushing the BCI system towards an on-line application, on one side, a reduced amount of stimuli as requested by the BCI was investigated, more complex scenarios were developed providing more freedom to the user and further connections towards a realistic scenario considering the brain fluctuations in involved while processing the external stimuli and deciding. This thesis brings novel research investigations in the context of user interest and needs within a BCI system, targeting the enhancement of the interaction between the computer and the human brain.

Performing an overview of the investigation and findings presented in this thesis, all the key points proposed in the beginning have been fulfilled. By means of the two experimental studies focused on the user, the advantages and importance of considering user needs and desires have been highlighted, accordingly.

6.2 Future perspectives towards BCI applications

In addition to the future works mentioned for each study, this thesis also paves the way to further long-term research. In the train of thoughts for future developments, different development and implementation issues arise to the BCI for the use in real-life applications. On the strength of the successful feasibility studies investigated in this thesis, could we transfer the techniques investigated here to real-world scenarios? This is certainly a difficult problem, as many objectives arise along with particular concerns. Repetitive stimuli in form of a presentation are displayed in these offline laboratory studies, where the user is restricted to few permissible movements and tasks, while in 'out of the lab' scenarios, continuous brain activity investigation and detection are required, and more dynamic movements are involved. Plus, a peaceful environment was available in the laboratory settings, compared to industry circumstances and other 'out of the lab' situations where more background noise and distractions appear. To translate the scenarios towards real-life neurotechnological applications, first the repetitive stimulus presentation approach has to be switched to a non-repetitive corresponding application of e.g. information seeking (Gamberini et al., 2015), operator monitoring (Venthur et al., 2010), video games (Naumann et al., 2017), where the investigated neural correlates focus more on the continuous oscillatory aspects of brain activity, e.g. triggered by workload (Schultze-Kraft et al., 2012, 2016b), attention (Jung et al., 1997) or even the levels of cognitive processing, within a continuous online monitoring and detection of the EEG activity (Kübler et al., 2006; Schultze-Kraft et al., 2016b), as compared to SMR, or event related potentials scenarios. Moreover, the signal processing and machine learning methods have to be adjusted for online detection (Blankertz et al., 2006a; Schultze-Kraft et al., 2012). Further, in the long term, special feedback has to be provided to the user, such as the respective application should automatically adapt in real-time according to the corresponding user mental state.

In dynamic real-life situations, where the users perform additional movements or complex physical activities (Gramann et al., 2011; Zander and Kothe, 2011; Zander et al., 2014; Jungnickel and Gramann, 2016) the challenge increases as further attention and more optimal approaches have to be considered for extracting the neural information and neglecting the activity coming from noisy sources. Furthermore, the key remains to the BCI system to ease the Human-Computer Interaction by silently detecting the corresponding user

mental state (e.g. cognitive) and adapt the BCI application accordingly, for example reducing, increasing or highlighting the content of interest in an information seeking application. In this case, a more comfortable interaction is required from the user when the BCI automatically detects the corresponding mental state or the respective intention, without the need for the user to clumsily control his sensory-motor brain oscillations, as in the case of a motor-imagery based scenario, where the user has to perform as many motor-imagery movements as the number of decisions he wants to perform. This will ease the human-computer interaction by reducing the complexity of user's requirements and more certainly will trigger increased user interest in using a BCI application.

While the present research relates to the first measures that need to be taken in order to switch in-lab settings to a more realistic situation, by integrating user self-chosen tasks and richer and complex stimuli and scenarios, the participants were still constrained to no additional body movements and small eye movements between stimuli. Inevitably, a lot of work needs to be performed in order to accomplish reliable real-time BCI implementation, such as online classification in both studies, the transfer from the induced levels paradigm to an application based on natural fluctuations considering the second study, with no controlled scenario and no constrained activity for the users.

In terms of hardware, more portable systems can be used (Mullen et al., 2015), more wearable designs (Nikulin et al., 2010, Debener et al., 2015), using dry (Popescu et al., 2007) or water-based electrodes (Volosyak et al., 2010) which drastically reduce the experiment preparation (Guger et al., 2012), even though additional care might be necessary related to signal quality while are more sensitive to artifacts. Despite the challenges and limitations that BCI is currently facing, there are still strong reasons to believe that many types of BCI applications will most likely be viable in the near and far future (Vansteensel et al., 2017). Given the fact that BCI is a young research field so far, more likely great advances will be performed in the years to come, which will open a broad exciting research.

Closing Statement

Preserving the time for further research, as last written words in this thesis, I would like us to contemplate further on brain functioning and its tremendous hidden secrets, highlighting the miracle of brain and the continuous journey that brain research provides which will endlessly carry on.

Appendix

A.1 Additional theoretical foundations – Chapter 2

A.1.1 Statistical analysis

1. Standard Error of the Mean (*SEM*)

While the sample mean is an unbiased estimator, the variation of the error in the sample mean with respect to the true mean can be estimated by e.g. standard deviation (σ) or standard error of the mean, SEM:

$$SEM(x) = \frac{\sigma(x)}{\sqrt{n}}, \quad (\text{A.1.1})$$

where:

$SEM(x)$ – standard error of the mean for data x ,
 $\sigma(x)$ – standard distribution of the data x
 n – size of the data

2. Hypothesis testing

Hypothesis testing is divided into three categories: parametric, non-parametric and semi-parametric testing. The parametric hypothesis tests are frequently used to measure the quality of the sample parameters or to test whether the estimates on a given parameter are equal for two samples. Statistical hypothesis testing assumes a preliminary null hypothesis and aims at rejecting or confirming it based on the probability of the observed data (low or high) considering a specific α level of significance.

- *Student's t-test*

A t-test checks if the data follows a Student's t-distribution (Fisher, 1925) with mean zero (one sample t-test) or determines if two sets of data have equal means (two sample t-test) or the pairwise difference between two data vectors has zero mean (paired sample t-test). It is most commonly applied in case of normal distribution and when the variation of the data is unknown.

- *Kolmogorov–Smirnov test (KS test)*

Kolmogorov–Smirnov test (KS test) is a non-parametric test that quantifies the difference between the empirical distribution function of one sample and the cumulative distribution

Appendix

function of a reference distribution, e.g. normal distribution. In case of two sample data vectors, it computes the difference between the empirical distribution functions of the two samples (Wayne, 1990).

- *Wilcoxon signed-rank test*

The Wilcoxon signed-rank test is a non-parametric test that determines whether the means of two dependent samples differ. It can be used as an alternative to the paired Student's t-test, when the population cannot be assumed to be normally distributed (Gibbons, Chakraborti, 2011).

- *Shapiro Wilk test*

The Shapiro-Wilk goodness-of-fit test (Shapiro and Wilk, 1965, Royston, 1995) evaluates the hypothesis of normal distribution data, with a higher tolerance for skewness and kurtosis deviations. It is generally considered more powerful as compared with other alternatives, such as KS test for example (Razali and Wah, 2011).

- *Chi-squared goodness of fit test*

The most common measure for testing the variance of the data is the Chi-squared goodness of fit test (Chernoff and Lehmann, 1954). This statistical model detects how good it fits a set of observations by measuring the inconsistencies between the observed values and the expected values considering the specified hypothesis. Generally, the hypothesis refers to a well curve fit of the data and the model determine the exact curve shape of the data while minimizing the mean squared error. Shortly, it determines if the sample data has a specified distribution, usually a normal distribution, where the parameters (mean and variance) are estimated from the data.

- *Bartlett test*

Bartlett test (Bartlett, 1937) analyses if k samples come from populations with equal variances, named homoscedasticity or homogeneity of variance. It is generally used for testing the assumptions of statistical test which refer to equality of variance across groups or samples. Bartlett's test is sensitive to non-normality. When the samples come from non-normal distributions, Bartlett's test is simply testing for non-normality, instead of variance analysis. In this case, Levene's test and the Brown–Forsythe test are more appropriate, because are less sensitive to departures from normality (Snedecor and Cochran, 1989).

- *Brown & Forsythe test (modified Levene test)*

The modified Levene test (Brown–Forsythe) analyzes the statistical significance of group variances equality (Brown and Forsythe, 1974). It can be used as a replacement for Bartlett test, when the data distribution is non-normal.

- *Mauchly's test*

Mauchly's test (Mauchly, 1940) validates the sphericity characteristic of the data. The sphericity condition refers to equal variances of the differences between all possible within-participant variables pairs (i.e., levels variables). More precisely, all response variables have similar variance, and each pair of response variables share a common correlation.

- *ANOVA*

The statistical ANOVA measure (Krzanowski, 1988), determines if several groups (levels) have similar mean related to one or more data sets (or factors). Depending on the number of factors, it is termed one-way, two-way or n -way ANOVA. ANOVA is a linear model, with the following assumptions for the probability distribution of the responses: i) Independence of samples; ii) Normality – the distributions of the residuals are normal (However, for large sample sizes, non-normality is accepted because the distribution of the sample means will always be large); iii) Equality (or "homogeneity ") of variances between levels, called homoscedasticity; iv) Sphericity (assumption for the repeated-measure of ANOVA): the variances of the differences between all possible pairs of within-participant conditions are equal (homogeneity between levels and factors). For testing normality distribution, e.g. the Chi-squared goodness of fit test, Kolmogorov–Smirnov test, Shapiro Wilk (Shapiro and Wilk, 1965) test can be used, while for homogeneity, Bartlett test (Bartlett, 1937) or Brown & Forsythe Levene test (Brown and Forsythe, 1974) are good estimations, and for sphericity e.g. Mauchly's test (Mauchly, 1940) is appropriate.

The conventional ANOVA measure assumes a between-participants design by considering different groups. Therefore, in case of an experiment with multiple conditions or cases, where all the participants performed all conditions, the assumption of independence of samples is not valid any more. A good measure in this case is the repeated measure of ANOVA (rm-ANOVA), (also known as a within-participant design), which accounts for inter-participant variability and has therefore more statistical veracity. Similarly, it can compare the data between multiple levels considering one, two or n factors (one-way, two-way or n -way rm-ANOVA, in accordance).

- *Multiple comparisons*

Multiple means comparisons can help identifying differences between data means, for example as in the case of the Bonferroni correction.

Bonferroni correction

When multiple comparisons are performed, or multiple hypotheses are tested, the possibility for a rare event to appear increases, and so does the probability of incorrectly rejecting the null hypothesis. This effect is diminished by the Bonferroni procedure (Bonferroni, 1936) which corrects the original p -value by testing each individual hypothesis or sample considering an α/m significance level (thresholding). The parameter m can represent the number of hypothesis and the number of data samples.

- *Bootstrapping*

Bootstrapping is an approach of statistical inference that makes few assumptions regarding the underlying probability distribution that characterize the data (Efron, 1982; Efron and Tibshirani, 1993). The bootstrapping procedure can be used to test for statistical significance, in three different ways non-parametric, parametric, and semi-parametric. While in practice, because nonparametric intervals consider parametric assumptions, the categorization rather arbitrary. In the following, the non-parametric version is described.

In a situation where confidence intervals are requested for a set of observations, for whom there is no possibility to estimate the standard error, the statistic sample can be appropriately assumed to reflect the broader population from which it was drawn. Considering the sample as a model of the population, uniform random number numbers of observation are resampled in the data with replacement for which bootstrap estimates are computed. Assuming that these bootstrap observations similarly vary to the sample statistic (null hypothesis), the probability of obtaining a different statistic is then computed. If the probability value is sufficiently low, the null hypothesis is rejected and the observations are statistically different. Typically 95% of the bootstrap estimates should fall within the 95% confidence limits of the sample statistic, that is a 5% significance level.

3. Correlation

- *Spearman's rank correlation coefficient*

Spearman's rank correlation coefficient (Spearman's rho, ρ) is a nonparametric measure of rank correlation (Best and Roberts, 1975), analyzing the statistical dependence between two variables rankings. It is similar to the Pearson's correlation (Pearson, 1895) except it assesses linear or non-linear monotonic relationships between the two variables and ranges from -1 (opposite correlation) to +1 (highly correlation, similar or identical), while Pearson's correlation considers only linear relationships. The significance is determined by using the permutation test, on the null hypothesis of no correlation, against the alternative of a nonzero correlation.

A.1.2 Measures of signal quality

Signal-to-noise ratio (SNR) is a measure that compares the magnitude of a desired signal to the magnitude of the background noise. SNR is defined as the ratio between the signal power and the power in the noise and it is expressed in decibels according to the International System of Units.

$$SNR = 10 \log_{10} \frac{P(\mathbf{x}_s)}{P(\mathbf{x}_n)} \quad (\text{A.1.2})$$

where \mathbf{x}_s is the desired signal and \mathbf{x}_n is the noise.

Another similar measure, Peak signal to noise ratio is computed by:

$$PSNR = 10 \log_{10} \frac{M^2}{MSE} \quad (\text{A.1.3})$$

where M is the maximum value of the signal \mathbf{x} and MSE is the mean squared error computed by: $MSE(\mathbf{x}) = \frac{1}{m} \sum_{i=1}^m (\mathbf{x}_s(i) - \mathbf{x}_n(i))$ with m – the length of \mathbf{x}_s .

A.1.3 Signal processing

A.1.3.1 *Signal filtering and time to frequency transformations*

1. *Discrete Fourier Transform filtering – time to frequency transformation*

Discrete Fourier Transform (DFT) (Smith, 2007b) decomposes a temporal signal into the frequency domain, represented by the amount of oscillations with different frequencies f . Hence, the DFT of a signal $\mathbf{s}(t)$, with $t = 1, \dots, N$ (samples) is given by:

$$\mathcal{F}(f) = \sum_{t=0}^{N-1} \mathbf{s}(t) e^{\frac{-2i\pi ft}{N}} \quad (\text{A.1.4})$$

Further, for signal filtering using DFT, the coefficients of $\mathcal{F}(f)$ that relate to unwanted frequencies are all set to zero. Next, the obtained signal is transformed back in the temporal domain, by performing the inverse DFT as defined below:

$$\mathcal{F}(t) = \frac{1}{N} \sum_{k=0}^{N-1} \mathbf{s}(k) e^{\frac{2i\pi tk}{N}} \quad (\text{A.1.5})$$

The DFT is applied to the signal in windowing manner (Smith, 1997), setting the desired window width and the overlay of the windows for a better resolution.

The DFT filtering can be also applied in the online case by the implementation of the Fast Fourier Transform (FFT), described below.

2. Fast Fourier Transform (FFT) – time to frequency transformation

The Fast Fourier Transform (FFT) (Smith, 1997; Frigo and Johnson, 2005) transforms a signal from the temporal domain to the frequency domain by a fast calculation of the discrete Fourier transform (DFT) which is done by factorizing the DFT matrix into a product of sparse (mostly zero) factors.

3. Finite Impulse Response (FIR) filtering

The Finite Impulse (FIR) filters are linear filters that consider the last M samples of a raw signal $\mathbf{s}(t)$. Thus, the filtered signal $\mathbf{y}(t)$ is computed as:

$$\mathbf{y}(t) = \sum_{k=0}^M a_k \mathbf{s}(t - k) \quad (\text{A.1.6})$$

where a_k represents the filter coefficients (Smith, 1997).

Depending on the desired frequency response, several different FIR designs can be implemented. Among the variety, a common filter design is the Equiripple filter, based on the Parks-McClellan method (McClellan and Parks, 2005). Considering a specific filter order, N , the method finds a set of $N + 1$ optimal coefficients that minimize the maximum deviation of the frequency response from the ideal and desired response (Rabiner and Gold, 1975) and aims at minimizing the error in the pass and stop bands by considering Chebyshev approximation (Parks and McClellan, 1972).

Due to their great performances in the frequency domain, FIR filters have been commonly used for filtering the EEG signals (Dornhege et al., 2006; Gouy-Pailler et al., 2007).

4. Infinite Impulse Response (IIR) filtering (with zero phase shifting)

In addition to the FIR filters, the Infinite Impulse Response (IIR) filters employ also the P previous outputs of the filters, based on recursive formula:

$$\mathbf{y}(t) = \sum_{k=0}^M a_k \mathbf{s}(t - k) + \sum_{k=1}^P b_k \mathbf{y}(t - k) \quad (\text{A.1.7})$$

Compared to FIR filter, the IIR filtering is produced with a reduced number of coefficients. However, their performances slightly tend to reduce in the frequency domain (Smith, 1997). The most used IIR filters in the brain signals preprocessing step of a BCI, are: Chebychev, Butterworth, or elliptic filters, which differ in the frequency response, e.g. different ripples (Smith, 1997; Dornhege et al., 2004a; Martinez et al., 2007). Another common IIR filter type is the feedback Comb filter (Smith, 2007a), named after the type of its frequency response which is represented by a sequence of equally distant notches, resembling a comb structure. Simply, the response contains a repeated series of impulses delayed and replied from the signal itself, that decrease in amplitude over time.

5. Wavelet filtering

A wavelet is a sort of oscillation with the amplitude varying from zero, and then coming back to zero, and can be different shaped in order to better represent a biological electrical signal (brain signal, heart signal, etc.). There are different kinds of wavelets, among which we mention the Daubechies wavelet family, a specific wavelet type because they are orthogonal (Daubechies, 1990) and are specific to discrete analysis. The wavelets are created using a time-frequency transformation, named Discrete Wavelet Transform (DWT) considering discrete time signals. Continuous wavelet transformation may also be used for obtaining accurate time-frequency representations of the analog signals. In this case, different wavelets can be applied such as: Morlet (Lemm et al., 2004) or Mexican hat wavelets (Bostanov, 2004). For this thesis, we restrict to the discrete wavelet filtering for the preprocessing step (3.2.1.1), while for the time-frequency analysis we use different methods described in Section 3.3.4.1 and detailed in Appendix A.1.3.4.

The main advantages of wavelet transform over Fourier transform is that it has a better temporal resolution due to the representation of both frequency of the signals and the time corresponding to those frequencies and has a smaller algorithm complexity. The DWT of a signal $\mathbf{x}(t)$ is computed by a series of filters: first a low-pass filter in convolution with its impulse response and secondly, the signal is also decomposed separately using high-pass filters. The results are subsampled by 2 and processed again, then subsampled by 2 and the resulted low-pass filter is further processed several times (wavelet order) using the same procedure.

The wavelet filter implementation is constructed by calculating the wavelet coefficients of a discrete group of children wavelets for a given mother wavelet $\psi(t)$ in $L^2(\mathbb{R})$:

$$\Psi_{m,n}(t) = \frac{1}{\sqrt{a^m}} \Psi\left(\frac{t-na^m}{a^m}\right), \quad (\text{A.1.8})$$

where m is a scale factor, n is a shift parameter, and $a > 1$.

After the desired filtering, the signal is reconstructed backwards, step by step, using the below formula. For orthogonal wavelets, the reconstruction computation coincides with the decomposition calculation.

$$\mathbf{x}(t) = \sum_{m \in \mathbb{Z}} \sum_{n \in \mathbb{Z}} \langle \mathbf{x}, \Psi_{m,n} \rangle \cdot \Psi_{m,n}(t) \quad (\text{A.1.9})$$

If we look at the signal as a cumulation of the scaling function and wavelets, the signal can be also reconstructed in terms of a sum of the scaling function, $\varphi(t)$ – father wavelet, given by the low-pass spectrum (Mallat, 1989) and the wavelet sequence, $\psi(t)$ – mother wavelet, given by the high-pass filtering, where each of them is also formed as an aggregation of the corresponding wavelets over the entire scale (wavelet order):

$$\mathbf{x}(t) = \sum_k \lambda_{m-1}(k) \varphi(2^{m-1}t - k) + \sum_k \gamma_{m-1}(k) \psi(2^{m-1}t - k), \quad (3.7)$$

where m is the scale and the coefficients $\lambda_{m-1}(k)$ and $\gamma_{m-1}(k)$ are computed by taking the complex inner products of the L^2 norm in the Hilbert space:

$$\lambda_{m-1}(k) = \langle \mathbf{x}(t), \varphi_{m,k}(t) \rangle = \frac{1}{\sqrt{a^m}} \int \mathbf{x}(t) \varphi_{m,k}^*(t) dt \quad (\text{A.1.10})$$

$$\gamma_{m-1}(k) = \langle \mathbf{x}(t), \psi_{m,k}(t) \rangle = \frac{1}{\sqrt{a^m}} \int \mathbf{x}(t) \psi_{m,k}^*(t) dt \quad (\text{A.1.11})$$

In case of Daubechies wavelet, the scaling sequence (low-pass filter) and the wavelet sequence (band-pass filter), are normalized to have sum and the sum of squares equal to $\sqrt{2}$, therefore $a = 2$. In addition, for the order $m=5$ for example, it has 5 vanishing moments (the

wavelet coefficients are zero for polynomials of order less than $m-1$). For a better overview of the structure (Wasilewski, n.d.), the figure below shows the scaling function, $\varphi(t)$ – father wavelet and the wavelet sequence, $\psi(t)$ – mother wavelet, for Daubechies wavelet of order 5:

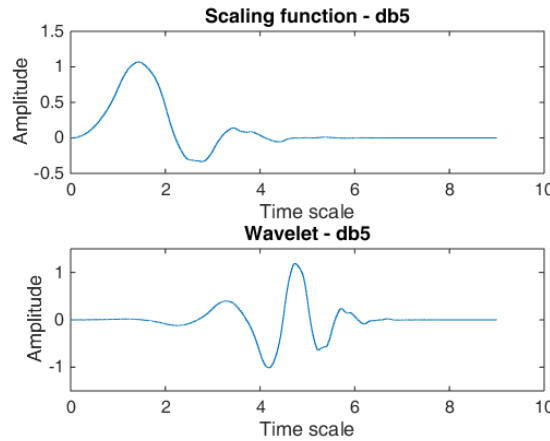


Fig. A.1.1 Scaling and wavelet functions for the Daubechies wavelet of order 5.

A.1.3.2 Temporal analysis - signal envelope

The amplitude evolution of the signal in a specific frequency band, namely the envelope, can be estimated by e.g. Hilbert transform (Bracewell, 1999; Oppenheim et al., 1999), a moving average filter, Root Mean Square (RMS) with a sliding window. The Hilbert transform estimates the imaginary part of the analytical signal that contains only a real part and can be calculated by applying the Fourier transform to the signal, then replacing the Fourier coefficients corresponding to negative frequencies with zeros, and applying the inverse Fourier transform (Marple, 1999). The envelope is then computed by taking the absolute value of the Hilbert transform.

On the other hand, the RMS of the signal is computed by: $RMS(\mathbf{x}) = \sqrt{\frac{1}{N} \sum_{n=1}^N |\mathbf{x}_n|^2}$.

The signal envelope is a good measure for representing the ERD/ERS effects (Clochon, 1996), the upper envelope of the signal is usually considered (the positive amplitude extremes of the oscillating signal).

A.1.3.3 Spectral estimation

1. Periodogram

Periodogram (Schuster, 1898) is a nonparametric estimation of the power spectral density. It is computed based on the Fourier transform, using a rectangular window. The periodogram helps investigating the amplitude vs frequency characteristics of a given entity. Considering a signal $\mathbf{x}(n)$, the periodogram can be defined by:

$$\hat{P}(f) = \frac{\Delta t}{N} \left| \sum_{n=0}^{N-1} \mathbf{x}(n) e^{-i2\pi f n} \right|^2 \quad (\text{A.1.12})$$

with $f \in (-\frac{1}{2} \Delta t ; \frac{1}{2} \Delta t]$ the frequency and N the number of samples.

2. Welch periodogram (P_{welch})

Welch periodogram is another method of Spectral Density Estimation (SDE) that approximates the power spectral density of a signal based on the Welch method (Welch, 1967), involving averaging over overlapping segments. While Periodogram described

previously is not a perfect estimator of the true spectral power of a signal, the Welch method reduces the periodogram variance by dividing the signal into overlapped segments. After computing the periodogram of these segments multiplied by a window function (e.g. Hamming window), it averages them in order to estimate the PSD, which diminishes the variability as a result. In addition, the overlapping procedure preserves the information which could have been lost by the windowing procedure in periodogram, which is the reason why is also called a ‘modified periodogram’.

A.1.3.4 Time-frequency representations

1. Time-frequency representation based on PSD

For generating a time-frequency representation (TFR) of an epoch or a continuous signal, the power spectral density of a signal $P(\mathbf{x}(t))$ computed for example by FFT, Periodogram, has to be applied for a number of segments in overlapping manner, for example based on the Welch method. Briefly:

$$10 * \log_{10}(TFR(\mathbf{x}(t), f)) = \frac{1}{N_w} \sum_{k=1}^{N_w} P(\mathbf{x}_k(t), f) \quad (\text{A.1.13})$$

where N_w is total number of windows and overlaps and f is the frequency range.

In the end, the logarithmic power of the TFR is computed and the TFR of the epoch (after the stimulus onset) or continuous signal is normalized by the mean baseline spectrum.

2. Short-time Fourier transform (STFT)

Short-Time Fourier Transform (STFT) is a Fourier based transformation that detects the changes over time of sinusoidal frequency and phase information in relation to local segments within a signal. Mainly, it requires a multiplication of the original signal $\mathbf{x}(n)$ by a windowing function ω that has a non-zero value for a short time interval, followed by a Fourier transformation computed on the windowed signal. Referring to the discrete computation, it can be described by:

$$\mathbf{X}(m, \omega) = \sum_{n=-\infty}^{+\infty} \mathbf{x}(n)\omega(n - m)e^{-j\omega n} \quad (\text{A.1.14})$$

Therefore, to obtain the Time-Frequency Representation (TFR) the Fourier Transform is applied with a fixed size sliding window for different signal segments with a level of overlapping between them.

Although it is variously used in EEG analysis (Coyle et al., 2005; Herman et al., 2005), it shows a shortcoming related to the constant temporal and spectral resolution for all frequency bands, due to the fixed length window employment. Obtaining distinct levels of details in different frequency bands is overcome by the Wavelet Time-Frequency analysis described in the next Section A.1.3.4.3.

3. Wavelet time-frequency representation

As previously described in Section A.1.3.1.5 wavelet transform decomposes a signal into multiple functions. The advantage of wavelet transform over the Fourier Transform is that it allows simultaneous signal analysis at different scales of resolution, offering a good instrumentality for EEG analysis (Samar et al., 1999). A fine scale (less number of cycles) corresponds to high frequencies giving high temporal resolution, while on the other hand a rough scale (more cycles) relates to low frequencies and gives high frequency resolution.

For generating time-frequency representations of the signal $\mathbf{x}(t)$ in continuous form, the Continuous Wavelet Transform (CWT) is applied, defined by:

$$\mathbf{X}_{CWT}(m, n) = \int_{-\infty}^{\infty} \mathbf{x}(t) \psi_{m,n}(t) dt \quad (\text{A.1.15})$$

where $\psi_{m,n}(t)$ is the mother wavelet defined in Eq. A.1.8.

The best practice for time-frequency decomposition in the context of EEG signals is to consider a suitable wavelet type. A good option is considered to be the Morlet wavelet type, applied with a Gaussian window (Cohen, 2014). This suits with the Gaussian distribution of the EEG data and does not introduce more artifacts due to the Morlet smooth edges shape characteristics.

A.1.4 Regularize a discriminant analysis classifier (Matlab implementation)

The implementation below (Guo et al., 2007) aims to regularize a discriminant analysis classifier by tuning the two parameters, γ and δ , which identify the redundant features and reduce the higher number of features by finding a tradeoff between the number of model features and the classification accuracy.

Considering Σ the covariance matrix of the data \mathbf{X} , and $\hat{\mathbf{X}} = \mathbf{X} - \mathbf{1}\bar{\mathbf{x}}^T$ the centered data (where $\mathbf{1}$ is the vector of ones and length n , and $\bar{\mathbf{x}}$ is the vector of column time point averages).

The regularized covariance matrix $\hat{\Sigma}$ is: $\hat{\Sigma} = (1 - \gamma) \Sigma + \gamma \mathbf{D}$, where \mathbf{D} is the diagonal matrix $\mathbf{D} = \text{diag}(\hat{\mathbf{X}}^T \hat{\mathbf{X}})$.

Further, considering \mathbf{C} the correlation matrix of \mathbf{X} and $\hat{\mathbf{C}}$ the regularized correlation matrix $\hat{\mathbf{C}} = (1 - \gamma) \mathbf{C} + \gamma \mathbf{I}$, with \mathbf{I} the identity matrix, the linear term in the regularized discriminant analysis classifier for a data point x is:

$$(\mathbf{x} - \boldsymbol{\mu}_0)^T \hat{\Sigma}^{-1} (\boldsymbol{\mu}_k - \boldsymbol{\mu}_0) = ((\mathbf{x} - \boldsymbol{\mu}_0)^T \mathbf{D}^{-1/2}) (\hat{\mathbf{C}}^{-1} \mathbf{D}^{-1/2} (\boldsymbol{\mu}_k - \boldsymbol{\mu}_0)), \quad (\text{A.1.16})$$

where $\boldsymbol{\mu}_k$ is be the mean vector of the elements of \mathbf{X} in class k , $\boldsymbol{\mu}_0$ the overall mean vector (the mean of the rows of \mathbf{X}).

The parameter δ controls the magnitude of the last term in Eq. A.1.16, such as $\hat{\mathbf{C}}^{-1} \mathbf{D}^{-1/2} (\boldsymbol{\mu}_k - \boldsymbol{\mu}_0) \leq \delta$ and the feature vectors which do not pass this evaluation are neglected for classification.

Appendix

The Matlab implementation from the Statistics and Machine Learning toolbox examples (using *fitcdiscr* and *cvshrink* functions) is provided in the code below, where **X** represents the feature vectors matrix and **z** is the label information vector:

```
cls = fitcdiscr(X', z);
[err, gamma, delta, numpred] = cvshrink(cls, ...
    'NumGamma',24,'NumDelta',24,'kfold',5,'Verbose',1);
plot(err, numpred, 'k.')
xlabel('Error rate');
ylabel('Number of features');
prompt = 'Set the threshold: mininum no. of features'
thresh = input(prompt) %based on the plot could be between 2000-3000
minerr = min(min(err));
% Subscripts of error producing minimal error
[p, q] = find(err < minerr + 1e-4);
% Convert from subscripts to linear indices
idx = sub2ind(size(delta),p,q);
low3000 = min(min(err(numpred <= thresh)));
lownum = min(min(numpred(err == low3000)));
[r,s] = find((err(:, :) == low3000) & (numpred(:, :) == lownum));
r=r(1);s=s(1);
gamma(r); delta(r,s);
% Set the regularization parameters
cls.Gamma = gamma(r);
cls.Delta = delta(r,s);
Acc=1-resubLoss(cls);
```

A.2 Supplementary material for the motor imagery study – Chapter 4

A.2.1 EEG activity detection

For an overview over the distribution of the data, see for example the scatter plot (C3 vs C4 channels) of the imagery trigger pull data, shown in Appendix Fig. A.2.1. Normalized means of the combined feature vectors (temporal and spectral values) for all trials are represented. We observe very close mean classes for left and right imagery movements, while the mean for the no movement class is distant from the other two. This makes it easier when discriminating the no movement task, while more errors are obtained for left and right movement classification. In any case, the decision boundaries cannot be easily represented in this bi-dimensional representation, because the actual decision is done in a multi-dimensional higher complex space. Considering the distribution, there is a visible positive correlation between both electrodes, effect produced due to volume conduction.

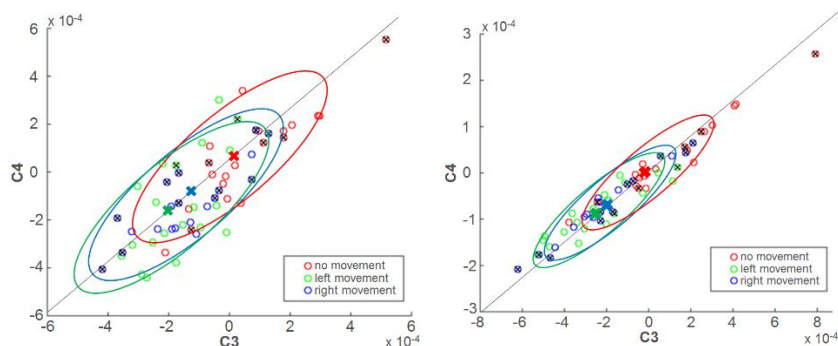


Fig. A.2.1 Scatter plot of C3 vs C4 electrodes showing the distribution of the imagery trigger pull data (Vo. St.). The normalized mean values of the temporal and spectral features for each trial are depicted here as empty circles (right figure) and only for the temporal features (left figure). The elipsoid is an approximation of the class covariance and the filled cross represents the mean of the class. The small black crosses inside the circle data points represent a wrong classified trial given by rLDA shrink for the first CV fold.

A.2.2 EMG activity detection

1. EMG recording

To confirm the absence of real movement, the surface electromyogram was also recorded, which detects the muscles contraction corresponding to left/right arm or left/right index finger movement. To include all fingers and arm activity, the muscle activity was recorded by two electrodes placed on the extensor digitorum communis muscle (Sunderland, 1945; Jones, 2010). In addition to the hardware equipment for EEG acquisition, two EMG100C modules were added for the EMG activity. Two disposable electrodes EL503 were applied on each forearm, placed 3 cm away from each other, in parallel, on the representative muscle fibers.

2. EMG pre-processing

Preliminary noise cancelling (Altimari et al., 2012) was performed over the EMG signals considering the following filtering techniques which aims at preserving the signal of interest in the frequency band from 50 to 500 Hz. The process consist in the following steps: i) signals were re-referenced to a common signal, due do different grounding; ii) the DC

Appendix

voltage (0.06V DC offset) was subtracted from the recorded EMG signal in order to remove network interference (3 Hz cutoff frequency by Butterworth filter of order 4); iii) electrical noise removal with high pass Butterworth filter of 10 Hz cutoff frequency (Butter); iv) a 500 Hz low pass Butterworth filter to remove high frequency harmonics; v) power line interference cancelling with a 50 Hz Notch filter of third order; vi) signal correction with absolute value; vii) random noise reduction with a 5-point moving average FIR filter; viii) root mean square detection (RMS) to measure overall muscular effort, i.e. to extract the muscle contractions, if any.

3. Automatic muscle activity detection

The final correction step given by absolute value and root mean square application provides a clean signal that easily allows the identification of the muscle contractions. The muscle contractions (flexions and extensions) are automatically detected by a peaks and troughs detection technique based on a thresholding (see below [Matlab code](#)). The first step of the algorithm detects the highest peaks in amplitude, considering a minimum possible distance between them. When a peak is detected, the local minima are located within the close proximity of the peaks. In the second step, the algorithm finds the lowest amplitudes, choosing the closest position before and after the timing of the respective peak. And finally, the onset of the muscle contraction, the amplitude and the duration of the movement are computed.

While analyzing the signals, no contractions were detected according an automatic peak and troughs detection algorithm (no peaks of amplitude higher than 1mV), as it can be observed in the following figure, Fig. [A.2.2](#).

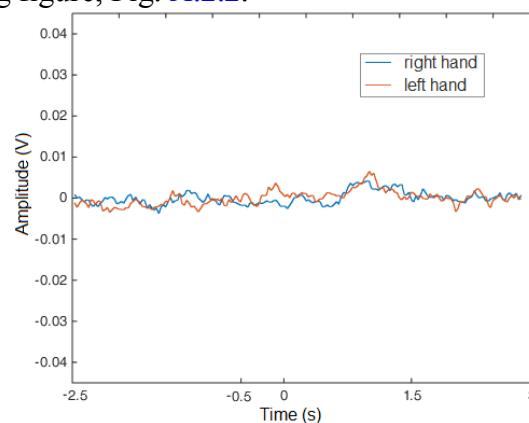


Fig. A.2.2 Average EMG signals over all trials for the left and right motor imagery movement (finger button press experiment with Vis. St.), segmented according to the experiment timing (-2.5s to 3s).

EMG activity detection algorithm (Matlab code):

```

% detection of spikes/ muscle contraction
function [nr_p,peakLocations,nr_t,troughLocations]=detect(y,type)

switch type
    case 'left'
        min_p_h = 0.0145; min_p_dist = 200; % minimum peak height and
distance
        min_t_h = 0.0145; min_t_dist = 200; % minimum troughs height and
distance
    case 'right'
        min_p_h = -0.01; min_p_dist = 300;
        min_t_h = -0.007; min_t_dist = 200;
end
% peaks detection
x = linspace(0,length(y),length(y));
[peaks,peakLocations]=findpeaks(y,'MINPEAKHEIGHT',min_p_h,'MINPEAKDISTAN
CE',min_p_dist);
% troughs detection
[troughs, troughLocations] = findpeaks(-
y,'MINPEAKHEIGHT',min_t_h,'MINPEAKDISTANCE',min_t_dist);
k=1; width = zeros(size(peaks));
nr_p = numel(peaks);
nr_t = numel(troughs);
for ii = 1:nr_p
    trough_before = troughLocations( ...
        find(troughLocations < peakLocations(ii), 1,'last') );
    t_b(k)=troughs( ...
        find(troughLocations < peakLocations(ii), 1,'last') );
    t_loc_b(k)=trough_before;

    trough_after = troughLocations( ...
        find(troughLocations > peakLocations(ii), 1,'first') );
    t_a(k)=troughs( ...
        find(troughLocations > peakLocations(ii), 1,'first') );
    t_loc_a(k)=trough_after;
    width(ii) = trough_after - trough_before;
k=k+1;
end
end

```


A.3 Supplementary material for the Depth of cognitive processing study – Chapter 5

A.3.1 Artifactual components

Three examples of artifactual components detected by ICA with MARA (IC1, IC4, IC49) are presented in Fig. A.3.1, in comparison with the characteristics of a neural component (IC15). In the examples below, IC1 is a typical eye blink artifact with strong frontal activation and a typical front to back scalp map distribution, with steep power spectrum and increases in lower frequencies, and various variations in the ERP image. The IC4 component shows a muscle artifact characterized by a lateral out of the scalp spatial distribution, an increased spectrum in higher frequencies and highly non-stationary activity in the continuous ERP image, characteristic to muscle usage. IC49 shows an increased localized activity around one channel, CPz, with negative spectrum and repeating artifacts segments in the ERP image, visible in the second part of the continuous data, representing an acquisition artifact such as loose electrode or bad conductance. On the other hand, IC5 characterizes a neural component with an alpha peak around 10 Hz, and considering the spatial distribution it indicates a parietal brain source with regular ERP image and smooth activity.

The bottom plots in Fig. A.3.1 shows the MARA features values that are used to categorize the components (recall section 3.2.2.2). An artifactual component is characterized by high value for lambda representing high spectrum values in the 20-50Hz range, signifying muscle activity. High value considering local skewness suggest the existence of outliers in the time series of the respective component. An Increased 'range in pattern' value and Current Density Norm characterize a noisy scalp map activity. While a neural component is indicated by high FitError and 8-13Hz value, revealing a typical alpha peak.

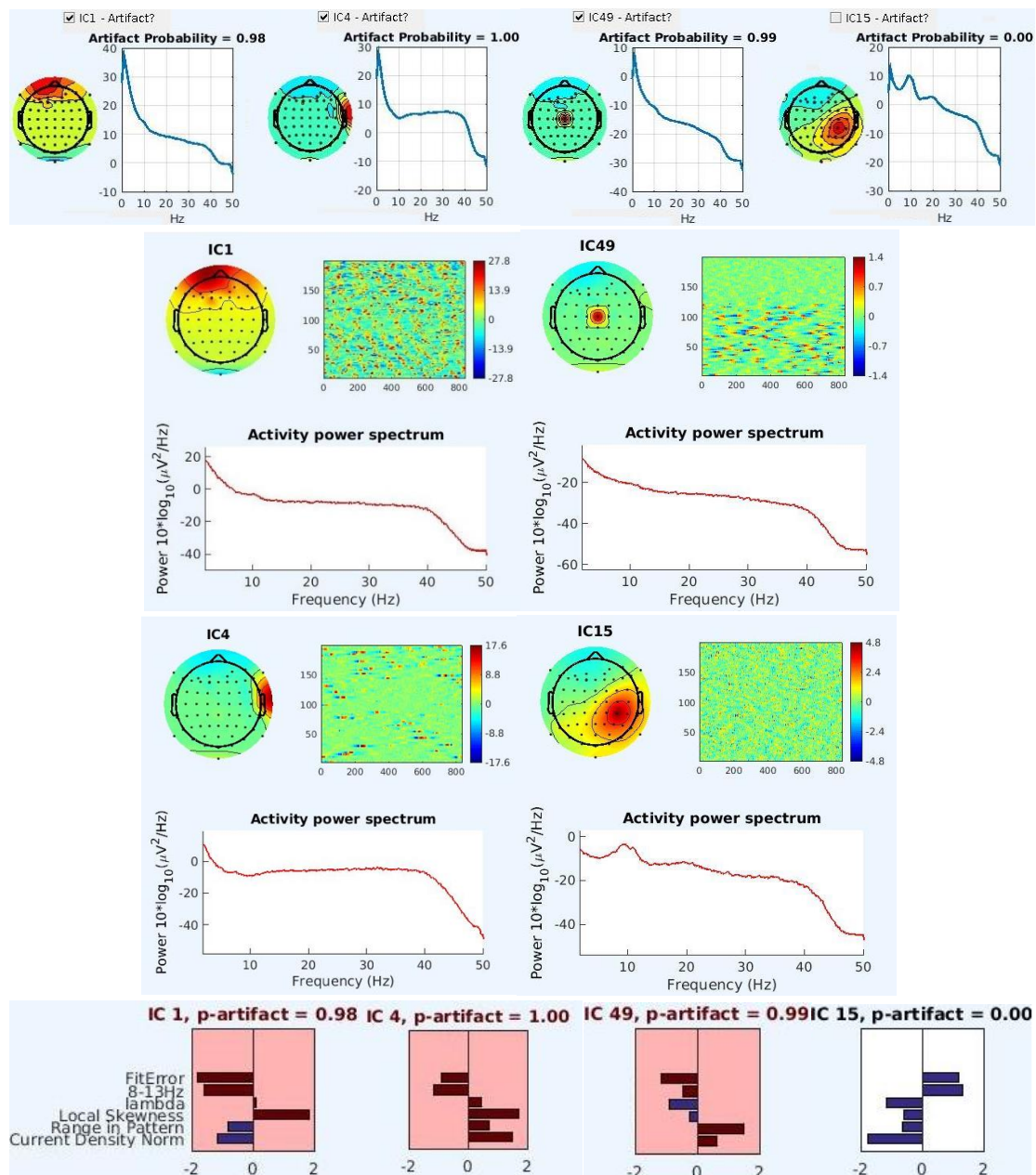


Fig. A.3.1 Example of artifactual components (IC1, IC4, IC49) detected by ICA with MARA for participant P5 on the memory data, as compared to non-artifactual neural components (IC15). In total, 45 components out of 62 were rejected for this participant. The four top plots show the characteristics of the components considering spatial distribution (scalp topographies), power spectrum (log power spectral density) and ERP image on continuous EEG data. The continuous ERP image shows the entire data splitted on rows with the beginning of the recording starting on the first upper row and continuing from left to right along the rows and ending on the bottom row. The four bottom plots show the values of the six features as computed by MARA, in relation to the corresponding probability.

A.3.2 ERP analysis

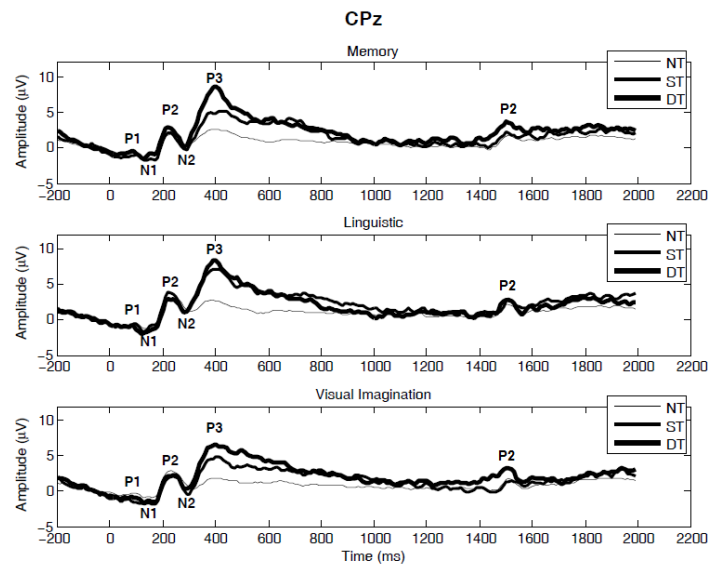


Fig. A.3.2 Event-related potentials corresponding to the cognitive activity depicted in the temporal evolution of the EEG signal, at channel CPz.

The ERP image (Fig. A.3.3) considering the temporal evolution of all NT trials show no visible synchrony between trials, effect related to mind wandering, except the 250ms point corresponding to the stimulus appearance. Further, strong temporal synchronicities are observed within each trial. For the ERP image in the ST trials, strong correlations are observed between trials at the 400ms peak corresponding to the color detection and later increased activity at different times corresponding to mental calculations. In rest, no other fluctuations are observed in amplitude (blue). For the DT case, the ERP image shows strong similar amplitude increases between trials at the 400ms peak and later increased activity, temporally localized around 800 – 1000ms, with a varied starting point contingent upon each trial. This activity most probably relates to the second decision that is performed in the deep processing task.

Appendix

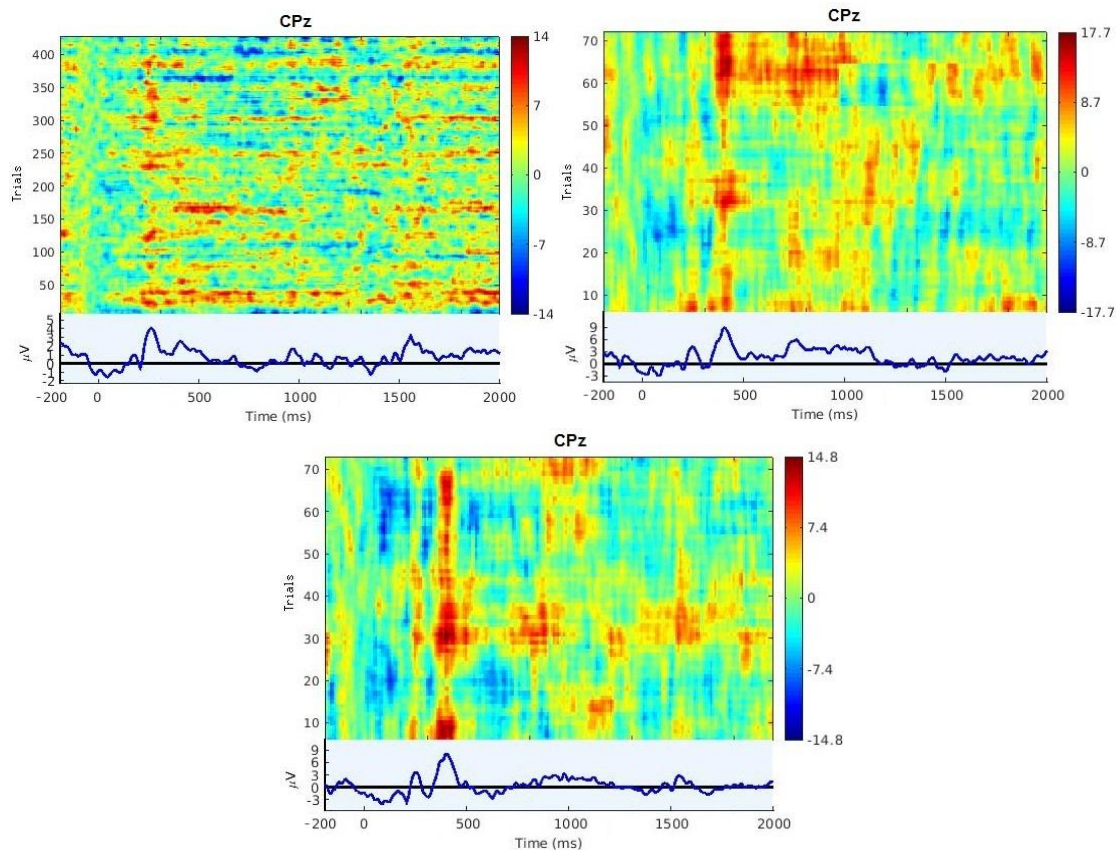


Fig. A.3.3 Temporal evolution of the trials and mean ERP corresponding to the memory condition, related to no-processing (upper left), shallow (upper right) and deep processing (bottom), as detected by channel CPz, for participant P5. The timing considers 200ms of pre-stimulus interval and 2000ms post-stimulus, with the stimulus onset at 0ms.

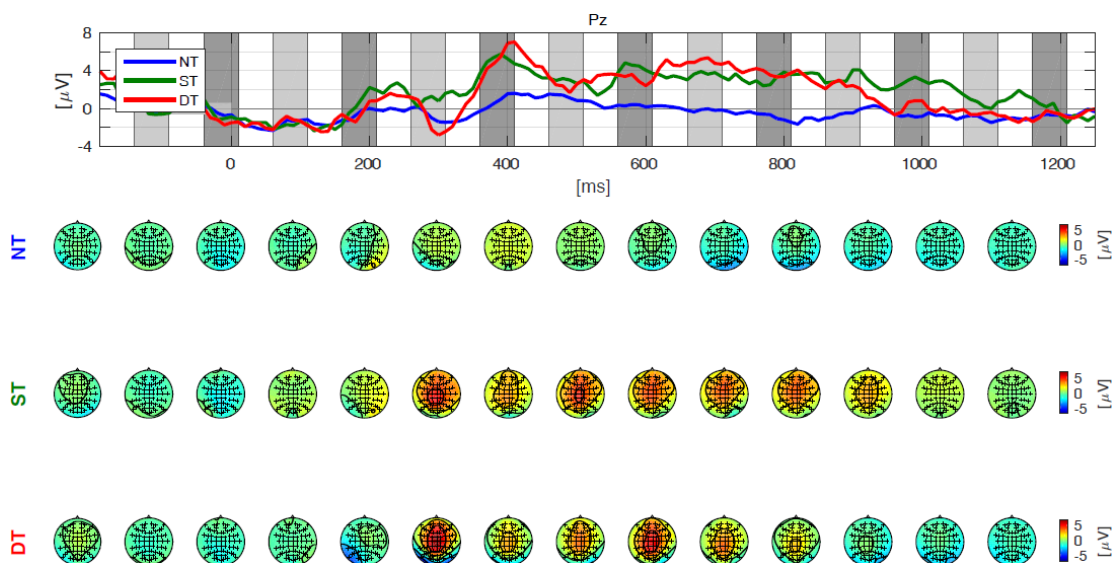


Fig. A.3.4 Temporal and spatial distribution of the mean ERP of participant P5 for the NT, ST and DT processing levels considering the memory condition at electrode Pz. Timing interval: -200ms to 1250ms.

Small differences are observed between the DT+ and DT- levels (Fig. A.3.5), represented by a higher amplitude for the DT+ level at 400 ms with more pronounced differences after 600ms and a more pronounced lateral occipital negativity for the DT- level for the visual imagination case. Due to higher trial to trial variability within the deep level, no considerable differences are observed in the grand average, which might be pronounced at the trial level.

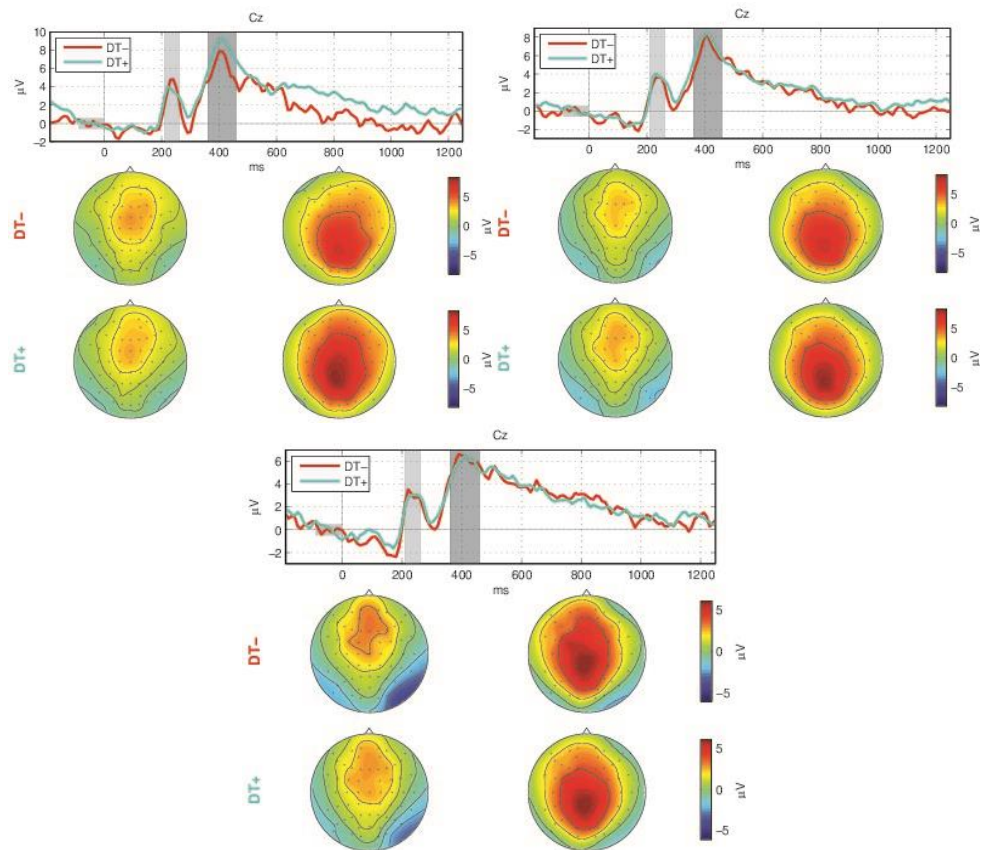


Fig. A.3.5 Grand average ERPs for the DT+ and DT- levels considering the memory, language and visual imagination conditions at electrode Cz.

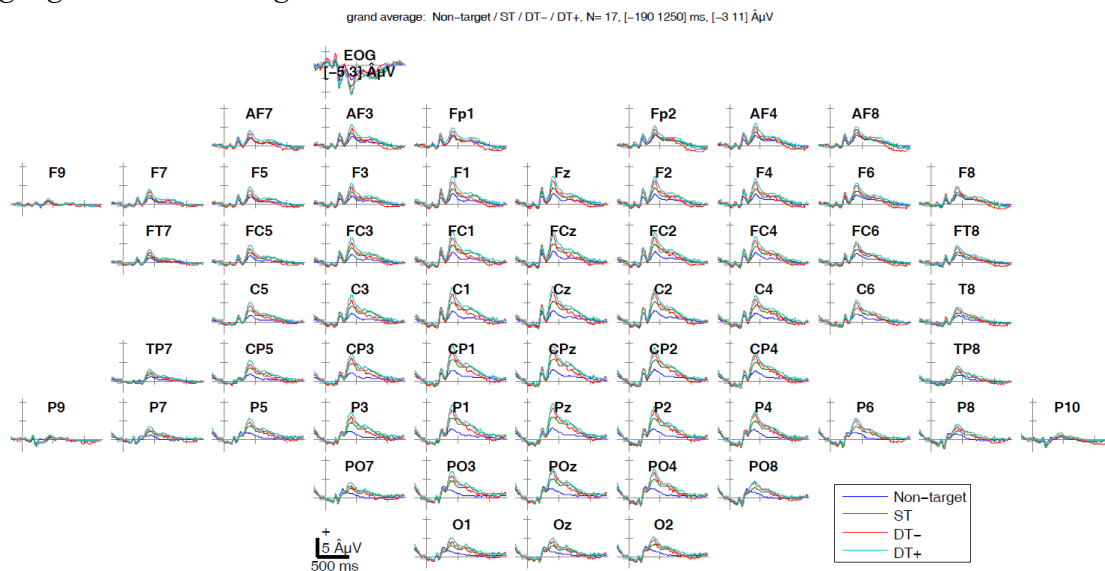


Fig. A.3.6 Grand average ERP considering all electrodes and all processing levels (NT blue, ST green, DT- red and DT+ cyan) for the language condition.

Appendix

For a detailed view of the amplitude discriminability over all channels, the *signed* r^2 computed pair-wise between classes using additional Bonferroni correction is shown in Fig. A.3.7 in form of channels vs time matrix. The threshold to account for multiple comparisons related to the number of time-points, channels, conditions and event types, is set as α/m , where $\alpha = 0.05$ and $m = no_of_samples \times no_of_classes$ (*no_of_samples* represents the entire number of time points and *no_of_classes* is the number of *conditions*, equal to three).

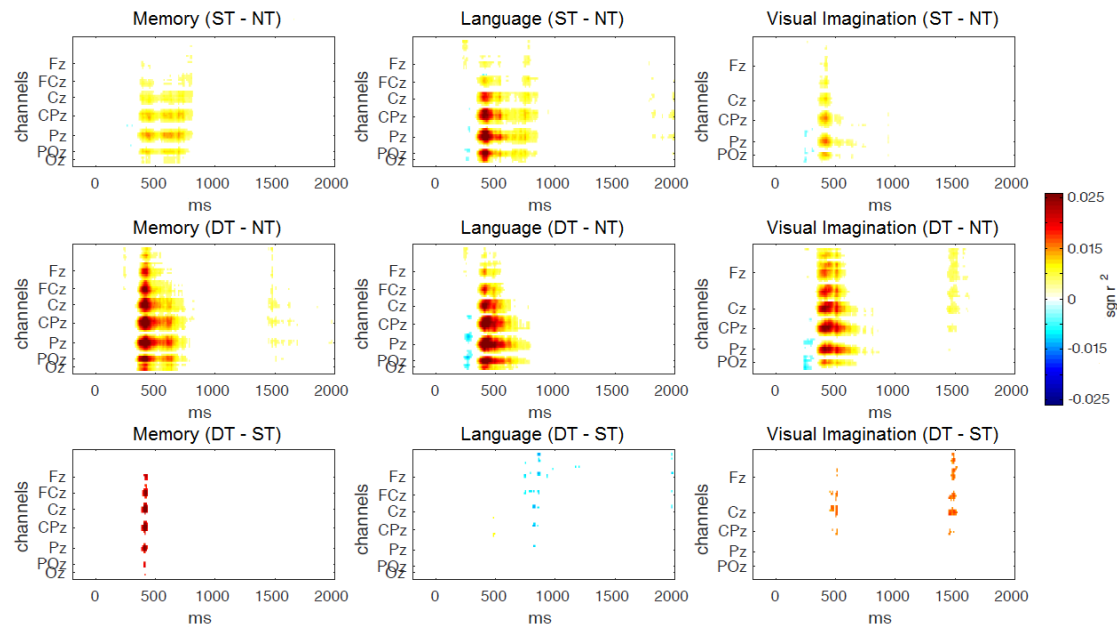


Fig. A.3.7 Statistical temporal differences between classes (upper plots: ST-NT; middle plots: DT-NT; bottom plots: DT-ST) considering signed r^2 at midline channels (frontal, central, parietal and occipital locations) for the Memory, Language and Visual Imagination conditions ($p \leq 0.05$ with Bonferroni correction). The channels are ordered from front to back of the head (from top to bottom in each scalp topography figure). The color bar on the right shows the scale of the plots in terms of $sign\ r^2$ values from -0.025 to 0.025.

As shown in the upper figure, highest discrimination is encountered for the central and parietal channels: FCz, Cz, CPz, Pz, when comparing between a higher level of processing and a smaller level.

A.3.3 ERD/ERS analysis

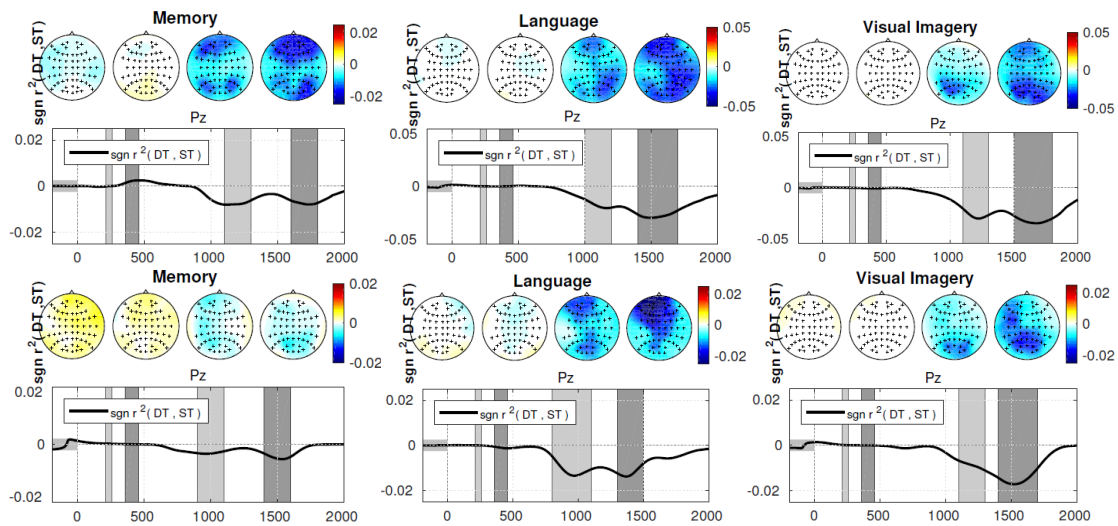


Fig. A.3.8 Grand-average ERD/ERS signed r^2 discriminability between DT and ST for the alpha (8-14 Hz; top plots) and the beta band (16-20 Hz; bottom plots) at location Pz. From left to right: memory, language and visual imagination conditions. The four scalp plots refer to different temporal intervals (shaded in grey). Take into consideration the scale difference: -0.02 - 0.02 scale for most of the graphs, compared to -0.05 - 0.05.

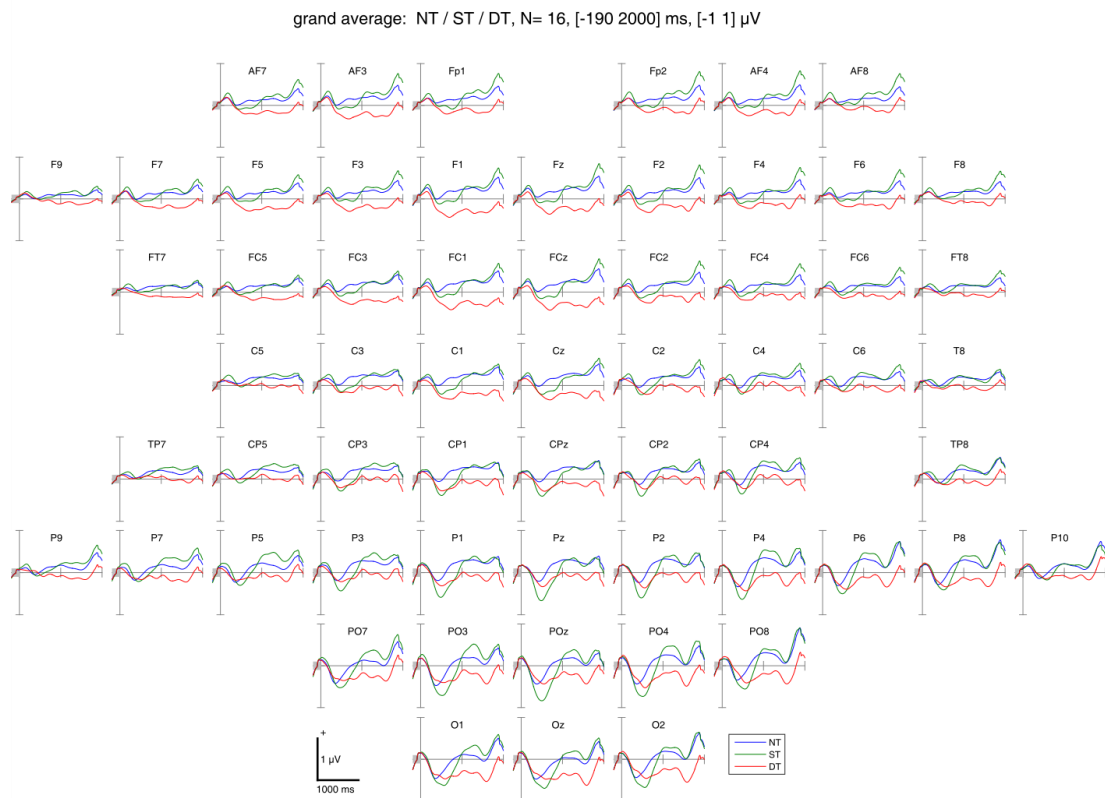


Fig. A.3.9 Grand average ERD/ERS curves on 8-14 Hz considering all electrodes and all processing levels for the memory condition. (Figure taken from Nicolae et al., 2017a, with permission).

Appendix

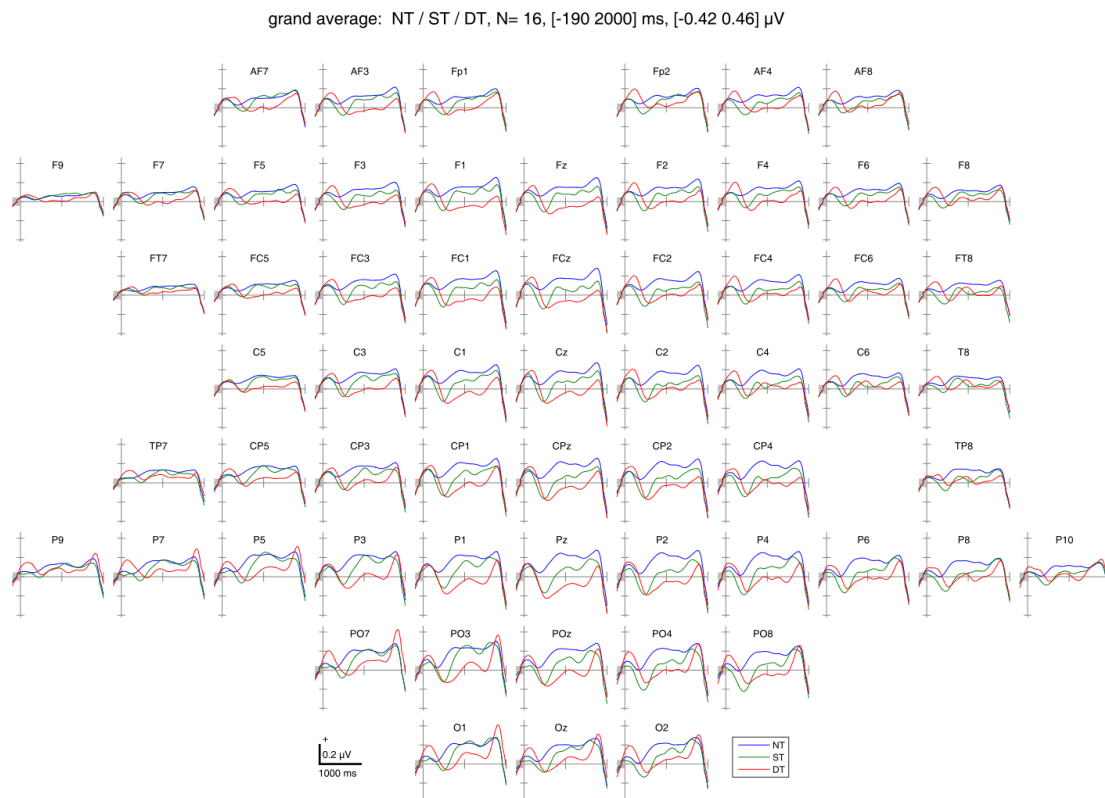


Fig. A.3.10 Grand average ERD/ERS curves on 16-20Hz considering all electrodes and all processing levels for the memory condition. (Figure taken from Nicolae et al., 2017a, with permission).

A.3.4 Discriminatory analysis

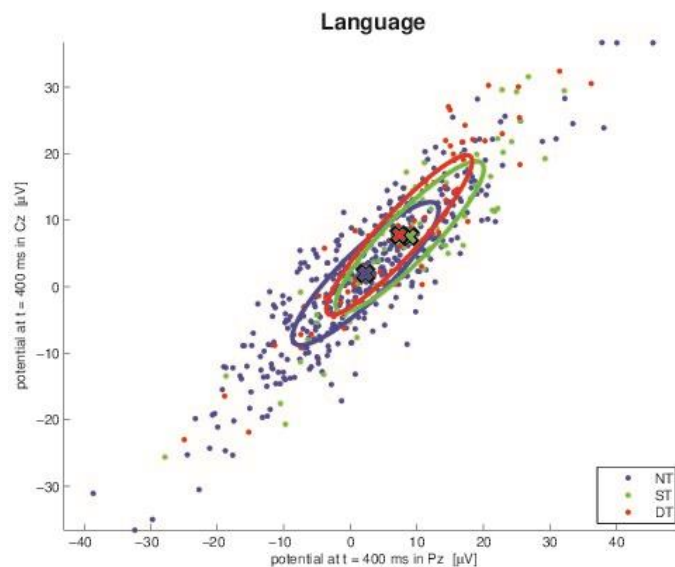


Fig. A.3.11 Scatter plot of Pz vs Cz electrodes showing the distribution of the language data ($t = 400$ ms) considering the NT (blue), ST (green) and DT (red) classes. Normalized mean values for each trial related to participant P5 are presented. The ellipsoids are covariance approximations of the classes and the filled crosses represents class means.

Few participants (P7, P10, P13, P14) have smaller classification performances in some of the conditions (underlined values in Tab. A.3.1), which correlate with a portion of the second group of participants selected according to behavioral results, as analyzed in Nicolae et al., (2018). However, no significant statistical difference was encountered related to behavioral groups, and additionally no difference according to BCI experience, gender, language – mother tongue vs. second spoken language ($p > 0.05$ two-sample t- test). Although, the difference in language processes for non-native speakers as compared to native speakers might generate longer delays in ERPs, which are not currently investigated in this work.

Tab. A.3.1 ERP and multi band CSP with SSD binary classification performance with shrink rLDA over all conditions and participants³ (Table taken from Nicolae et al., 2018, with permission)

Participant	Memory			Language			Visual imagination		
	NT-ST	NT-DT	ST-DT	NT-ST	NT-DT	ST-DT	NT-ST	NT-DT	ST-DT
P1	0.6361	0.8198	0.7499	0.8282	0.8452	0.7507	0.6885	0.9484	0.7312
P2	0.8558	0.9359	0.7330	0.8171	0.7980	0.6621	0.8514	0.8735	0.6728
P3	0.8342	0.8819	0.7889	0.8630	0.8016	0.8139	0.7730	0.8935	0.6466
P4	0.8087	0.9501	0.7572	0.7943	0.9043	0.7827	0.8258	0.9097	0.7846
P5	0.7165	0.8220	0.6894	0.7703	0.9657	0.7787	0.8143	0.9304	0.7198
P6	0.7571	0.8792	0.7062	0.8212	0.9553	0.7508	0.6587	0.8321	0.6353
P7	0.6299	<u>0.6160</u>	0.6497	0.7907	0.8880	0.7197	0.7388	0.8729	0.7177
P8	0.7341	0.8040	0.6678	0.7350	0.8329	0.6539	0.7380	0.8541	0.7630
P9	0.7650	0.8556	0.7945	0.8502	0.8735	0.8040	0.8199	0.9194	0.7820
P10	0.6983	0.9165	0.7485	<u>0.6574</u>	0.9728	<u>0.5616</u>	0.7488	0.8878	0.6921
P11	0.8742	0.8714	0.7047	0.9073	0.9534	0.6455	0.8588	0.9306	0.6888
P12	0.7613	0.9524	0.7382	0.9432	0.9787	0.6920	0.9091	0.9581	0.7363
P13	<u>0.9201</u>	0.8095	0.6508	0.9254	0.8531	<u>0.5755</u>	0.8941	<u>0.7287</u>	0.6356
P14	0.7278	0.9133	0.7457	0.7572	0.9045	0.7151	<u>0.5858</u>	0.9386	0.7178
P15	0.7731	0.9362	0.6501	0.8600	0.9333	0.7767	0.7825	0.9235	0.7116
Mean	0.7661	0.8643	0.7183	0.8214	0.8974	0.7122	0.7792	0.8934	0.7090
SEM	0.0213	0.0222	0.0126	0.0195	0.0159	0.0204	0.0230	0.0150	0.0124

- Testing ANOVA assumptions:

The classification performance and the residuals manifest a normal distribution (Shapiro Wilk test, $p > 0.008$ for residuals), not presenting high variability between participants, except few outliers analyzed in the following. Only the NT-DT case show near-normality residuals (leptokurtic and left-skewed, respectively) for the Memory ($p > 0.008$) and Visual imagination ($p > 0.0138$) performances, observable in Fig. A.3.12. These effects are not extreme overall, residuals do not emerge too far from normality and are generated by one outlier in each group (underlined values in Tab. A.3.1), therefore the effects can be disregarded due to the robustness of rm-ANOVA with respect to the normality assumption.

³ Note: Participants numbers here do not correspond with the data in Nicolae et al., (2017b), while two participants data have been initially rejected (originally P8 and P11)

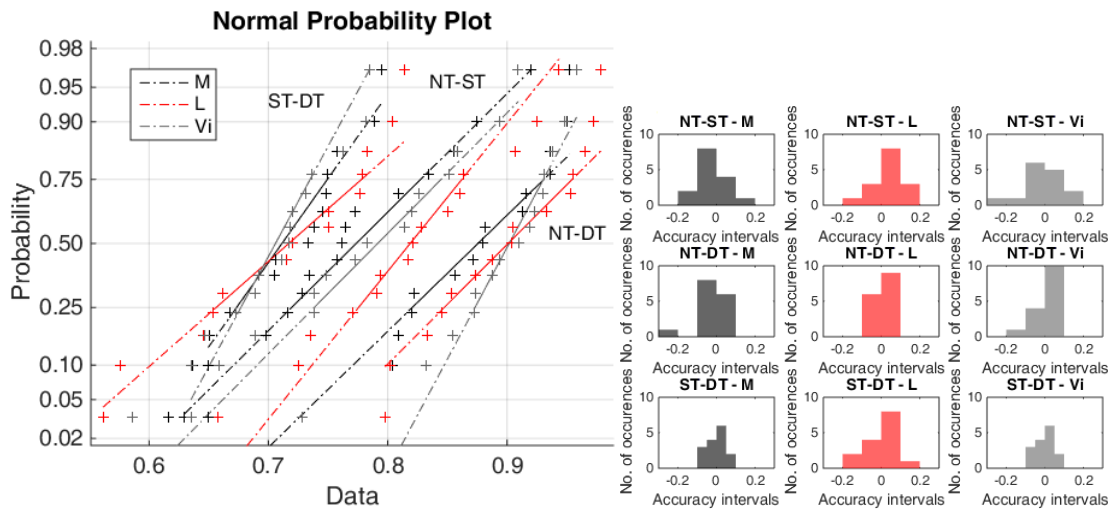


Fig. A.3.12 The normal distribution graphs of the binary ERP-mCSP classifier performance. The normal probability plot of the data (left) and the histogram of the residuals for each class (right). Figure modified (scaled and color coded) from Nicolae et al., 2018, with permission.

Considering homogeneity of variance checked with Barletttest, all groups variances are equal ($p > 0.05$), except the NT-ST group for the Language – Visual imagination variance comparison, $p = 0.0302$, which shows in Fig. A.3.13 slightly non-normality of the residuals (right skewed), given also by slightly unequal number of points between observed and fitted values in the linear model, and slightly unequal variances, differently spread between the sides of the mean predicted value of 0. The effect is not strong and can be overlooked due to equal sample sizes between groups, nearly and the ratio of any pair of variances does not exceed 3.5 (rule of thumb; Dean and Voss, 1999). While Barletttest is very sensitive to non-normality, the homogeneity is verified also with Levene test based on group medians, which is more appropriate, and shows significant homogeneity ($F = 0.31$; $p > 0.58$ Brown & Forsythe Test).

The sphericity of data was detected as significant by Mauchly's test ($p > 0.27$).

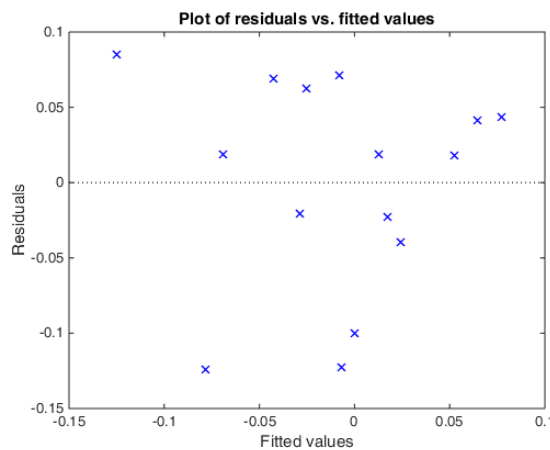


Fig. A.3.13 The variance distribution graph of the residuals between Language and Visual imagination for the NT-ST group, considering binary ERP-mCSP classifier performance.

Tab. A.3.2 ERP-mCSP with SSD (JAD and OVR) multi-class classification performances with shrink rLDA over all conditions and participants⁴

Participant	Memory		Language		Visual imagination	
	JAD	OVR	JAD	OVR	JAD	OVR
P1	0.4998	0.5153	0.6082	0.6227	0.5464	0.5655
P2	0.6689	0.6595	0.5581	0.5630	0.5938	0.5994
P3	0.6239	0.6150	0.5980	0.5808	0.5541	0.5536
P4	0.6764	0.6826	0.6204	0.6407	0.6365	0.6435
P5	0.5468	0.5602	0.6926	0.6932	0.6385	0.6415
P6	0.6040	0.6103	0.6478	0.6476	0.5444	0.5611
P7	<u>0.4136</u>	<u>0.4193</u>	0.5888	0.6058	0.5791	0.5948
P8	0.5273	0.5262	0.5607	0.5733	0.5885	0.5920
P9	0.5999	0.6112	0.6395	0.6346	0.7182	0.7024
P10	0.6470	0.6671	0.6657	0.6458	0.6378	0.6356
P11	0.6207	0.6194	0.6531	0.6670	0.6661	0.6830
P12	0.6830	0.7209	0.7016	0.7206	0.6897	0.7016
P13	0.5090	0.5204	0.5794	0.5627	<u>0.4469</u>	<u>0.4409</u>
P14	0.6441	0.6447	0.6289	0.6416	0.5727	0.5957
P15	0.6323	0.6400	0.6714	0.6698	0.6384	0.6500
<i>Mean</i>	0.5931	0.6008	0.6276	0.6313	0.6034	0.6107
<i>SEM</i>	0.0200	0.0204	0.0117	0.0122	0.0176	0.0174

- *Testing anova assumptions:*

Considering the multi classification JAD results, the residuals are normally distributed according to Shapiro Wilk test ($p > 0.1244$),

Further, all groups have equal variances ($p > 0.05$ by Barletttest), except the language – visual imagination variance comparison, where $p = 0.0149$. This is observed in Fig. A.3.14 by slightly non-normal distribution (unequal number of points between observed and fitted values, slightly right skewed). However, variances of the residuals are equally spread on either side of the mean predicted value, zero and ratios of any two variances are small, does not exceed three (Dean and Voss, 1999). In addition, homogeneity is significant with Brown & Forsythe Levene test ($F = 1.6$; $p > 0.22$). Based on these facts, the slight disturbance can be omitted.

Considering data sphericity, the Mauchly's test result is positive ($p > 0.4$).

⁴ Note: Participants numbers here do not correspond with the data in Nicolae et al., (2017b), while two participants data have been initially rejected (originally P8 and P11)

Appendix

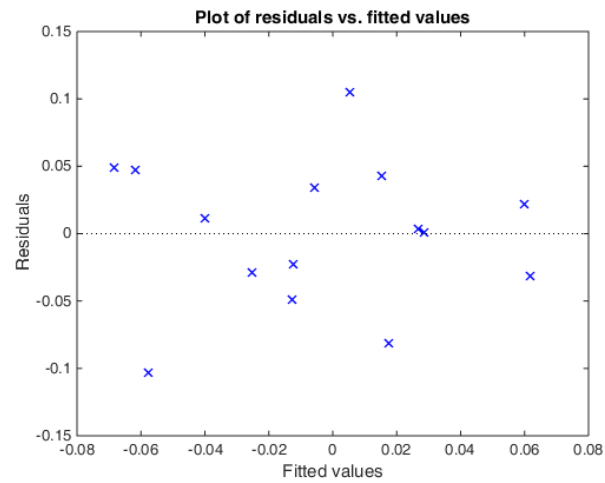


Fig. A.3.14 The variance distribution graph of the residuals between Language and Visual imagination, considering the multi-class ERP-mCSP classifier performance.

In the case when the normality and homogeneity failed badly, then the Kruskal-Wallis test is preferred instead of ANOVA (Kruskal and Wallis, 1952).

Bibliography

- Acqualagna L., Blankertz B., (2013). Gaze-Independent BCI-Spelling Using Rapid Visual Serial Presentation (RSVP). *Clin Neurophysiol.*, **124**, 901-908
- Acqualagna, L., and Blankertz, B. (2015). "Neural correlates of relevant stimuli processing for brain computer interfaces," in Engineering in Medicine and Biology Society (EMBC), 2015 37th Annual International Conference of the IEEE (Milano: IEEE)
- Acqualagna L, Bosse S, Porbadnigk AK, Curio G, Müller KR, Wiegand T, Blankertz B (2015) EEG-based classification of video quality perception using steady state visual evoked potentials (SSVEPs) *J Neural Eng* **12** 026012
- Acqualagna L, Botrel L, Vidaurre C, Kübler A, Blankertz B (2016) Large-Scale Assessment of a Fully Automatic Co-Adaptive Motor Imagery-Based Brain Computer Interface *PLoS ONE* **11** 1-19
- Adrian, E. D., & Matthews, B. H. (1934). The Berger rhythm: potential changes from the occipital lobes in man. *Brain*, 57(4), 355-385.
- Allison B. Z., S. Dunne, R. Leeb, J. D. R. Millan, and A. Nijholt. (2012) Towards practical braincomputer interfaces: bridging the gap from research to real-world applications. Springer Science & Business Media, 2012.
- Allwein E, R. Schapire, and Y. Singer, (2000) Reducing multiclass to binary: A unifying approach for margin classifiers. *Journal of Machine Learning Research*, vol. 1, pp. 113.141, 2000.
- Altimari, L. R., Dantas, J. L., Bigliassi, M., Kanthack, T. F. D., de Moraes, A. C., & Abrão, T. (2012). Influence of different strategies of treatment muscle contraction and relaxation phases on EMG signal processing and analysis during cyclic exercise. *Computational Intelligence in Electromyography Analysis-A Perspective on Current Applications and Future Challenges*. G.R. Naik (Ed). INTECH.
- Amari, S., Cichocki, A., & Yang, H. H. (1996). A new learning algorithm for blind signal separation. *Advances in Neural Information Processing Systems*, 8, 757-763.
- Anderson, J. R., & Reder, L. M. (1979). An elaborative processing explanation of depth of processing. L.; S. Cermak and FIM Craik, Eds., *Levels of Processing in Human Memory* (Erlbam), 385-404.
- Anderson C. W., E. A. Stolz, and S. Shamsunder. (1998) Multivariate autoregressive models for classification of spontaneous electroencephalographic signals during mental tasks. *IEEE Transactions on Biomedical Engineering*, 45:277–286.
- Aricò, P., Borghini, G., Di Flumeri, G., Colosimo, A., Pozzi, S., & Babiloni, F. (2016a). A passive brain-computer interface application for the mental workload assessment on professional air traffic controllers during realistic air traffic control tasks. *Progress in brain research*, 228, 295-328.
- Aricò, P., Borghini, G., Di Flumeri, G., Colosimo, A., Bonelli, S., Golfetti, A., Pozzi, S., Imbert, J.-P., Granger, G., Benhacene, R., et al. (2016b). Adaptive automation triggered by EEG-based mental workload index: A passive brain-computer interface application in realistic air traffic control environment. *Frontiers in Human Neuroscience*, 10. doi: 10.3389/fnhum.2016.00539.
- Ariely, D. and Berns, G. S. (2010). Neuromarketing: the hope and hype of neuroimaging in business. *Nature Reviews Neuroscience*, 11(4):284–292.
- Armitage, R. (1995). The distribution of EEG frequencies in REM and NREM sleep stages in healthy young adults. *Sleep: Journal of Sleep Research & Sleep Medicine*.
- Baars, B. J., & Gage, N. M. (2010). *Cognition, brain, and consciousness: Introduction to cognitive neuroscience*. Academic Press.

Bibliography

- Badia, S. B., Morgade, A. G., Samaha, H., & Verschure, P. F. M. J. (2013). Using a hybrid brain computer interface and virtual reality system to monitor and promote cortical reorganization through motor activity and motor imagery training. *IEEE Transactions on Neural Systems and Rehabilitation Engineering*, 21(2), 174-181.
- Barry, R. J., Clarke, A. R., Johnstone, S. J., Magee, C. A., & Rushby, J. A. (2007). EEG differences between eyes-closed and eyes-open resting conditions. *Clin. Neurophysiology*, 118(12), 2765-2773.
- Bartlett, M. S. (1937). "Properties of sufficiency and statistical tests". *Proceedings of the Royal Statistical Society, Series A* 160, 268–282 JSTOR 96803
- Bartlett, M.S. (1950). "Periodogram Analysis and Continuous Spectra". *Biometrika*. **37** (1-2): 1–16. doi:10.1093/biomet/37.1-2.1
- Bartz D M and Müller K-R (2013) Generalizing analytic shrinkage for arbitrary covariance structures *Adv. Neural Inf. Proc. Syst.* **26** 1869–77
- Bashashati A, M. Fatourehchi, R. K. Ward, and G. E. Birch. (2007) A survey of signal processing algorithms in brain-computer interfaces based on electrical brain signals. *Journal of Neural engineering*, 4(2):R35–57.
- Basile, L. F., Sato, J. R., Alvarenga, M. Y., Henrique, N. Jr., Pasquini, H. A., Alfenas, W., et al. (2013). Lack of systematic topographic difference between attention and reasoning beta correlates. *PLoS ONE* 8:e59595. doi: 10.1371/journal.pone.0059595
- Başar, E., Başar-Eroğlu, C., Karakaş, S., & Schürmann, M. (1999). Are cognitive processes manifested in event-related gamma, alpha, theta and delta oscillations in the EEG?. *Neuroscience letters*, 259(3), 165-168.
- Başar, E., Başar-Eroglu, C., Karakaş, S., & Schürmann, M. (2001). Gamma, alpha, delta, and theta oscillations govern cognitive processes. *International journal of psychophysiology*, 39(2), 241-248.
- Başar E., M. Schurmann, C. Başar-Eroglu, and S. Karakaş. (1997). Alpha oscillations in brain functioning: an integrative theory. *International Journal of Psychophysiology*, 26(1-3):5–29.
- Bauer, M., Oostenveld, R., Peeters, M., & Fries, P. (2006). Tactile spatial attention enhances gamma-band activity in somatosensory cortex and reduces low-frequency activity in parieto-occipital areas. *Journal of Neuroscience*, 26(2), 490-501.
- Bayliss J. D. and D. H. Ballard, (2000) "Recognizing evoked potentials in a virtual environment," *Adv. Neural Inform. Process. Syst.*, vol. 12.
- Bear, M. F., Connors, B. W., Paradiso, M. A. (2007). *Neuroscience: Exploring the Brain*, 3rd edition. Lippincott Williams & Wilkins: USA.
- Beatty, J., A. Greenberg, W. P. Deibler, and J. F. O'Hanlon (1974). Operant control of occipital theta rhythm affects performance in a radar monitoring task. *Science* 183.4127, pp. 871–873.
- Bell AJ, Sejnowski TJ (1995). "An Information-Maximization Approach to Blind Separation and Blind Deconvolution". In: *Neural Comput* 7.6, pp. 1129–1159.
- Berka, C. et al., (2007) "EEG correlates of task engagement and mental workload in vigilance, learning, and memory tasks", *Aviat. Space Environ. Med.* 78, B231–B244.
- Berger P. D. H. (1929) Über das Elektrenkephalogramm des Menschen. *Archiv für Psychiatrie und Nervenkrankheiten*, 87(1):527–570, 2, 11.
- Berger, H. (1933) Über das Elektrenkephalogramm des Menschen *Archiv f. Psychiatrie* 98: 231- 254. <https://doi.org/10.1007/BF01814645>
- Berger, B., Omer, S., Minarik, T., Sterr, A., & Sauseng, P. (2014). Interacting memory systems—does EEG alpha activity respond to semantic long-term memory access in a working memory task?. *Biology*, 4(1), 1-16.
- Besserve, M., K. Jerbi, F. Laurent, S. Baillet, J. Martinerie, and L. Garnero. (2008) Classification methods for ongoing EEG and MEG signals. *Biol. Res.*, 40(4):415–437.

- Best, D.J. and D.E. Roberts (1975) "Algorithm AS 89: The Upper Tail Probabilities of Spearman's rho", *Applied Statistics*, 24:377-379.
- Bianchi L, Mattia D, Goebel R, Owen A M, Pellas F, Müller-Putz G, Laureys S, Kubler A 2014 Brain-Computer Interfaces for Assessment and Communication *IGI Global* 181-214
- Bießmann F, Dähne S, Meinecke F C, Blankertz B, Gørgen K, Haufe S (2012) On the interpretability of linear multivariate neuroimaging analyses: filters, patterns and their relationship *Proc. of the 2nd NIPS Workshop on Machine Learning and Interpretation in Neuroimaging* 12177881
- Birbaumer N (2006) Breaking the silence: brain–computer interfaces (BCI) for communication and motor control *Psychophysiology* **43** 517–532
- Birbaumer N, Murguialday A. R., and Cohen L. (2008) Brain–computer interface in paralysis. *Current opinion in neurology*, 21(6):634–638.
- Birbaumer N, Cohen L (2007). “Brain-computer interfaces: communication and restoration of movement in paralysis”. In: *J Physiol* 579, pp. 621–636.
- Birbaumer N, Ghanayim N, Hinterberger T, Iversen I, Kotchoubey B, Kübler A, Perelmouter J, Taub E, Flor H (1999). “A spelling device for the paralysed”. In: *Nature* 398, pp. 297–298.
- Bishop, C. M. (2007). *Pattern Recognition and Machine Learning (Information Science and Statistics)*. Springer US.
- Blanchard G and B. Blankertz. (2004) BCI competition 2003–data set Iia: spatial patterns of self-controlled brain rhythm modulations. *IEEE Transactions on Biomedical Engineering*, 51(6):1062–1066.
- Blankertz B, Acqualagna L, Dähne S, Haufe S, Schultze-Kraft M, Sturm I, Uscumlic M, Wenzel M, Curio G, Müller K (2016) The Berlin Brain-Computer Interface: Progress Beyond Communication and Control *Front Neuroscience* 10 530, <http://doi.org/10.3389/fnins.2016.00530>
- Blankertz B., Curio G., and K.-R. Müller. (2002) Classifying single trial EEG: Towards brain computer interfacing. In T. G. Diettrich, S. Becker, and Z. Ghahramani, editors, *Advances in Neural Inf. Proc. Systems (NIPS 01)*, volume 14, pages 157–164.
- Blankertz B., Dornhege G., M. Krauledat, K.-R. Müller, and G. Curio. (2007) The non-invasive Berlin Brain-Computer Interface: Fast acquisition of effective performance in untrained subjects. *Neuroimage*, 37(2):539–550. URL <http://dx.doi.org/10.1016/j.neuroimage.2007.01.051>.
- Blankertz B., Dornhege G., M. Krauledat, K.-R. Müller, V. Kunzmann, F. Losch, and G. Curio. (2006a) The Berlin brain-computer interface: EEG-based communication without subject training. *IEEE Trans. Neural Sys. Rehab. Eng.*, 14(2):147–152.
- Blankertz, B., Dornhege, G., Lemm, S., Krauledat, M., Curio, G., and Müller, K. R. (2006b). The Berlin Brain-Computer Interface: Machine Learning Based Detection of User Specific Brain States. *J Universal Computer Sci*, 12(6), 581-607.
- Blankertz B, Jacucci G, Gamberini L, Spagnolli A, Freeman J, eds. (2015) Symbiotic Interaction, 4th International Workshop, Symbiotic 2015, Proceedings *Springer International Publishing* 9359
- Blankertz, B., Tangermann, M., Vidaurre, C., Dickhaus, T., Sannelli, C., Popescu, F., ... & Müller, K. R. (2009). Detecting mental states by machine learning techniques: the Berlin brain–computer interface. In *Brain-computer interfaces* (pp. 113-135). Springer, Berlin, Heidelberg.
- Blankertz B, Kawanabe M, Tomioka R, Hohlefeld F, Nikulin V, Müller KR (2008a). “Invariant Common Spatial Patterns: Alleviating Nonstationarities in Brain-Computer Interfacing”. In: *Advances in Neural Information Processing Systems 20*. Ed. by J Platt, D Koller, Y Singer, and S Roweis. Cambridge, MA: MIT Press, pp. 113–120.
- Blankertz B, Lemm S, Treder M, Haufe S, Müller K R (2011) Single-trial analysis and classification of ERP components—a tutorial, *NeuroImage* **56** 814-825

Bibliography

- Blankertz B., F. Losch, M. Krauledat, G. Dornhege, G. Curio, and K.-R. Müller. (2008b) The Berlin Brain-Computer Interface: Accurate performance from first-session in BCI-naïve subjects. *IEEE Trans Biomed Eng*, 55(10):2452–2462. URL <http://dx.doi.org/10.1109/TBME.2008.923152>.
- Blankertz B, Müller K. R., D. J. Krusienski, G. Schalk, J. R. Wolpaw, A. Schlogl, G. Pfurtscheller, J. D. R. Millan, M. Schroder, and N. Birbaumer. (2006c) The BCI competition III: Validating alternative approaches to actual BCI problems. *IEEE Transactions on Neural Systems and Rehabilitation Engineering*, 14(2):153–159.
- Blankertz B, Sannelli C, Halder S, Hammer EM, Kübler A, Müller KR., Curio, G., and Dickhaus, T. (2010a) Neurophysiological predictor of SMR-based BCI performance *Neuroimage* 51 1303–9
- Blankertz B, Tangermann M, Vidaurre C, Dickhaus T, Sannelli C, Popescu F, Fazli S, Danóczy M, Curio G, Müller K R (2010b) Detecting Mental States by Machine Learning Techniques: The Berlin Brain-Computer Interface, *Brain-Computer Interfaces Revolutionizing Human-Computer Interaction The Frontiers Collection Springer* 113-135
- Blankertz B, Tangermann M, Vidaurre C, Fazli S, Sannelli C, Haufe S, Maeder C, Ramsey LE, Sturm I, Curio G, Müller K R (2010c) The Berlin Brain-Computer Interface: Non-Medical Uses of BCI Technology *Open Access Front Neuroscience* 4 198
- Blankertz B, Tomioka R, Lemm S, Kawanabe M, Müller K R (2008c) Optimizing spatial filters for robust EEG single-trial analysis *IEEE Signal Processing Magazine* 25 41–56
- Blythe D, W. Samek, K. R. Müller, (2011) Stationary Linear Discriminant Analysis - Classifying Non-Stationary Features in Brain-Computer Interfacing, Conference Abstract: Bernstein Conference on Computational Neuroscience (BCCN '11).
- Böhning, D. (1992). Multinomial logistic regression algorithm. *Annals of the Institute of Statistical Mathematics*, 44(1), 197-200.
- Bock, R. D. (1997). The nominal categories model. In *Handbook of modern item response theory* (pp. 33-49). Springer New York.
- Bonferroni, C. E., (1936). *Teoria statistica delle classi e calcolo delle probabilità*. Pubblicazioni del R Istituto Superiore di Scienze Economiche e Commerciali di Firenze 8, 3–62.
- Boostani, R., B. Graimann, M.H.Moradi, and G. Pfurtscheller. (2007) A comparison approach toward finding the best feature and classifier in cue-based BCI. *Medical and Biological Engineering and Computing*, 45(4):403–412.
- Borghini, G., L. Astolfi, G. Vecchiato, D. Mattia, and F. Babiloni (2014). Measuring neurophysiological signals in aircraft pilots and car drivers for the assessment of mental workload, fatigue and drowsiness. *Neuroscience & Biobehavioral Reviews* 44, pp. 58–75.
- Bostanov V. (2004) BCI competition 2003–data sets Ib and IIb: feature extraction from event-related brain potentials with the continuous wavelet transform and the t-value scalogram. *IEEE Transactions on Biomedical Engineering*, 51(6):1057–1061.
- Bracewell, (1999) R. N., *The Fourier Transform and Its Applications*. McGraw-Hill, 3rd ed.
- Brouwer A-M, Hogervorst M A, van Erp J B F, Heffelaar T, Zimmerman P H and Oostenveld R (2012) Estimating workload using EEG spectral power and ERPs in the n-back task *J. Neural Eng.* 9 045008
- Brown, Morton B.; Forsythe, Alan B. (1974). "Robust tests for the equality of variances". *Journal of the American Statistical Association*. 69: 364–367. doi:10.1080/01621459.1974.10482955. JSTOR 2285659.
- Brunner C, Birbaumer N, Blankertz B, Guger C, Kübler A, Mattia D, del R. Millán J, Miralles F, Nijholt A, Opisso E, Ramsey N, Salomon P, Müller-Putz GR (2015). BNCI Horizon 2020: towards a roadmap for the BCI community. *Brain Comput Interfaces* 2 (1):1–10
- Bünau P., F. C. Meinecke, F. Kir'aly, and K.-R. Müller, (2009) "Finding Stationary Subspaces in Multivariate Time Series", *Physical Review Letters*, 103: 214101.

- Buzsáki G., (2006) *Rhythms of the brain*, Oxford Univeristy Press.
- Buzsáki G, Draguhn A (2004) Neuronal oscillations in cortical networks *Science* **304** 1926–1929
- Buzsáki, G. and da Silva, F.L., (2012). High frequency oscillations in the intact brain. *Progress in neurobiology*, 98(3), pp.241-249.
- Buzsáki, G., Anastassiou, C. A., and Koch, C. (2012). The origin of extracellular fields and currents- EEG, ECoG, LFP and spikes. *Nature Reviews Neuroscience*, 13(6):407-420.
- Cardoso J-F and A. Souloumiac. (1996) Jacobi angles for simultaneous diagonalization. *SIAM J.Mat.Anal.Appl.*, vol. 17, no. 1, p. 161.
- Carrasco D. G., J. A. Cantalapedra, (2016) Effectiveness of motor imagery or mental practice in functional recovery after stroke: a systematic review, *Neurología*, vol. 31(1), pp. 43—52.
- Carter, R. (2014). *The human brain book*. Penguin.
- Caton, Richard. (1875) 'The electric currents of the brain'. *British Medical Journal, Section F, Physiology*. 2
- Chatterjee, A., Aggarwal, V., Ramos, A., Acharya, S., & Thakor, N. V. (2007). A brain-computer interface with vibrotactile biofeedback for haptic information. *Journal of neuroengineering and rehabilitation*, 4(1), 40.
- Chen Y N, Mitra S, Schlaghecken F (2008) Sub-processes of working memory in the N-back task: an investigation using ERPs *Clin Neurophysiol* **119** 1546–1559
- Chernoff, H.; Lehmann, E. L. (1954). "The Use of Maximum Likelihood Estimates in χ^2 Tests for Goodness of Fit". *The Annals of Mathematical Statistics*. 25 (3): 579–586. doi:10.1214/aoms/1177728726.
- Christensen, J. C., J. R. Estep, G. F. Wilson, and C. A. Russell (2012). The effects of day-to-day variability of physiological data on operator functional state classification. *NeuroImage* 59.1, pp. 57–63.
- Clochon, P., Fontbonne, J. M., Lebrun, N., & Etévenon, P. (1996). A new method for quantifying eeg event-related desynchronization: amplitude envelope analysis. *Electroencephalography and clinical neurophysiology*, 98(2), 126-129.
- Cohen L., "Time–Frequency Analysis," *Prentice-Hall*, New York, (1995). ISBN 978-0135945322
- Cohen M. X. (2014) *Analyzing Neural Time Series Data: Theory and Practice*. MIT Press.
- Cohen, M.X. (2016). Comparison of linear spatial filters for identifying oscillatory activity in multichannel data. *Journal of neuroscience methods*, Vol. 278, pp. 1-12. Doi: <https://doi.org/10.1016/j.jneumeth.2016.12.016>
- Cohen, R. A., & Waters, W. F. (1985). Psychophysiological correlates of levels and stages of cognitive processing. *Neuropsychologia*, 23(2), 243-256.
- Collinger, J. L.,Wodlinger, B., Downey, J. E.,Wang,W., Tyler-Kabara, E. C.,Weber, D. J.,McMorland, A. J. C., Velliste, M., Boninger, M. L., and Schwartz, A. B. (2013). High-performance neuroprosthetic control by an individual with tetraplegia. *The Lancet*, 381(9866):557–564. doi: 10.1016/S0140-6736(12)61816-9.
- Constine, J. (2017, Apr 19). Facebook is building brain-computer interfaces for typing and skin-hearing. Retrieved from <https://techcrunch.com/2017/04/19/facebook-brain-interface/>
- Cox, DR (1958). "The regression analysis of binary sequences (with discussion)". *J Roy Stat Soc B*. 20: 215–242. JSTOR 2983890.
- Coyle, S.M., Ward, T.E., and Markham, C.M. (2007) Brain-computer interface using a simplified functional near-infrared spectroscopy system. *Journal of neural engineering*, 4:219–226.
- Coyle, D., G. Prasad, and T. M. McGinnity. (2005) A time-frequency approach to feature extraction for a brain-computer interface with a comparative analysis of performance measures. *EURASIP J. Appl. Signal Process.*, 2005(1):3141–3151.

Bibliography

- Craik F I M, Lockhart R S (1972) Levels of processing: A framework for memory research *Journal of Verbal Learning and Verbal behavior* **11** 671-684
- Craik, F.I.M. and E. Tulving, (1975) "Depth of processing and the retention of words in episodic memory." *Journal of Experimental Psychology: General*, 104, 268-294.
- Curio, G., (1999). High frequency (600 Hz) bursts of spike-like activities generated in the human cerebral somatosensory system. *Electroencephalogr. Clin. Neurophysiol. Suppl.* 49, 56–61.
- Curran E. A. and M. J. B. Stokes. (2003) Learning to control brain activity: a review of the production and control of EEG components for driving brain-computer interface (BCI) systems. *Brain and Cognition*, pages 326–336.
- Dähne S, Meinecke FC, Haufe S, Höhne J, Tangermann M, Müller KR, Nikulin VV (2014a). "SPoC: a novel framework for relating the amplitude of neuronal oscillations to behaviorally relevant parameters". In: *Neuroimage* 86.0, pp. 111–122.
- Dähne S, Nikulin VV, Ramírez D, Schreier PJ, Müller KR, Haufe S (2014b). "Finding brain oscillations with power dependencies in neuroimaging data". In: *Neuroimage* 96, pp. 334–348.
- Dähne, S., Höhne, J., Schreuder, M., and Tangermann, M. (2011). Band power features correlate with performance in auditory brain-computer interface. In *Front. Hum. Neurosci. Conference Abstract: XI International Conference on Cognitive Neuroscience (ICON XI)*
- Daly, J. J. and Wolpaw, J. R. (2008). Brain–Computer Interfaces in neurological rehabilitation. *The Lancet Neurology*, 7(11):1032–1043.
- Daubechies I. (1990) The wavelet transform, time-frequency localization and signal analysis. *Information Theory, IEEE Transactions on*, 36(5):961–1005.
- de Moor, J. W. (2003) Building a brain interface. wwwf.bio.uu.nl/LAB/NE/scripties/Building_a_Brain_Interface.pdf.
- Dean and Voss, (1999) *Design and Analysis of Experiments*, page 112.
- Debener, S., Emkes, R., De Vos, M., and Bleichner, M. (2015). Unobtrusive ambulatory EEG using a smartphone and flexible printed electrodes around the ear. *Scientific reports*, 5.
- Debener, S., Herrmann, C. S., Kranczioch, C., Gembris, D., & Engel, A. K. (2003). Top-down attentional processing enhances auditory evoked gamma band activity. *Neuroreport*, 14(5), 683-686.
- Debener, S., Ullsperger, M., Siegel, M., & Engel, A. K. (2006). Single-trial EEG–fMRI reveals the dynamics of cognitive function. *Trends in cognitive sciences*, 10(12), 558-563.
- Delorme, A., & Makeig, S. (2004). EEGLAB: an open source toolbox for analysis of single-trial EEG dynamics including independent component analysis. *Journal of neuroscience methods*, 134(1), 9-21.
- Delorme, A., Mullen, T., Kothe, C., Acar, Z. A., Bigdely-Shamlo, N., Vankov, A., & Makeig, S. (2011). EEGLAB, SIFT, NFT, BCILAB, and ERICA: new tools for advanced EEG processing. *Computational intelligence and neuroscience*, 2011, 10.
- Dickter, C. L., & Kieffaber, P. D. (2013). *EEG methods for the psychological sciences*. Sage.
- Dohrmann, G. J. (1983). *Manter and Gatz's essentials of clinical neuroanatomy and neurophysiology*: S. Gilman, SS Winans, editors. pp. 218. Philadelphia: FA Davis, 1982. *Surgical Neurology*, 20(1), 87.
- Donchin E, Kubovy M, Kutas M, Johnson R Jr, Herning R I (1973) Graded changes in evoked response (P300) amplitude as a function of cognitive activity *Perception and Psychophysics* **14** 319-324
- Donchin E. (1981), Surprise!... Surprise? *Psychophysiology*, 18, 493-513.
- Donchin, E. (1979). Event-related potentials: A tool in the study of human information processing. In H. Beegleiter (Ed.), *Evoked Brain Potentials and Behavior*, pp. 13-88. New York: Plenum Press.
- Dornhege, G., Blankertz, B., Curio, G. and Müller, K.R., (2003). Combining features for BCI. In *Advances in Neural Information Processing Systems* (pp. 1139-1146).

- Dornhege G, B. Blankertz, G. Curio, and K.R. Müller. (2004a) Boosting bit rates in non-invasive EEG single-trial classifications by feature combination and multi-class paradigms. *IEEE Transactions on Biomedical Engineering*, 51(6):993–1002.
- Dornhege G, B. Blankertz, M. Krauledat, F. Losch, G. Curio, and K.-R. Müller. (2006) Combined optimization of spatial and temporal filters for improving brain-computer interfacing. *IEEE Trans. Biomed. Eng.*, 53(11):2274–2281.
- Dornhege G, Blankertz B, Curio G, Müller K R (2004b) Increase Information Transfer Rates in BCI by CSP Extension to Multi-class, *Advances in Neural Information Processing Systems*, *MIT Press* **16** 733-740
- Dornhege G, del R Millán J der R, Hinterberger T, McFarland D, Müller K R, eds. (2007) *Toward Brain-Computer Interfacing*. Cambridge MA: *MIT Press* 520
- Dubin, “Mark Brodmann Areas in the Human Brain with an emphasis on vision and language.”, University of Colorado, (2017), retrieved from <http://spot.colorado.edu/~dubin/talks/brodmann/brodmann.html>
- Duda, R. O., P. E. Hart, and D. G. Stork (2001). *Pattern Classification*. 2nd edition. Wiley & Sons.
- Duncan-Johnson C C, Kopell B. S. (1981) *The stroop effect: Brain potentials localize the source of interference*, *Science*, vol. 214, 938-940.
- Efron, B., (1982). The Jackknife, the Bootstrap, and other Resampling Plans. J. W. Arrowsmith, pp. 92.
- Efron, B., and R. Tibshirani, (1993): *An Introduction to the Bootstrap*. Chapman & Hall, 456 pp.
- Farquhar J, Hill N J (2013) Interactions Between Pre-Processing and Classification Methods for Event-Related-Potential Classification - Best-Practice Guidelines for Brain-Computer Interfacing *Neuroinformatics* **11** 175-192
- Farwell L, Donchin E (1988). “Talking off the top of your head: toward a mental prosthesis utilizing event-related brain potentials”. In: *Electroencephalogr Clin Neurophysiol* 70, pp. 510–523.
- Fatourechi M, A. Bashashati, R. Ward, and G. Birch. (2007) EMG and EOG artifacts in brain computer interface systems: A survey. *Clinical Neurophysiology*, 118(3):480–494.
- Fazli, S., Dähne, S., Samek, W., Bießmann, F., & Müller, K. R. (2015). Learning from more than one data source: data fusion techniques for sensorimotor rhythm-based brain–computer interfaces. *Proceedings of the IEEE*, 103(6), 891-906.
- Fedele, T., (2014) High-frequency electroencephalography (hf-EEG): Non-invasive detection of spike-related brain activity, PhD thesis. Doi: <http://dx.doi.org/10.14279/depositonce-4110>
- Feshchenko, Vladimir A.; Reinsel, Ruth A.; Veselis, Robert A. (2001). "Multiplicity of the α Rhythm in Normal Humans". *Journal of Clinical Neurophysiology*. 18 (4): 331–44. doi:10.1097/00004691-200107000-00005. PMID 11673699
- Fisch, B. J., & Spehlmann, R. (1999). *Fisch and Spehlmann's EEG primer: basic principles of digital and analog EEG*. Elsevier Health Sciences.
- Fisher, R. A. (1925). *Statistical methods for research workers*. Genesis Publishing Pvt Ltd.
- Francis, J. G. (1961). The QR transformation a unitary analogue to the Ir transformation|part 1. *The Computer Journal*, 4(3):265 {271.
- Friedman J. H. (1989) Regularized discriminant analysis. *Journal of the American statistical association*, 84(405):165–175.
- Friedman, J. H. K. (1997) On bias, variance, 0/1-loss, and the curse-of-dimensionality. *Data Mining and Knowledge Discovery*, 1(1):55–77.
- Frigo M. and Johnson S. G., (2005) "The Design and Implementation of FFTW3," *Proceedings of the IEEE* **93** (2), 216–231. Invited paper, Special Issue on Program Generation, Optimization, and Platform Adaptation.

Bibliography

- Fuentemilla, L., Marco-Pallarés, J., & Grau, C. (2006). Modulation of spectral power and of phase resetting of EEG contributes differentially to the generation of auditory event-related potentials. *Neuroimage*, *30*(3), 909-916.
- Fukunaga K (1990) Introduction to statistical pattern recognition *Academic Press* Boston 2nd edition 591
- Fukunaga, K. (2013). Introduction to statistical pattern recognition. Academic press.
- Furman, D., Reichart, R., & Pratt, H. (2016). Finger flexion imagery: EEG classification through physiologically-inspired feature extraction and hierarchical voting. In *Brain-Computer Interface (BCI), 2016 4th International Winter Conference on* (pp. 1-4). IEEE.
- Galán, F., M. Nuttin, E. Lew, P. W. Ferrez, G. Vanacker, J. Philips, and J. d. R. Millán (2008). A brain-actuated wheelchair: asynchronous and non-invasive brain-computer interfaces for continuous control of robots. *Clinical Neurophysiology* *119*.9, pp. 2159–2169.
- Gamberini L, Spagnolli A, Blankertz B, Kaski S, Freeman J, Acqualagna L, Barral O, Bellio M, Chech L, Eugster M, Ferrari E, Negri P, Orso V, Pluchino P, Minelle F, Serim B, Wenzel M, and Jacucci G (2015) Developing a Symbiotic System for Scientific Information Seeking: The MindSee Project, Symbiotic Interaction, Lecture Notes in Computer Science, *Springer International Publishing* **9259** 68-80
- Ganis, G., Lacey, S. and Lawson, R., eds. (2013). “Multisensory Imagery”. In *Visual Mental Imagery*. Springer Science Business Media LLC. 9-28. doi: 10.1007/978-1-4614-5879-1_2
- Ganis, G., Thompson, W. L., Kosslyna, S. M. (2004). Brain areas underlying visual mental imagery and visual perception: an fMRI study. *Cognitive Brain Research*. **20**: 226–241. doi: 10.1016/j.cogbrainres.2004.02.012
- Garrett, D., Peterson, D. A., Anderson, C. W., & Thaut, M. H. (2003). Comparison of linear, nonlinear, and feature selection methods for EEG signal classification. *IEEE Transactions on neural systems and rehabilitation engineering*, *11*(2), 141-144.
- Gevins, A., Leong, H., Du, R., Smith, M. E., Le, J., DuRousseau, D., Zhang, J. and Libove, J. (1995). Towards measurement of brain function in operational environments. *Biological Psychology* *40*.1, pp. 169–186.
- Gevins A and Smith M E (2003) Neurophysiological measures of cognitive workload during human-computer interaction *Theor. Issues Ergon. Sci.* *4* 113–31
- Gevins A, Smith M E, McEvoy L, Yu D (1997) High-resolution EEG mapping of cortical activation related to working memory: effects of task difficulty, type of processing, and practice *Cerebral cortex* **7**(4) 374-85
- Gibbons, J. D., and S. Chakraborti. (2011) *Nonparametric Statistical Inference*, 5th Ed., Boca Raton, FL: Chapman & Hall/CRC Press, Taylor & Francis Group.
- Gomez-Ramirez, J., Freedman, S., Mateos, D., Velazquez, J. L. P., & Valiante, T. (2017). Eyes closed or Eyes open? Exploring the alpha desynchronization hypothesis in resting state functional connectivity networks with intracranial EEG. *bioRxiv*, 118174.
- Gotz T, Curio G, Witte OW, Witte H and Hauelsen J (2009). High-frequency oscillations in EEG and MEG recordings are modulated by cognitive context. *Front. Comput. Neurosci. Conference Abstract: Bernstein Conference on Computational Neuroscience*. doi: 10.3389/conf.neuro.10.2009.14.148
- Gouy-Pailler, C., S. Achard, B. Rivet, C. Jutten, E. Maby, A. Souloumiac, and M. Congedo. (2007) Topographical dynamics of brain connections for the design of asynchronous brain-computer interfaces. In *Proc. Int. Conf. IEEE Engineering in Medicine and Biology Society (IEEE EMBC)*, pages 2520–2523.

- Graimann B., B. Allison, G. Pfurtscheller (2010) Brain-computer interfaces: A gentle introduction. In: *Brain-Computer Interfaces*. Springer. p. 1–27.
- Gramann, K., Gwin, J.T., Ferris, D.P., Oie, K., Jung, T.P., Lin, C.T., Liao, L.D. and Makeig, S., (2011). Cognition in action: imaging brain/body dynamics in mobile humans. *Reviews in the Neurosciences*, 22(6), pp.593-608.
- Green MD, Swets JA (1966). *Signal detection theory and psychophysics*. Huntington, NY: Krieger.
- Greene, William H. (2012). *Econometric Analysis* (Seventh ed.). Boston: Pearson Education. pp. 803–806. ISBN 978-0-273-75356-8.
- Griggs, R.A.: *Psychology: A Concise Introduction*. p. 69 (2012)
- Groppe, D. M., Bickel, S., Keller, C. J., Jain, S. K., Hwang, S. T., Harden, C., & Mehta, A. D. (2013). Dominant frequencies of resting human brain activity as measured by the electrocorticogram. *NeuroImage*, 79, 223–233. <http://doi.org/10.1016/j.neuroimage.2013.04.044>
- Grosse-Wentrup M, Bus M, (2008) Multiclass Common Spatial Patterns and Information Theoretic Feature Extraction, *IEEE Transactions on Biomedical Engineering*, Vol. 55, No. 8.
- Guger C, Edlinger G, Harkam W, Niedermayer I, Pfurtscheller G (2003) How Many People are Able to Operate an EEG-based Brain-Computer Interface (BCI)? *IEEE Trans Neural Syst Rehabil Eng*. **11** 145–147
- Guger, C., Krausz, G., Allison, B. Z., and Edlinger, G. (2012) Comparison of dry and gel based electrodes for p300 brain–computer interfaces. *Frontiers in neuroscience*, 6.
- Guillot, A., et. al. (2009) Brain Activity during Visual Versus Kinesthetic Imagery: An fMRI Study. *Human Brain Mapping* 30, pp. 2157 – 2172
- Gundel, A., Wilson, G. F. (1992). Topographical changes in the ongoing EEG related to the difficulty of mental tasks. *Brain Topogr.* **5**: 17–25. doi: 10.1007/BF01129966
- Guo, Y., T. Hastie, and R. Tibshirani. (2007) Regularized Discriminant Analysis and Its Application in Microarray. *Biostatistics*, Vol. 8, No. 1, pp. 86–100.
- Gysels E. and Celka P. (2004) Phase synchronization for the recognition of mental tasks in a brain-computer interface. *IEEE Transactions on Neural Systems and Rehabilitation Engineering*, 12(4):406–415.
- Haegens, S., B.F. Händel, O. Jensen, (2011a) Top–down controlled alpha band activity in somatosensory areas determines behavioral performance in a discrimination task *J. Neurosci.*, 31, pp. 5197-5204, 10.1523/JNEUROSCI.5199-10.2011
- Haegens, S, Nácher V, Hernández A, Luna R, Jensen O, Romo R. (2011b) Beta oscillations in the monkey sensorimotor network reflect somatosensory decision making. *Proc Natl Acad Sci U S A.*, 108:10708–10713. doi: 10.1073/pnas.1107297108.
- Halme, H.L. and Parkkonen, L., (2016). Comparing Features for Classification of MEG Responses to Motor Imagery. *PloS one*, 11(12), p.e0168766.
- Hammon P.S. and de Sa V.R. (2007) Preprocessing and meta-classification for brain-computer interfaces. *IEEE Transactions on Biomedical Engineering*, 54(3):518–525.
- Handy T. C., (2004) *Event-Related Potentials - A method Handbook*, The MIT Press.
- Hanley J A and McNeil B J (1982) The meaning and use of the area under a receiver operating characteristic (roc) curve *Radiology* **143** 29–36
- Hassanien A E, Taher Azar A, eds. (2015) *Brain-Computer Interfaces: Current Trends and Applications Springer* **74**
- Hastie T., Tibshirani R., Friedman J. (2008) “The Elements of Statistical Learning”, Section 4.3, p.106-119.
- Haufe S, Dähne S, Nikulin V V (2014a) Dimensionality reduction for the analysis of brain oscillations *NeuroImage* **101** 583-597

Bibliography

- Haufe, S., Kim J.-W., I.-H. Kim, A. Sonnleitner, M. Schrauf, G. Curio, and B. Blankertz (2014c). Electrophysiology-based detection of emergency braking intention in real-world driving. *Journal of Neural Engineering* 11.5, p. 056011.
- Haufe S, Meinecke F, Görge K, Dähne S, Haynes J, Blankertz B, Biessmann F (2014b) On the interpretation of weight vectors of linear models in multivariate neuroimaging *Neuroimage* **87** 96-110
- Haufe, S., M. S. Treder, M. F. Gugler, M. Sagebaum, G. Curio, and B. Blankertz (2011). EEG potentials predict upcoming emergency breakings during simulated driving. *Journal of Neural Engineering* 8.5, pp. 056001+.
- Haykin, S. (2009). *Neural Networks and Learning Machines*. New Jersey: Pearson Education, Inc.
- Herman, P., G. Prasad, and T.M. McGinnity. (2005) Investigation of the type-2 fuzzy logic approach to classification in an EEG-based brain-computer interface. In 27th Annual International Conference of the Engineering in Medicine and Biology Society, IEEE-EMBS 2005, pp. 5354–5357.
- Hinterberger, T., Neumann, N., Pham, M., Kübler, A., Grether, A., Hofmayer, N., ... & Birbaumer, N. (2004). A multimodal brain-based feedback and communication system. *Experimental brain research*, 154(4), 521-526.
- Höhne J, Bartz D, Hebart MN, Müller KR, Blankertz B (2016) Analyzing neuroimaging data with subclasses: a shrinkage approach *Neuroimage* **124** 740-751
- Höhne J, Schreuder M, Blankertz B, Tangermann M (2011a). “A novel 9-class auditory ERP paradigm driving a predictive text entry system”. In: *Front Neuroscience* 5, p. 99.
- Höhne J, Tangermann M (2014). “Towards User-Friendly Spelling with an Auditory Brain-Computer Interface: The CharStreamer Paradigm”. In: *PLoS ONE* 9.6, e98322
- Hoerl, A. E., and Kennard, R. W. (1970). Ridge regression: Biased estimation for nonorthogonal problems. *Applications to nonorthogonal problems, Technometrics*, 12(1):55-82.
- Hohmann, M. R., Fomina, T., Jayaram, V., Widmann, N., Förster, C., Just, J., M. Synofzik, B. Schölkopf, L. Schöls, & Grosse-Wentrup, M. (2016). A cognitive brain–computer interface for patients with amyotrophic lateral sclerosis. *Progress in brain research*, 228, 221-239.
- Holm A, Lukander K, Korpela J, Sallinen M, Müller KM (2009) Estimating brain load from EEG. *Scientific World Journal* 9: 639-651.
- Huang, R. S., Jung, T. P., Makeig, S. (2007a). Event-related brain dynamics in continuous sustained-attention tasks. *Foundations of augmented cognition*, 65-74.
- Huang, R. S., Jung, T. P., Makeig, S. (2007b). Multi-scale EEG brain dynamics during sustained attention tasks *Proc. of the 32th Int. Conf. on Acoustics, Speech and Signal Processing* 1173-1176
- Hughes, S. W., & Crunelli, V. (2005). Thalamic mechanisms of EEG alpha rhythms and their pathological implications. *The Neuroscientist*, 11(4), 357-372.
- Hyvärinen A, Karhunen J, Oja E (2004). *Independent component analysis*. Vol. 46. John Wiley & Sons.
- Hyvärinen, A., & Oja, E. (2000). Independent component analysis: algorithms and applications. *Neural Networks*, 13, 411-430.
- Hwang, H.-J., Kim, S., Choi, S., and Im, C.-H. (2013). EEG-based brain-computer interfaces: A thorough literature survey. *International Journal of Human–Computer Interaction*, 29(12):814–826. doi: 10.1080/10447318.2013.780869.
- Hwang, H. J., Kwon, K., & Im, C. H. (2009). Neurofeedback-based motor imagery training for brain–computer interface (BCI). *Journal of neuroscience methods*, 179(1), 150-156.
- Jain, A.K., R.P.W. Duin, and J. Mao. (2000) Statistical pattern recognition: A review. *IEEE Transactions on Pattern Analysis and Machine Intelligence*, 22(1):4–37.

- Jaušovec, N. and Jaušovec, K., (2000). EEG activity during the performance of complex mental problems. *International Journal of Psychophysiology*, 36(1), pp.73-88.
- Jensen, O. and L. L. Colgin (2007). Cross-frequency coupling between neuronal oscillations. *Trends in cognitive sciences* 11.7, pp. 267–269.
- Ji, H., Li, J., Cao, L., & Wang, D. (2012). A EEG-Based brain computer interface system towards applicable vigilance monitoring. *Foundations of Intelligent Systems*, 743-749.
- Jones, J.: Human body, Our Index Finger. *Answers magazine* (2010), (retrieved from <https://answersingenesis.org/human-body/our-index-finger/>)
- Jung, T. P., Makeig, S., Lee, T. W., McKeown, M. J., Brown, G., Bell, A. J., & Sejnowski, T. J. (2000) Independent component analysis of biomedical signals. In *Proc. Int. Workshop on Independent Component Analysis and Signal Separation*, 633-644.
- Jung T-P, Makeig S, Stensmo M and Sejnowski T (1997) Estimating alertness from the EEG power spectrum *IEEE Trans. Biomed. Eng.* 44 60–9
- Jungnickel, E. and Gramann, K., (2016) Mobile brain/body imaging (MoBI) of physical interaction with dynamically moving objects. *Frontiers in human neuroscience*, 10.
- Kachenoura A, L. Albera, L. Senhadji, and P. Comon. (2008) ICA: A potential tool for BCI systems. *IEEE Signal Processing Magazine*, 25(1):57–68.
- Kandel, E.R., Schwartz, J.H. and Jessell, T.M. eds., (2000). *Principles of neural science* (Vol. 4, pp. 1227-1246). New York: McGraw-hill.
- Kaplan, A., Vasilyev, A., Liburkina, S., & Yakovlev, L. (2016). Poor BCI Performers Still Could Benefit from Motor Imagery Training. In *International Conference on Augmented Cognition* (pp. 46-56). Springer International Publishing.
- Kappenman, E. S., & Luck, S. J. (2010). The Effects of Electrode Impedance on Data Quality and Statistical Significance in ERP Recordings. *Psychophysiology*, 47(5), 888–904. <http://doi.org/10.1111/j.1469-8986.2010.01009.x>
- Kauppi J.-P., M. Kandemir, V.-M. Saarinen, L. Hirvenkari, L. Parkkonen, A. Klami, R. Hari, and S. Kaski. (2015) Towards brain-activity-controlled information retrieval: Decoding image relevance from meg signals. *NeuroImage*, 112:288–298.
- Kawanabe M, Samek W, Müller KR, Vidaurre C (2014). “Robust Common Spatial filters with a Maxmin Approach”. In: *Neural Computation* 26.2, pp. 1–28.
- Keirn Z. A. and J. I. Aunon. (1990) A new mode of communication between man and his surroundings. *IEEE Transactions on Biomedical Engineering*, 37(12):1209–1214.
- Khoshnam, M., Kuatsjah, E., Zhang, X., & Menon, C. (2017, April). Hands-Free EEG-Based Control of a Computer Interface Based on Online Detection of Clenching of Jaw. In *International Conference on Bioinformatics and Biomedical Engineering* (pp. 497-507). Springer, Cham.
- Kim, K. H., Kim, J. H., Yoona, J., and Jung, K. Y. (2008). Influence of task difficulty on the features of event-related potential during visual oddball task. *Neurosci. Lett.* 445, 179–183. doi: 10.1016/j.neulet.2008.09.004
- Kirchner W K (1958) Age differences in short-term retention of rapidly changing information *J. Exp.Psychol.* **55** 352–358
- Klimesch, W. (1996). Memory processes, brain oscillations and EEG synchronization. *International journal of psychophysiology*, 24(1), 61-100.
- Klimesch, W. (1997). EEG-alpha rhythms and memory processes. *International Journal of Psychophysiology*, 26(1), 319-340.
- Klimesch W (1999) EEG alpha and theta oscillations reflect cognitive and memory performance: a review and analysis *Brain Research Reviews* **29** 169–195

Bibliography

- Klimesch, W. (2003). "Interindividual differences in oscillatory EEG activity and cognitive performance". In: Reinvang I, Greenlee MW, Herrmann M, eds. *The cognitive neuroscience of individual differences*. 87–99.
- Klimesch W (2012) Alpha-band oscillations, attention, and controlled access to stored information *Trends Cogn Sci.* **16** 606–617
- Klimesch, W., Doppelmayr, M., Pachinger, T. and Russegger, H. (1997). Event-related desynchronization in the alpha band and the processing of semantic information. *Cognitive Brain Research*. 6(2): 83-94. doi: 10.1016/S0926-6410(97)00018-9
- Klimesch, W., M. Doppelmayr, H. Russegger, T. Pachinger, and J. Schwaiger. (1998) Induced alpha band power changes in the human eeg and attention. *Neuroscience letters*, 244(2):73–76.
- Klimesch, W., Pfurtscheller, G., Schimke, H. (1992). Pre- and post-stimulus processes in category judgement tasks as measured by event-related desynchronization (ERD). *Journal of Psychophysiology*. 6(3): 185-203.
- Klimesch, W., Schimke, H., Pfurtscheller, G. (1993). Alpha frequency, cognitive load and memory performance. *Brain Topography* 5(3) 241–251. Doi: 10.1007/BF01128991
- Klimesch, W., Schimke, H., Schwaiger, J. (1994). Episodic and semantic memory: an analysis in the EEG theta and alpha band. *Electroenceph. Clin. Neurophysiol.* 91: 428–441. doi: 10.1016/0013-4694(94)90164-3
- Klöppel S., T. van Eimeren, V. Glauche, A. Vongerichten, A. Münchau, R.S.J. Frackowiak, C. Büchel, C. Weiller, and H.R. Siebner (2007) The effect of handedness on cortical motor activation during simple bilateral movements, *NeuroImage* 34, pp. 274–280. doi:10.1016/j.neuroimage.2006.08.038
- Kohavi, R. and Provost, F., (1998). Guest editors' introduction: On applied research in machine learning. *Machine learning*, 30(2), 127-132.
- Kohlmorgen J., G. Dornhege, M. Braun, B. Blankertz, K.-R. Müller, G. Curio, K. Hagemann, A. Bruns, M. Schrauf, and W. Kincses. (2007) Improving human performance in a real operating environment through real-time mental workload detection, in: G. Dornhege, J. del R. Millán, T. Hinterberger, D. McFarland, and K.-R. Müller, eds., *Toward Brain-Computer Interfacing*, pages 409–422, MIT press, Cambridge, MA.
- Kohlmorgen J, S. Lemm, (2001) An On-line Method for Segmentation and Identification of Non-stationary Time Series Neural Networks for Signal Processing XI, IEEE.
- Kolak, D., Hirstein, W., Mandik, P., & Waskan, J. (2006). *Cognitive science: An introduction to mind and brain*. Routledge.
- Kolb B. and Whishaw I. Q. (1980) *Fundamentals of Human Neuropsychology*, W. H. Freeman.
- Koles Z J (1991) The quantitative extraction and topographic mapping of the abnormal components in the clinical EEG. *Electroencephalography and Clinical Neurophysiology.* **79** 440–447
- Kowalczyk A. and Chapelle O. (2005) An Analysis of the Anti-Learning Phenomenon for the Class Symmetric Polyhedron, in Sanjay Jain, Hans Ulrich Simon, Etsuji Tomita, eds., *Algorithmic Learning Theory: 16th International Conference, ALT, Springer*, pp. 78-91, 2005. doi: 10.1007/11564089_8
- Krauledat M., G. Dornhege, B. Blankertz, G. Curio, and K.-R. Müller. (2004) The Berlin brain-computer interface for rapid response. *Biomed Tech*, 49(1):61–62.
- Krepki, R., Blankertz, B., Curio, G., & Müller, K. R. (2007). The Berlin Brain-Computer Interface (BBCI)–towards a new communication channel for online control in gaming applications. *Multimedia Tools and Applications*, 33(1), 73-90.
- Kronegg J, G. Chanel, S. Voloshynovskiy, and T. Pun. (2007) EEG-based synchronized brain-computer interfaces: A model for optimizing the number of mental tasks. *IEEE Transactions on Neural Systems and Rehabilitation Engineering*, 15(1):50–58.

- Kruskal, W. H., & Wallis, W. A. (1952). Use of ranks in one-criterion variance analysis. *Journal of the American statistical Association*, 47(260), 583-621. doi:10.1080/01621459.1952.10483441.
- Krzanowski, W. J. (1988) *Principles of Multivariate Analysis: A User's Perspective*. New York: Oxford University Press.
- Kublanovskaya, V. N. (1962). On some algorithms for the solution of the complete eigenvalue problem. *USSR Computational Mathematics and Mathematical Physics*, 1(3):637-657.
- Kübler, A., Halder, S., Furdea, A., & Hösle, A. (2008). Brain painting—BCI meets art. na.
- Kübler A, Müller KR (2007) An Introduction to Brain Computer Interfacing. In: Dornhege G, Millán J der R, Hinterberger T, McFarland D J and Müller K R (eds) *Toward brain-computer interfacing MIT press* 1–25
- Kübler A, V.K. Mushahwar, L.R. Hochberg, and J.P. Donoghue. (2006) BCI meeting 2005-workshop on clinical issues and applications. *IEEE Transactions on Neural Systems and Rehabilitation Engineering*, 14(2):131–134.
- Kübler A., F. Nijboer, J. Mellinger, T. M. Vaughan, H. Pawelzik, G. Schalk, D. J. McFarland, N. Birbaumer, and J. R. Wolpaw. (2005) Patients with ALS can use sensorimotor rhythms to operate a brain-computer interface. *Neurology*, 64(10):1775–1777.
- Hunter, J. D. (2007). Matplotlib: A 2D graphics environment. *Computing In Science & Engineering*, 9(3), 90-95. DOI: <http://www.dx.doi.org/10.5281/zenodo.573577>
- Lachaux J P, George N, Tallon-Baudry C, Martinerie J, Hugueville L, Minotti L, Kahane P, Renault B (2005) The many faces of the gamma band response to complex visual stimuli *NeuroImage* 25 491 – 501
- Lafrance, C. and Dumont, M., (2000). Diurnal variations in the waking EEG: comparisons with sleep latencies and subjective alertness. *Journal of sleep research*, 9(3), pp.243-248.
- Lalor, E., S. P. Kelly, C. Finucane, R. Burke, R. Smith, R. Reilly, and G. Mc-Darby. (2005) Steady-state VEP-based brain-computer interface control in an immersive 3-D gaming environment. *EURASIP journal on applied signal processing*.
- Lebedev, M.A. and Nicolelis, M.A.L. (2006) Brain-machine interfaces: past, present and future. *Trends in Neurosciences*, 29(9):536–546.
- Lécuyer, A., F. Lotte, R. B. Reilly, R. Leeb, M. Hirose and M. Slater, (2008) "Brain-Computer Interfaces, Virtual Reality, and Videogames," in *Computer*, vol. 41, no. 10, pp. 66-72. doi: 10.1109/MC.2008.410
- Ledoit, O. and M. Wolf (2004). A well-conditioned estimator for largedimensional covariance matrices. *Journal of multivariate analysis* 88.2, pp. 365–411.
- Lee, H, Choi, S, (2009) Group nonnegative matrix factorization for EEG classification. Intern. Conf. on Artificial Intelligence and Statistics, FL, USA
- Lee, H, Yoo, J, Choi, S, (2010) Semi-supervised nonnegative matrix factorization *IEEE Signal Process Lett*, 17, pp. 4-7
- Lemm S, Blankertz B, Curio G, Müller KR (2005). “Spatio-Spectral Filters for Improving Classification of Single Trial EEG”. In: *IEEE Trans Biomed Eng* 52.9, pp. 1541–1548.
- Lemm S, Blankertz B, Dickhaus T, Müller KR (2011). “Introduction to machine learning for brain imaging”. In: *Neuroimage* 56, pp. 387–399.
- Lemm S, Müller K R, Curio G (2009) A Generalized Framework for Quantifying the Dynamics of EEG Event-Related Desynchronization *PLoS Comput Biol* 5 e1000453
- Lemm S., Schafer, C., & Curio, G. (2004). BCI competition 2003-data set III: probabilistic modeling of sensorimotor/spl mu/rhythms for classification of imaginary hand movements. *IEEE Transactions on Biomedical Engineering*, 51(6), 1077-1080.
- Lepage, K. Q., Kramer, M. A., & Chu, C. J. (2014). A statistically robust EEG re-referencing procedure to mitigate reference effect. *Journal of neuroscience methods*, 235, 101-116.

Bibliography

- Leuthardt, E.C., K.J. Miller, G. Schalk, R.P.N. Rao, and J.G. Ojemann. (2006) Electrocorticography-based brain computer interface-the Seattle experience. *IEEE Transactions on Neural Systems and Rehabilitation Engineering*, 14(2):194–198.
- Levin, R.B., Levin and Richard B., (2000). Devices and methods for maintaining an alert state of consciousness through brain wave monitoring. U.S. Patent 6,167,298.
- Lezak M. D. *Neuropsychological Assessment*, -- Oxford Univ Press, 1983
- Li, S., Hong, B., Gao, X., Wang, Y., & Gao, S. (2011). Event-related spectral perturbation induced by action-related sound. *Neuroscience letters*, 491(3), 165-167.
- Lloyd, D., (2007) “What do Brodmann areas do? Or: Scanning the Neurocracy”, Trinity College, Hartford, CT: Program in Neuroscience.
- Long, J. S. (1997) *Regression Models for Categorical and Limited Dependent Variables*. Sage Publications.
- Lotte F, Congedo M, Lécuyer A, Lamarche F, Arnaldi B (2007a). “A review of classification algorithms for EEG-based brain-computer interfaces”. In: *J Neural Eng* 4, R1–R13.
- Lotte, F., A. Lécuyer, F. Lamarche, and B. Arnaldi. (2007b) Studying the use of fuzzy inference systems for motor imagery classification. *IEEE Transactions on Neural System and Rehabilitation Engineering*, 15(2):322–324.
- Lu, N., & Yin, T. (2015). Motor imagery classification via combinatory decomposition of ERP and ERSP using sparse nonnegative matrix factorization. *Journal of neuroscience methods*, 249, 41-49.
- Luck S. J., (2005) *An introduction to the Event-Related Potential technique*, The MIT Press, pp. 45-64.
- Luck, S. J. (2014). *An introduction to the event-related potential technique*. MIT press.
- Mak JN, Wolpaw JR (2009). “Clinical applications of brain-computer interfaces: current state and future prospects”. In: *Biomedical Engineering, IEEE Reviews in 2*, pp. 187–199.
- Makeig, S. (1993). Auditory event-related dynamics of the EEG spectrum and effects of exposure to tones. *Electroencephalography and clinical neurophysiology*, 86(4), 283-293.
- Makeig, S., et al., (2002) “Dynamic brain sources of visual evoked responses”, *Science* 295:690–694.
- Makeig, S. and Jung, T. P. (1996). Tonic, phasic, and transient EEG correlates of auditory awareness in drowsiness. *Cognitive Brain Research* 4.1, pp. 15–25.
- Makeig, S., Bell, T., Lee, T. W., Jung, T. P., & Enghoff, S. (2000a). EEGLAB: ICA toolbox for psychophysiological research. WWW Site, Swartz Center for Computational Neuroscience, Institute of Neural Computation, University of San Diego California. www.sccn.ucsd.edu/eeglab/
- Makeig, S., Bell, A.J., Jung, T-P and Sejnowski, T.J., (1996) "Independent component analysis of electroencephalographic data," In: D. Touretzky, M. Mozer and M. Hasselmo (Eds). *Advances in Neural Information Processing Systems* 8:145-151, MIT Press, Cambridge, MA.
- Makeig S, S. Debener, J. Onton, A. Delorme, (2004) “Mining event-related brain dynamics”, *Trends Cogn. Sci.* 8, 204–210.
- Makeig S, S. Enghoff, Tzyy-Ping Jung, and T.J. Sejnowski. (2000b) A natural basis for efficient brain-actuated control. *IEEE Transactions on Rehabilitation Engineering*, 8(2):208–211.
- Makeig, S., G. Leslie, T. Mullen, D. Sarma, N. Bigdely-Shamlo, and C. Kothe. (2011) First demonstration of a musical emotion bci. In *Affective Computing and Intelligent Interaction*, pages 487–496. Springer.
- Mallat, S. (1989), "A theory for multiresolution signal decomposition: the wavelet representation," *IEEE Pattern Anal. and Machine Intell.*, vol. 11, no. 7, pp 674–693.
- Marple, S. L. (1999) “Computing the Discrete-Time Analytic Signal via FFT.” *IEEE Transactions on Signal Processing*. Vol. 47, pp. 2600–2603.
- Martel A, Dähne S and Blankertz B (2014) EEG predictors of covert vigilant attention *J. Neural Eng.* 11 035009

- Martinez, P., H. Bakardjian, and A. Cichocki. (2007) Fully online multicommand brain-computer interface with visual neurofeedback using SSVEP paradigm. *Comput. Intell. Neuroscience*, 1.
- Mason S G and G. E. Birch. (2000) A brain-controlled switch for asynchronous control applications. *IEEE Transactions on Biomedical Engineering*, 47(10):1297–1307.
- Mason S.G. and G.E. Birch. (2003) A general framework for brain-computer interface design. *IEEE Transactions on Neural Systems and Rehabilitation Engineering*, 11(1):70–85.
- Matousek, M. and I. Petersén (1983). A method for assessing alertness fluctuations from EEG spectra. *Electroencephalography and clinical neurophysiology* 55.1, pp. 108–113.
- Mauchly, J. W. (1940) “Significance Test for Sphericity of a Normal n-Variate Distribution. The Annals of Mathematical Statistics. Vol. 11, pp. 204–209.
- McClellan, J. H., and Parks, T. W. (2005). A personal history of the Parks-McClellan algorithm. *IEEE Signal Processing Magazine*, 22(2), 82-86.
- McFarland, D. J. and Wolpaw, J. R. (2005) Sensorimotor rhythm-based braincomputer interface (BCI): feature selection by regression improves performance. *IEEE Transactions on Neural Systems and Rehabilitation Engineering*, 13(3):372–379.
- McFarland D J, L.M.McCane, S. V. David, and J. R.Wolpaw. (1997) Spatial filter selection for EEG-based communication. *Electroencephalographic Clinical Neurophysiology*, 103(3):386–394.
- McFarland D. J., C. W. Anderson, K.-R. Müller, A. Schlogl, and D. J. Krusienski. (2006) BCI meeting 2005-workshop on BCI signal processing: feature extraction and translation. *IEEE Transactions on Neural Systems and Rehabilitation Engineering*, 14(2):135 – 138.
- McFarland D. J., J. R. Wolpaw, (2010) Chapter 4 – Brain–Computer Interfaces for the Operation of Robotic and Prosthetic Devices, *Advances in Computers*, Volume 79, pp. 169–187, [http://doi.org/10.1016/S0065-2458\(10\)79004-5](http://doi.org/10.1016/S0065-2458(10)79004-5)
- McFarland D. J., L. A. Miner, T. M. Vaughan, and J. R. Wolpaw. (2000) Mu and beta rhythm topographies during motor imagery and actual movements. *Brain topography*, 12(3): 177–186.
- McLachlan, G. (2004). *Discriminant analysis and statistical pattern recognition* (Vol. 544). John Wiley & Sons.
- McLeod, S. A. (2007). Levels of Processing. Retrieved from www.simplypsychology.org/levelsofprocessing.html
- Mecklinger A, Kramer AF, Strayer DL (1992) Event related potentials and EEG components in a semantic memory search task. *Psychophysiology* 29:104–119
- Melinscak, F., Montesano, L., & Minguez, J. (2014). Discriminating between attention and mind wandering during movement using EEG. In *Proc 6th BCI Int Conf* (Vol. 2014, pp. 314-317).
- Mellinger, J., G. Schalk, C. Braun, H. Preissl, W. Rosenstiel, N. Birbaumer, and A. Kübler. (2007) An MEG-based brain-computer interface (BCI). *Neuroimage*, 36(3):581–593.
- MettingVanRijn, A. C., Kuiper, A. P., Dankers, T. E., & Grimbergen, C. A. (1996, October). Low-cost active electrode improves the resolution in biopotential recordings. In *Engineering in Medicine and Biology Society, 1996. Bridging Disciplines for Biomedicine. Proceedings of the 18th Annual International Conference of the IEEE* (Vol. 1, pp. 101-102). IEEE.
- Meyer L, Grigutsch M, Schmuck N, Gaston P, Friederici A D (2015) Frontal-posterior theta oscillations reflect memory retrieval during sentence comprehension *Cortex* 71 205-218
- Millán J. del R. and J. Mouriño. (2003) Asynchronous BCI and local neural classifiers: An overview of the Adaptive Brain Interface project. *IEEE Transactions on Neural Systems and Rehabilitation Engineering*, Special Issue on Brain-Computer Interface Technology.
- Millán J. del R., J. Mouriño, F. Cincotti, F. Babiloni, M. Varsta, and J. Heikkinen. (2000) Local neural classifier for EEG-based recognition of mental tasks. In *IEEE-INNS-ENNS International Joint Conference on Neural Networks*.

Bibliography

- Millán, J.D.R., Franzé, M., Mouriño, J., Cincotti, F. and Babiloni, F., (2002). Relevant EEG features for the classification of spontaneous motor-related tasks. *Biological cybernetics*, 86(2), pp.89-95.
- Millán J. del R., R. Rupp, G. Müller-Putz, R. Murray-Smith, C. Giugliemma, M. Tangermann, C. Vidaurre, F. Cincotti, A. Kübler, R. Leeb, C. Neuper, K.-R. Müller, and D. Mattia. (2010) Combining brain-computer interfaces and assistive technologies: State-of-the-art and challenges. *Frontiers in Neuroprosthetics*, 4. doi: 10.3389/fnins.2010.00161.
- Mokienko O.A., L.A. Chernikova, A.A. Frolov, and P.D. Bobrov, (2014) Motor imagery and its practical application, *Neurosci. Behav. Physiol.*, vol. 44, pp. 483–489.
- Moore, M.M. (2003) Real-world applications for brain-computer interface technology. *IEEE Transactions on Neural Systems and Rehabilitation Engineering*, 11(2):162–165.
- Morone, G., Pisotta, I., Pichiorri, F., Kleih, S., Paolucci, S., Molinari, M., ... & Mattia, D. (2015). Proof of principle of a brain-computer interface approach to support poststroke arm rehabilitation in hospitalized patients: design, acceptability, and usability. *Archives of physical medicine and rehabilitation*, 96(3), S71-S78.
- Mullen, T. R., Kothe, C. A. E., Chi, Y. M., Ojeda, A., Kerth, T., Makeig, S., Jung, T.-P., and Cauwenberghs, G. (2015). Real-time neuroimaging and cognitive monitoring using wearable dry EEG. *IEEE Transactions on Biomedical Engineering*, 62(11):2553–2567.
- Mühl C, Jeunet C, Lotte F (2014) EEG-based Workload Estimation Across Affective Contexts *Frontiers in Neurosciences Neuroprosthetics* 8 00114
- Müller KR, Anderson C W, Birch G E (2003) Linear and nonlinear methods for brain-computer interfaces *IEEE Transactions on Neural Systems and Rehabilitation Engineering* 11 165–169
- Müller KR, Blankertz B (2006). “Toward non-invasive Brain-Computer Interfaces”. In: *IEEE Signal Process Mag* 23.5, pp. 125–128.
- Müller KR., M. Krauledat, G. Dornhege, G. Curio, and B. Blankertz. (2004) Machine learning techniques for brain-computer interfaces. *Biomed Tech*, 49(1):11–22.
- Müller KR, Tangermann M, Dornhege G, Krauledat M, Curio G, Blankertz B (2008). “Machine learning for real-time single-trial EEG-analysis: From brain-computer interfacing to mental state monitoring”. In: *J Neurosci Methods* 167(1): 82–90. URL <http://dx.doi.org/10.1016/j.jneumeth.2007.09.022>
- Müller-Gerking J, Pfurtscheller G, Flyvbjerg H (1999) Designing optimal spatial filters for single-trial eeg classification in a movement task *Clinical Neurophysiology*, 110 787-798
- Müller-Putz, G. R., R. Scherer, C. Brauneis, and G. Pfurtscheller (2005). Steady-state visual evoked potential (SSVEP)-based communication: impact of harmonic frequency components. *Journal of Neural Engineering* 2.4, pp. 123–130.
- Muthukumaraswamy, S. D. (2013). High-frequency brain activity and muscle artifacts in MEG/EEG: a review and recommendations. *Frontiers in Human Neuroscience*, 7, 138. <http://doi.org/10.3389/fnhum.2013.00138>
- Naem M, C. Brunner, R. Leeb, B. Graimann, and G. Pfurtscheller. (2006) Seperability of four-class motor imagery data using independent components analysis. *Journal of Neural Engineering*, 3:208–216.
- Nakata, H., Sakamoto, K., Otsuka, A., Yumoto, M., and Kakigi, R. (2013). Cortical rhythm of No-go processing in humans: an MEG study. *Clin. Neurophysiol.* 124, 273–282. doi: 10.1016/j.clinph.2012.06.019
- Naumann L., Schultze-Kraft M., Dähne S., Blankertz B. (2017) Prediction of Difficulty Levels in Video Games from Ongoing EEG. In: Gamberini L., Spagnolli A., Jacucci G., Blankertz B., Freeman J. (eds) *Symbiotic Interaction. Symbiotic 2016. Lecture Notes in Computer Science*, vol 9961. Springer, Cham

- Netter F. H., (1983) The CIBA Collection of Medical Illustrations, Vol. I: Nervous System, Part I: Anatomy and Physiology, CIBA Pharmaceutical Company.
- Neuper C., G. Müller, A. Kubler, N. Birbaumer, and G. Pfurtscheller. (2003) Clinical application of an eeg-based brain–computer interface: a case study in a patient with severe motor impairment. *Clinical neurophysiology*, 114(3):399–409.
- Neuper, C. and Pfurtscheller, G. (2009). Neurofeedback training for BCI control. In *Brain-Computer Interfaces* (pp. 65-78). Springer Berlin Heidelberg.
- Neuper C., R. Scherer, M. Reiner, and G. Pfurtscheller. (2005) Imagery of motor actions: Differential effects of kinesthetic and visual–motor mode of imagery in single-trial eeg. *Cognitive Brain Research*, 25(3):668–677.
- Nicolae I E**, Acqualagna L, and Blankertz B (2015a) Neural Indicators of the Depth of Cognitive Processing for User-Adaptive Neurotechnological Applications *Proc. Int. Conf. of the IEEE Engineering in Medicine and Biology Society* 1484-1487
- Nicolae I E**, Acqualagna L, and Blankertz B (2015b) Tapping Neural Correlates of the Depth of Cognitive processing for Improving Human Computer Interaction 4th International Workshop on Symbiotic Interaction, Lecture Notes in Computer Science *Springer* **9359** 126-131
- Nicolae I E**, Acqualagna L, and Blankertz B (2016a) Investigating Depth of Cognitive Processing in the Brain Dynamics of Oscillations *Proc. of 6th International BCI meeting* Verlag der TU Graz 186
- Nicolae, I. E.**, (2013) „An improved stimuli system for brain-computer interface applications”, Proc. of the 5th Intern. Conf. on Electronics, Computers and Artificial Intelligence, 27 -29 June 2013, Pitesti, Romania, Vol. 3, pp. 49 – 53 (Extended version published also in: *Intern. Journ. of Monitoring and Surveillance Technologies Research, Special Issue on Biomedical Monitoring Technologies*, 1(4), 1-8, October-December 2013, DOI: 10.4018/ijmstr.2013100101)
- Nicolae I. E.**, Acqualagna L and Blankertz B. (2017a). “Assessing the Depth of Cognitive Processing as the Basis for Potential User-State Adaptation”. *Front. Neurosci.* **11**:548, 2017a. doi: 10.3389/fnins.2017.00548
- Nicolae I-E**, Acqualagna L and Blankertz B. (2017b). Assessing the Depth of Cognitive Processing as the Basis for Potential User-State Adaptation – Data set. Depositonce, Technische Universität Berlin. doi: <http://dx.doi.org/10.14279/depositonce-6173>
- Nicolae I. E.**, G. M. Ungureanu, R. Strungaru, L. Acqualagna, B. Blankertz, (2018) *Enhanced classification for the depth of cognitive processing depicted in neural signals*, UPB Scientific Bulletin, Series C, Vol. 80, Iss. 1, 2018, ISSN 2286-3540, pp. 135-146.
- Nicolae I. E.**, M. M. C. Ștefan, B. Hurezeanu, D. D Taralunga, R. Strungaru, T. M Vasile, O. A. Bajenaru, G. M. Ungureanu, (2016b) “Investigating Motor Imagery Tasks by Their Neural Effects – a Case Study”, Proc. of the 38th Annual International Conference of the IEEE Engineering in Medicine and Biology Society (EMBC), 17-20 August, 2016, Orlando, Florida, pp. 5861-5864, DOI: 10.1109/EMBC.2016.7592061
- Nicolae I. E.**, M. Ungureanu, L. Acqualagna, R. Strungaru and B. Blankertz, (2015c) “Spectral Perturbations of the Depth of Cognitive Processing for Brain-Computer Interface Systems”, 5-th edition of the International Conference on e-Health and Bioengineering (EHB 2015), 19-21 November, Iasi, Romania, pp. 1-4, DOI: 10.1109/EHB.2015.7391473
- Nicolae I.E.**, G. M. Ungureanu, and R. Strungaru, (2014a) „ICA Analysis of Real and Motor Imagery Movements in a Brain-Computer Interface Stimuli System”, Proc. of the 6th International Conference on Electronics, Computers and Artificial Intelligence (ECAI), 23-25 oct, 2014, Bucharest, Romania, Vol. 6 – No. 6, pp. 7-10, DOI: 10.1109/ECAI.2014.7090216
- Nicolae I.E.**, G. M. Ungureanu, and R. Strungaru, (2014b) “Motor Imagery Mental Tasks in Brain-Computer Interface Applications”, Workshop on Smart Healthcare and Healing Environments,

Bibliography

- AMI'14, 11-13 nov, Eindhoven, The Netherlands, 12 pages, Online accession: http://www.smarthealth-ami.id.tue.nl/SHHE2014/submissions/shhe2014_submission_9.pdf
- Nicolas-Alonso LF, Gomez-Gil J (2012). "Brain computer interfaces, a review". In: *Sensors* 12.2, pp. 1211–1279.
- Niedermeyer E, Silva F H L (2005) *Electroencephalography: Basic Principles, Clinical Applications, and Related Fields Philadelphia: Williams & Wilkins 5*
- Niedermeyer, E. (1997). "Alpha rhythms as physiological and abnormal phenomena". *International Journal of Psychophysiology*. 26 (1–3): 31–49. doi:10.1016/S0167-8760(97)00754-X. PMID 9202993.
- Nikulin, V. V., Kegeles, J., and Curio, G. (2010). Miniaturized electroencephalographic scalp electrode for optimal wearing comfort. *Clinical Neurophysiology*, 121(7):1007–1014.
- Nikulin, V. V., Linkenkaer-Hansen, K., Nolte, G., Lemm, S., Müller, K. R., Ilmoniemi, R. J., & Curio, G. (2007). A novel mechanism for evoked responses in the human brain. *European Journal of Neuroscience*, 25(10), 3146-3154.
- Nikulin V V, Nolte G, Curio G 2011 A novel method for reliable and fast extraction of neuronal EEG/MEG oscillations on the basis of spatio-spectral decomposition *NeuroImage* **55** 1528–1535
- Okazaki, M., Kaneko, Y., Yumoto, M., Arima, K. (2008). Perceptual change in response to a bistable picture increases neuromagnetic beta-band activities. *Neurosci Res*. 61: 319–328. doi: 10.1016/j.neures.2008.03.010
- Onton, J., Delorme, A., & Makeig, S. (2005). Frontal midline EEG dynamics during working memory. *Neuroimage*, 27(2), 341-356.
- Oppenheim, A. V.; Schaffer, R. W.; Buck J. R. (1999). *Discrete-time signal processing*. Upper Saddle River, N.J.: Prentice Hall. ISBN 0-13-754920-2.
- Osaka, M. (1984). Peak alpha frequency of EEG during a mental task: Task difficulty and hemispheric differences. *Psychophysiology*, 21(1), 101-105.
- Palaniappan, R. (2005) Brain computer interface design using band powers extracted during mental tasks. In *Proceedings of the 2nd International IEEE EMBS Conference on Neural Engineering*.
- Palva, S., Palva, M. (2007). New vistas for α -frequency band oscillations. *Trends in Neurosciences* **30**: 150–158. doi: 10.1016/j.tins.2007.02.001
- Parks, T., & McClellan, J. (1972). Chebyshev approximation for nonrecursive digital filters with linear phase. *IEEE Transactions on Circuit Theory*, 19(2), 189-194.
- Parra, L., Alvino, C., Tang, A. C., Pearlmutter, B. A., Yeung, N., Osman, A., and Sajda, P., (2002) "Linear spatial integration for single trial detection in encephalography", *NeuroImage*.
- Parra, L. C., Spence, C. D., Gerson, A. D., Sajda, P., (2005). Recipes for the linear analysis of EEG. *Neuroimage* 28 (2), 326–341.
- Pearson K (20 June 1895) "Notes on regression and inheritance in the case of two parents," *Proceedings of the Royal Society of London*, 58 : 240–242.
- Pesonen, M., Hämäläinen, H., Krause, C. M. (2007). Brain oscillatory 4–30 Hz responses during a visual n-back memory task with varying memory load. *Brain Research*. 1138: 171–177. doi: 10.1016/j.brainres.2006.12.076
- Pfurtscheller G and Neuper C. (2001) Motor imagery and direct brain-computer communication. *proceedings of the IEEE*, 89(7):1123–1134.
- Pfurtscheller G, Brunner C., A. Schlogl, and F.H. Lopes da Silva. (2006) Mu rhythm (de)synchronization and EEG single-trial classification of different motor imagery tasks. *NeuroImage*, 31(1):153–159.
- Pfurtscheller G., D. Flotzinger, and J. Kalcher. (1993) Brain-computer interface-a new communication device for handicapped persons. *journal of microcomputer application*, 16:293–299.

- Pfurtscheller G, da Silva Lopes F H (1999) Event-related EEG/MEG synchronization and desynchronization: basic principles *Clin. Neurophysiol.* **110** 1842–1857
- Pfurtscheller, G., & Aranibar, A. (1979). Evaluation of event-related desynchronization (ERD) preceding and following voluntary self-paced movement. *Clinical Neurophysiology*, 46(2), 138–146.
- Pfurtscheller G. and Aranibar A. (1977) Event-related cortical desynchronization detected by power measurements of scalp eeg. *Electroencephalography and clinical neurophysiology*, 42(6): 817–826.
- Pfurtscheller G. and Klimesch W. (1992) Event-related synchronization and desynchronization of alpha and beta waves in a cognitive task. In *Induced rhythms in the brain*, pages 117–128. Springer.
- Pfurtscheller, G., C. Neuper, C. Brunner, and F. L. da Silva. (2005) Beta rebound after different types of motor imagery in man. *Neuroscience letters*, 378(3):156–159.
- Pfurtscheller G., Neuper Ch., D. Flotzinger, M. Pregenzer, (1997) EEG based discrimination between imagination of right and left hand movement, *Electroencephalography and clinical Neurophysiology* 103, pp. 642-651.
- Pfurtscheller, G., Müller G. R, J. Pfurtscheller, H. J. Gerner, and R. Rupp (2003). ‘Thought’–control of functional electrical stimulation to restore hand grasp in a patient with tetraplegia. *Neuroscience letters* 351.1, pp. 33–36.
- Pham D-T. (2001) Joint approximate diagonalization of positive definite matrices. *SIAM J. on Matrix Anal. and Appl.*, vol. 22, no. 4, pp. 1136. 1152.
- Plourde, G., D.R. Stapells, T.W. Picton, (1991) The human auditory steady-state evoked potentials, *Acta Otolaryngol.*, 491, pp. 153-160
- Polich J (1989). “Frequency, intensity, and duration as determinants of P300 from auditory stimuli”. In: *J Clin Neurophysiol* 6.3, p. 277.
- Polich J (2007). “Updating P300: an integrative theory of P3a and P3b”. In: *Clin Neurophysiol* 118, pp. 2128–2148.
- Polich J, Ellerson PC, Cohen J (1996). “P300, stimulus intensity, modality, and probability”. In: *Int J Psychophysiol* 23, pp. 55–62.
- Polich J, Kok A (1995) Cognitive and biological determinants of P300: an integrative review *Biological Psychology* **41** 103-146
- Pomer-Escher, A., Tello, R., Castillo, J., & Bastos-Filho, T. (2014). Analysis of mental fatigue in motor imagery and emotional stimulation based on EEG. In XXIV Congresso Brasileiro de Engenharia Biomedica-CBEB.
- Pope A T, Bogart E H and Bartolome D S (1995) Biocybernetic system evaluates indices of operator engagement in automated task *Biol. Psychol.* 40:187–95
- Popescu, F., Fazli, S., Badower, Y., Blankertz, B., and Müller, K.-R. (2007). Single trial classification of motor imagination using 6 dry EEG electrodes. *PLoS ONE*, 2(7):1–5.
- Porbadnigk, A. K., N. Görnitz, C. Sannelli, A. Binder, M. Braun, M. Kloft, and K.-R. Müller. (2015) Extracting latent brain states–towards true labels in cognitive neuroscience experiments. *NeuroImage*, 120:225–253.
- Porbadnigk A K, Treder M S, Blankertz B, Antons J N, Schleicher R, Möller S, Curio G and Müller K-R (2013) Single trial analysis of the neural correlates of speech quality perception *J. Neural. Eng.* **10** 056003
- Rabiner, L. R., and Gold, B. (1975). *Theory and application of digital signal processing*. Englewood Cliffs, NJ, Prentice-Hall, Inc., 1975. 777 p., 1.
- Ramachandran V S, (nov 2009) “The neurons that shaped”, TED talks. Retrieved from https://www.ted.com/talks/vs_ramachandran_the_neurons_that_shaped_civilization/transcript?language=en

Bibliography

- Ramoser, H., Müller-Gerking, J., and Pfurtscheller, G. (2000). Optimal spatial filtering of single trial EEG during imagined hand movement. *IEEE Transactions on Rehabilitation Engineering*, 8(4):441-446.
- Razali, N. M., & Wah, Y. B. (2011). Power comparisons of shapiro-wilk, kolmogorov-smirnov, lilliefors and anderson-darling tests. *Journal of statistical modeling and analytics*, 2(1), 21-33.
- Regan, D. (1989). *Human Brain Electrophysiology: Evoked Potentials and Evoked Magnetic Fields in Science and Medicine*. Elsevier, New York.
- Rimbert, S., Avilov, O., & Bougrain, L. (2017). Discrete motor imageries can be used to allow a faster detection. In *7th Graz Brain-Computer Interface Conference 2017*.
- Roland, P. E., & Gulyás, B. (1995). Visual memory, visual imagery, and visual recognition of large field patterns by the human brain: functional anatomy by positron emission tomography. *Cerebral Cortex*, 5(1), 79-93.
- Royston P. "Remark AS R94", *Applied Statistics* (1995), Vol. 44, No. 4, pp. 547-551.
- Rutkove S. B., *Introduction to Volume Conduction, The Clinical Neurophysiology Primer*, I pp 43-53, 2007
- Samar V J, A. Bopardikar, R. Rao, and K. Swartz. (1999) Wavelet analysis of neuroelectric waveforms: A conceptual tutorial. *Brain and Language*, 66(1):7-60.
- Samek W, Kawanabe M, Müller KR (2014). "Divergence-based Framework for Common Spatial Patterns Algorithms". In: *Biomedical Engineering, IEEE Reviews in 7*, pp. 50-72.
- Samek, W., Nakajima, S., Kawanabe, M., & Müller, K. R. (2017). On robust parameter estimation in brain-computer interfacing. *Journal of neural engineering*, 14(6), 061001.
- Samek W, Vidaurre C, Müller KR, Kawanabe M (2012). "Stationary Common Spatial Patterns for Brain-Computer Interfacing". In: *Journal of Neural Engineering* 9.2, p. 026013.
- Sannelli, C., Dickhaus, T., Halder, S., Hammer, E. M., Müller, K. R., & Blankertz, B. (2010). On optimal channel configurations for SMR-based brain-computer interfaces. *Brain topography*, 23(2), 186-193.
- Sannelli C, Vidaurre C, Müller KR, Blankertz B (2011). "Common Spatial Pattern Patches - an Optimized Filter Ensemble for Adaptive Brain-Computer Interfaces". In: *J Neural Eng* 8.2, 025012 (7pp).
- Schack, B., Klimesch, W., Sauseng, P. (2005). Phase synchronization between theta and upper alpha oscillations in a working memory task. *Int J Psychophysiol.* 57: 105-114. doi: 10.1016/j.ijpsycho.2005.03.016
- Schäfer, J., K. Strimmer, et al. (2005). A shrinkage approach to largescale covariance matrix estimation and implications for functional genomics. *Statistical applications in genetics and molecular biology* 4(1), p. 32. doi: 10.2202/1544-6115.1175
- Scherer, R., F. Lee, A. Schlögl, R. Leeb, H. Bischof, and G. Pfurtscheller. (2008) Towards self-paced brain-computer communication: Navigation through virtual worlds. *IEEE, Transactions on Biomedical Engineering*, 55(2):675-682.
- Schlögl, C. Vidaurre, K. R. Müller, (2010) *Adaptive Methods in BCI Research - An Introductory Tutorial, Brain-Computer Interfaces, Springer, The Frontiers Collection*.
- Schmidt, E. A., Kincses, W. E., Schrauf, M., Haufe, S., Schubert, R., and Curio, G. (2007). "Assessing drivers' vigilance state during monotonous driving," in *Proceedings of the Fourth International Symposium on Human Factors in Driving Assessment, Training, and Vehicle Design* (Washington, DC), 138-145.
- Schmidt, E. A., Schrauf, M., Simon, M., Fritzsche, M., Buchner, A., and Kincses, W. E. (2009). Drivers' misjudgement of vigilance state during prolonged monotonous daytime driving. *Accid. Anal. Prev.* 41, 1087-1093. doi: 10.1016/j.aap.2009.06.007

- Scholler S, Bosse S, Treder M S, Blankertz B, Curio G, Müller K-R and Wiegand T (2012) Towards a direct measure of video quality perception using EEG *IEEE Trans. Image Process.* 21 2619–29
- Scholz, S., Schneider, S. L., & Rose, M. (2017). Differential effects of ongoing EEG beta and theta power on memory formation. *PloS one*, 12(2), e0171913.
- Scheer, H.J., Curio, G. and Burghoff, M., (2009). Measurement of high frequency EEG signals with very low noise amplifiers: Brain oscillations above 600 Hz measured non-invasively. In 4th European Conference of the International Federation for Medical and Biological Engineering (pp. 1302-1304). Springer, Berlin, Heidelberg.
- Schreuder M, Blankertz B, Tangermann M (2010). “A New Auditory Multi-class Brain-Computer Interface Paradigm: Spatial Hearing as an Informative Cue”. In: *PLoS ONE* 5.4, e9813., URL <http://dx.doi.org/10.1371/journal.pone.0009813>.
- Schroder, M., Bogdan, M., Hinterberger, T., & Birbaumer, N. (2003, March). Automated EEG feature selection for brain computer interfaces. In *Neural Engineering, 2003. Conference Proceedings. First International IEEE EMBS Conference on* (pp. 626-629). IEEE.
- Schubert, R., M. Tangermann, S. Haufe, C. Sannelli, M. Simon, E. A. Schmidt, W. E. Kincses, and G. Curio (2008). „Parieto-occipital alpha power indexes distraction during simulated car driving.“ In: *International Journal of Psychophysiology*. Vol. 69. 3.
- Schultze-Kraft, M., D. Birman, M. Rusconi, C. Allefeld, K. Görden, S. Dähne, B. Blankertz, and J.-D. Haynes (2015). „Predicting and interrupting movement intentions with a closed loop BCI.“ In: *Annual Meeting of the Organization for Human Brain Mapping (OHBM)*, Honolulu, USA.
- Schultze-Kraft, M., Birman, D., Rusconi, M., Allefeld, C., Görden, K., Dähne, S., Blankertz, B., and Haynes, J.-D. (2016a). The point of no return in vetoing self-initiated movements. *Proceedings of the National Academy of Sciences*, 113(4):1080–1085. doi: 10.1073/pnas.1513569112.
- Schultze-Kraft, M., Gugler, M., Curio, G. and Blankertz, B., (2012). Towards an Online Detection of Workload in Industrial Work Environments. In *34th Annual International Conference of the IEEE EMBS*, pp. 4792-4795.
- Schultze-Kraft, M., Dähne, S., Gugler, M., Curio, G., Blankertz, B. (2016b). Unsupervised classification of operator workload from brain signals. *J Neural Eng.* **13**. doi: 10.1088/1741-2560/13/3/036008
- Schuster, Arthur (January 1898). "On the investigation of hidden periodicities with application to a supposed 26 day period of meteorological phenomena". *Terrestrial Magnetism*. **3** (1): 13–41. doi:[10.1029/TM003i001p00013](https://doi.org/10.1029/TM003i001p00013)
- Sejdić E.; Djurović I.; Jiang J. (2009). "Time-frequency feature representation using energy concentration: An overview of recent advances". *Digital Signal Processing*. **19** (1): 153–183. doi:[10.1016/j.dsp.2007.12.004](https://doi.org/10.1016/j.dsp.2007.12.004).
- Sergeant, J., Geuze, R., van Winsum, W. (1987). Event-Related Desynchronization and P300. *Psychophysiology*. **24**(3): 272-277. doi: 10.1111/j.1469-8986.1987.tb00294.x
- Shapiro, S. S.; Wilk, M. B. (1965). "An analysis of variance test for normality (complete samples)". *Biometrika*. 52 (3–4): 591–611. doi:10.1093/biomet/52.3-4.591. JSTOR 2333709. MR 0205384. p. 593
- She, H.C., Jung, T.P., Chou, W.C., Huang, L.Y., Wang, C.Y. and Lin, G.Y., (2012). EEG dynamics reflect the distinct cognitive process of optic problem solving. *PloS one*, 7(7), p.e40731.
- Sheth, B. R., Sandkühler, S., Bhattacharya, J. (2009). Posterior beta and anterior gamma oscillations predict cognitive insight. *Journal of Cognitive Neuroscience*. **21**: 1269–1279. doi: 10.1162/jocn.2009.21069
- Shirer W R, Ryali S, Rykhlevskaia E, Menon V, Greicius M D (2012) Decoding subject-driven cognitive states with whole-brain connectivity patterns *Cereb. Cortex* **22** 158–165

Bibliography

- Smith J. O., (Sept. 2007a) Introduction to Digital Filters with Audio Applications, <http://ccrma.stanford.edu/~jos/filters/>, online book.
- Smith J. O. (2007b) Mathematics of the discrete Fourier transform (DFT): with audio applications. Julius Smith.
- Smith S.W. (1997) The Scientist & Engineer's Guide to Digital Signal Processing. ISBN 0-9660176-3-3.
- Snedecor, George W. and Cochran, William G. (1989), Statistical Methods, Eighth Edition, Iowa State University Press. ISBN 978-0-8138-1561-9
- Spironelli, C. and Angrilli, A., (2010). Developmental aspects of language lateralization in delta, theta, alpha and beta EEG bands. *Biological psychology*, 85(2), pp.258-267.
- Stapel, J. C., Hunnius, S., van Elk, M., & Bekkering, H. (2010). Motor activation during observation of unusual versus ordinary actions in infancy. *Social Neuroscience*, 5(5-6), 451-460.
- Staudigl, T., Vollmar, C., Noachtar, S., Hanslmayr, S., (2015). Temporal-Pattern Similarity Analysis Reveals the Beneficial and Detrimental Effects of Context Reinstatement on Human Memory. *J. Neurosci.* 35, 5373–5384. doi:10.1523/JNEUROSCI.4198-14.2015
- Stavrinou, M. L., Moraru, L., Cimponeriu, L., Della Penna, S., & Bezerianos, A. (2007). Evaluation of cortical connectivity during real and imagined rhythmic finger tapping. *Brain topography*, 19(3), 137.
- Stikic M, Johnson R R, Levendowski D J, Popovic D P, Olmstead R E and Berka C (2011) EEG-derived estimators of present and future cognitive performance *Frontiers Hum. Neurosci.* 5 70
- Stipacek, A., Grabner, R. H., Neuper, C., Fink, A., Neubauer, A. C. (2003). Sensitivity of human EEG alpha band desynchronization to different working memory components and increasing levels of memory load. *Neuroscience Letters*. **353**(3): 193–196. doi: 10.1016/j.neulet.2003.09.044
- Stone J.V. (2004); "Independent Component Analysis: A Tutorial Introduction", The MIT Press Cambridge, Massachusetts, London, England; ISBN 0-262-69315-1
- Sturm, I., M. Treder, D. Miklody, H. Purwins, S. Dähne, B. Blankertz, and G. Curio (2015). Extracting the neural representation of tone onsets for separate voices of ensemble music using multivariate EEG analysis. *Psychomusicology: Music, Mind, and Brain* 25.4, p. 366.
- Subasi, A., & Gursoy, M. I. (2010). EEG signal classification using PCA, ICA, LDA and support vector machines. *Expert Systems with Applications*, 37(12), 8659-8666.
- Sugiyama M, Krauledat M, Müller K R (2007) Covariate Shift Adaptation by Importance Weighted Cross Validation *Journal of Machine Learning Research* **8** 1027–1061
- Sunderland, S., (1945) "The Actions of the Extensor Digitorum Communis, Interosseus and Lumbrical Muscles," *Am. J. Anat.* 77, p. 189.
- Swartz B. E. (1998). "The advantages of digital over analog recording techniques". *Electroencephalography and Clinical Neurophysiology*. **106** (2): 113–7. doi:10.1016/S0013-4694(97)00113-2. PMID 9741771.
- Tallon-Baudry C, Bertrand O, Delpuech C, Pernier J. (1996) Stimulus specificity of phase-locked and non-phase-locked 40 Hz visual responses in human. *J. Neurosci.*, 1996; 16: 4240-9.
- Tallon-Baudry, C., Bertrand, O., Fischer, C., 2001. Oscillatory synchrony between human extrastriate areas during visual short-term memory maintenance. *J. Neurosci.* 21, RC177.
- Talukdar, U., & Hazarika, S. M. (2016). Estimation of Mental Fatigue During EEG Based Motor Imagery. In *IHCI* (pp. 122-132).
- Tangermann M, Höhne J, Stecher H, Schreuder M (2012a). "No Surprise — Fixed Sequence Event-Related Potentials for Brain-Computer Interfaces". In: *Engineering in Medicine and Biology Society (EMBC), 2012 Annual International Conference of the IEEE. IEEE*, pp. 2501–2504.
- Tavakolan, M., Yong, X., Zhang, X., & Menon, C. (2016). Classification scheme for arm motor imagery. *Journal of medical and biological engineering*, 36, 12.

- Telenczuk, B., Baker, S.N., Herz, A.V. and Curio, G., (2011). High-frequency EEG covaries with spike burst patterns detected in cortical neurons. *Journal of neurophysiology*, 105(6), pp.2951-2959.
- The Australian National University. (17 July 2003), "*Star count: ANU astronomer makes best yet*". Archived from [the original](#) on July 24, 2005. Retrieved 2 November 2010.
- Thompson, M. & Thompson, L. (2003) *The Neurofeedback Book: An Introduction to Basic Concepts in Applied Psychophysiology*, Wheat Ridge, CO: Association for Applied Psychophysiology.
- Thut, G., A. Nietzel, S. A. Brandt, and A. Pascual-Leone (2006). α -Band electroencephalographic activity over occipital cortex indexes visuospatial attention bias and predicts visual target detection. *The Journal of Neuroscience* 26.37, pp. 9494–9502.
- Tomioka R, G. Dornhege, K. Aihara, and K.-R. Müller. (2006) An iterative algorithm for spatio-temporal filter optimization. In *Proceedings of the 3rd International Brain-Computer Interface Workshop and Training Course 2006*, pages 22–23.
- Tomioka R, Müller KR (2010). "A regularized discriminative framework for EEG analysis with application to brain-computer interface". In: *Neuroimage* 49 (1), pp. 415–432.
- Tomioka, R., Aihara, K., & Müller, K. R. (2007). Logistic regression for single trial EEG classification. *Advances in neural information processing systems*, 19, 1377.
- Treder, M. S. and B. Blankertz (2010). (C)overt attention and visual speller design in an ERP-based brain-computer interface. *Behavioral and brain functions* 6.1, p. 1.
- Treder M S, Schmidt N M, Blankertz B (2011) Gaze-independent brain-computer interfaces based on covert attention and feature attention *J Neural Eng* 8 066003
- Treder M. S., H. Purwins, D. Miklody, I. Sturm, and B. Blankertz. (2014) Decoding auditory attention to instruments in polyphonic music using single-trial eeg classification. *Journal of neural engineering*, 11(2):026009.
- Trejo, L. J., Kubitz, K., Rosipal, R., Kochavi, R. L., & Montgomery, L. D. (2015). EEG-based estimation and classification of mental fatigue. *Psychology*, 6(05), 572.
- Tsui C S, Gan J Q, Hu H (2011) A self-paced motor imagery based brain-computer interface for robotic wheelchair control *Clin. EEG Neurosci.* 42 225-9
- Ullsperger, P., Neumann, U., Gille, H. G., Pietschmann, M. (1987). P300 and anticipated task difficulty. *Intern. Journal of Psychophysiology*. 5(2): 145–149. doi: 10.1016/0167-8760(87)90018-3
- Ušćumlić M, Blankertz B (2016) Active visual search in non-stationary scenes: coping with temporal variability and uncertainty *J Neural Eng* 13 016015
- Vaid and Singh, (2015) "De-noising of EEG signal for emotion recognition", International Conference on Signal Processing, Computing and Control (ISPCC), Wagnaghat, pp. 159-162. doi: 10.1109/ISPCC.2015.7375017
- van Erp J B, Brouwer A M, Zander T O (2015) Editorial: Using neurophysiological signals that reflect cognitive or affective state *Frontiers in Neuroscience* 9 00193
- van Erp J B, Lotte, F., Tangermann M. (2012) Brain-Computer Interfaces: Beyond Medical Applications. *Computer -IEEE Computer Society-, IEEE*, 45 (4), pp.26-34. 10.1109/MC.2012.107; hal-00688344
- Vanacker, G., J.R. Millán, E Lew, P.W. Ferrez, F. Galán Moles, J. Philips, H. Van Brussel, and M. Nuttin. (2007) Context-based filtering for assisted brain actuated wheelchair driving. *Computational Intelligence and Neuroscience*, Article ID 25130, 12 pages.
- Vanni S., A. Revonsuo, and R. Hari. (1997) Modulation of the parieto-occipital alpha rhythm during object detection. *The Journal of neuroscience: the official journal of the Society for Neuroscience*, 17(18):7141–7147, Sept. 12
- Vansteensel, M. J., Kristo, G., Aarnoutse, E. J., & Ramsey, N. F. (2017). The brain-computer interface researcher's questionnaire: from research to application. *Brain-Computer Interfaces*, 4(4), 236-247.

Bibliography

- Varela F, Lachaux J P, Rodriguez E, Martinerie J (2001) The brain web: phase synchronization and large-scale integration *Nat. Rev. Neurosci.* 2 229–239
- Vaughan H. G., Jr., (1969) The relationship of brain activity to scalp recordings of event-related potentials, In E. Donchin & D. B. Lindsey (Eds.), *Average Evoked Potentials: Methods, Results and Evaluations* (pp. 45-75). Washington, D.C.: U.S. Government Printing Office.
- Vaughan T M, D.J. McFarland, G. Schalk, W.A. Sarnacki, D.J. Krusienski, E.W. Sellers, and J.R. Wolpaw. (2006) The wadsworth BCI research and development program: at home with BCI. *IEEE Transactions on Neural Systems and Rehabilitation Engineering*, 14(2):229–233.
- Vecchiato, G., Borghini, G., Aricò, P., Graziani, I., Maglione, A. G., Cherubino, P., & Babiloni, F. (2016). Investigation of the effect of EEG-BCI on the simultaneous execution of flight simulation and attentional tasks. *Med. Biol. Engineering and Computing*, 54(10), 1503-1513.
- Ventur B, B. Blankertz, M. F. Gugler, G. Curio, (2010) “Novel Applications of BCI Technology: Psychophysiological Optimization of Working Conditions in Industry”, *Proceedings of the IEEE Conference on Systems, Man and Cybernetics (SMC2010)*.
- Vidal, J.-J. (1973). *Toward Direct Brain-Computer Communication*. *Annual review of Biophysics and Bioengineering*, 2(1):157–180.
- Vidaurre C, Kawanabe M, Bünau P, Blankertz B, Müller KR (2011a). “Toward Unsupervised Adaptation of LDA for Brain-Computer Interfaces”. In: *IEEE Trans Biomed Eng* 58.3, pp. 587 – 597.
- Vidaurre C, Sannelli C, Müller KR, Blankertz B (2011b). “Co-adaptive calibration to improve BCI efficiency”. In: *J Neural Eng* 8.2, 025009 (8pp).
- Vidaurre C, Sannelli C, Müller K R, Blankertz B (2011c) Machine-learning-based co-adaptive calibration for brain-computer interfaces *Neural Comput.* 23 791-816
- Vidaurre C, Sannelli C, Samek W, Dähne S, and Müller K R (2015) Machine learning methods of the Berlin brain-computer interface *Proceedings Volumes (IFAC-PapersOnline)* 20 48 447-452
- Vidaurre C., B. Blankertz, (2010) Towards a Cure for BCI Illiteracy, *Open Access Brain topography*, 23:194-198
- Volosyak, I., Valbuena, D., Malechka, T., Peuscher, J., and Gräser, A., (2010) Brain–computer interface using water-based electrodes. *Journal of neural engineering*, 7(6):066007.
- Wasilewski, F. (n.d.). PyWavelets - Wavelet Browser. Retrieved from <http://wavelets.pybytes.com/wavelet/db5/>
- Wayne D. W. (1990). "Kolmogorov–Smirnov one-sample test". *Applied Nonparametric Statistics* (2nd ed.). Boston: PWS-Kent. pp. 319–330. ISBN 0-534-91976-6.
- Weiskopf, N., K. Mathiak, S.W. Bock, F. Scharnowski, R. Veit, W. Grodd, R. Goebel, and N. Birbaumer. (2004) Principles of a brain-computer interface (BCI) based on real-time functional magnetic resonance imaging (fMRI). *IEEE Transactions on Biomedical Engineering*, 51(6):966–970, 2004.
- Welch, P. D. (1967), "The use of Fast Fourier Transform for the estimation of power spectra: A method based on time averaging over short, modified periodograms", *IEEE Transactions on Audio and Electroacoustics*, AU-15 (2): 70–73, doi:10.1109/TAU.1967.1161901
- Wenzel, M. A., J.-E. Golenia, and B. Blankertz (2016). Classification of eye fixation related potentials for variable stimulus saliency. *Frontiers in neuroscience* 10.
- Winkler, I., Haufe, S., & Müller, K. R. (2015). Removal of muscular artefacts for the analysis of brain oscillations: Comparison between ICA and SSD. In *ICML Workshop on Statistics, Machine Learning and Neuroscience (Stamfins 2015)*.
- Winkler, I., Haufe, S., and Tangermann, M. (2011). Automatic classification of artifactual ICA components for artifact removal in EEG signals. *Behavioral and Brain Functions*. 7: 30. doi: 701 10.1186/1744-9081-7-30

- Wolpaw J.R. (2007) Brain-computer interfaces as new brain output pathways. *J Physiol*, 579:613–619.
- Wolpaw J R and D.J. McFarland. (2004) Control of a two-dimensional movement signal by a noninvasive brain-computer interface in humans. *Proc Natl Acad Sci U S A*, 101(51):49–54.
- Wolpaw JR., N. Birbaumer, DJ. McFarland, G. Pfurtscheller, TM. Vaughan, (2002) Brain-computer interfaces for communication and control. *Clinical Neurophysiology*, 113(6), pp. 767–779.
- Wolpaw J R, D. J. McFarland, G. W. Neat, and C. A. Forneris. (1991) An EEG based brain-computer interface for cursor control. *Electroencephalography and clinical neurophysiology*, 78:252–259.
- Wolpaw J R, Wolpaw E W, eds. (2012) Brain-computer interfaces: principles and practice *Oxford University press* 0001
- Wolpaw, J.R., Loeb, G.E., B.Z. Allison, E. Donchin, O.F. do Nascimento, W.J. Heetderks, F. Nijboer, W.G. Shain, and J. N. Turner. (2006) BCI meeting 2005–workshop on signals and recording methods. *IEEE Transaction on Neural Systems and Rehabilitation Engineering.*, 14(2):138–141.
- Wu W, X. Gao, and S. Gao. (2005) One-versus-the-rest (OVR) algorithm: An extension of common spatial patterns(CSP) algorithm to multi-class case. In *27th Annual International Conference of the Engineering in Medicine and Biology Society, IEEE-EMBS 2005*, pp. 2387– 2390.
- Yordanova, J., Kolev, V., Polich, J. (2001). P300 and alpha event-related desynchronization (ERD). *Society for Psychophysiological Research*. **38(1)**: 143–152. doi: 10.1111/1469-8986.3810143
- Zander T. O. and C. Kothe. (2011) Towards passive brain–computer interfaces: applying brain–computer interface technology to human–machine systems in general. *Journal of neural engineering*, 8(2):025005.
- Zander, T.O., Brönstrup, J., Lorenz, R. and Krol, L.R., (2014). Towards BCI-based implicit control in human–computer interaction. In *Advances in Physiological Computing* (pp. 67-90). Springer London.
- Zhong, M., F. Lotte, M. Girolami, and A. Lécuyer. (2008) Classifying EEG for brain computer interfaces using gaussian processes. *Pattern Recognition Letters*, 29:354–359.
- Ziehe A, P. Laskov, G. Nolte, and K.R. Müller, (2004) “Afast algorithm for joint diagonalization with nonorthogonal transformations and its application to blind source separation,” *J. Mach. Learn. Res.*, vol. 5, pp. 777–800.
- Ziehe, A., & Müller, K. R. (1998). TDSEP—an efficient algorithm for blind separation using time structure. In *ICANN 98* (pp. 675-680). Springer, London.
- Ziehe, A., Muller, K. R., Nolte, G., Mackert, B. M., & Curio, G. (2000). Artifact reduction in magnetoneurography based on time-delayed second-order correlations. *IEEE Transactions on biomedical Engineering*, 47(1), 75-87.